INVESTIGATING THE THERMAL BEHAVIOR DIFFERENCES BETWEEN
BEET AND CANE SUGAR SOURCES

BY

YINGSHUANG LU

DISSERTATION

Submitted in partial fulfillment of the requirements
for the degree of Doctor of Philosophy in Food Science and Human Nutrition
with a concentration in Food Science
in the Graduate College of the
University of Illinois at Urbana-Champaign, 2016

Urbana, Illinois

Doctoral Committee:

       Research Assistant Professor Dawn M. Bohn, Chair
       Professor Shelly J. Schmidt, Director of Research
       Professor Keith R. Cadwallader
       Associate Professor Kent D. Rausch
       Research Chemist Danielle L. Gray
       Leonard C. Thomas, DSC Solutions LLC

Abstract

The melting behavior of sucrose has been well studied over a long period of time. However, one aspect that needed further study was the wide variation in melting temperature reported in the literature for sucrose, as well as other simple sugars (e.g., glucose and fructose). Based on previous work carried out in the Schmidt laboratory, the initial loss of crystalline structure in sucrose, glucose, and fructose was attributed to thermal decomposition, rather than thermodynamic melting. Recently, a number of sucrose samples were investigated in the Schmidt laboratory and a marked difference in the thermal behavior of beet versus cane sucrose samples was observed. In general, sucrose from sugarcane sources exhibited two endothermic peaks in the DSC thermogram, one small peak proceeded by one large peak; whereas, sucrose from sugarbeet sources exhibited only one large endothermic peak. The thermal behavior of both beet and cane sucrose sources also exhibited heating rate dependency, with Tmonset values for both small and large peaks increasing as heating rate increased; however, the degree of thermal stability, based on results from an ampule heating study, was much greater for beet compared to cane sucrose sources. To date, no published research was found relating the presence and magnitude of the small endothermic DSC peak to the plant source of the sucrose – suagrbeet versus sugarcane. Thus, the main objective of this research was to identify the cause and underlying mechanism of the presence of the small endothermic DSC peak in cane sucrose sources. A variety of analytical methods and techniques were applied to approach this research objective, including moisture content analysis, pH, conductivity ash content, total sulfite content measurements, single crystal X-ray diffraction (SXRD), X-ray Micro-Computed Tomography (Micro-CT), Differential Scanning Calorimetry (DSC),

High Performance Liquid Chromatography (HPLC), and Confocal Raman imaging and spectroscopy. From this study we found that the pH, conductivity ash, and moisture content values varied widely within and between sugar sources, and were not able to explain the small endothermic DSC peak difference between beet and cane sucrose sources. However, impurities in the mother liquor occlusions in beet, Chinese cane, and Sugar in the Raw appear to play a major role in thermally stabilizing the sucrose molecule. Beet and Chinese cane sucrose sources contained residual sulfite from the sulfitation processing step; whereas, analytical and commercial cane sources, which usually do not undergo sulfitation, were below the detection limit. Thus, sulfite content appears to explain the absence of the small endothermic DSC peak. Also, by addition of different concentrations of potassium sulfite, we were able to control the thermal behavior of laboratory-recrystallized Sigma sucrose, demonstrating that low concentrations of sulfite can completely inhibit the small endothermic DSC peak in cane sources. In the case of Sugar in the Raw, the high conductivity ash and pH appear to be responsible for inhibition of the small endothermic DSC peak. Overall, this research reveals that the composition and chemistry of the mother liquor occlusions, formed within the sucrose crystal during the crystallization process, are responsible for the thermal behavior of the various sucrose sources studied herein, In addition, this study makes a substantial contribution to the investigation of the thermal behavior of crystalline sucrose at the molecular level, since no previous research was found that explored the internal crystalline structure and vibrational modes of "as is" and heated crystalline beet and cane sucrose samples, which were examined using Micro-CT and Confocal Raman imaging and spectroscopy, respectively. Overall, this research provides a comprehensive and more detailed understanding of the thermal behavior

of sucrose, regardless of its source, which, in turn, is critical to the processing of and reactions

in sucrose containing foods, such as baking and caramelization.

Acknowledgement

First of all, I would like to thank and express sincere gratitude to my academic advisor Dr. Shelly J Schmidt, for the motivation and guidance she provided to me during my study and research in the past five years. Under her seasoned guidance, I enriched my knowledge, broadened my expertise, and sharpened my research skills significantly. It is truly an honor and blessing to have worked with Dr. Schmidt. Her personal characteristics, such as persistence and passion for science and education, will forever encourage me to be devoted to Food Science and its relevant research work in the future.

I sincerely thank all my committee members: Dr. Dawn Bohn, Dr. Keith Cadwallader, Dr. Kent Rausch, Dr. Danielle Gray, and Leonard Thomas for their encouragement and kind help. I am also grateful for the in depth help and support provided by Leonard Thomas, Dr. Danielle Gray, Dr. John Jerrell, Dr. Leilei Yin, Dr. Pawan Takhar, and Dr. Wu Heng-liang, especially for their willingness to share their expertise to help with my experimental design and data analysis. I am also grateful for the expert assistance of Mary An Godshall, retired, formerly with the Sugar Processing Research Institute, Inc., (SPRI, New Orleans, LA) and the assistance of Mark Muhonen, formerly with United Sugar Corporation (Clewiston, FL).

Last but not least, this journey would not have been possible without my family and friends. I would like to express my heart full gratitude to my parents Wei Lu, Shuying Liu, my grandfather Shufa Lu, my husband Peng Wang, and other family members for their unconditional love and support. I am also grateful for the help given by the whole Schmidt lab group, especially to our previously graduated PhD students, Dr. Sarah Scholl, Dr. Michelle Schwenk, and my undergraduate research assistant Haena Yun. In addition, I would like to thank our department

office administrator Barb Vandeventer and my friends in FSHN, as well as all other collaborators who have helped me with my study, research, and life. I look forward to continuing our collaboration in the future.

Table of Contents

Chapter 1: Introduction

1.1 Rationale and significance

The melting behavior of sucrose has been well studied over a long period of time. However, one aspect that needed further study was the wide variation in melting temperature reported in the literature for sucrose (e.g., Shah and Chakradeo 1936; Power 1958; Shallenberger and Birch, 1975; Lee and others 2011a), as well as other simple sugars (e.g., glucose and fructose). Based on previous work carried out in the Schmidt laboratory, the initial loss of crystalline structure in sucrose, glucose, and fructose was attributed to thermal decomposition, rather than thermodynamic melting (Lee and others 2011a and b). Recently, a number of sucrose samples were investigated in the Schmidt laboratory and a difference in the thermal behavior of beet versus cane sucrose samples was observed. In general, sucrose from sugarcane sources exhibited two endothermic peaks in the DSC thermogram, one small peak proceeded by one large peak; whereas, sucrose from sugarbeet sources exhibited only one large endothermic peak (Lu and others 2013). Thermal behavior of both beet and cane sucrose sources also exhibited heating rate dependency, with Tmonset values for both small and large peaks increasing as heating rate increased. Additionally, the magnitude of the small peak was observed to increase with increasing heating rate. Based on the literature review, as well as preliminary research studies carried out in the Schmidt laboratory, there are a number of factors that appear to influence the presence and magnitude of the small endothermic DSC peak in sucrose. However, to date, no published research was found that relates the presence and magnitude of the small endothermic peak to the plant source of the sucrose – sugarbeet versus sugarcane. Thus, the long-term goal of this research is to identify the cause and

underlying mechanism of the presence of the small endothermic DSC peak in cane sucrose sources.

1.2 Objectives

The specific objectives of this research are to:

Objective 1: Investigate the thermal behavior differences between beet and cane sucrose sources using thermal analysis (Chapter 3).

Objective 2: Determine the physicochemical characteristics of both "as is" and laboratory prepared beet and cane sucrose samples that are responsible for the observed thermal differences between the two sugar sources (Chapters 4 and 5).

Objective 3: Control the presence and magnitude of the small endothermic DSC peak in sucrose samples by manipulating sample properties and laboratory crystallization conditions (e.g., impurities and/or solvent type). The variables examined will be based upon the key characteristics identified in Objective 2 (Chapters 5 and 6).

Objective 4: Explore the thermal behavior of crystalline sucrose from different sources at the molecular level using confocal Raman imaging microscopy equipped with a hot stage (Chapter 7).

1.3 References

Lee JW, Thomas LC, Schmidt SJ. 2011a. Investigation of the heating rate dependency associated with the loss of crystalline structure in sucrose, glucose, and fructose using a thermal analysis approach (Part I). Journal of Agricultural and Food Chemistry, (59):684-701.

Lee JW, Thomas LC, Jerrell   J, Feng H, Cadwallader KR, Schmidt SJ. 2011b. Investigation of thermal decomposition as the kinetic process that causes the loss of crystalline structure in sucrose using a chemical analysis approach (Part II). Journal of Agricultural and Food Chemistry, (59):702-712.

Lu Y, Lee JW, Thomas L, Schmidt SJ. 2013. Differences in the thermal behavior of beet and cane sugars. Proceedings of the 74th Annual Institute of Food Technologists, Chicago, Ill.

Powers HEC. 1958. Sucrose crystal inclusions. Nature, 182:715-717.

Shah SV, Chakradeo YM. 1936. A note on the melting point of cane sugar.   Journal of Current Science. P652-3

Shallenberger RS. 1978. Intrinsic chemistry of fructose. Pure and Applied Chemistry 50:1409-1420.

Chapter 2: Literature review

2.1 Sources of sucrose

Much of the world's food comes from some 150 plant species cultivated as crops. Sugar (the common name for sucrose) is obtained from two main crops: sugarbeet and sugarcane. Currently, approximately 20% of the global sugar comes from sugarbeet, a root crop mainly grown in the temperate zones in the north; whereas the remaining 80% is extracted from sugarcane – a tall, bamboo-like grass largely grown in tropical countries (Fairtrade and Sugar 2013). However, these global sugar percentages are influenced by production costs and associated developments in technology, such as production of biofuel from sugarcane biomass. The United States is among the world's largest sugar producers and has both large and well-developed cane sugar and beet sugar industries. In fact, the beet sugar industry has grown a great deal in the United States since the early twentieth century. Since the mid-1990s, cane sugar has accounted for approximately 45% of the total sugar produced in the U.S., and beet sugar for approximately 55% of production (USDA 2013). Sucrose is one of the most important pure chemicals produced abundantly in the world. The refinement level of granulated sucrose is very high, with purity usually reaching greater than 99% (Table 2.1).

2.2 Structure of sucrose

Sucrose can be manufactured through the photosynthesis process by green plants. Sucrose is a disaccharide consisting of two monosaccharide units (Figure 2.1): D-glucose and D-fructose formed by an α-1, 2 glycosidic linkage (Hirschmüller 1953), with the chemical formula $C_{12}H_{22}O_{11}$ and scientific name α-D-glucopyranosyl-β-D-fructofuranoside. The confirmation of crystalline sucrose reveals that the glucose and fructose residues are fixed in

their relative orientation by two intramolecular hydrogen bonds between O-6f-H...O-5g and

O-1f-H...O-2g of 1.895 and 1.851 Å length, respectively. Sucrose crystallizes as an anhydrous

monoclinic crystal and belong to space group $P2_1$ (Mathlouthi and Reiser 1995). Each sucrose

molecule is surrounded by 12 neighbors and formed a highly dense packing structure. The

crystal structure of sucrose obtained by neutron and X-ray diffraction is reported in Table 2.1,

and the packing pattern (labeled with unit cell) of sucrose crystal is recorded in Figure 2.2.

2.3 Processing of refined white sugar from sugar beet and sugar cane

The process of extracting sucrose from either sugarbeet or sugarcane involves many

processing steps. The flowchart of the typical unit operations included in the manufacturing of

sucrose from sugarbeet and sugarcane plant sources are illustrated in Figures 2.3 and 2.4,

respectively. One major difference between white refined beet and cane sugar processing is

that beet sugar is produced in one continuous process, while cane sugar is generally produced

in two separate processes. Another difference is that the sugar beet process routinely includes

a sulfitation step, whereas sugar cane usually does not. Juice sulfitation is the process of adding

sulfur dioxide (SO_2) to the juice at approximate 30 ppm to reduce color and prevent color

formation in the next steps of operation (Clarke and Godshall, 1988; Asadi 2007). SO_2 inhibits

the browning (Maillard) reaction that forms coloring compounds during evaporation and

crystallization. Among cane sugar processors worldwide, there is mixed interest in the use of

sulfitation. In the United States, sulfitation has rarely been used in cane raw sugar factories

since the 1950's (Andrews and Godshall 2002). The aforementioned processing variations may

result in physicochemical differences between sucrose produced from sugarbeet versus

sugarcane plant sources. However, both beet and cane sugar end products need to meet the

same international quality standards, in terms of sucrose content, color, invert sugar, and ash content (Schiweck and Clarke 1994). Specifications valid within the European Economic Community (EC) have been accepted by many countries in the world, which are commonly used in international white sugar trading. Codex Alimentarius and Food Chemical Codex are the quality and safety standards for both beet and cane sugars subscribed to by the United States.

In beet sugar production in the U.S. (Figure 2.3), the beets are washed, sliced, and the sugar is extracted using a diffusion technique with 70°C hot water (diffusion juice). After several clarification steps using carbonation and sulfitation, thin juice is evaporated to thick juice (68 to 74% solids). Thick juice is mixed with back re-melted (i.e., melt in the sugar processing industry means dissolve) raw sugar crystallized from run-off syrups and is called standard liquor. White sugar is crystallized from standard liquor and molasses is produced as a by-product.

The first process in cane sugar production in the U.S. (Figure 2.4) is when dilute juice from washed, milled cane is clarified to produce clarified juice, evaporated to evaporator syrup (62 to 69% solids), and crystallized to raw sugar. Molasses is run-off syrup from the centrifugal separation of crystals and syrup. Raw sugar is a golden yellow/brown color with crystals containing approximately 97 to 98 % sucrose, with the remainder consisting of moisture, invert sugars, and non-sugar compounds, including colored compounds (Clarke and others 1997). The raw sugar is transported to refineries where the sugar is washed to remove the syrup coating and then melted (washed raw liquor), clarified to produce clarified liquor, decolorized to produce decolorized liquor, and then crystallized to white refined sugar with molasses as a by-product.

2.4 Physical and chemical differences between beet and cane sugar sources

Though refined white beet and cane sugars both contain greater than 99% sucrose (Table 2.1), differences in their instrumental aroma profile (Acree and others 1976; Parliment and others 1977; Monte and Maga 1982; Marsili and others 1994; Pihlsgard 1997; Magne and others 1998), sensory properties (Urbanus and others 2014a and b), and product performance (Urbanus and others 2014a and b) have been reported in the literature. Some of the differences between cane and beet sugars are due to the plant materials themselves, while others are due to processing differences. For example, beet and cane sugars exhibit a difference in their carbon isotope ratio (C_{13} to C_{12}), where the ratio is approximately 25% in beet sugar and 11% in cane sugar (Bubnik, 1995). This difference in isotope ratio is attributed to the varying CO_2 fixation during the photosynthesis of sugar beet, a C3 plant, and sugar cane, a C4 plant (Schiweck and Clarke 1994). Two other differential plant material markers are raffinose and theanderose. Though raffinose is present in both sugar sources, levels are higher in beet sugar compared to cane sugar as quantified using chromatography (Vaccari and Mantovani, 1995; Morel du Boil 1997; Eggleston 2004). Theanderose is present only in cane sugar and is thought to be a natural constituent of sugar cane (Morel du Boil 1996). Both raffinose and theanderose affect the sugar crystal growth and morphology (Liang and others 1989; Morel du Boil 1992). A number of studies conducted by the Sugar Processing Research Institute (New Orleans, LA) have focused on the identification and comparison between beet and cane sugars in regards to their odor, color, pH, ash, invert sugar, and polysaccharide content (Godshall 1986 and 1994). Preliminary compositional analysis of white refined beet and cane sugar complied by Godshall (2013) is given in Appendix A.

Due to the sulfitation step in sugar beet production, beet sugar should have a higher sulfur content compared to cane sugar. Lee and Schmidt (2014), using ICP analysis, determined that the sulfur content was higher in white refined beet sugar (125.15±3.09 mg/kg commercial grade United Sugar) compared to white refined cane sugar (41.82±0.92 mg/kg in analytical grade Sigma and 59.00±3.62 mg/kg in commercial grade C&H). Additionally, based on our own research, we observed that analytical grade sucrose samples (cane base) have a larger particle size compared to commercial beet and cane sucrose samples. Also, we found that beet sugar samples are always shiner compared to cane sugar samples. Generally, dull appearance relates to defects within the crystalline structure of a material. For example, the single crystal aluminum oxide specimen is very transparent, whereas the polycrystalline and porous (~5% porosity) materials are translucent and opaque, respectively (Callister and Rethwisch 2012).

2.5 Analytical techniques

Differential scanning calorimetry (DSC)

Standard differential scanning calorimetry (SDSC), generally abbreviated as DSC, is the most frequently used thermal technique, in which the difference in the amount of heat inputs into a sample and a reference is measured as a function of temperature, while the sample and the reference are subjected to a controlled temperature program (Lee, 2010).

There are two types of DSC instruments: power compensation and heat-flux DSC. A cross sectional diagram of a power compensation DSC cell and a typical heat-flux DSC cell are showed in Figure 2.5 and 2.6. In a powder compensation DSC, separate furnaces (heater) are used for the sample pan and the reference pan. The sample and the reference are heated at the same rate and maintained at the same temperature while the electrical power used by their heaters

was monitored. As a sample undergoes different thermal events (endothermic or exothermic), more or less heat must flow into the sample pan to maintain its temperature, so that it is always the same as reference pan. The difference in heat output between the sample furnace and reference furnace at any given temperature is recorded and the total heat flow signal is plotted as a function of temperature or time, thus generating a typical DSC thermogram. In traditional heat-flux DSC instruments, heat is transferred through a disk made of the alloy (constantan body) and up to the sample and reference pans using a single heat source. The difference in heat flow to the sample pan and reference pan is monitored by chromel-constantan area thermocouples formed by the junction of the constantan body and a chromel disc welded to the underside of each platform. The difference in temperature between the sample pan and reference pan is amplified by a variable high gain amplifier, and then electronically scaled to read directly as heat flow, thus generating a typical DSC thermogram (Lin 2007 and Lee 2010). Unlike other heat-flux DSC instruments, the Q2000 DSC (TA instruments, New Castle, DE) has another component, a chromel/constantan wire, which is named Tzero thermocouple (Figure 2.7). This wire is symmetrically located between the sample and reference sensor platforms and functioned as an independent measurement and furnace control sensor. Equipped with chromel/constantan results in a better instrument resolution and baseline generation, which is important for heat capacity measurements and quantification of weak and broad phase transitions (Lee 2010).

DSC is commonly used to measure transitions in material structure, since every change in structure is associated with heat absorption or release (Thomas and Schmidt 2010). A DSC thermal profile contains both qualitative and quantitative information about material

transitions, such as the glass transition, crystallization, curing, melting, and decomposition

(Figure 2.8). For some of these transitions, DSC can report not only the transition temperature

and total heat involved, but also reveals kinetic information about the reaction. In recent years,

the thermal behavior of sucrose has been studied using DSC (Beckett et al 2006; Lee and others

2011a and b; Magoń and others 2014). Three melting parameters, onset melting temperature,

Tmonset; peak melting temperature, Tmpeak; and enthalpy of melting, ΔH (J/g) are usually

measured by heating a crystalline material at a specified heating rate to a temperature where

the melting endothermic peak is complete (Lee 2010).

Thermogravimetric analysis (TGA)

Thermogravimetric analysis (TGA) can be used to determine the weight change of a

sample as a function of time and/or temperature using a thermal analyses controller and

associated software, which comprise a thermal analysis system. The TGA measures the amount

and rate change in a material, either as a function of increasing temperature, or isothermally as

a function of time, in a controlled atmosphere. It can be used to characterize any material that

exhibits a weight change and to detect phase changes due to decomposition, oxidation, or

dehydration. This information helps the scientist or engineer identify the percent weight

change and correlate chemical structure, processing, and end-use performance (TA Instruments

2006).

The essential components of TA Q500 TGA analyzer are: balance, sample platform, furnace,

heat exchanger, mass flow controller and cabinet. The balance is considered as the key to the

TGA system, since it provides precise weight measurement of material. The sample platform is

used to load and unload sample to and from the balance. The TGA furnace controls the sample

atmosphere and temperature. The heat from the furnace will be dissipated by the heat exchanger. The two TGA mass flow controllers control the purge gas to the balance and furnace. All other system electronics and mechanics are housed in the cabinet. A schematic diagram in Figure 2.9 is used to illustrate the inside structure of the TGA instrument.

Today, the TGA technique is widely used in pharmaceutical, materials, and food science research. TGA can evaluate the presence of bulk water and identify the temperature when decomposition occurs by measuring weight loss or gain in a material during thermal process (Thomas and Schmidt 2010). Since TGA can detect weight changes caused by decomposition, evaporation, hydrated or solvated solids, and gas adsorption or desorption, thus it is considered to be an important technique to compare thermal stability among sugar samples and to further investigate thermal decomposition related loss of crystalline structure in sucrose (Lee, 2010).

High performance liquid chromatography (HPLC)

In order to quickly and accurately quantify the amount of sucrose and its decomposition components under different heat treatments, proper analytical methods are required. In 1915, the hydrolysis products (invert sugars) of beet and cane sucrose were quantified using Fehling's titration test (Hubbard and Mitchel 1915). To date, more advanced analytical techniques have been developed and applied to the similar research purpose. High performance liquid chromatography (HPLC) is a chromatographic technique used to separate the components in a mixture, to identify each component, and to quantify each component. It relies on pumps to pass a pressurized liquid and a sample mixture through a column filled with a sorbent, leading to the separation of the sample components. Therefore, HPLC has been utilized to determine sugar decomposition components, since it is known to be a successful technique for separating,

identifying, and quantifying sugars and their thermal degradation products (Bonn 1985, Yuan

1996 and 1999, Lee 2011b).

Powder X-ray diffraction (PXRD)

X-ray powder diffraction (PXRD) was first developed by Max Von Laue in 1912 (Formica,

1997). When the X-ray incident beam is diffracted by the crystalline material, the distances

between the atomic planes could be measured by applying Bragg's Law (Equation 2.1),

$$n\lambda=2d\sin\theta \qquad\qquad \text{Equation 2.1}$$

where n is the order of the diffraction, λ is the wavelength of the X-ray, d is the distance

between atomic layers in a crystal, and θ is the angle between the incident ray and the

scattering planes. Scattered waves that are in phase (parallel, but out of phase with the original

X-ray) are collected by a detector (Figure 2.10). The X-ray generator and detector move through

a series of angles to collect data of the structure. When the scattered wave over a range of

angles (°2θ) detected, a diffraction pattern is created, and thus the lattice parameters of the

material can be determined (Scholl 2014). In many cases, the sample is rotated, while the

either/or/both source and detector are moved on a continuous arc.

PXRD is a nondestructive technique, which can be applied to identify crystalline phases

and orientation, to determine structure properties such as lattice parameters (10-4Å), strain,

grain size, preferred orientation, thermal expansion, to measure thickness of thin films and

multi-layers and to determine atomic arrangement. If a sample contains some amorphous

material, the disorder structure of the sample will result in background noise. For example, if

the sample is completely amorphous, the broad signal at low angles that appears to give no

peaks (Suryanarayana and Norton 1998).

Single crystal X-ray diffraction (SXRD)

Single crystal X-ray diffractometers utilize either 3- or 4-circle goniometers. These circles refer to the four angles (2θ, χ, φ, and ω) that define the relationship between the crystal lattice, the incident ray, and the detector. Each sample held by a thin glass fiber is attached to brass pins and mounted onto the goniometer head. Adjustment of the X, Y and Z orthogonal directions allows centering of the crystal within the X-ray beam. X-rays leave the collimator and are directed at the crystal. Rays are either transmitted through the crystal, reflected off the surface, absorbed by the sample, or diffracted by the crystal lattice. A beam stop is located directly opposite the collimator to block transmitted rays and prevent burn-out of the detector. Reflected rays cannot be picked up by the detector, which is due to the angles involved. Diffracted rays at the correct orientation for the configuration are then collected by the detector (Figure 2.11). Modern single-crystal diffractometers are designed to use CCD (charge-coupled device) technology to transform the X-ray photons into an electrical signal, which are then sent to a computer for processing (Clark and Dutrow 2015).

Single crystal X-ray diffraction (SXRD) is used to determine the crystalline structure, such as the inter- and intra- molecular bonding, bond distance, bond angle, and molecular packing pattern. SXRD provides the best structure evidence for polymorphs (Huang 2004). Polymorphism indicates the phenomenon that the same chemical compound exhibits different crystal forms (Authier and Chapuis 2014). Besides basic crystallographic information (unit cell, molecular packing, bond lengths and angles) such structural features as absolute and relative configurations, hydrogen-bonding pattern, crystal disorder and conformational polymorphism may be obtained (Yu and others 1998); however the data collected from single-crystal

diffraction is limited by the quality of the selected crystal (Lin 2007). Compared to PXRD, SXRD could provide detailed crystal structure, including unit cell dimensions, bond-lengths, bond-angles and site-ordering information and determine the crystal-chemical controls on mineral chemistry. Limitations of SXRD, such as it demands a single, robust (stable), optically clear sample, generally between 50 to 250 microns in size, and relatively longer time for data collecting should also be considered during analysis. The major difference between experimental operation of SXRD and PXRD is illustrated in Figure 2.12.

X-ray computed microtomography (Micro-CT)

X-ray computed microtomography (micro-CT) is derived from the oldest true 3D imaging method (Elliott 2008 and Kalender 2005). Lab-based micro-CT systems are now commercially available that can routinely produce cell-scale images of intact samples. Like its clinical progenitor, micro-CT reconstructs a stack of cross-sectional images from a series of projection images taken at closely spaced angles through a half or full rotation (of the sample, rather than the source and detector). Micro-CT is a 3D complement to serial sectioning, and can give histological resolutions throughout a complete volume (Metscher 2013). When micro-CT is working, the X-ray beams are more focused using collimators, which have a fan shape. The X-ray beam moves around the object in a circle at small angular increments and the sensors take measurements for each position. Many independent ray values are collected along the fan, and then give a multitude of rays for each angular value. A high-speed computer is used to convert these ray values, in terms of reconstructing the object using a method known as "Filtered Back Projection" into a 2-dimensional slice.

The Xradia Bio Micro-CT (MicroXCT-400, Figure 2.13) is a high-resolution 3D X-ray imaging system, which is optimized for non-destructive imaging of complex internal structures. It enables accelerated, highly efficient analysis of structures examined in a variety of applications, for examples, semiconductor packaging development and failure analysis, life-science research, rock microstructure modeling for oil and gas exploration, and in situ measurement during imaging. The Xradia MicroXCT-400 provides the unique ability to reveal the internal structure with full 3D imaging of features down to <1.0 micron resolution (from: LOT-QuantumDesign GmbH), thus can be utilized to visualize the internal structure of sucrose crystals.

Raman spectroscopy

Raman spectroscopy has been proved to be an effective tool for studying molecular structures and interactions (Mathlouthi 1986). It is a sensitive, reliable, and non-destructive technique, which can be used in situ (Castro and others 2005). Raman spectrum is plotted as the intensity of the collected photons versus wavenumbers. Wavenumbers have the unit of cm^{-1}, which is the reciprocal of the wavelength. Wavenumbers (w) represent the difference between the frequency of laser wavelength (v_0) and frequency of scattered light (v_m) that calculated by Equation 2.2, where c is the speed of light.

$$w = \frac{v_m}{c} - \frac{v_0}{c} \qquad \text{Equation 2.2}$$

Raman shifts are currently measured by Raman spectrometers. There are mainly two commercial forms of Raman spectrometers: dispersive Raman and Fourier-transform (FT)-Raman instruments. The diagrams for these two types are illustrated in Figure 2.15 (a) and (b), respectively. Dispersive Raman systems utilizes a grating and multi-channel detector, such as charge-coupled device (CCD), whereas FT-Raman systems use a multiplexer and inverse

Fourier-transformation to obtain the Raman spectrum. Laser wavelengths used in dispersive Raman are 514, 532, 633, 785 and 850 nm, on the other hand longer wavelength, 1064 nm, is preferred in FT-Raman systems (Gizem Gezer 2015).

The reason for the observed Raman shift is due to vibrational modes of the molecules, which are highly selective to specific molecular bonds. Raman Effect only occurs when the polarizability of the molecule changes, unlike Infra-Red spectroscopy, which requires a change in the dipole moment of a molecule. The peak position of a bond is determined by three factors: the force constant, vibration mode of the bond (e.g. stretching and bending vibrational types in Figure 2.14), and the reduced mass of the molecules involved in the bond. The peak positions of stretching vibrations for the same molecule is observed at higher wavenumbers compared to bending ones. Stronger bonds (e.g. C=C) compared to weaker bonds (e.g. C-C) also occurs at higher wavenumbers. In addition, the molecules with low molecular weight, hence low reduced mass occur at smaller wavenumbers. These rules can be applied to molecules in the absence of other molecules. When there are surrounding molecules, the band position might shift or overlap since the width of a peak is influenced by the surrounding molecules (Gizem Gezer 2015). Some of the commonly used characterizing Raman peaks are recorded in Table 2.3. Therefore, Raman spectroscopy could potentially be utilized to study the vibrational modes in sucrose crystals refined from different sources.

2.6 Thermal behavior of sucrose

Thermodynamic melting occurs at a single, time-independent (i.e., heating-rate independent) temperature (often reported as Tm onset), where the crystalline solid and corresponding liquid phases are in thermodynamic equilibrium at a constant pressure without

chemical changes (Wunderlich 1990a; Lee and others 2011a,). The parameters associated with

the melting process (onset melting temperature, Tmonset; peak melting temperature, Tmpeak;

and enthalpy of melting, ΔH) are usually measured by heating a crystalline material at a

specified heating rate to a temperature, where the melting endothermic peak is complete.

Melting point variation

The crystallization and melting behavior of sucrose has been under investigated for a

number of years. However, one aspect of the melting behavior of sucrose that needed further

study was the wide variation in melting temperature reported in the literature for sucrose, as

well as other sugars (e.g., glucose and fructose). Though a consistent, uniform melting

temperature is expected for a crystalline material, the melting temperature for sucrose has

been found to vary widely, beginning in early studies and continuing to the present. Examples

of early studies include work by Shah and Chakradeo (1936) and Powers (1956 and 1958). Shah

and Chakradeo (1936) reported a sucrose melting point of 182°C, but gave a table of sucrose

melting point values recorded in the literature, varying from 160 to 186°C. Melting parameters

for more recent studies still exhibit a wide range of values, examples of which are summarized

in Appendix B.

Shah and Chakradeo (1936) mentioned a number of possible factors responsible for the

reported melting point variation including "slow heating and consequent partial decomposition

into glucose and fructozone or even partial hydrolysis into glucose and fructose due to the

presence of traces of water," and differences in the melting point determination methods, as

well as the purity of sucrose. These authors concluded that the melting temperature was

dependent upon the purity of the sample alone. Powers (1956 and 1958) reported that the

presence of water inside the sucrose crystal structure is in the form of mother syrup (or liquor) inclusions, which was used as an explanation for the widely varying melting point of sucrose observed in the literature (160 to 186°C).

Over the years, researchers have offered a number of possible explanations for the wide range of melting temperatures of sucrose, including impurities (Hirschmüller 1953; Kamoda 1960; Beckett and others 2006), polymorphism (Kishihara and others 2001; Lee and Lin 2007; Lee and Chang 2009), superheating (Wunderlich 1990b), liquefaction (used to explain the large variation observed in the melting parameters for isomerizable materials, such as fructose, glucose, and galactose) (Shallenberger 1978; Horton and Walaszek 1982), and thermal decomposition (Shah and Chakradeo 1936; Lee and others 2011a and b) and/or mutarotation (Hurtta and others 2004a; Lappalainen and others 2006) in addition to melting. However, according to Lee and others (2011a), these explanations do not completely account for the observed variation. Rather, Lee and others (2011a and b) noted that the sucrose melting parameters tended to increase strongly with increasing heating rate, leading to their conclusion that the initial loss of crystalline structure in sucrose is associated with the kinetic process of thermal decomposition.

Another unique observation, related to the wide range of melting parameters, is the appearance of a small endothermic DSC peak prior to the large endothermic DSC peak observed in thermal profiles of some sucrose samples. Most recent studies conducted using DSC clearly reveals that the appearance of small endothermic peak in sucrose samples (Lee and others 2011a and b; Saavedra-Leos and others 2012; Mathlouthi and Roge 2012; Magoń and others 2014; Kinugawa and others 2015), one example is given in Figure 3.1 (Magoń and others 2014).

A variety of factors discussed in the literature that have been found to affect the presence and magnitude of the small peak. Beckett and others (2006) reported that the appearance of the small endothermic peak is highly dependent on the purity of the sucrose. For example, the size of the peak decreased when the sucrose was recrystallized in the presence of KCl. They also observed that the appearance of the small peak could be affected by the recrystallization conditions. For example, by introducing a stirring step or increasing the temperature of the recrystallization solution, the small peak decreased. Additionally, Kawakami and others (2006) found that by "annealing" the recrystallized amorphous sucrose samples at variety of time and temperature combinations, defects in the crystal structure were partially modified, which resulted in the alteration of the melting behavior of sample (number and magnitude of peaks in DSC thermograms).

Several hypotheses have been suggested in the literature that attempt to explain the presence of the small endothermic DSC peak, which can be grouped in five categories and summarized as follows. The presence of the small endothermic peak in crystalline sucrose is attributed to: 1) amorphous content and described as i) presence of partially amorphous, fine sucrose crystals (<50 μm), which produces a glass transition just prior to the melting peak (Mathlouthi and Roge 2012); ii) presence of some amorphous fraction (highly concentrated mother liquor) in the granules, which produces a small devitrification peak (Bhandari and Hartel 2002); 2) water - entrapped, surface, or hydrate and described as i) partial decomposition into glucose during slow heating or hydrolysis into glucose and fructose due to the presence of traces of water (Shah and Chakradeo 1936); ii) a non-stoichiometric entrapment of water in the crystal lattice and the affinity of added impurities for available water (Maulny 2004; Beckett

2006); iii) formation of a hydrate of sucrose (Miller 2001); iv) solubilization (heat of solution) of the surface of the crystals by residual moisture (Bhandari and Hartel 2002); 3) impurities and defects and described as i) a non-stoichiometric entrapment of water in the crystal lattice and the affinity of added impurities for available water (Maulny 2004; Beckett 2006); ii) formation of different crystal structures due to the type and amount of impurities present in the mother liquor (Okuno 2003); iii) defects in the lattice structure produced during crystallization (Kawakami and others 2006); 4) polymorphism and described as i) conformational polymorphism about the glycosidic linkage (Lee and Lin 2007a and b; Lee and Chang 2009); ii) formation of different crystal structures due to the type and amount of impurities present in the mother liquor (Okuno 2003); 5) decomposition or hydrogen bond breaking that described as i) partial decomposition into glucose during slow heating or hydrolysis into glucose and fructose due to the presence of traces of water (Shah and Chakradeo 1936); ii) breaking of some hydrogen bonds prior to the melting of the crystal structure (Reynhardt 1990); 6) particle size differences among sucrose samples (Magoń and others 2014).

Although researchers have tried to identify the cause of the small peak (as listed above), no literature was found tying the existence of the small peak to the source of the sucrose. Recently, a number of sucrose samples were investigated in the Schmidt laboratory and a difference in the thermal behavior of beet versus cane sucrose samples was observed. In general, sucrose from cane sources exhibited two endothermic peaks in the DSC thermogram, one small and one large peak; whereas, sucrose from beet sources exhibited only one large endothermic peak.

Thermal decomposition of sucrose

A large number of publications, over the years, have investigated the thermal

decomposition of sucrose, both in the presence and in the absence of an aqueous solution

(Richards and Shafizadeh 1978 and 1986; Lee and others 2011b). Under both conditions, the

first step in the sucrose thermal decomposition pathway is the splitting of the glycosidic linkage

between the glucose and fructose moieties via a form of sucrose hydrolysis (i.e., protonation of

the glycosidic oxygen). What remains somewhat controversial is the timing and mechanism of

this initial thermal decomposition step in relation to sucrose melting (e.g., Roos and others

2012; Schmidt and others 2012; Roos and others 2013). A number of publications have

suggested that thermal decomposition accompanies (along with or right after) sugar melting in

sucrose, as well as glucose, and fructose (Kamoda 1960; Örsi 1973; Mauch 1975; Roos 1995;

Hurtta 2004; Kishihara 2004; Sakamoto and others 2006; Liu and others 2006). Based on

heating rate dependency studies, the onset temperature of melting increases with increased

heating rate (especially in the 1 to 5°C/min heating rate range) has been observed. There is

mounting evidence to reveal that thermal decomposition is involved in the initiation of the loss

of crystalline structure in sucrose (Lee and others 2011a and b; Schmidt and others 2012).

In 1953, Hirschmüller reported that even at a temperature below the melting point, the

decomposition of sucrose could occur slowly. A more rapid decomposition reaction could take

place when sucrose is further heated. Additionally, the formation of early decomposition

components, D-glucose and D-fructosan, could cause no weight loss. Later on, Gardiner (1966)

reported the yields of pyrolysis products of some hexoses and derived di-tri-, and

poly-saccharides. The thermal decomposition products 1, 6 -anhydro- β-D-glucopyranose and 1,

6 -anhydro- β-D-glucofuranose were detected in sucrose using Gas Chromatography. In 1978,

Richards and Shafizadeh reported that the initiating reaction of sucrose thermal decomposition is a first-order reaction, which yields D-glucose and a fructose derivative. Also they claimed the apparent temperature associated with these thermal events is considerably influence by the heating rate of DSC. Richards and Shafizadeh (1986) simplified the thermal degradation (decomposition) of sucrose into three predominant steps as confirmed by HPLC analysis: 1) The protonation of the glycosidic oxygen yields initial products (α-D-glucopyranose and fructose carbocation). This step is very sensitive to catalysis by trace amounts of acid. 2) The fructose carbocation is lost rapidly by several reaction channels, which may cyclize to form anhydrides. 3) The non-specific degradation to a variety of products such as hydroxymethyfurfural, fructose formed by adding a hydroxyl ion, or it could add to one of hydroxyl oxygen to another sucrose molecule to form a trisaccharide, such as kestoses. Eggleston and others (1996) reported on the catalytic nature of salts, which is associated with the thermal degradation of crystalline sucrose via DSC and TGA studies. In 2003, Šimkovic and others reported that the primary reaction of thermal degradation of sucrose is the splitting of glycosidic bond when it is isothermal heating at 185°C for 5 minutes, yielding glucopyranose isomers and 2, 6-anhydrofructose.

More recently, a number of studies on the loss of crystalline structure of sucrose that attributed the initial loss of crystalline structure to thermal decomposition, rather than thermodynamic melting were carried out by the Schmidt Laboratory (Lee and others 2011a to d). In addition of generating a more comprehensive schematic overview of the thermal decomposition of sucrose, they also reported that using fast scanning mode (standard DSC at 10°C/min heating rate), initial thermal decomposition components: glucose and 5-HMF were detected in the sucrose sample using HPLC, which was commensurate with the Tmonset of the

small DSC endothermic peak in analytical grade Sigma cane sucrose, measured approximately at 150°C. During slow, isotherm heating (quasi-isothermal MDSC 120°C for 3100 min), the same initial decomposition components: glucose and 5-HMF, were detected in the sucrose sample corresponding with the time (50 min) that the reversing heat capacity began to increase. This study clearly illustrated that not only is the loss of crystalline structure in sucrose initiated by thermal decomposition, but also that is achieved via a time-temperature combination process. In 2014, Magoń and others concluded that the shift to higher melting temperature values with increasing heating in the DSC is the result of superheating of sucrose, the minor accompanying from thermal lag and thermal decomposition. In another word, the authors believed that the observed heating rate dependence of the loss of crystalline structure in sucrose is due to superheating.

2.7 Morphology of sucrose and role of crystal defects

The morphology of sucrose grown in aqueous solution has been studied by a number of researchers (Ubbelohde 1965; Hartel and Shastry 1991; Bubnik and others 1992; Mullin 2001; Vaccari 2010; Roos and others 2013; Vaccari and Mantovani 1995, 1999a and b; Sgualdino and others 2005 and 2007). When sucrose crystals are grown in aqueous pure solution, there may be 15 possible faces, with 8 of the most important faces (Vavrinecz 1965). The missing of some faces is because that the faster growing phases will become smaller and smaller until they disappear; whereas the slower growing phases will gradually become large and larger. Thus, in the final shape, the crystal will only be made up of those slower growing faces (Vaccari 2010). Pure crystalline sucrose should always be the same regardless of plant source, since the molecular structure of the sucrose crystal is determined by physical constrains (Hartel and

Shastry 1991). However, mother liquor solution can remain on the crystals even after centrifugation, thus, the entrapped impurities can further impact the chemistry, composition and morphology of crystals. As previously mentioned, there are some differences between beet and cane sucrose that are sensitive to small levels of impurities present during processing. Since these impurities can play a large role during crystallization process, these differences may become quite important in controlling the formation of sugar crystals in a food product. Also, it is known that raffinose, a trisaccharide, is always present in beet sugar processing. In the presence of quite low concentration of raffinose in sucrose growing solution could result in a very simple morphology, particularly elongated on the *b* axis.

Another important area to explore in relation to the thermal behavior and the presence of the small peak in crystalline sucrose is the role of crystal defects. Thomas and Williams (1967), studying lattice imperfections in sucrose, showed that water is located in dislocation cores in the sucrose crystal structure, which can be liberated upon heating. The presence of water inside the sucrose crystal, observed using light microscopy, was first reported earlier by Powers (1956). Powers (1958) related the amount of water in the crystal to the size of the crystal, with large crystals (approaching an inch in length) containing more water (0.1 to 0.4%) compared to smaller crystals (0.01 to 0.04%). It is interesting to note that Powers (1958) explained the widely varying specific gravity and melting point values for sucrose given in the literature, 1.58 to 1.60 gram/cm3 and 160 to 186°C, respectively, to the presence of these water inclusions. Thomas and Williams (1967) also demonstrated that prolonged heating (6 hours) at 120°C under vacuum gave rise to decomposition "volcanoes" on the surface of the crystal, again likely situated at dislocation sites. Thomas and Williams (1967) also noted that regions of higher

24

imperfection density undergo preferential caramelization when sucrose crystals were heated. Eastmond (1970) reviewing the result of Thomas and Williams (1967), stated that these results demonstrate that lattice imperfections are important as reaction sites. Further evidence arises from the sensitivity of many of these reactions to the presence of very small concentrations of chemically inert impurities and from the general irreproducibility of reaction rates. The mother liquor solution in sucrose crystal is related to the instability of the surface structure that is due to the high growth rate of the various faces. This high growth rate can be reached through specific conditions of supersaturation, temperature, and stirring. Also, there is another cause, which should be responsible for particular disturbance of the surface of the crystal and, consequently, to promote the trapping of mother solution that is the boiling of the solution during the crystallization. Oftentimes the faster crystal growth rate and higher growing steps will result in rougher surfaces and deeper cavities (Vaccari 2010).

2.8 References

Acree TE, Lee CY, Butts RM, Barnard J. 1976. Geosmin, the earthy component of table beet odor. J Agric Food Chem 24(2):430–1.

Andrews LS, Godshall MA. 2002. Comparing the Effects of Sulphur Dioxide on Model Sucrose and Cane Juice Systems. Journal American Society of Sugarcane Technologists. 22: 90-101.

Asadi M. ed. 2007. Beet-sugar handbook. John Wiley & Sons, Inc.,Hoboken, New Jersey.

Authier A, Chapuis G. ed. 2014. A Little Dictionary of Crystallography. By IUCr Commission on Crystallographic Nomenclature. Chester, International Union of Crystallography. 238pp.

Beckett ST, Francesconi, MG, Geary PM, MacKenzie G, Maulny APE. 2006. DSC study of sucrose melting. Carbohydrate Research 341: 2591-2599.

Bensouissi A, Rousse C, Roge B, Mathlouthi M. 2007. Effect of Selected Impurities on Sucrose Crystal Growth Rate and Granulated Sugar Quality. p 147-65.

Bhandari B, Hartel R. 2002. Co-crystallization of Sucrose at High Concentration in the Presence of Glucose and Fructose. J. of Food Sci, 67: 1797–1802.

Bonn G.1985. High-performance liquid chromatographic elution behavior of oligosaccharides, monosaccharides and sugar degradation products on series-connected ion-exchange resin columns using water as the mobile phase. Journal of Chromatography 332:411-424.

Bubnik Z, Vaccari G, Mantovani G, Sgualdino G, Kadlec P. 1992. Effect of dextran, glucose and fructose on sucrose crystal elongation and morphology. Zuckerindustrie. 117(7): 557-561.

Bubnik, Z. et al. eds. 1995. Sugar Technologists Manual. Bartens, Berlin.

Callister WD, Rethwisch DG. 2012. Fundamentals of materials science and engineering: an integrated approach. 4th ed. Hoboken, N.J.: Wiley.

Castro K, Pérez-Alonso M, Rodríguez-Laso MD, et al (2005) On-line FT-Raman and dispersive Raman spectra database of artists' materials (e-VISART database). Anal Bioanal Chem 382:248–258. doi: 10.1007/s00216-005-3072-0.

China GB13104-2005 Sugar Hygiene Standard (National standard for sugars). 2005. Beijing.

Clark CM, Dutrow BL. 2015. Single-crystal X-ray Diffraction. Available from http://serc.carleton.edu/research_education/geochemsheets/techniques/SXD.html. Lasted accessed 12th Mar, 2016.

Clarke MA, Edye LA, Eggleston G. 1997. Sucrose decomposition in aqueous solution, and losses in sugar manufacture and refining. p 441-470.

Clarke MA, Godshall MA. eds. 1988. Chemistry and Processing of Sugarbeet and Sugarcane. Chapter 13, The nature of colorants in sugarcane and beet sugar manufacture. Elsevier Science. Publishers, Amsterdam.

Clarke MA. 2000. Sugarcane. In: Anonymous Kirk-Othmer Encyclopedia of Chemical Technology. John Wiley & Sons, Inc. p 1-26.

Colonna WJ, Samaraweera U, Clarke MA, Cleary M, Godshall MA, White JS, Updated by Staff. 2000. Sugar. In: Anonymous Kirk-Othmer Encyclopedia of Chemical Technology. John Wiley & Sons, Inc.

Dowling JF. 1990. Sugar products. In: Pennington NL, Baker CW, editors. Sugar a user's guide to sucrose. 1st ed. New York: Van Nostrand Reinhold. p 36-45.

Eastmond GC. 1970. Solid-state polymerization. Progress in Polymer Science, 2:1–46.

Eggleston G, Trask-Morrell BJ, Vercellotti JR. 1996. Use of differential scanning calorimetry and thermogravimetric analysis to characterize the thermal degradation of crystalline sucrose and dried sucrose-salt residues. J. Agric. Food. Chem. 44, 3319-3325.

Eggleston G. 2004. Differentiating cane white sugar from beet white sugar using ion chromatography profiles. SPRI Conference on Sugar Processing Research 209-14.

Elliott JC, Davis GR, Dover SD 2008. X-ray microtomography: Past and present. in Proceedings of SPIE - The International Society for Optical Engineering. San Diego, CA.

European Economic Community, Council Directive of 11 Dec., 1973 (73/437/EC), Off. J. E. C. no L 356, 27.12.73, pp. 71-78;First Commission Directive of 26 July, 1979 (79/786/EC), Off. J. E. C. no L 239, 22.9.79. p 24-52.

Fairtrade and Sugar 2013. Fairtrade Foundation. Available from http://www.fairtrade.org.uk/. Lasteded accessed 3rd Mar, 2014.

Formica J. 1997. Chapter 18, X-ray diffraction. In Handbook of Instrumental Techniques for Analytical chemistry, edited by Settle FA, Prentice Hall PTR, New Jersey. pp.339-353.

Gizem Gezer P. 2015. PhD dessertation "Manufacture and utilization of a biodegradable sensor platform from gold coated zein nanophotonic films to detect Acrylamide and Ara-h1 using SERS" University of Illinois, Urbana-Champaign.

Godshall MA, Grimm CC, Clarke MA. 1994. Sensory properties of white beet sugars. p 305-24.

Godshall MA. 1986. Flavors from beet and cane sugar products. From Proc. Sugar processing research conference. p 210-28.

Godshall MA. 2013. Industrial Uses of Sugar – Chocolate, Confectionery, Beverage, Bakery, Cereal and Dairy Products and Processes. U.K.: InformaAgra.

Haines PJ, Wilburn FW. 1995 Differential thermal analysis and differential scanning calorimetry. In Thermal Methods of Analysis, edited by Haines PJ. Blackie: London. P63-122.

Hartel R.W., Shastry A.V. Sugar crystallization in food products. (1991) Critical reviews in food science and nutrition, 30 (1), pp. 49-112.

Hirschmüller H. (1953) Chapter 1 – Chemical properties of sucrose, in   Principles of Sugar Technology, edited by Honig, Elsevier, Amsterdam, The Netherlands, Pages 1-17.

Horton D, Walaszek Z. 1982. Tautomeric equilibria of some sugars by partially relaxed, 13C pulse Fourier-transform, nuclear magnetic resonance spectroscopy. Carbohydrate Research 105:145-153.

Huang TC. 2004. Automatic X-ray single crystal structure analysis system for small molecule. The Rigaku J. 21(2), 43-46.

Hubbard WS, Mitchel WL. 1915. The hydrolysis of sugar solutions under pressure. The Journal 505 of Industrial and Engineering Chemistry (7):609-610.

Hurtta M, Pitkänen I, Knuutinen J. 2004a. Melting behaviour of D-sucrose, D-glucose and D-fructose. Carbohydrate Research 339:2267-2273.

Kalender WA. 2005. Computed Tomography: Fundamentals, System Technology, Image Quality, Applications. Erlangen: Publicis Corporate Publishing.

Kamoda, M. Studies on the properties of sucrose crystal. Proc. Res. Soc. Jpn. Sugar Refin. Technol. 1960, 27, 258-238.

Kawakami K, Miyoshi K, Tamura N, Yamaguchi T, and Ida Y. 2006. Crystallization of sucrose glass under ambient conditions: Evaluation of crystallization rate and unusual melting behavior of resultant crystals. Journal of Pharmaceutical Sciences, 95(6): 1354-1363.

Kinugawa K, Kinuhata M, Kagotani R, Imanaka H, Ishida N, Kitamatsu M, Nakanishi K, Imamura K. 2015. Inhibitory effects of additives and heat treatment on the crystallization of freeze-dried sugar. Journal of Food Engineering, 155, 37-44.

Kishihara, S.; Sakuda, H.; Miura, K.; Sakamoto, K.; Tachibana, Y.; Koizumi, Y.; Tatara, T. Transfiguration of the properties of granulated sugar on heating. Proc. Res. Soc. Jpn. Sugar Refin. Technol. 2004, 52, 1-5.

Lappalainen M, Pitkänen I, Heikkilä H, Nurmi J. 2006. Melting behaviour and evolved gas analysis of xylose. Journal of Thermal Analysis and Calorimetry 84:367-376.

Lee JW. 2010. PhD dessertation "Investigation of thermal decomposition as the cause of the loss of crystalline structure in sucrose, glucose, and fructose" University of Illinois, Urbana-Champaign.

Lee JW, Thomas LC, Schmidt SJ. 2011a. Investigation of the heating rate dependency associated with the loss of crystalline structure in sucrose, glucose, and fructose using a thermal analysis approach (Part I). Journal of Agricultural and Food Chemistry, (59):684-701.

Lee JW, Thomas LC, Jerrell J, Feng H, Cadwallader KR, Schmidt SJ. 2011b. Investigation of thermal decomposition as the kinetic process that causes the loss of crystalline structure in sucrose using a chemical analysis approach (Part II). Journal of Agricultural and Food Chemistry, (59):702-712.

Lee JW, Thomas, LC, Schmidt SJ. 2011c. Can the thermodynamic melting temperature of sucrose, glucose, and fructose be measured using rapid-scanning DSC? Journal of Agricultural and Food Chemistry, 59 (7): 3306–3310.

Lee JW, Thomas LC, Schmidt SJ. 2011d. Effects of heating conditions on the glass transition parameters of amorphous sucrose produced by melt-quenching. Journal of Agricultural and Food Chemistry, 59 (7): 3311–3319.

Lee JW, Schmidt SJ. 2014. Personal communication.

Lee T and Lin YS. 2007. Dimorphs of sucrose. International Sugar Journal, 109 (1303):440-445.

Liang B, Hartel RW, Berglund KA. 1989. Effects of raffinose on sucrose crystal growth kinetics and rate dispersion. AICHE J. 35(12):2053-7

Lin YS. 2007. Master thesis "Two Conformational Polymorphs of Sucrose". National Central University.

Liu, Y.; Bhandari, B.; Zhou, W. Glass transition and enthalpy relaxation of amorphous food saccharides: a review. J. Agric. Food. Chem. 2006, 54, 5701-5717.

LOT-QuantumDesign GmbH. Available from: http://www.lao.cz/data/ke-stazeni/MicroXCT_200_eu_1_.pdf. Lasted accessed Nov, 30th 2015.

Magne V, Mathlouthi M, Robilland B, Magne M, Mathlouthi B. 1998. Determination of some organic acids and inorganic anions in beet sugar by ionic HPLC. Food Chem 61(4):449–53.

Magoń A, Wurm A, Schick C, Pangloli P, Zivanovic S, Skotnicki M, Pyda M. 2014. Heat capacity and transition behavior of sucrose by standard, fast scanning and temperature-modulated calorimetry. Thermochimica Acta, 589: 183-196. Article reprinted in 2015, Thermochimica Acta, 603, 149-161.

Marsili RT, Miller N, Kilmer GJ, Simmons RE. 1994. Identification and quantitation of the primary chemicals responsible for the characteristic malodor of beet sugar by purge-and-trap GC-MS-OD techniques. J Chromatogr Sci 32(5):165–71.

Mathlouthi M and Koenig JL. 1986. Vibrational spectra of carbohydrates. Adv Carbohydr Chem Biochem. 44:7-89.

Mathlouthi M and Roge B. 2012. Melting And Crystallization of Sugars: a structural approach. 2012 IFT Annual Meeting presentation. Las Vegas, NV.

Mathlouthi M, Reiser P, editors. (1995) Sucrose properties and applications. 1st ed. Bishopbriggs: Blackie Academic and Professional.

Mauch W.; Asseily S. Sorption characteristics of fructose, glucose, and sucrose melts subjected to various degrees of heat treatment. Forschungsber.-Inst. Zuckerind. Berlin 1975, 1, 127.

Maulny A. 2003. Co-crystallisation of sugars. Ph.D. Thesis, Department of Chemistry, University of Hull, Hull, UK.

Metscher BD. 2013. Biological applications of X-ray microtomography: imaging micro- anatomy, molecular expression and organismal diversity. Microsc Anal 27:13–16.

Miller MM. 2001. PhD dissertation "The effect of applied fields on crystallisation". Brunel University.

Mohomed K. 2013. Thermogravimetric Analysis Theory, Operation, Calibration and Data Interpretation (Instrumental training presentation). TA Instruments—Waters LLC.

Monte WC, Maga JA. 1982. Flavor chemistry of sucrose. Sugar Technol Rev 8(3):181–204.

Morel du Boil PG. 1992. Theanderose - A contributor to c-axis elongation in cane sugar processing. Int.Sugar J. 94(1120):90-4.

Morel du Boil PG. 1996. Theanderose – A characteristic of cane sugar crystals. Proc S Afr Sug Technol Ass 70140-4.

Morel du Boil PG. 1997. Theanderose - Distinguishing cane and beet Sugars. Int.Sugar J. 99(1179):102-6.

Morgan M. 1999. SUGAR, SUGAR / Cane and beet share the same chemistry but act differently in the kitchen. Available online http://www.sfgate.com/news/article/SUGAR-SUGAR-Cane-and-beet-share-the-same-2939081.php. Lasted accessed July 3, 2013.

Mullin JW. Crystallization, 4th ed.; Elsevier Butterworth-Heinemann: Oxford, UK, 2001; 594 pp.

Nawrocka A, Lamorska J. 2013. Determination of food quality by using spectroscopic methods. Advances in Agrophysical Research, pages 347–367.

Okuno M, Nakai N, Kishihara S. 2003. Melting Point of Sucrose Crystals Prepared in Various Solvents. Proceedings of research Society of Japan Sugar Refineries' Technologists, (51):1-6.

Örsi, F. Kinetic studies on the thermal decomposition of glucose and fructose. J. Therm. Anal. 1973, 5, 329-335.

Parliment T, Kolor M, Maing I. 1977. Identification of the major volatile components cooked beets. J Food Sci 42(6):1592–3.

Pasztor AJ. 1997. Thermal analysis techniques in Handbook of Instrumental Techniques for Analytical chemistry, Settle FA ed. rentice Hall PTR, Upper Saddle River, New Jersey, USA, 1997, pp.909-917 (993pp).

Pihlsgard P. 1997. The properties of sugar focusing on odours and flavours—a literature review. SIK Rapport (634).

Potter R, Mansel R, inventors; University of South Florida, assignee. 1992 Jul. 7, 1992. Assay for the detection of beet sugar adulteration of food products. U.S. patent 5128243.

Powers HEC. 1956. Growth of sucrose crystals. Nature, 178:139-140.

Powers HEC. 1958. Sucrose crystal inclusions. Nature, 182:715-717.

Reynhardt EC. 1990. An NMR, DSC and X-ray investigation of the disaccharides sucrose, maltose and lactose, Molecular Physics: An International Journal at the Interface Between Chemistry and Physics, 69:6, 1083-1097.

Richards GN (1986). Initial steps in thermal degradation of sucrose. Int. Sugar J. 88, 145-148.

Richards GN, Shafizadeh F (1978). Mechanism of thermal degradation of sucrose: A preliminary study. Aust. J. Chem. 31, 1825-1832.

Roos YH, Franks F, Karel M, Labuza TP, Levine H, Mathlouthi M, Reid D, Shalaev E, Slade L. 2012. Comment on the melting and decomposition of sugars, Journal of Agricultural and Food Chemistry, 60: 10359–10362.

Roos YH, Karel M, Labuza TP, Levine H, Mathlouthi M, Reid D, Shalaev E, Slade L. 2013. Melting and Crystallization of Sugars in High-Solids Systems, Journal of Agricultural and Food Chemistry, 61:3167-3178.

Roos, YH. Food components and polymers. In Phase Transitions in Foods, 1st ed.; Taylor, S. L., Ed.; Academic Press: San Diego, CA, 1995; Chapter 5, pp 109-156.

Saavedra-Leos MZ, Grajales-Lagunes A, González-García R, Toxqui-Terán A, Pérez-García SA, Abud-Archila MA, Ruiz-Cabrera MA. 2012. Glass Transition Study in Model Food Systems Prepared with Mixtures of Fructose, Glucose, and Sucrose. Journal of Food Science, 77:5, 118-126.

Sakamoto, K.; Kishihara, S.; Miura, K.; Sakuda, H.; Koizumi, Y.; Tachibana, Y.; Kataoka-Shirasugi, N. Browning of granulated sugar on heating below melting point. Proc. Res. Soc. Jpn. Sugar Refin. Technol. 2006, 54, 15-21.

Schiweck H, Clarke M, Pollach G. 1994. Sugar. Ullmann's Encyclopedia of Industrial Chemistry 34:557-628.

Schmidt SJ, Thomas LC, Lee, JW. 2012. Response to comment on the melting and decomposition of sugars. Journal of Agricultural and Food Chemistry, 60: 10363-10371.

Scholl SK. 2014. PhD dessertation "Investigation of glucose hydrate formation and loss: parameters, mechanisms, and physical stability" University of Illinois, Urbana-Champagin.

Sgualdino G, Aquilano D, Fioravanti R, Vaccari G, Pastero L. Growth kinetics, adsorption and morphology of sucrose crystals from aqueous solutions in the presence of raffinose(2005). Crystal Research and Technology, 40 (10-11), pp. 1087-1093.

Sgualdino G, Aquilano D, Pastero L, Vaccari G. Face-by-face growth of sucrose crystals from aqueous solutions in the presence of raffinose II: growth morphology and segregation. J. Cryst. Growth 2007, 308, 141–150.

Shah SV, Chakradeo YM. 1936. A note on the melting point of cane sugar.   Journal of Current Science. P652-3

Shallenberger RS. 1978. Intrinsic chemistry of fructose. Pure and Applied Chemistry 50:1409-1420.

Šimkovic I, Šurina I, Vričan M. 2003. Primary reactions of sucrose thermal degradation. Journal of Analytical and Applied Pyrolysis, 70 (2), pp. 493-504.

Standard for sugars. CODEX STAN 212-1999 (Amd. 1-2001). P 1-6. Available from http://famis.comesa.int/pdf/Sugar_FDHS_6_CXS_212.pdf. Lasted accessed 3rd Mar, 2014.

Sugar & Sweeteners. USDA 2012. Available from http://www.ers.usda.gov/topics/crops/sugar-sweeteners/background.aspx#.UwUVghxRSX0. Lasted accessed 3rd Mar, 2014.

Suryanarayana C, Norton MG. 1998. X-ray Diffraction: A Practical Approach. New York NY: Plenum Press. 281 p.

TA Instruments DSC Brochure 2012. Available from http://www.tainstruments.com/wp-content/uploads/2012-DSC-Brochure-r1.pdf. Lasted accessed 12th Mar 2016.

TGA Q Series Getting Started Guide. Revision K. 2006. by TA Instruments—Waters LLC.

The University of Liverpool. 2000. Available from: http://www.matter.org.uk/diffraction/geometry/reciprocal_lattice.htm. Lasted accessed 12th Mar, 2016.

Thomas JM, Williams JO. 1967. Lattice imperfections in organic solids. Part 2. Sucrose. Transactions of the Faraday Society, 63: 1922-1928.

Thomas LC, Schmidt SJ 2010. Chapter 31, Thermal Analysis. In: Nielsen SS, editor. Food Analysis. 4th ed. New York, NY: Springer. pp 555-571.

Ubbelohde, A. R. Melting and Crystal Structure; Clarendon Press: Oxford, UK, 1965; 325 pp.

Urbanus BL, Cox GO, Eklund EJ, Ickes CM, Schmidt SJ, Lee S. 2014a. Sensory Differences Between Beet and Cane Sugar Sources. J. Food Sci. 79:1763–1768.

Urbanus BL, Schmidt SJ, Lee S. 2014b. Sensory Differences between Product Matrices Made with Beet and Cane Sugar Sources. J. Food Sci. 79:2354-2361.

Vaccari G, Mantovani G. 1995. Sucrose crystallization. In: Mathlouthi M, Reiser P, editors. Sucrose properties and applications. 1st ed. Bishopbriggs: Blackie Academic and Professional. p 33-72.

Vaccari G. 2010 The Sugar Crystal: A Chameleon. 2010 SPRI Award Presentation. Proc. of the SPRI 2010 Conference on Sugar Processing, New Orleans, LA.

Vaccari G., Mantovani G., Sgualdino G., Tamburini E., Aquilano D. Fructo-oligosaccharides and sucrose crystal growth morphology I. Experimental growth habits.(1999) Zuckerindustrie, 124 (1), pp. 34-39.

Vaccari G., Sgualdino G., Tamburini E., Lodi G., Aquilano D., Mantovani G. Fructo-oligosaccharides and sucrose crystal growth morphology II. Verification of nonsucrose absorption through chromatographic analysis and X-ray diffractometry (1999) Zuckerindustrie, 124 (7), pp. 536-540.

Vandenabeele P. 2013. Practical Raman spectroscopy: an introduction. John Wiley & Sons.

Vavrinecz G. 1965. Atlas of Sugar Crystals. Verlag Dr. A. Bartens, Berlin, Germany.

Wunderlich B. 1990a. Thermometry. In: Wunderlich B, author. Thermal Analysis. San Diego, CA: Academic Press. p 79-121.

Wunderlich B. 1990b. Differential thermal analysis. In: Wunderlich B, author. Thermal Analysis. San Diego, CA: Academic Press. p 123-218.

Yu L, Reutzel SM, Stephenson GA. 1998. Physical characterization of polymorphic drugs: an integrated characterization strategy. PSTT 1(3), 118-127.

Yuan JP, Chen F. 1999. Simultaneous separation and determination of sugars, ascorbic acid and furanic compounds by HPLC-dual detection. Food Chem. 64, 423-427.

Yuan JP, Guo SY, Li L (1996). Simultaneous determination of sugars and their degradation 649 products 5-HMF by HPLC. Chinese Journal of Analytical Chemistry 24:57-60.

2.9 Figures and Tables
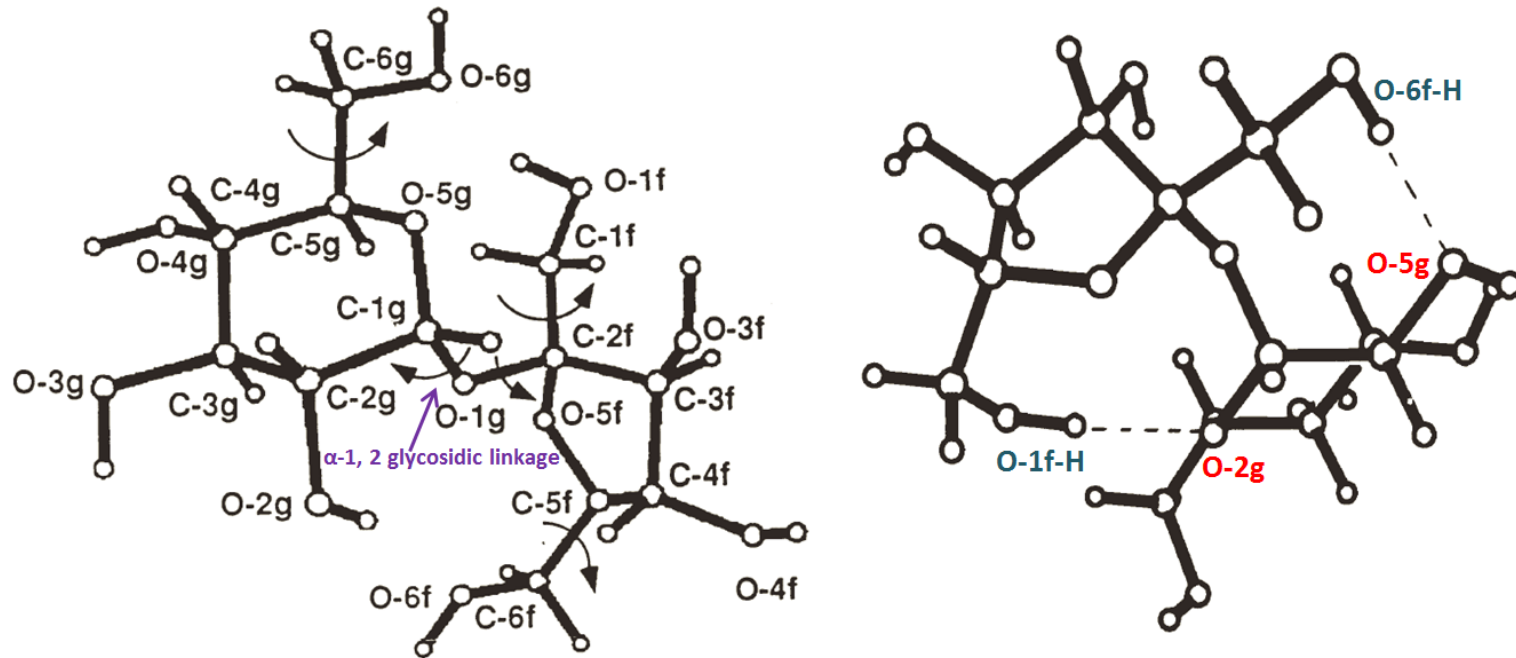
Figure 2.1 The chemical structure of sucrose (adapted from Perez, 1995).
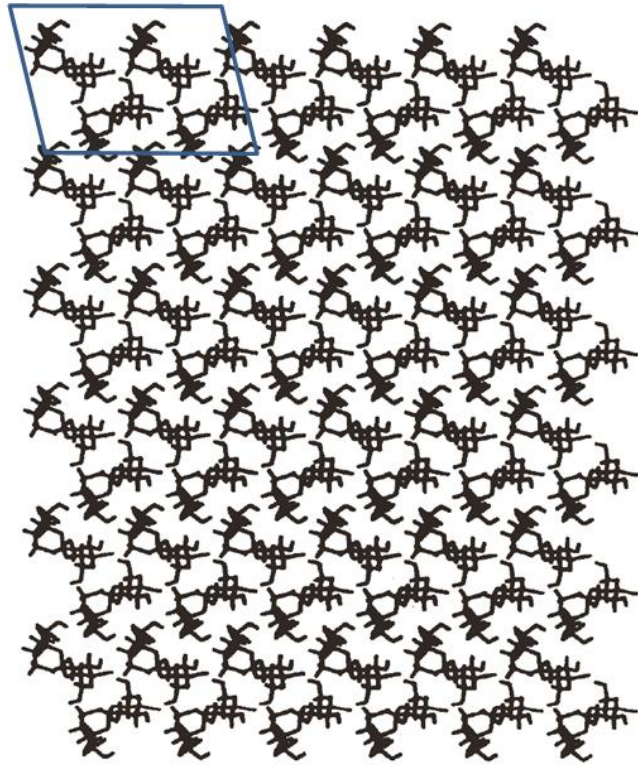
Figure 2.2 Packing pattern (labeled with unit cell) of sucrose (Immel, 2003)
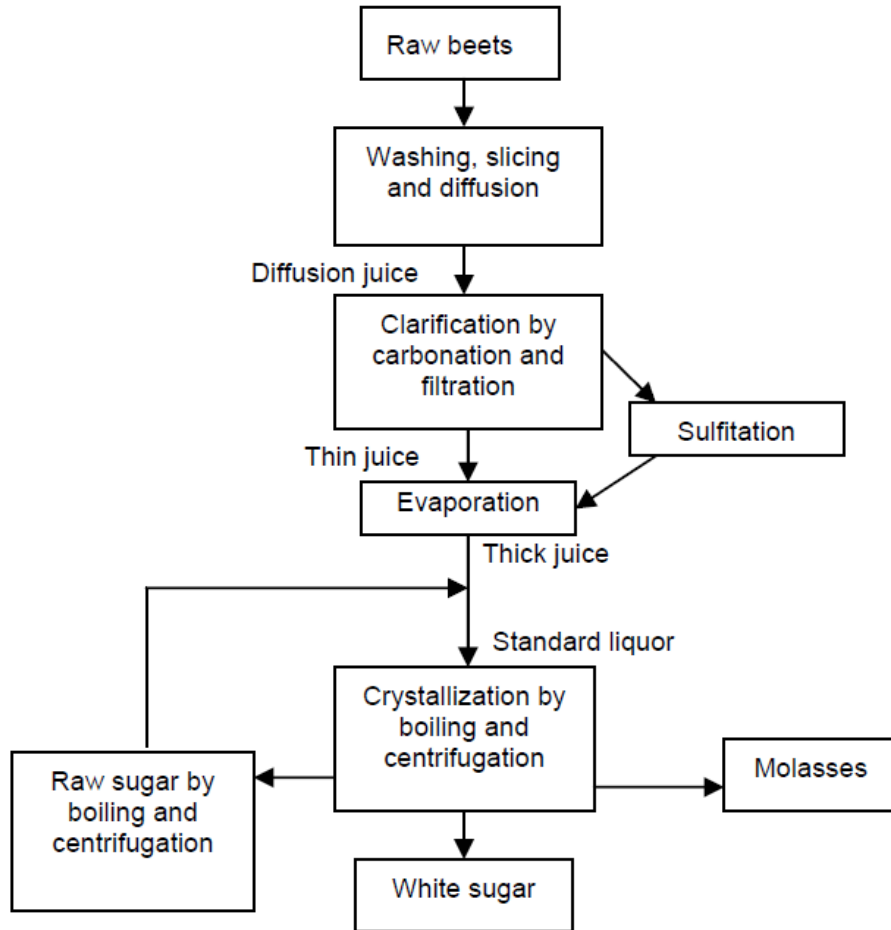
Figure 2.3 Process flowchart for the production of white refined beet sugar in the U.S. (Clarke and others 1997).
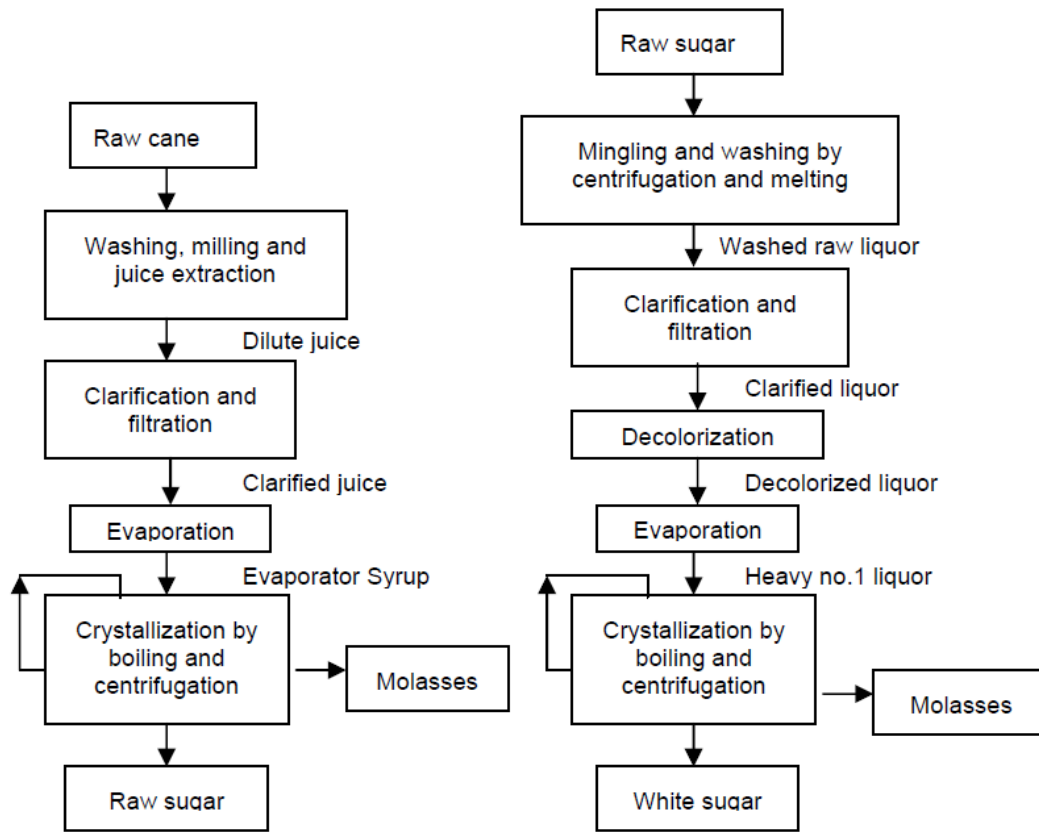
Figure 2.4 Process flowchart for the production of white refined cane sugar in the U.S. (Clarke and others 1997).
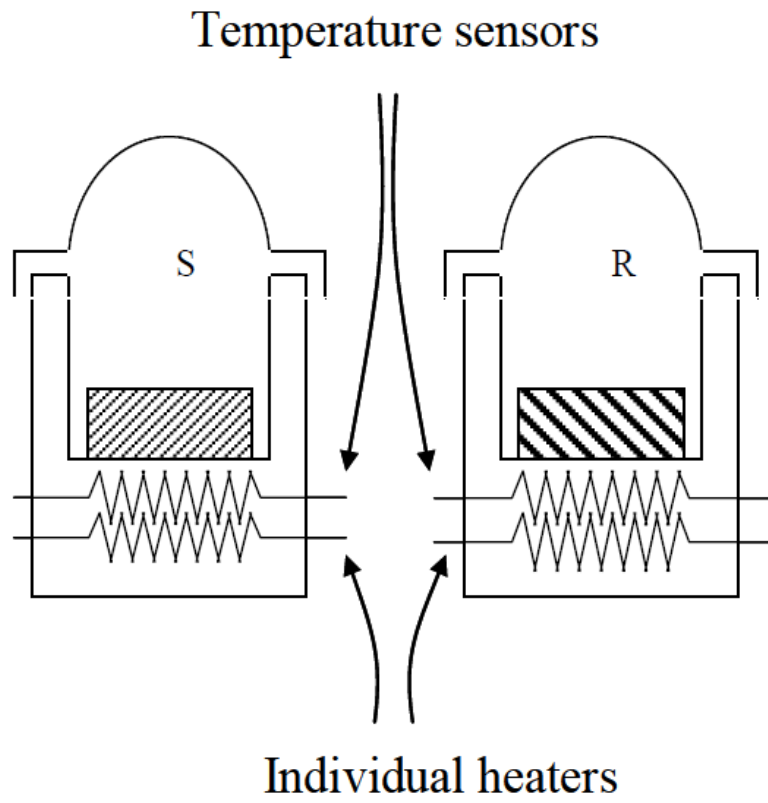
Figure 2.5 Schematic diagram of a power compensation DSC (Haines and Wilburn, 1995).
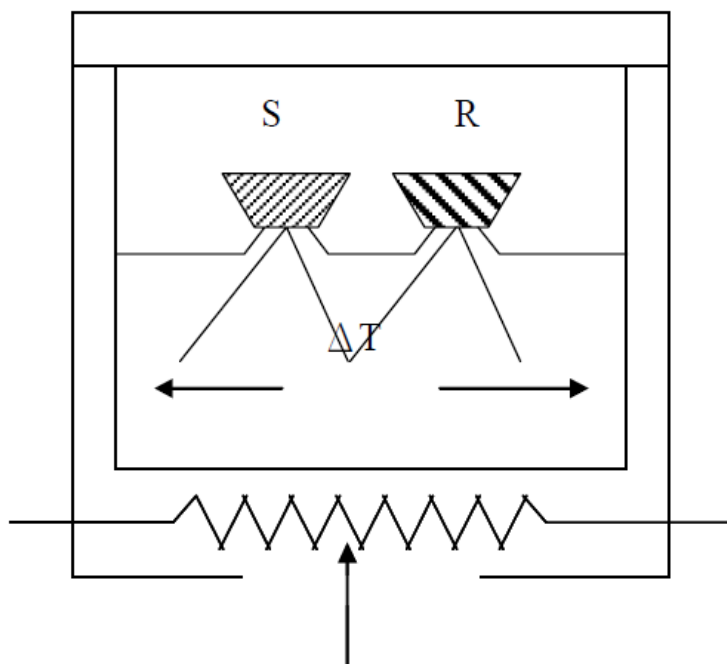
Single heat source

Figure 2.6 Schematic diagram of a typical heat-flux DSC (Pasztor, 1997)
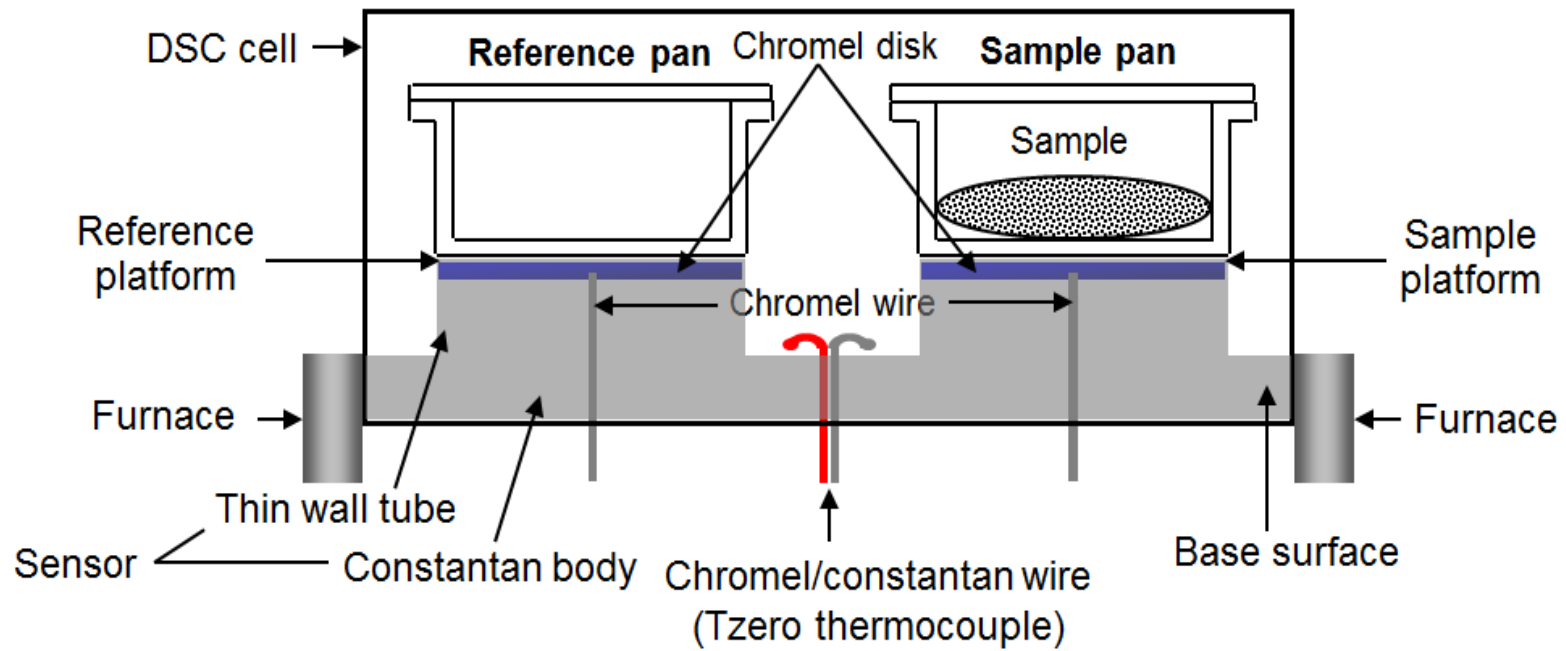
Figure 2.7 Schematic diagram of a heat-flux DSC (Lee, 2010)
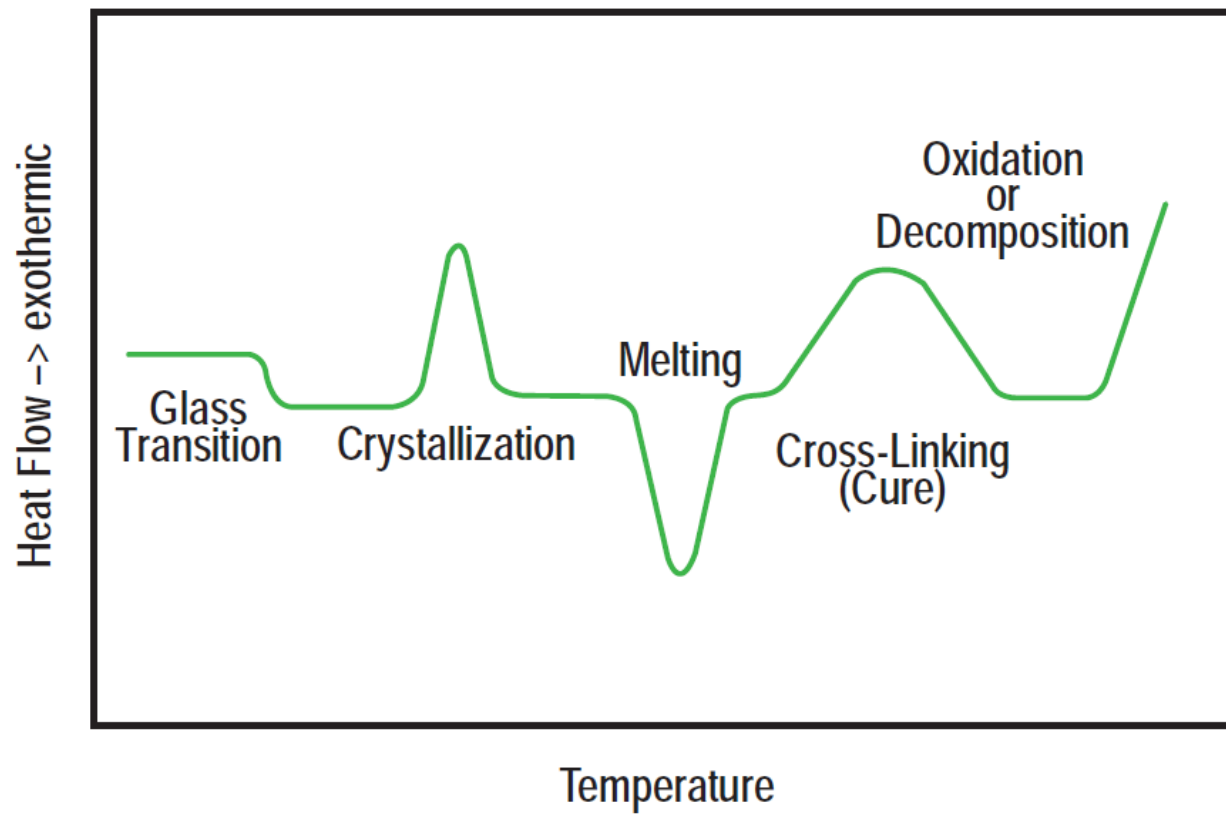
Figure 2.8 Illustration for the common information about material transitions in DSC thermal profile (TA Instruments DSC Brochure 2012)
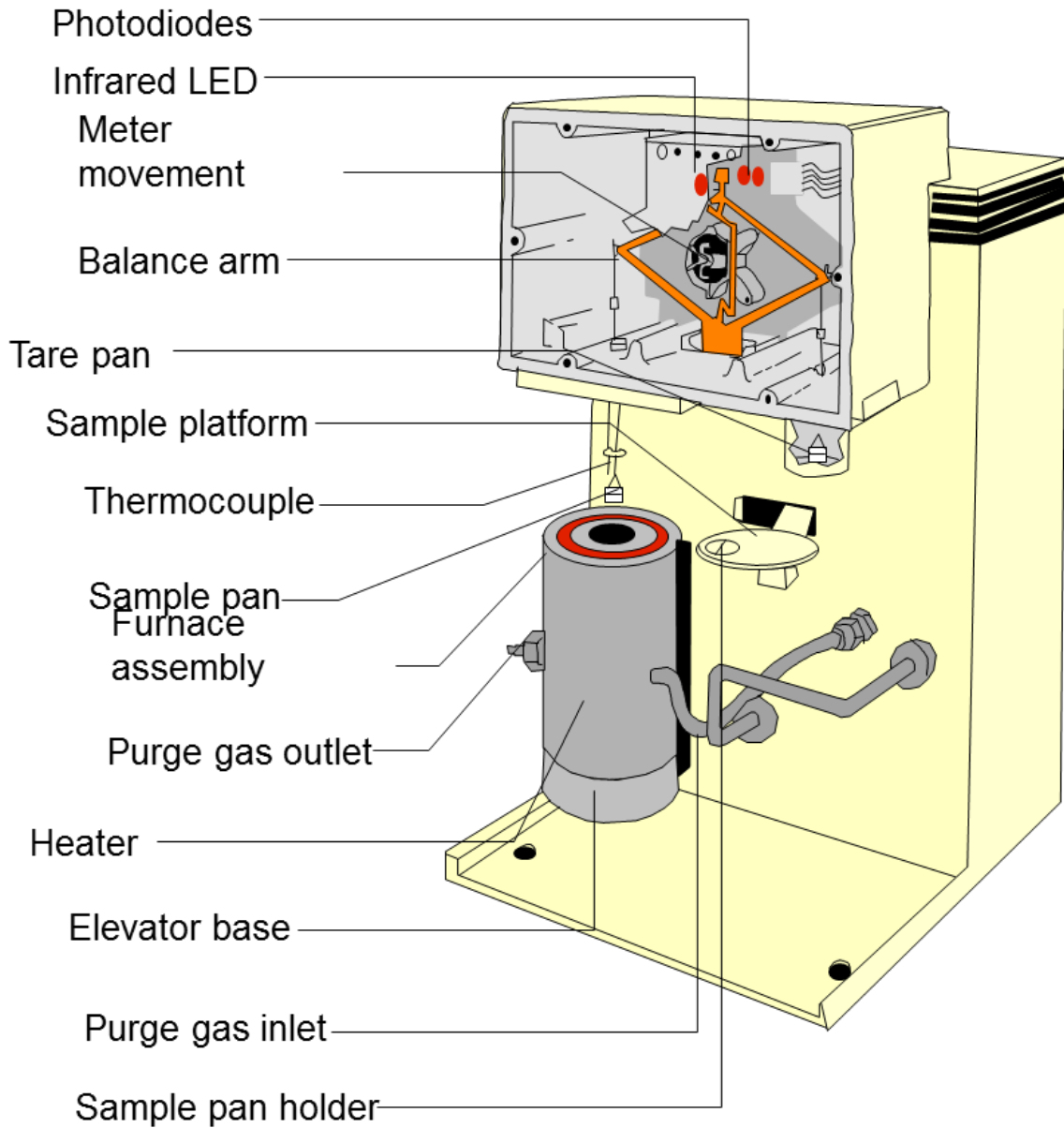
Figure 2.9 Schematic diagram of TA Q500 TGA (Mohomed 2013).
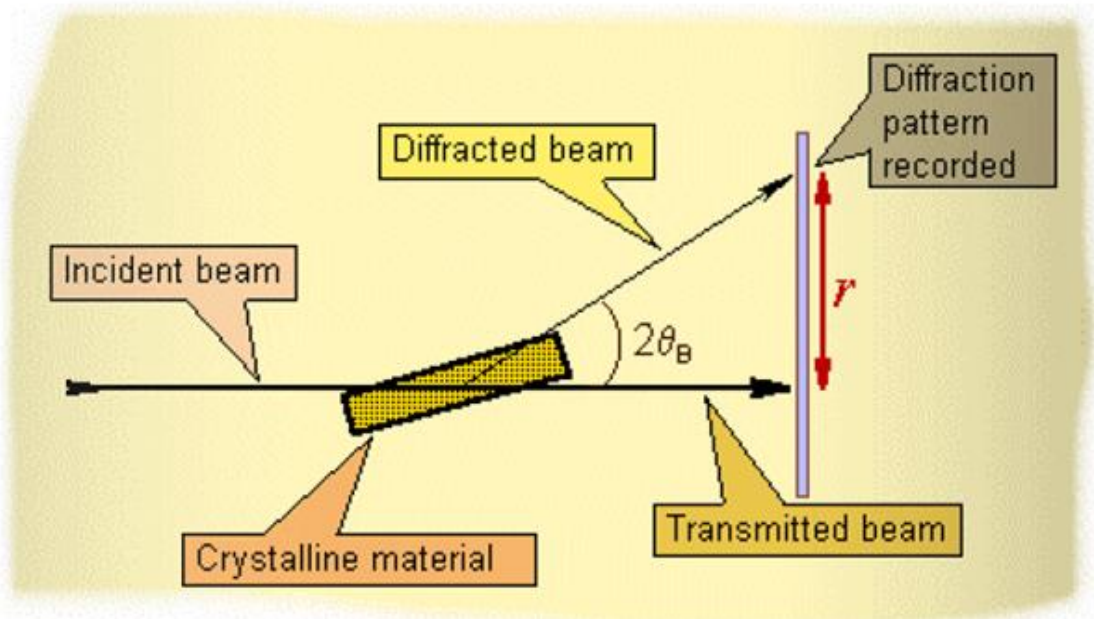
Figure 2.10 Schematic experimental setup for PXRD (University of Liverpool 2000).
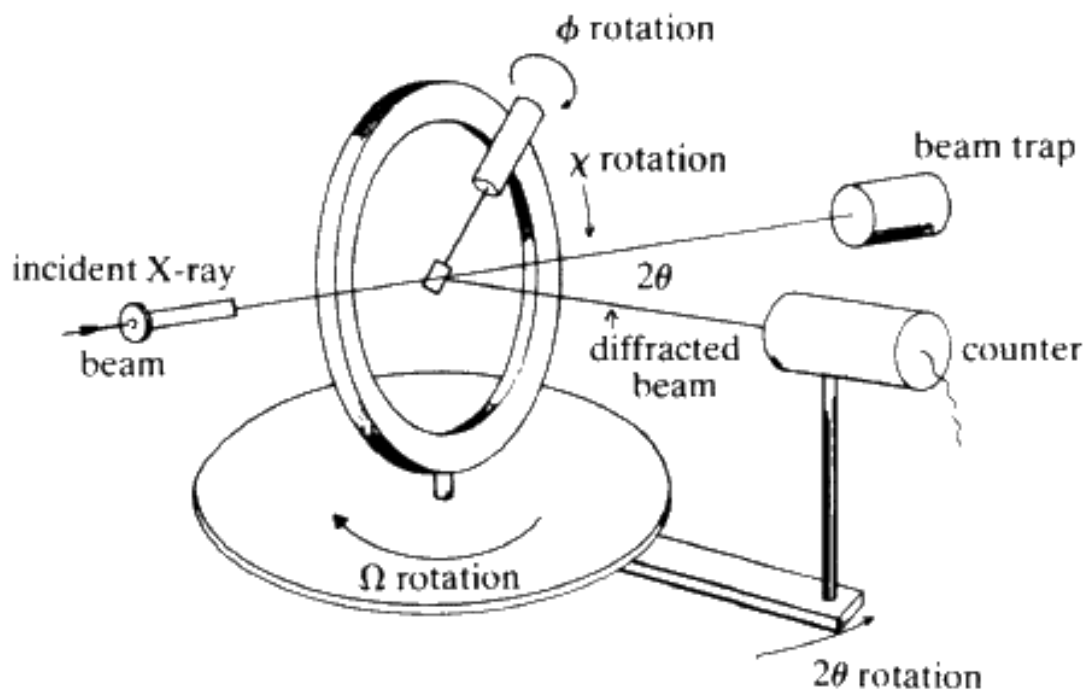
Figure 2.11 Schematic experimental setup for SXRD (Clark and Dutrow 2015).
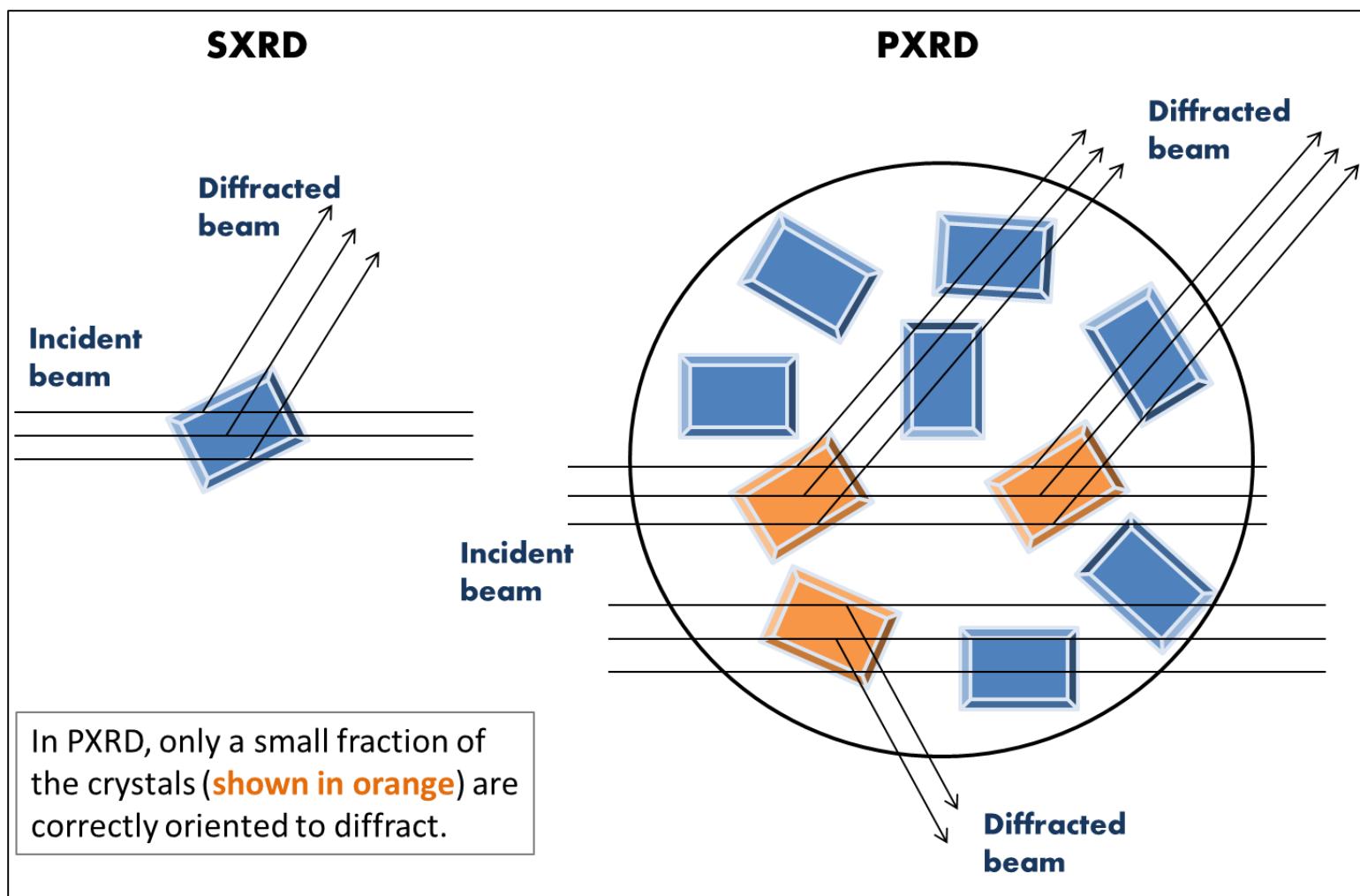
Figure 2.12 The major difference between SXRD and PXRD

Figure 2.13 MicroXCT-400 High Resolution 3D X-ray Imaging System (from: LOT-QuantumDesign GmbH).
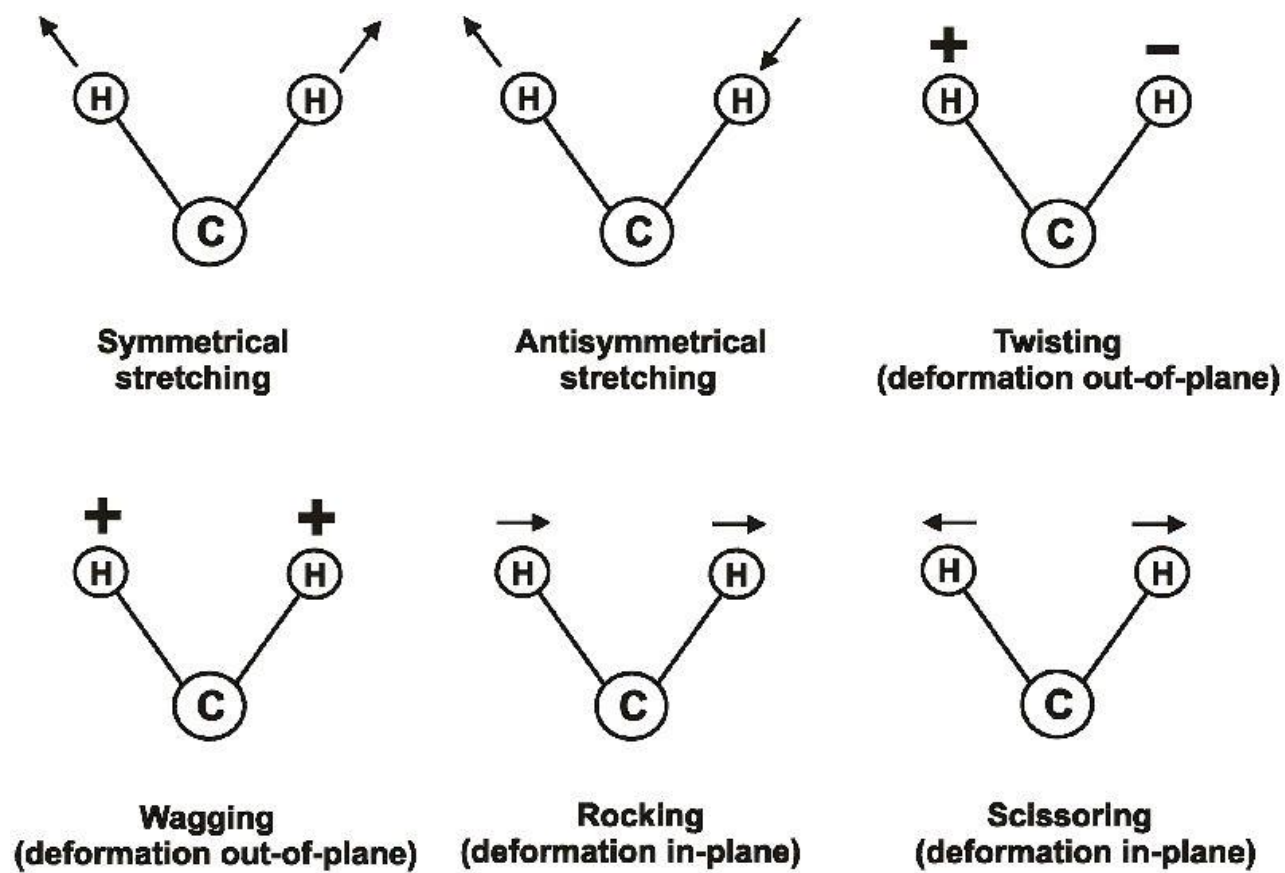
Figure 2.14. Different modes of molecular vibrations for a three-atom molecule (Nawrocka and Joanna 2013).
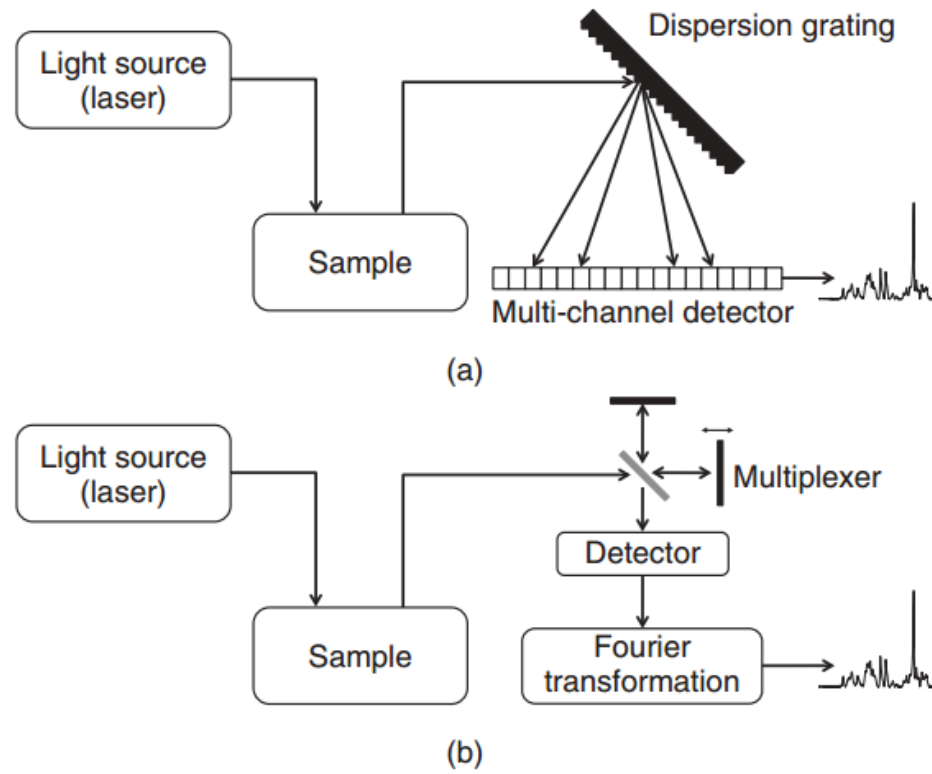
Figure 2.15. Diagram of dispersive Raman (a) and FT-Raman instruments (b) (Vandenabeele, 2013)

Table 2.1 Sucrose purity reported in the scientific and technical literature.

Reference	Purity (% of sucrose)	Source of sucrose
Dowling 1990	>99.8%	Beet and cane white refined sugar
Potter and Mansel 1992	99.96%	White refined sugar, SNS[a]
Schiweck and Clarke 1994	99.8%	Beet and cane white refined sugar
Vaccari and Mantovani 1995	99.9%	White refined sugar, SNS[a]
Morgan 1999	99.95%	Beet and cane white refined sugar
Clarke 2000	99.9%	White refined sugar, SNS[a]
Colonna and others 2000	99.96%	White refined sugar, SNS[a]
Maulny 2003	99.96	White refined sugar, SNS[a]
Maulny 2003	96 to 99%	Raw sugar, SNS[a]
Asadi 2007	99.96%	White refined sugar, SNS[a]
Asadi 2007	99.95%	Beet and cane white refined sugar
Bensouissi and others 2007	99.7-99.8%	White refined sugar, SNS[a]
Sigma-Aldrich Product information	≥99.5%	Cane GC grade
China GB13104-2005	99.5%	Chinese cane white granulated sugar
China GB13104-2005	97.9%	Chinese cane soft sugar
China GB13104-2005	89%	Chinese cane brown sugar

[a]SNS – source not specified

Table 2.2 Crystal structure of sucrose obtained by neutron and X-ray diffraction (Mathlouthi, 1995).

	Neutron	X-ray
a (Å)	10.8633 (5)	10.8648 (15)
b(Å)	8.7050 (4)	8.7028 (12)
c(Å)	7.7585 (4)	7.7578 (11)
β(°)	102.945 (6)	102.956 (15)
Cell volume	715	
Space group	$P2_1$	
Z	2	
D (calc)	1.590 Mgm^{-3}	

Table 2.3 Wavenumbers for some molecular groups (Vandenabeele, 2013)

Vibration		Wavenumbers (cm^{-1})	Raman-intensity[1]
O–H stretch	ν(O–H)	3650–3000	w
N–H stretch	ν(N–H)	3500–3300	m
C–H stretch of alkynes	ν($\equiv$C–H)	3350–3300	w
C–H stretch of alkenes	ν(= C–H)	3100–3000	s
C–H stretch of alkanes	ν(–C–H)	3000–2750	s
C$\equiv$C stretch of alkynes	ν(C$\equiv$C)	2250–2100	vs
C=C stretch of alkenes	ν(C=C)	1750–1450	vs–m
C–C stretch of aliphatic chains and cycloalkanes	ν(C–C)	1150–950	s–m
CC stretch of aromates [(substituted) benzene molecules]	ν(CC)	1600, 1580, 1500, 1450, 1000	s–m m–w s
C=O stretch	ν(C=O)	1870–1650	s–w
Antisymmetric C–O–C stretch	ν_{asym}(COC)	1150–1060	w
Symmetrical C–O–C stretch	ν_{sym}(COC)	970–800	s–m
CH$_2$ bending vibrations, antisymmetric CH$_3$ bend	δ(CH$_2$), δ_{asym}(CH$_3$)	1470–1400	m

Chapter 3: Differences in the thermal behavior of beet and cane sucrose sources

3.1 Abstract

Two main crops are utilized for production of sucrose (i.e., table sugar) - sugarbeet and sugarcane. Despite the nearly identical chemical composition of the two sucrose sources, some differences in aroma and performance in products have been reported. However, to date, little published research was found that explores the thermal property differences between these two sources of sucrose. Thus, the objective of this research was to investigate the thermal behavior of beet and cane sucrose. To accomplish this purpose, three thermal methods were employed, Differential Scanning Calorimetry (DSC), Thermal Gravimetric Analysis (TGA), and heating in an ampule. DSC thermograms of seventeen beet and thirty cane sucrose samples were obtained at 10°C/min. A subset of samples were also analyzed at 1, 5, and 25°C/min for heating rate dependency assessment. A distinct difference was observed between the DSC thermograms of beet and cane sucrose at 10°C/min. All seventeen beet samples exhibited only one large endothermic DSC peak, with an average onset temperature (Tmonset) of 188.41±0.37; whereas twenty-six of the thirty cane samples exhibited two endothermic DSC peaks, one small peak proceeded by one large peak, with average Tmonset values of 153.80±6.05 and 187.39±1.72, respectively. The four remaining cane samples, which contained either high ash content or processing added impurities, exhibited only one large endothermic DSC peak, similar to the DSC thermograms for beet sucrose sources. All beet and cane sucrose samples studied exhibited heating rate dependency; however, the extent of dependency varied widely as a function of both heating rate and sucrose sample category type. No clear TGA weight loss trend was observed between the three sucrose samples examined, analytical grade Sigma cane, US

beet, and US cane; however, during the ampule heating study, the thermal stability, in order

from least to most stable, was: analytical grade Sigma cane << US cane < US beet. Future

studies will focus on ascertaining the underlying cause(s) of the thermal behavior differences

between beet and cane sucrose sources. Understanding the thermal differences between beet

and cane sugars and how to account for these differences during processing is of value to the

food industry, as these sugars are often used interchangeably based on market price.

3.2 Introduction

Sucrose, commonly termed sugar or table sugar, is an important commodity worldwide

and is produced using mainly sugarbeet and sugarcane plant sources. Though both refined

white beet and cane sugars commonly contain greater than 99% sucrose (Table 2.1),

differences in their instrumental aroma profile (Acree and others 1976; Parliment and others

1977; Monte and Maga 1982; Marsili and others 1994; Pihlsgard 1997; Magne and others 1998),

sensory properties (Urbanus and others 2014a and b), and product performance (Urbanus and

others 2014a and b) have been reported in the literature. Some of the differences between

beet and cane sugars are due to the plant materials themselves, while others are due to

processing differences. For example, due to the difference in their CO_2 fixation pathways,

sugarbeet, a C3 plant, and sugarcane, a C4 plant, exhibit a difference in their carbon isotope

ratio (C_{13} to C_{12}), where the ratio is approximately 25% in beet sugar and 11% in cane sugar

(Bubník and others 1995). The selective rejection of C_{13} is greater in the C3 pathway than in the

C4 pathway (Ferneluis 1984). Two other differential plant material markers are raffinose and

theanderose. Though raffinose is present in both sugar sources, levels are higher in beet sugar

compared to cane sugar, as quantified using chromatography (Vaccari and Mantovani, 1995;

Morel du Boil 1997; Eggleston 2004). Theanderose is present only in cane sugar and is thought to be a natural constituent of the sugarcane plant (Morel du Boil 1996). Both raffinose and theanderose affect sugar crystal growth and morphology (Liang and others 1989; Morel du Boil 1992). A number of studies conducted by the Sugar Processing Research Institute, Inc. (SPRI, New Orleans, LA) have focused on the identification of and comparison between beet and cane sugars in regards to their odor, color, pH, ash, invert sugar, and polysaccharide content (Godshall 1986, 1994, and 2013, Appendix A).

The crystallization and melting behavior of sucrose has been under investigation for a number of years. However, one aspect of the melting behavior of sucrose that needed further study was the wide variation in melting temperature reported in the literature for sucrose, as well as other sugars, such as glucose and fructose. Though a consistent, uniform melting temperature is expected for a crystalline material, the melting temperature for sucrose has been found to vary widely, as reported in earlier, as well as more recent studies. Examples of early studies include work by Shah and Chakradeo (1936) and Powers (1956 and 1958). Shah and Chakradeo (1936) reported a sucrose melting point of 182°C, but also gave a table of melting point values from the literature ranging from 160 to 189°C. These authors mentioned a number of possible factors responsible for the reported melting point variation, including "slow heating and consequent partial decomposition into glucose and fructozone or even partial hydrolysis into glucose and fructose due to the presence of traces of water," differences in the melting point determination methods, and sucrose purity. Based on their experiments, Shah and Chakradeo (1936) concluded that the sucrose melting point was dependent upon the purity of the sample alone. Powers (1956 and 1958) reported the presence of water, in the form of

mother syrup (or liquor) inclusions, inside the sucrose crystal structure and in his 1958 article implicated these inclusions as an explanation for the widely varying melting point of sucrose reported in the literature, given in the article as 160 to 186°C.

In addition to these studies, over the years, researchers have offered a number of possible explanations for the wide range of sucrose melting temperatures, including impurities (Hirschmüller 1953; Kamoda 1960; Beckett and others 2006), polymorphism (Kishihara and others 2001; Lee and Lin 2007; Lee and Chang 2009), superheating (Tammann 1910; Hellmuth and Wunderlich 1965; Wunderlich 1990b; Magoń and others 2014), liquefaction (used to explain the large variation observed in the melting parameters for isomerizable materials, such as fructose, glucose, and galactose) (Tombari and others 2007), and thermal decomposition and/or mutarotation (Hurtta and others 2004b; Lappalainen and others 2006) in addition to melting. However, according to Lee and others (2011a), these explanations do not completely account for the observed variation. Rather, Lee and others (2011a and b) demonstrated that analytical grade Sigma cane sucrose melting parameters tended to increase strongly with increasing heating rate, leading to their conclusion that the initial loss of crystalline structure in sucrose is associated with the kinetic process of thermal decomposition.

Another unique observation, related to the wide range of sucrose melting temperatures, is the appearance of a small endothermic peak prior to the large endothermic peak observed in some sucrose DSC thermograms. The presence of this small DSC endothermic peak in sucrose can be observed in a number of recent articles, which have included an example DSC thermogram (e.g., Lee and others 2011a and b; Saavedra-Leos and others 2012; Mathlouthi and Roge; 2012; Magoń and others 2014; Kinugawa and others 2015). As an example, a DSC

thermogram of analytical grade Sigma cane sucrose, at a heating rate of 10 K/min, from Magoń

and others (2014, Figure 6 therein) is provided in Figure 3.1. Magoń and others (2014) refer to

the two endothermic DSC peaks as minor and major peaks and report Tmpeak values of 430 K

(157°C) and 465 K (192°C), respectively (Tmonset values at 10 K/min estimated from Figure 13

in Magoń and others (2014) were 426 K [153 °C] and 458 K [185 °C]). A variety of factors have

been reported to affect the presence and magnitude of the small peak. Beckett and others

(2006) reported that the appearance of the small endothermic peak is highly dependent on the

purity of the sucrose. For example, the magnitude of the small peak decreased when the

sucrose was recrystallized in the presence of KCl. They also observed that the appearance of

the small peak was affected by the recrystallization conditions. For example, by introducing a

stirring step or increasing the recrystallization temperature, the magnitude of the small peak

decreased. Kawakami and others (2006) reported that the DSC thermograms of recrystallized

amorphous sucrose also exhibited two peaks, with the peaks varying in magnitude depending

on the %RH and temperature of the recrystallization conditions. However, upon annealing of

the recrystallized amorphous samples, the magnitude of the first (small) peak decreased and

ultimately disappeared.

A number of hypotheses have been suggested in the literature to explain the presence of

the small endothermic DSC peak. These hypotheses were grouped into six categories and are

summarized in Table 3.1. Though there may be merit to some of these hypotheses, preliminary

research from our laboratory (Lu and others 2013) focused on a new factor that appears to

substantially influence the presence and magnitude of the small endothermic DSC peak in

sucrose – the plant source from which the sucrose was extracted. Little previous research was

found tying the existence of the small peak to the plant source of the sucrose. Also, little previous research was found that mentioned studying the melting behavior of beet sucrose (Kamoda 1960; Beckett and others 2006). Unfortunately, most studies do not report the plant source of the sucrose used. Therefore, the objective of this research was to investigate the thermal behavior differences between beet and cane sucrose sources using thermal analysis methods.

3.3 Materials and Methods

Materials

Two analytical grade crystalline sucrose samples were purchased from Sigma-Aldrich Co. (St. Louis, MO; #S0389, ≥ 99.5%) and Fisher Scientific Inc. (Pittsburgh, PA; S5-500; Certified ACS, purity not reported). Both analytical grade sucrose samples are isolated from canesugar. Product information for the analytical grade sucrose samples, provided by each company, are included in Appendix C. Ten beet and 10 cane sucrose samples were obtained from SPRI (New Orleans, LA). Origin information for these sugars is provided in Appendix D. One beet and one cane sample were obtained directly from United Sugar (US) Corporation (Clewiston, FL). The remaining beet and cane samples were obtained from markets in the United States and abroad. One Chinese cane sample (called Lump Candy) was purchased in the US, but was produced in Guangdong, China. The samples from abroad included: two cane sugar samples from the same market in Beijing, China, two cane samples from markets in Mexico and Brazil, and one beet sample from a market in Sweden. Sample information for all commercially available sugars is given in Appendix E. All sugars were tested "as is" without further purification or modification.

Methods

DSC analysis of beet and cane sucrose sources

DSC experiments were carried out using a Q2000 (TA Instruments, New Castle, DE), equipped with a RCS 90 refrigerated cooling system. The DSC was calibrated for enthalpy and temperature using a standard indium sample (Tmonset of 156.6°C, ΔH of 28.71 J/g, TA Instruments, New Castle, DE) prior to sample measurements. Hermetic aluminum Tzero pans and lids (TA Instruments, New Castle, DE) were used for all calibration and sample measurements, including an empty pan as the reference. Dry nitrogen, at a flow rate of 50 mL/min, was used as the purge gas. All experiments were conducted in at least duplicate, but most were done in triplicate. Universal Analysis (UA) software (version 4.4a, TA instrument, New Castle, DE) was used to obtain the melting parameters (onset melting temperature, Tm onset; peak melting temperature, Tm peak; and enthalpy of melting, ΔH J/g) and plot the average heat flow signals. The specific experimental conditions described below were selected based on previous research carried out in the Schmidt laboratory (Lee and others 2011a).

DSC characterization of beet and cane sucrose sources

Hermetically sealed sugar samples (17 beet samples and 30 cane samples), approximately 3 mg, were equilibrated at 25°C and then heated at rate of 10°C/min to 220°C. The end temperature was selected so as to ensure coverage of the entire endothermic peak for all samples tested.

Heating rate dependency of beet and cane sucrose sources

For the heating rate dependency study, DSC thermal thermograms of nine selected sucrose samples were obtained at three additional heating rates, 1, 5, and 25°C/min. The nine samples included: two analytical grade cane samples (Sigma and Fisher), three white refined

beet samples (US beet, Pioneer beet, and Meijer beet), two white refined cane samples (US cane and C&H cane), one high ash cane sample (sample number 11 in Appendix D from SPRI, New Orleans, LA), and one Turbinado cane sugar sample (Sugar in the Raw, Brooklyn, NY). The heating rate dependency values (ΔTmonset, °C) were calculated by subtracting the lower heating rate Tmonset (e.g., Tmonset at 1°C/min) from the higher heating rate Tmonset (e.g., Tmonset at 25°C/min).

TGA analysis of beet and cane sucrose sources

Before sample analysis, the TGA Q500 (TA instrument, New Castle, DE) was calibrated for weight and temperature measurement using indium (melting onset 156.6°C). Approximately 100 mg of each crystalline sucrose sample (analytical grade Sigma cane, US beet, and US cane samples) was heated from 25°C to 250°C at a heating rate of 10°C/min. A large sample size was used to improve sensitivity. Helium gas was used to improve heat transfer between the sample and the thermocouple, which is at the edge of the pan containing the sample. The derivative weight loss signals were plotted as a function of temperature using the Universal Analysis (UA) software (version 4.4a, TA instrument, New Castle, DE). To facilitate comparison, the TGA data were plotted with the DSC data using the UA software. The TGA data were displayed as % weight loss as a function of temperature, while the DSC data were displayed as heat flow as a function of temperature.

Ampule heating study of beet and cane sucrose sources

Approximately 2 g of analytical grade Sigma cane, US beet, and US cane sucrose samples were weighed into glass ampules, flame-sealed, and placed into a beaker. The beaker was then placed into a Gas Chromatograph (GC) oven (Agilent Technologies, Inc., Santa Clara, CA) and the

temperature ramped from 40°C to 160°C at 30°C/min and held at 160°C for 180 minutes. At 15

minute intervals, samples were briefly removed from the oven and examined for physical

changes. Images were taken, for total color difference analysis, using a Canon PowerShot ELPH

300 HS 12.1 Megapixel Digital Camera. For consistency of lighting and background conditions, a

photo studio light box was used (Figure 3.2). The Hunter color system *L* (+ values represent

lightness and – values represent darkness), *a* (+ values represent redness and – values

represent greenness), and *b* (+ values represent yellowness and – values represent blueness)

color space values were analyzed using Color Companion software (DMI digital interactive LLC)

for recorded digital photographs. This Color Companion analysis method was successfully used

to monitor the color stability of a tea polyphenol compound in the solution and solid state (Li

and others 2013). In the study herein, the total color difference (TCD) values were used to

quantify the total color change for each sucrose sample held isothermally over time at 160°C in

a GC oven, where TCD values (or ΔE) were calculated using Equation 3.1,

$$\mathbf{\Delta E} = \sqrt{\mathbf{\Delta L^2} + \mathbf{\Delta a^2} + \mathbf{\Delta b^2}} \qquad \text{Equation 3.1}$$

where ΔL^2, Δa^2, and Δb^2 are the squared differences in *Lab* color space values. Initial *Lab*

values for each "as is" sucrose sample were used for the TCD calculations, at each time point

evaluated. Triplicate trials were conducted for this study.

3.4 Results and Discussion

DSC characterization of beet and cane sucrose sources

Resultant DSC parameters for the 47 sucrose samples studied herein are summarized in

Table 3.2. A distinct difference can be observed between the thermal profiles of beet and cane

sucrose sources at 10°C/min. All 17 beet samples studied exhibited only one large endothermic

peak with an average Tmonset value of 188.41 ± 0.37°C; whereas, 26 of the 30 cane samples

exhibited two endothermic peaks, one small peak (average Tmonset = 153.80 ± 6.05°C)

proceeded by one large peak (average Tmonset = 187.39 ± 1.72°C). This large difference in the

average temperatures at which the initial thermal event begins in the majority of cane (small

peak) compared to beet (large peak) sucrose samples (34.61°C lower in cane sources, calculated

from Table 3.2) indicates that the loss of crystalline structure in sucrose extracted and refined

from sugarcane begins at a much lower temperature compared to that extracted from

sugarbeet. For a visual comparison of the differences in the thermal behavior, representative

DSC thermograms and associated Tmonset values of analytical grade Sigma cane, white refined

beet and cane (US beet and US cane), and Sugar in the Raw (discussed further below) are

plotted in Figure 3.3.

Most research studies do not include in the materials section the source of sucrose used

and currently, at least in the United States, the source of sucrose is not required on the product

label, so it is difficult to determine a relation between thermal behavior and sucrose source

based on the literature values. Only a few studies were found that identified and included both

beet and cane sucrose sources in their thermal behavior research (Kamoda 1960; Beckett and

others 2006), as mentioned in the introduction. Kamoda (1960), using a heating disc apparatus,

reported a rather wide variation in melting temperature, but found no difference in the melting

temperature of beet (7 beet samples with melting temperatures ranging from 184.6 to 188.4°C)

versus cane (11 cane samples with melting temperatures ranging from 172.2 to 190.6°C)

sucrose sources. Whereas, Beckett and others (2006), using DSC, reported that 2 of the sucrose

samples studied exhibited two endothermic peaks (both identified as cane sources) and 2

samples exhibited one endothermic peak (one beet sucrose source and one source that was not identified). Beckett and others (2006) discussed the influence of sucrose source on the melting temperature, but mainly tied the number of peaks in the sucrose DSC thermogram to the amount and type of impurities present.

Perhaps the lack of research on the topic of thermal property differences between beet and cane sucrose sources is related to the assumption that both sucrose sources are very high in purity (Table 3.1) and, thus, their thermal behavior should not vary widely. Additionally, some researchers may have overlooked the small peak in cane sucrose DSC thermograms, because the heat flow intensity scale may have been adjusted to fully display the large endothermic peak, causing the small peak to be visually enveloped into the baseline.

As can be observed in Table 3.2, 4 of the 30 cane samples exhibited only one large endothermic peak - high ash cane (SPRI, New Orleans, LA; Appendix D), Sugar in the Raw (Turbinado cane sugar, Appendix E), and Chinese granulated and caster (Appendix E) - similar to the beet sucrose samples studied. The high ash cane (0.107% conductivity ash from SPRI) and Sugar in the Raw (raw sugars ranged from 0.35 to 0.61% ash content using a conductometric method for 29 different plantations, Gillett 1949a and b) samples have relatively high impurity levels compared to white refined sugar (0.01 to 0.03% conductivity ash for both white refined beet and cane samples, Appendix D). The Chinese granulated and caster cane samples, obtained from a market in Beijing, China, were produced using sulfitation (Huo 2008). In the United States, sulfitation is routinely used in beet sugar processing, but is not usually used in the production of white refined cane sugar. Sulfitation is the process of adding sulfur dioxide (SO_2) to the sugarbeet juice to decrease the pH and minimize color formation during

subsequent processing steps (Clarke and Godshall, 1988; Clark and others 1997; Asadi 2005).

Thus, these 4 cane sucrose samples contain excess (high ash content cane and Sugar in the Raw

samples) or processing added (residual sulfite in both Chinese cane samples) impurities. We

hypothesis that the thermal behavior differences observed for these four cane samples, with

only one large endothermic peak, are potentially associated with the presence of these

impurities. The results also suggest that the presence of only one large peak observed in the

beet sucrose DSC thermograms (also could be observed as the absence of the small peak) may

also be related to the presence of impurities.

As a general rule, the purer the crystalline material the higher and sharper the melting

peak (Widmann and Scherrer 1991; Cassel 2008) and for most crystalline materials, the

presence of even a small quantity of impurities will lower the melting point by a few degrees

and broaden the melting temperature range (Callister and Rethwisch 2012). Since impurities

cause defects in the crystalline lattice, it is easier to overcome the intermolecular interactions

between the molecules, and consequently, a lower temperature is required for melting in the

presence of impurities. However, DSC melting temperature data collected herein do not follow

this commonly recognized principle. For example, the analytical grade Sigma cane sucrose

samples (Sigma and Fisher), with the highest purity, have a much lower Tmonset value (small

peak) compared to the Tmonset value for the substantially less pure Sugar in the Raw (cane)

sample, which exhibited only one large peak (see Figure 3.3).

Previous research studies have reported that impurities play an important, but rather

complicated, role in the thermal behavior of crystalline sucrose (Kamota 1960; Eggleston and

others 1996; Kishihara and others 2001; Okuno and others 2002a and b and 2003; Maulny 2003;

Beckett and others 2006). For example, Okuno and others (2002b) summarized that the addition of Na^+, K^+ or hydrogen carbonate ions (HCO_3^-) will increase the melting point of recrystallized sucrose; whereas, the addition of Ca^{2+} or Mg^{2+} will lower the melting point of recrystallized sucrose. In order to further investigate the role impurities play in the thermal behavior difference between and within beet and cane sucrose sources, additional research assessing the physicochemical characteristics of the sucrose sources, such as moisture content, pH, conductivity ash, and sulfite content, needs to be carried out.

Heating rate dependency of beet and cane sucrose sources

Thermodynamic melting occurs at a single, time-independent (i.e., heating-rate independent) temperature (often reported as Tm onset), where the crystalline solid and corresponding liquid phases are in thermodynamic equilibrium at constant pressure without chemical changes (Lee and others 2011, Roos 1995, Wunderlich 1990a). The parameters associated with the melting process (onset melting temperature, Tmonset; peak melting temperature, Tmpeak; and enthalpy of melting, ΔH) are usually measured by heating a crystalline material at a specified rate to a temperature where the melting endothermic peak is complete.

In previous research, the melting parameters for analytical grade Sigma cane sucrose were shown to exhibit strong heating rate dependency, 12.96°C for the small peak and 12.95°C for the large peak for heating rates ranging from 2 to 10°C/min, compared to indium (0.75°C) and mannitol (0.39°C) for heating rates ranging from 1 to 25°C (Lee and others 2011a). In order to determine if heating rate dependency is a common behavior of sucrose samples in general, nine sucrose samples (3 beet and 6 cane samples) were examined at 3 heating rates, in addition

to 10°C/min. Resultant heating rate data (average DSC parameters and plotted DSC thermograms) were organized into 5 categories: analytical grade cane (Table 3.3 and Figure 3.4), white refined beet (Table 3.4 and Figure 3.5), white refined cane (Table 3.5 and Figure 3.6), high ash cane (Table 3.6 and Figure 3.7), and Sugar in the Raw (Table 3.7 and Figure 3.8). For comparison purposes, images taken after the samples were heated to 220°C, are also provided in Tables 3.4 to 3.8. The small peak was not measurable using the UA software for the white refined cane sucrose samples (US cane and C&H) at a heating rate of 1°C/min; however, a change in the slope of the heat flow curve was observed. This is expected, since a lower heating rate results in a slower reaction rate, making it more difficult to detect a distinct change in the DSC heat flow. The temperature at which the slope began to change was extrapolate from the heat flow curves and used as an estimate of the small T_{monset} value at 1°C/min in Table 3.4. However, T_{mpeak} and ΔH for the small peak at 1°C/min were not measurable.

As can be observed from Figure 3.9, heating rate dependency, and therefore time dependency, is a common behavior of all sucrose sample studied herein. However, as can be observed from Figure 3.9, the extent of the heating rate/time dependency (kinetics) varied widely as a function of both sucrose sample category type and heating rate.

In the case of sucrose sample category type, the heating rate dependency (1 to 25°C/min) was largest for the small peak for analytical grade Sigma cane (23.7°C) and white refined cane (23.5°C) samples and smallest for the white refined beet sucrose category (6.1°C for the one large peak), with the other categories falling in between (Figure 3.9). As was pointed out for the DSC T_{monset} values discussed in the previous section, it is an unexpected result for the more pure analytical grade cane sucrose to exhibit a larger heating rate dependency compared to the

less pure beet sucrose. Within the white refined cane samples, it is important to note that magnitude of the small peak (ΔH) for the more pure analytical grade cane sucrose samples (e.g., lower mineral content with an average ash content of 0.0009%), is larger and more distinct than the small peak for the less pure white refined cane sucrose samples (average ash content 0.02%), though their Tmonset values are similar. The underlying role impurities play in the thermal behavior difference between and within beet and cane sucrose sources once again, call for further investigation.

In the case of heating rate, in general, the increase in Tmonset is substantially larger for the lower heating rate range compared to the higher heating rate range, for both the small and large endothermic DSC peaks for all 5 sucrose sample categories. This trend can be observe in Figure 3.9 by noting the leveling off of the Tmonset curve with increasing heating rate for all sucrose samples studied.

In order to better illustrate the heating rate dependency (kinetic) of Tmonset, as influence by sugar type and heating rate, an Arrhenius plot was generated for a subset of sucrose sample categories, analytical grade cane, white refined cane, and white refined beet categories (Figure 3.10). Quantitative kinetic analysis is beyond the scope of this research. However, qualitative analysis of an Arrhenius plot (Figure 3.10) provides significant insight into processes occurring over the temperature range of loss in crystalline structure.

Three implications can be drawn from the data in Figure 3.10. First, a straight-line relationship is seen for the heating rate dependency of the small peak observed in analytical grade and white refined cane sucrose. This indicates that a single, independent process is

responsible for the heating rate dependency, which based on the work of Lee and others 2011a and b, we hypothesize to be associated with thermal decomposition.

Second, white refined beet sucrose samples exhibited two linear segments, from 1 to 5°C/min and from 5 to 25°C/min. This broken line behavior indicates that more than one processes is occurring. The 1 to 5°C/min line segment shows a slight increase in Tmonset with increasing heating rate; whereas, the 5 to 25°C/min line segment is nearly vertical, indicating that Tmonset is independent of heating rate. Usually, if Tmonset is independent of heating rate the loss of crystalline structure would be termed thermodynamic melting. However, since heating rate dependency is observed in the lower heating rate range, further testing is required to determine the underlying cause of this change in kinetic behavior as a function of heating. Thus, additional research into the purity of beet sucrose is also needed. Both aspects of beet sucrose characterization are currently under investigation in the Schmidt laboratory.

Third, the large peak in analytical grade and white refined cane sucrose behaves similarly to the white refined beet sucrose sample, indicating a larger heating rate effect at low heating rates compared to higher heating rates. The broken line behavior again indicates that more than one processes is occurring.

Similar heating rate dependency studies for sucrose, as well as other sugars, have been reported in the literature (Okuno and others 2003; Hurtta and others 2004a; Beckett and others 2006; Lappalainen and others 2006; Lee and others 2011a; Magoń and others 2014). Usually, the observation of heating rate dependency of the Tmonset values indicates that there is a kinetic process associated with the loss of crystalline structure occurring in the material. Based on previous research carried out by Lee and others (2011a and b) and further discussed by

Schmidt and others (2012), the kinetic process responsible for the initial loss of crystalline structure in analytical grade cane sucrose is thermal decomposition, though specifics of the underlying mechanism have yet to be established. The larger heating rate dependency exhibited by the analytical grade cane and white refined cane samples compared to the white refined beet sucrose samples suggests that the extent of the thermal decomposition event is greater in the case of cane sucrose than in the case of beet sucrose samples. However, additional research, employing HPLC analysis for quantification of select decomposition components, is needed to further investigate this assertion. Investigation of the factors responsible for the thermal behavior differences reported herein between beet and cane sucrose sources should prove quite valuable for determining the mechanism underlying this kinetic thermal event, as well.

TGA analysis of beet and cane sucrose sources

To investigate the relation between the Tmonset of the different sucrose sources, as measured by DSC, and the onset of initial thermal decomposition of the different sucrose sources, as detected by weight change as a function of temperature, thermogravimetric analysis (TGA) was also applied in this study to three samples – analytical grade Sigma cane, US beet, and US cane sucrose samples. DSC thermograms and TGA weight loss profiles, plotted as a function of temperature and obtained at the same heating rate (10°C/min), are shown in Figure 3.11. For easier visual interpretation of when weight loss begins, the TGA baseline for all three sucrose samples has been rotated to 100% weight at 50 and 100°C temperature points to compensate the baseline buoyancy caused by the noise of the instrument. A similar adjustment was made in Schmidt and others (2012) and is described in detail therein. TGA analysis

indicates that all three sucrose samples start to lose a very small amount of weight at essentially the same temperature, near 120°C at a heating rate of 10°C/min. The cause of this very small weight loss could be the beginning of thermal decomposition as discussed by Schmidt and others (2012). However, there appears to be no obvious relation between TGA weight loss onset or amount and DSC Tmonset or ΔH values. Lee and others (2011a) drew similar conclusions and went on to employ HPLC analysis for thermal decomposition component detection (Lee and others 2011b). The same approach will be utilized in this research, where a subsequent study will be carried out to investigate the thermal decomposition differences between beet and cane sucrose sources using HPLC analysis.

Ampule heating study of beet and cane sucrose sources

A suitable method to distinguish the color of two adjacent objects is to find the total color difference (TCD) between them. The TCD must account for variation in both luminance (L reflects lightness/darkness) and chrominance (a and b reflect redness and yellowness) (Valavanis and others 1996). Hunter color parameters and TCD have been widely used to describe color changes in food systems caused by browning reactions, such as the Maillard reaction, enzymatic browning, pigment degradation, and oxidation of ascorbic acid during thermal processing (Rhim and others 1989; Correia and others 2009; Silva and Silva 1999; Maskan 2006; Assawarachan and Noomhorm 2010; Saxena and others 2012; Kara and Erçelebi 2013; Giner and others 2013).

Visual inspection of color and phase changes in sealed ampules under isothermal heating conditions, 160°C for a total of 180 minutes, was recorded using digital images (Figure 3.12 A to N). The calculated TCD values for the three sucrose samples, analytical grade Sigma cane, US

beet, and US cane, are plotted in Figure 3.13. Prior to heat treatment, all three sucrose samples were composed of clear, white crystals (Figure 3.12A), where, based on visual inspection, the US beet sample appeared shinier than the Sigma cane and US cane samples.

At the beginning of holding at 160°C (from 0 to 15min, Figure 3.12B to C), visual color changes were slight, and TCD values increased only modestly for all three sugar samples (Figure 3.12). However, as holding time increased, Sigma cane was the first sample to exhibit a tan/brown color and the first to begin liquefying (at 45 mins, Figure 3.12F). After heating was complete (180 mins), Sigma cane visually appeared a dark brown color (Figure 3.12N), with a final TCD value of 57.3. US cane began to liquefied next (at 120 mins, Figure 3.12 J) and after heating was complete (180 mins, Figure 3.12N), exhibited a medium brown color with a final TCD value of 40.6. US beet did not liquefy over the 180 minute isothermal heating, displaying a grainy (crystalline) texture with a light brown color (180 mins, Figure 3.12N) and a TCD value of 25.0. It is interesting to note that even though the visual appearance of Sigma sucrose continued to darken from 105 to 180 mins, as can be observed in Figure 3.13, the TCD values did not increase, but rather remained relatively constant ranging from 55.21 to 57.26. It is convenient to reduce the Hunter color system *Lab* values to a single number; however, one limitation of using TCD values is that a single number can only indicates the magnitude of the color difference, not the direction. Thus, samples with the same TCD values will not necessarily have the same visual appearance (Nielsen 2009).

Traditionally, it has been thought that sucrose melts before it caramelizes; however, the results of the ampule heating study show that for all three sucrose samples a substantial change in color is observed prior to the solid to liquid phase transition. Even though all three

sucrose samples changed color before they changed phase, they did not change color at the same time. Analytical grade Sigma cane sucrose exhibited the least thermal stability, as reflected by quick color generation and the most rapid phase change. In contrast, the US beet sample exhibited the greatest thermal stability, with the slowest color development and most robust resistance to changing phase. This substantial difference in color generation kinetics, and phase change behavior, between beet and cane sucrose sources connects with and further supports the observed DSC thermal behavior differences, discussed above. For example, there is a direct connection between the ampule thermal stability and the heating rate dependency results. In general, the greater the heating rate dependency the less thermal stability is exhibited. This can be seen by comparing the heating rate dependency and thermal stability, based on the TCD, of analytical grade cane sucrose and white refined cane sucrose samples with that for white refined beet samples. The analytical grade cane sucrose and white refined cane sucrose samples exhibited greater heat rate dependency, 23.7 and 23.5°C (differences in small DSC peak Tmonset values between 1 and 25°C/min heating rates), respectively, and less thermal stability (57.3 and 40.6 TCD), compared to the beet sample which exhibited less heat rate dependency, 6.1°C (differences in DSC Tmonset values between 1 and 25°C/min heating rates), and less thermal stability (25.0 TCD).

3.5 Conclusions

Based on the research findings reported herein, beet and cane sucrose sources exhibit substantially different thermal behaviors, in terms of the number of endothermic DSC peaks (in general, one peak for beet samples and two peaks for cane samples), the extent of heating rate dependency (in general, cane > beet), and the degree of thermal stability (beet > cane). The

underlying cause(s) of these thermal differences, however, requires additional research, including investigation of the role impurities play in the thermal behavior of beet and cane sucrose sources, quantification using HPLC of potential thermal decomposition differences between beet and cane sucrose sources, and determination of structural and/or chemical differences between beet and cane sucrose sources. Lastly, this research shows that additional factors, besides market price, may need to be taken into account during sugar source selection by the food and pharmaceutical industries.

3.6 Acknowledgements

3.7 References

Acree TE, Lee CY, Butts RM, Barnard J. 1976. Geosmin, the earthy component of table beet odor. J Agric Food Chem 24(2):430–1.

Asadi M. ed. 2007. Beet-sugar handbook. John Wiley & Sons, Inc., Hoboken, New Jersey, USA.

Assawarachan R, Noomhorm A (2010) Changes in color and rheological behavior of pineapple concentrate through various evaporation methods. Int J Agric Biol Eng 3:74–84.

Beckett ST, Francesconi, MG, Geary PM, MacKenzie G, Maulny APE. 2006. DSC study of sucrose melting. Carbohydrate Research 341: 2591-2599.

Bensouissi A, Rousse C, Roge B, Mathlouthi M. 2007. Effect of Selected Impurities on Sucrose Crystal Growth Rate and Granulated Sugar Quality. p 147-65.

Bhandari B, Hartel R. 2002. Co-crystallization of Sucrose at High Concentration in the Presence of Glucose and Fructose. J. of Food Sci, 67: 1797–1802.

Bubník Z, Kadlec P, Urban D, Bruhns M. 1995. Sugar technologists manual. Chemical and physical data for sugar manufacturers and users Bartens Pub. Co., Berlin, Germany.

Callister WD, Rethwisch DG. 2012. Fundamentals of materials science and engineering : an integrated approach. 4th ed. Hoboken, N.J.: Wiley.

Cassel RB. 2008. TA283. How Tzero^{TM} technology improves DSC performance. Part V: Reducing thermal lag. TA instruments: Applications library search [Internet]. New Castle, DE: TA instruments; c 2008 [Accessed 2008 Aug 20]. Available from: http://www.tainstruments.co.jp/application/pdf/Thermal_Library/Applications_Briefs/TA285.PDF.

China GB13104-2005 Sugar Hygiene Standard (National standard for sugars). 2005. Beijing.

Clarke MA. 2000. Sugarcane. In: Anonymous Kirk-Othmer Encyclopedia of Chemical Technology. John Wiley & Sons, Inc. p 1-26.

Colonna WJ, Samaraweera U, Clarke MA, Cleary M, Godshall MA, White JS, Updated by Staff. 2000. Sugar. In: Anonymous Kirk-Othmer Encyclopedia of Chemical Technology. John Wiley & Sons, Inc.

Correia P, Leitão A, Beirão-da-Costa ML (2009) The effect of drying temperatures on morphological and chemical properties of dried chestnuts flours. J Food Eng 90:325–332.

Dowling JF. 1990. Sugar products. In: Pennington NL, Baker CW, editors. Sugar a user's guide to sucrose. 1st ed. New York: Van Nostrand Reinhold. p 36-45.

Eggleston G, Trask-Morrell BJ, Vercellotti JR. 1996. Use of differential scanning calorimetry and thermogravimetric analysis to characterize the thermal degradation of crystalline sucrose and dried sucrose-salt residues. J. Agric. Food. Chem. 44:3319-3325.

Eggleston G. 2004. Differentiating cane white sugar from beet white sugar using ion chromatography profiles. SPRI Conference on Sugar Processing Research 209-214.

European Economic Community, Council Directive of 11 Dec., 1973 (73/437/EC), Off. J. E. C. no L 356, 27.12.73, pp. 71-78;First Commission Directive of 26 July, 1979 (79/786/EC), Off. J. E. C. no L 239, 22.9.79. p 24-52.

Fernelius WC. 1984. Thumbnail sketches: Is sugar from sugar beets the same as sugar from sugar cane? Journal of Chemical Education, 61 (3): 249.

Gillett TR. 1949a. Conductometric Measurement of Ash in White. Sugars Analytical Chemistry 21(9): 1081-1084.

Gillett TR. 1949b. Conductometric Determination of Ash in Raw Sugars. Sugars Analytical Chemistry 21(9): 1084-1086.

Giner MJ, Hizarci Õ, Martí N, et al (2013) Novel approaches to reduce brown pigment formation and color changes in thermal pasteurized tomato juice. Eur Food Res Technol 236:507–515.

Godshall MA. 1986. Flavors from beet and cane sugar products. From Proc. Sugar processing research conference. p 210-28.

Godshall MA, Grimm CC, Clarke MA. 1994. Sensory properties of white beet sugars. p 305-24.

Godshall MA. 2013. Industrial Uses of Sugar – Chocolate, Confectionery, Beverage, Bakery, Cereal and Dairy Products and Processes. U.K.: InformaAgra.

Hellmuth, E.; Wunderlich, B. Superheating of linear high-polymer polyethylene crystals. J. Appl. Phys. 1965, 36 (10): 3039-3044.

Hirschmüller H. 1953. Chemical properties of sucrose. In: Honig P, editor. Principles of Sugar Technology. New York, NY: Elsevier Publishing Company. p 1-17.

Horton D, Walaszek Z. 1982. Tautomeric equilibria of some sugars by partially relaxed, 13C pulse Fourier-transform, nuclear magnetic resonance spectroscopy. Carbohydrate Research 105:145-153.

Hurtta M, Pitkänen I, Knuutinen J. 2004a. Melting behaviour of D-sucrose, D-glucose and D-fructose. Carbohydrate Research 339:2267-2273.

Hurtta M, Pitkänen I. 2004b. Quantification of low levels of amorphous content in maltitol. Thermochimica Acta 419:19-29.

Kara Ş, Ercęlebi EA (2013) Thermal degradation kinetics of anthocyanins and visual colour of Urmu mulberry (Morus nigra L.). J Food Eng 116:541–547.

Kamoda M. 1960. Proceedings of the Research Society of Japan Sugar Refineries' Technologists. 27, 158–238.

Kawakami K, Miyoshi K, Tamura N, Yamaguchi T, and Ida Y. 2006. Crystallization of sucrose glass under ambient conditions: Evaluation of crystallization rate and unusual melting behavior of resultant crystals. Journal of Pharmaceutical Sciences, 95(6): 1354-1363.

Kinugawa K, Kinuhata M, Kagotani R, Imanaka H, Ishida N, Kitamatsu M, Nakanishi K, Imamura K. 2015. Inhibitory effects of additives and heat treatment on the crystallization of freeze-dried sugar. Journal of Food Engineering, 155, 37-44.

Kishihara S, Okuno M, Fujii S, Kawasaki K, Nishiura T. 2001. An opinion on structure of sucrose crystal. Proceedings of the Research Society of Japan Sugar Refineries' Technologists 49:1-8.

Lappalainen M, Pitkänen I, Heikkilä H, Nurmi J. 2006. Melting behaviour and evolved gas analysis of xylose. Journal of Thermal Analysis and Calorimetry 84:367-376.

Lee JW, Thomas LC, Schmidt SJ. 2011a. Investigation of the heating rate dependency associated with the loss of crystalline structure in sucrose, glucose, and fructose using a thermal analysis approach (Part I). Journal of Agricultural and Food Chemistry, (59):684-701.

Lee JW, Thomas LC, Jerrell   J, Feng H, Cadwallader KR, Schmidt SJ. 2011b. Investigation of thermal decomposition as the kinetic process that causes the loss of crystalline structure in sucrose using a chemical analysis approach (Part II). Journal of Agricultural and Food Chemistry, (59):702-712.

Lee T and Chang GD. 2009. Sucrose conformational polymorphism. Crystal Growth and Design, 9(8): 3551-3561.

Lee T and Lin YS. 2007. Dimorphs of sucrose. International Sugar Journal, 109 (1303):440-445.

Li N, Taylor LS, Ferruzzi MG, Mauer LJ. 2013. Color and chemical stability of tea polyphenol (-)-epigallocatechin-3-gallate in solution and solid states. Food Res Int 53:909–921.

Liang B, Hartel RW, Berglund KA. 1989. Effects of raffinose on sucrose crystal growth kinetics and rate dispersion. AICHE J. 35(12):2053-7.

Lin YS. 2007. Master thesis "Two Conformational Polymorphs of Sucrose". National Central University.

Lu Y, Lee JW, Thomas L, Schmidt SJ. 2013. Differences in the thermal behavior of beet and cane sugars. Proceedings of the 74th Annual Institute of Food Technologists, Chicago, Ill.

Magne V, Mathlouthi M, Robilland B, Magne M, Mathlouthi B. 1998. Determination of some organic acids and inorganic anions in beet sugar by ionic HPLC. Food Chem 61(4):449–53.

Magoń A, Wurm A, Schick C, Pangloli P, Zivanovic S, Skotnicki M, Pyda M. 2014. Heat capacity and transition behavior of sucrose by standard, fast scanning and temperature-modulated calorimetry. Thermochimica Acta, 589: 183-196. Article reprinted in 2015, Thermochimica Acta, 603, 149-161.

Marsili RT, Miller N, Kilmer GJ, Simmons RE. 1994. Identification and quantitation of the primary chemicals responsible for the characteristic malodor of beet sugar by purge-and-trap GC-MS-OD techniques. J Chromatogr Sci 32(5):165–71.

Maskan M (2006) Production of pomegranate (Punica granatum L.) juice concentrate by various heating methods: colour degradation and kinetics. J Food Eng 72:218–224.

Mathlouthi M and Roge B. 2012. Melting And Crystallization of Sugars: a structural approach. 2012 IFT Annual Meeting presentation. Las Vegas, NV.

Maulny A. 2003. Co-crystallisation of sugars. Ph.D. Thesis, Department of Chemistry, University of Hull, Hull, UK.

Miller, MM. 2001. The effect of applied fields on crystallisation. Brunel University.

Monte WC, Maga JA. 1982. Flavor chemistry of sucrose. Sugar Technol Rev 8(3):181–204.

Morel du Boil PG. 1992. Theanderose - A contributor to c-axis elongation in cane sugar processing. Int.Sugar J. 94(1120):90-4.

Morel du Boil PG. 1996. Theanderose – A characteristic of cane sugar crystals. Proc S Afr Sug Technol Ass 70140-4.

Morel du Boil PG. 1997. Theanderose - Distinguishing cane and beet Sugars. Int.Sugar J. 99(1179):102-6.

Morgan M. 1999. SUGAR, SUGAR / Cane and beet share the same chemistry but act differently in the kitchen. San Fransisco Chronicle [serial online]. Nov. 27, 2012. Available from http://www.sfgate.com/news/article/SUGAR-SUGAR-Cane-and-beet-share-the-same-2939081.php#page-1. Posted on March 31, 1999.

Morus nigra L. 2013. Thermal degradation kinetics of anthocyanins and visual colour of Urmu mulberry. Journal of Food Engineering, 116 (2), pp. 541-547.

Okuno, M.; Kishihara, S.; Fujii, S.; Kawasaki, K. Analysis of structure of sucrose crystal by differential scanning calorimetry. Proc. Res. Soc. Jpn. Sugar Refin. Technol. 2002a, 50, 11-18.

Okuno, M.; Kishihara, S.; Fujii, S.; Kawasaki, K. Melting point of sucrose crystal prepared in sucrose solution containing various impurities. Proc. Res. Soc. Jpn. Sugar Refin. Technol. 2002b, 50, 19-27.

Okuno M, Nakai N, and Kishihara S. 2003. Melting Point of Sucrose Crystals Prepared in Various Solvents. Proceedings of research Society of Japan Sugar Refineries' Technologists, (51):1-6.

Parliment T, Kolor M, Maing I. 1977. Identification of the major volatile components cooked beets. J Food Sci 42(6):1592–3.

Pihlsgard P. 1997. The properties of sugar focusing on odours and flavours—a literature review. SIK Rapport (634).

Reynhardt EC. 1990. An NMR, DSC and X-ray investigation of the disaccharides sucrose, maltose and lactose, Molecular Physics: An International Journal at the Interface Between Chemistry and Physics, 69:6, 1083-1097.

Rhim JW, Nunes R V, Jones V a, Swartzel KR (1989) Kinetics of Color Change of Grape Juice Generated using Linearly Increasing Temperature. J Food Sci 54:776–777.

Roos YH. 1995. Food components and polymers. In: Taylor SL, editor. Phase Transitions in Foods. 1st ed. San Diego, CA: Academic Press. p 109-156.

Roos YH, Franks F, Karel M, Labuza TP, Levine H, Mathlouthi M, Reid D, Shalaev E, Slade L. 2012. Comment on the melting and decomposition of sugars, Journal of Agricultural and Food Chemistry, 60: 10359–10362.

Roos YH, Karel M, Labuza TP, Levine H, Mathlouthi M, Reid D, Shalaev E, Slade L. 2013. Melting and Crystallization of Sugars in High-Solids Systems, Journal of Agricultural and Food Chemistry, 61:3167-3178.

Powers HEC. 1958. Sucrose crystal inclusions. Nature, 182:715-717.

Potter R, Mansel R, inventors; University of South Florida, assignee. 1992 Jul. 7, 1992. Assay for the detection of beet sugar adulteration of food products. U.S. patent 5128243.

Saavedra-Leos MZ, Grajales-Lagunes A, González-García R, Toxqui-Terán A, Pérez-García SA, Abud-Archila MA, Ruiz-Cabrera MA. 2012. Glass Transition Study in Model Food Systems Prepared with Mixtures of Fructose, Glucose, and Sucrose. Journal of Food Science, 77:5, 118-126.

Saxena A, Maity T, Raju PS, Bawa a. S (2012) Degradation kinetics of colour and total carotenoids in jackfruit (Artocarpus heterophyllus) bulb slices during hot air drying. Food Bioprocess Technol 5:672–679.

Schiweck H, Clarke M, Pollach G. 1994. Sugar. Ullmann's Encyclopedia of Industrial Chemistry 34:557-628.

Schmidt SJ, Thomas LC, Lee, JW. 2012. Response to comment on the melting and decomposition of sugars. Journal of Agricultural and Food Chemistry, 60: 10363-10371.

Shah SV, Chakradeo YM. 1936. A note on the melting point of cane sugar.   Journal of Current Science. P652-3.

Shallenberger RS. 1978. Intrinsic chemistry of fructose. Pure and Applied Chemistry 50:1409-1420.

Silveira L, Moreira LM, Conceição VGB, et al (2009) Determination of sucrose concentration in lemon-type soft drinks by dispersive Raman spectroscopy. Spectroscopy 23:217–226.

Standard for sugars. CODEX STAN 212-1999 (Amd. 1-2001). P 1-6. Available from http://famis.comesa.int/pdf/Sugar_FDHS_6_CXS_212.pdf.

Sucrose SigmaUltra. Product Information. Sigma-Aldrich Co. St. Louis, MO. Available from http://www.sigmaaldrich.com/content/dam/sigma-aldrich/docs/Sigma/Product_Information_Sheet/1/s9378pis.pdf.

Sucrose SigmaUltra. Product Information. Sigma-Aldrich Co. St. Louis, MO. Available from http://www.sigmaaldrich.com/content/dam/sigma-aldrich/docs/Sigma/Product_Information_Sheet/1/s9378pis.pdf.

Tammann G. 1910. Zur Uberhitzung von Kristallen. Z. Phys. Chem. 1910, 68, 251-257.

Tombari E, Ferrari C, Salvetti G, Johari GP. 2007. Spontaneous liquefaction of isomerizable molecular crystals. J. Chem. Phys. 126:0211071-4.

Urbanus BL, Cox GO, Eklund EJ, Ickes CM, Schmidt SJ, Lee S. 2014a. Sensory Differences Between Beet and Cane Sugar Sources. J. Food Sci. 79:1763–1768.

Urbanus BL, Schmidt SJ, Lee S. 2014b. Sensory Differences between Product Matrices Made with Beet and Cane Sugar Sources. J. Food Sci. 79:2354-2361.

Vaccari G, Mantovani G. 1995. Sucrose crystallization. In: Mathlouthi M, Reiser P, editors. Sucrose properties and applications. 1st ed. Bishopbriggs: Blackie Academic and Professional. p 33-72.

Valavanis KP, Zheng J, Paschos G (1996) A total color difference measure for segmentation in color images. J Intell Robot Syst 16:269–313.

Widmann G, Scherrer O. 1991. A new program for DSC purity analysis. Journal of Thermal Analysis 37:1957-1964.

Wunderlich B. 1990a. Thermometry. In: Wunderlich B, author. Thermal Analysis. San Diego, CA: Academic Press. p 79-121.

Wunderlich B. 1990b. Differential thermal analysis. In: Wunderlich B, author. Thermal Analysis. San Diego, CA: Academic Press. p 123-218.

3.8 Figures and Tables
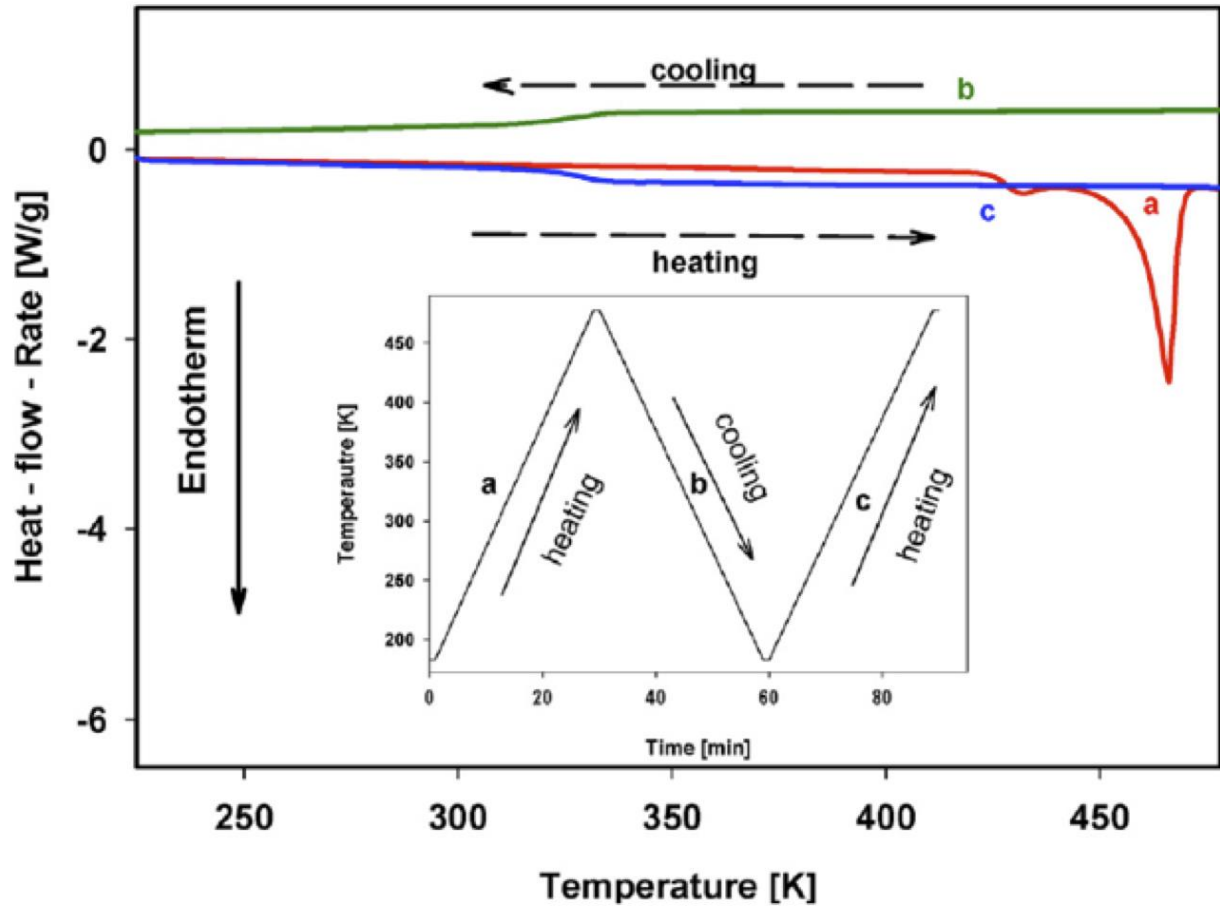
Figure 3.1 DSC thermogram and associated inset temperature program for analytical grade Sigma cane sucrose at a heating rate of 10 K/min, excerpted from Magoń and others (2014). Heat flow curve a (red) is from the first heating of crystalline sucrose, heat flow curve b (green) is from cooling the melt, and heat flow curve c (blue) is the second heating of amorphous sucrose.
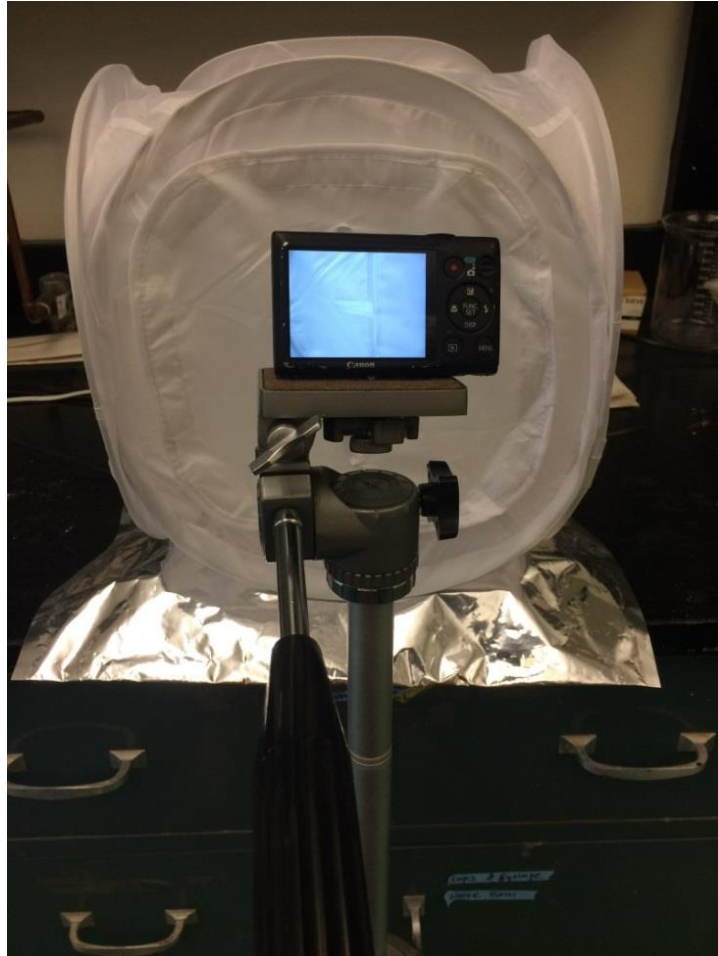
Figure 3.2 Photo studio light box arrangement used for all images taken.
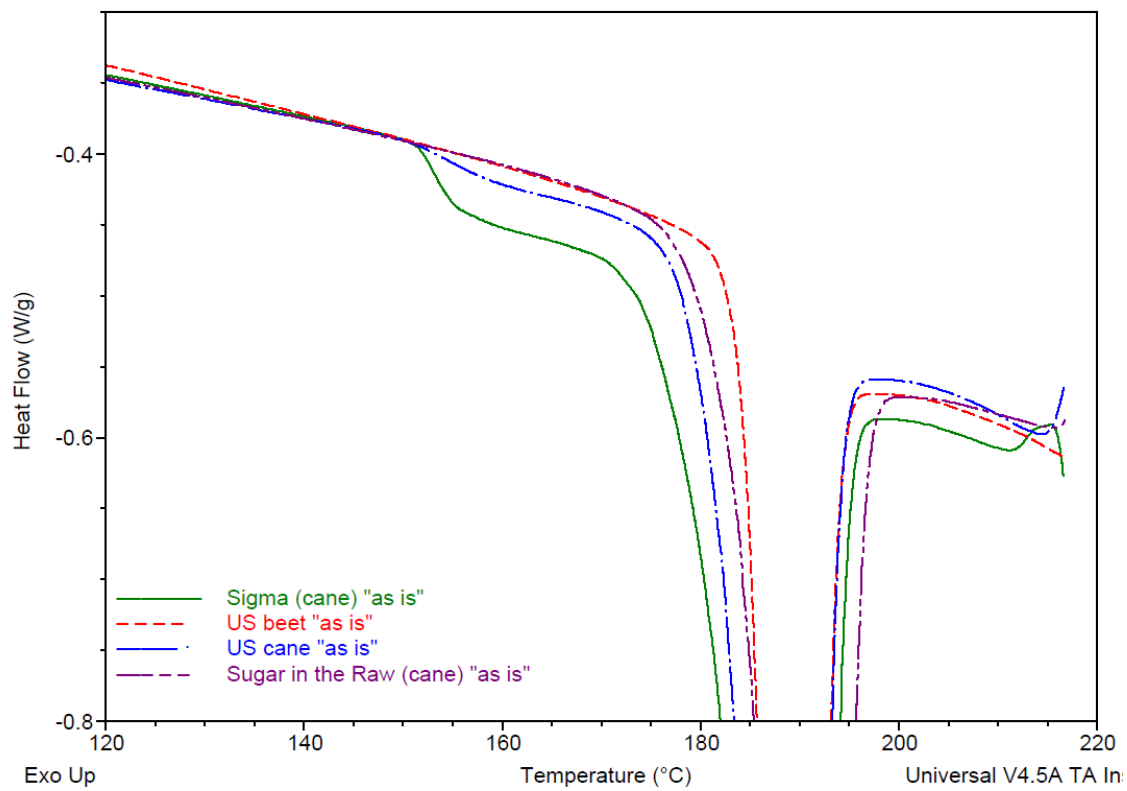
Figure 3.3 Example DSC thermograms of analytical grade Sigma cane, US beet, US cane, and Sugar in the Raw samples at a 10°C/min heating rate.

Table 3.1 Hypotheses associated with the appearance of the small endothermic DSC peak observed in sucrose samples. The terminology used by the original author(s) was retained, where possible, in order to best capture the essence of their hypothesis and to avoid any inadvertent misinterpretation. Note: Depending on the nature of the hypothesis, it may appear in more than one category.

| Categories	Hypotheses	References
Amorphous content	Presence of some amorphous fraction (highly concentrated mother liquor) in the granules, which produces a small devitrification peak	Bhandari and Hartel, 2002
	Presence of partially amorphous, fine sucrose crystals (<50 μm), which produce a glass transition just prior to the melting peak	Mathlouthi, 2012
Water (hydrate, surface, or entrapped)	Formation of a hydrate of sucrose	Miller 2001
	Solubilization (heat of solution) of the surface of the crystals by residual moisture	Bhandari and Hartel 2002
	A non-stoichiometric entrapment of water in the crystal lattice and the affinity of added impurities for available water	Maulny 2003; Beckett 2006
Impurities and defects	A non-stoichiometric entrapment of water in the crystal lattice and the affinity of added impurities for available water	Maulny 2003, Beckett 2006
	Formation of different crystal structures due to the type and amount of impurities present in the mother liquor	Okuno 2003
	Defects in the lattice structure produced during crystallization	Kawakami and others 2006
Polymorphism	Formation of different crystal structures due to the type and amount of impurities present in the mother liquor	Okuno 2003
	Conformational polymorphism about the glycosidic linkage	Lee and Lin 2007a and b; Lee and Chang 2009
Hydrogen bond breaking	Breaking of some hydrogen bonds prior to the melting of the crystal structure	Reynhardt 1990
Particle size	Particle size differences within the sample	Magoń and others 2014

Table 3.2 Average DSC parameters (Tm onset, Tm peak, ΔH) and associated standard deviations for various sucrose sample ramped from 25 to 220°C at 10°C/min. Number of samples within each sample type is given in parentheses. Dash indicates that the small peak was not observed.

Sample sources	Small Tm onset °C	Small Tm peak °C	Small ΔH (J/g)	Tm onset °C	Tm peak °C	ΔH (J/g)
Beet Sucrose (17)	—	—	—	188.41±0.37	190.33±0.33	132.53±5.02
Cane Sucrose (26)	153.80±6.05	168.99±7.53	4.79±2.20	187.39±1.72	190.07±0.74	132.40±6.08
High ash cane (1)	—	—	—	179.54±0.72	188.42±0.64	125.43±4.35
Sugar in the Raw (cane) (1)	—	—	—	188.34±1.64	191.67±0.05	129.80±0.57
Chinese granulated cane (1)	—	—	—	187.94±0.58	190.19±0.16	138.25±0.21
Chinese castor cane (1)	—	—	—	186.64±0.75	189.42±0.40	130.8±0.14

Table 3.3 Average DSC parameters (Tm onset, Tm peak, ΔH) and associated standard deviations for 2 analytical grade cane sucrose samples (Sigma and Fisher) as a function of heating rate.

Analytical Sucrose (2)	Small Tm onset °C	Small Tm peak °C	Small ΔH (J/g)	Tm onset °C	Tm peak °C	ΔH (J/g)	After heating to 220°C
1°C/min	133.08±1.31	141.30±4.12	2.10±1.56	170.57±1.38	177.36±1.42	136.18±5.27	
5°C/min	144.44±1.44	156.35±7.60	4.91±1.82	184.54±1.11	189.50±0.33	132.55±8.10	
10°C/min	151.26±0.73	169.25±4.89	7.34±0.85	187.56±0.25	190.80±0.37	127.99±2.90	
25°C/min	156.75±1.06	172.02±1.52	8.56±1.64	188.34±0.61	191.96±0.47	127.33±12.85	
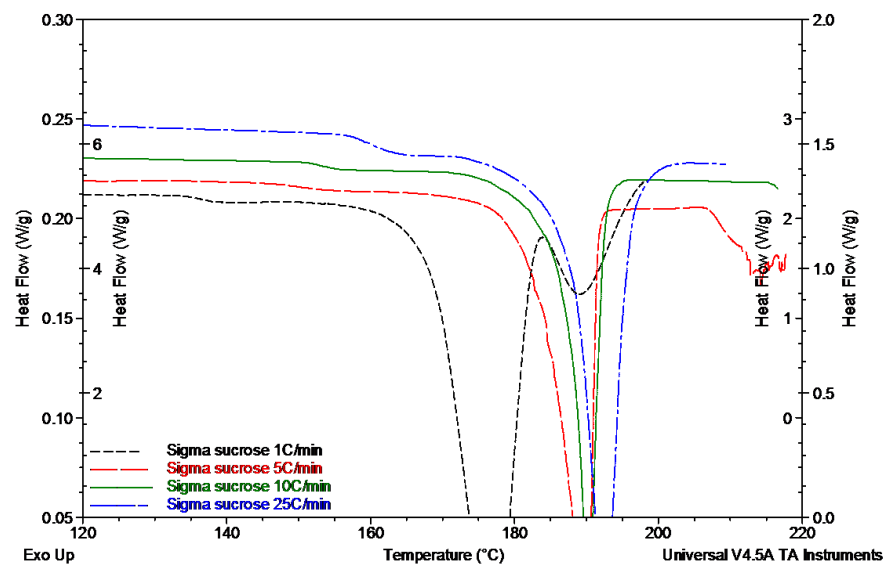
Figure 3.4 Example DSC thermograms of analytical grade Sigma cane sucrose at 1, 5, 10 and 25°C/min heating rates.

Table 3.4 Average DSC parameters (Tm onset, Tm peak, ΔH) and associated standard deviations for 3 white refined beet sucrose sources (US beet, Pioneer, and Meijer Brand) as a function of heating rate. The dash indicates that the small peak was not observed.

Beet Sucrose (3)	Small Tm onset °C	Small Tm peak °C	Small ΔH (J/g)	Tm onset °C	Tm peak °C	ΔH (J/g)	After heating to 220°C
1°C/min	—	—	—	182.43±0.85	185.60±0.91	127.22±10.05	
5°C/min	—	—	—	187.75±0.45	189.63±0.33	133.07±5.26	
10°C/min	—	—	—	188.01±0.31	190.03±0.40	131.25±3.91	
25°C/min	—	—	—	188.54±0.45	190.64±0.36	135.93±4.76	
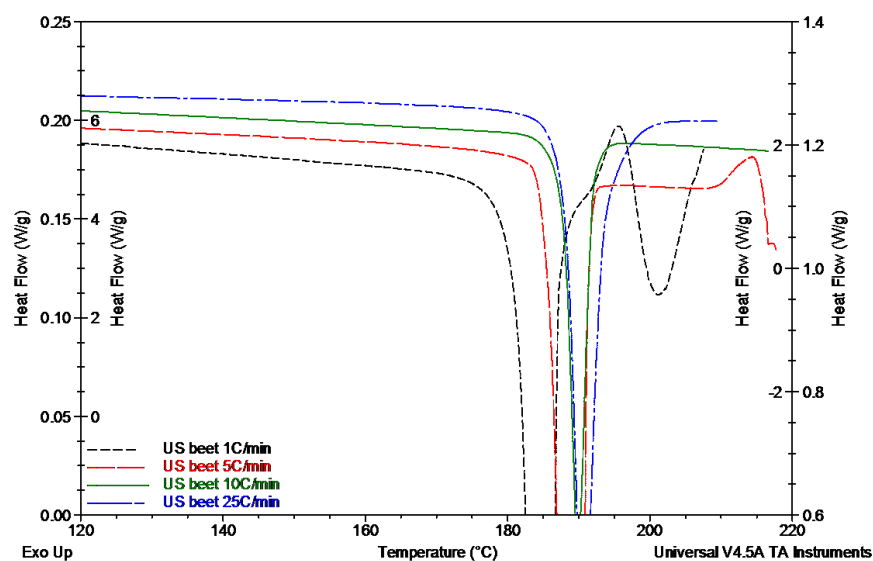
Figure 3.5 Example DSC thermograms of US beet at 1, 5, 10 and 25°C/min heating rates.

Table 3.5 Average DSC parameters (Tm onset, Tm peak, ΔH) and associated standard deviations for 2 white refined cane sucrose sources (US cane and C&H cane) as a function of heating rate. NM indicates the values were not measurable.

Cane Sucrose (2)	Small Tm onset °C	Small Tm peak °C	Small ΔH (J/g)	Tm onset °C	Tm peak °C	ΔH (J/g)	After heating to 220°C
1°C/min	133.28±0.65[a]	NM	NM	177.52±1.85	182.23±0.95	124.85±1.99	
5°C/min	144.35±1.11	165.52±1.99	2.76±1.74	186.85±0.47	189.24±0.25	135.98±2.31	
10°C/min	154.41±6.84	173.52±1.86	4.52±0.92	187.33±0.38	189.75±0.35	131.11±2.11	
25°C/min	156.81±0.84	174.62±2.43	4.01±1.65	188.26±0.19	190.68±0.25	136.60±3.56	

[a]The value at 1°C/min was extrapolate from the change in slope of the heat flow curves and used as an estimate of the small Tmonset value.
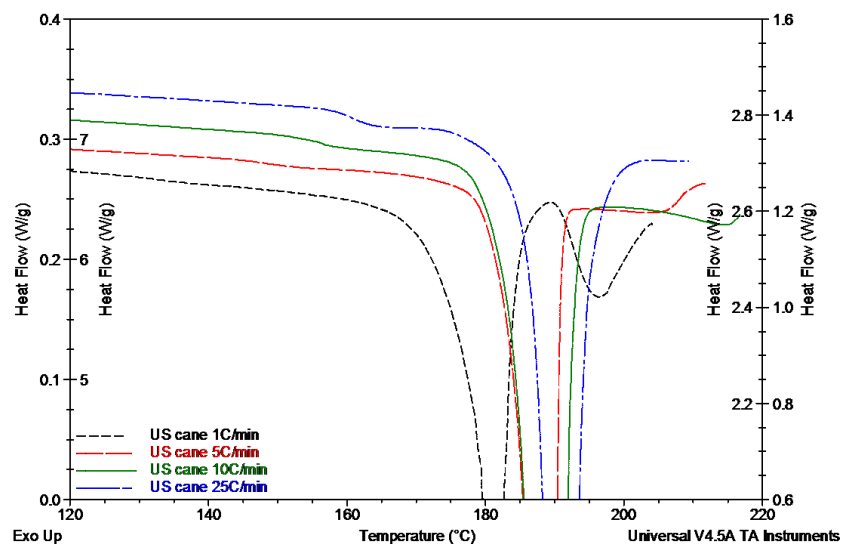
Figure 3.6 Example DSC thermograms of US cane at 1, 5, 10 and 25°C/min heating rates.

Table 3.6 Average DSC parameters and associated standard deviations for high ash cane sucrose as a function of heating rate. The dash indicates that the small peak was not observed.

High Ash Cane	Small Tm onset °C	Small Tm peak °C	Small ΔH (J/g)	Tm onset °C	Tm peak °C	ΔH (J/g)	After heating to 220°C
1°C/min	—	—	—	163.99±1.82	171.84±1.79	117.75±3.92	
5°C/min	—	—	—	173.86±0.28	183.06±0.54	131.35±1.06	
10°C/min	—	—	—	179.54±0.72	188.42±0.64	125.43±4.35	
25°C/min	—	—	—	186.10±0.50	189.58±0.06	135.20±0.42	
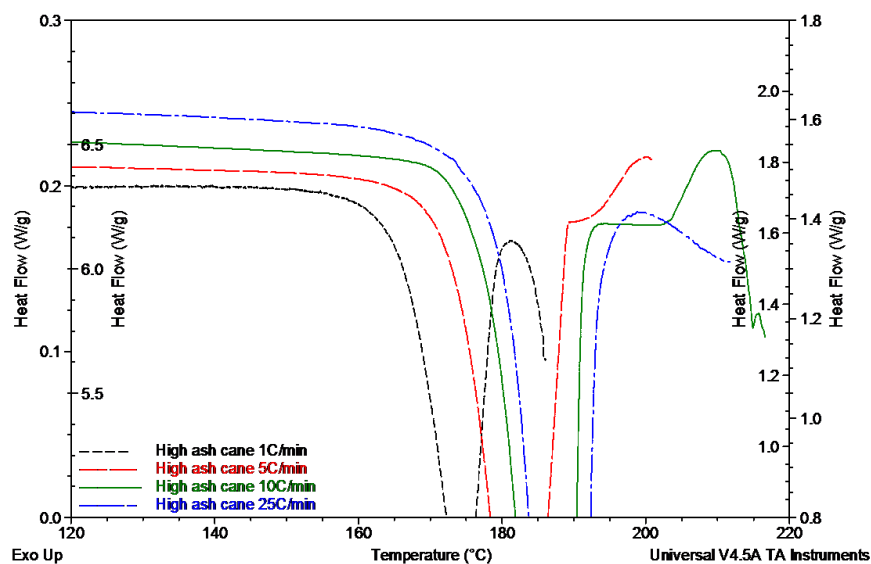
Figure 3.7 Example DSC thermograms of high ash cane at 1, 5, 10 and 25°C/min heating rates.

Table 3.7 Average DSC parameters and associated standard deviations for Sugar in the Raw (cane) sucrose as a function of heating rate. The dash indicates that the small peak was not observed.

Sugar in the Raw	Small Tm onset °C	Small Tm peak °C	Small ΔH (J/g)	Tm onset °C	Tm peak °C	ΔH (J/g)	After heating to 220°C
1°C/min	—	—	—	178.64±0.49	182.76±0.29	101.20±9.76	
5°C/min	—	—	—	187.38±0.95	190.05±0.43	120.80±1.41	
10°C/min	—	—	—	188.38±1.61	191.67±0.05	127.35±0.21	
25°C/min	—	—	—	188.61±2.25	194.10±2.45	127.95±6.43	
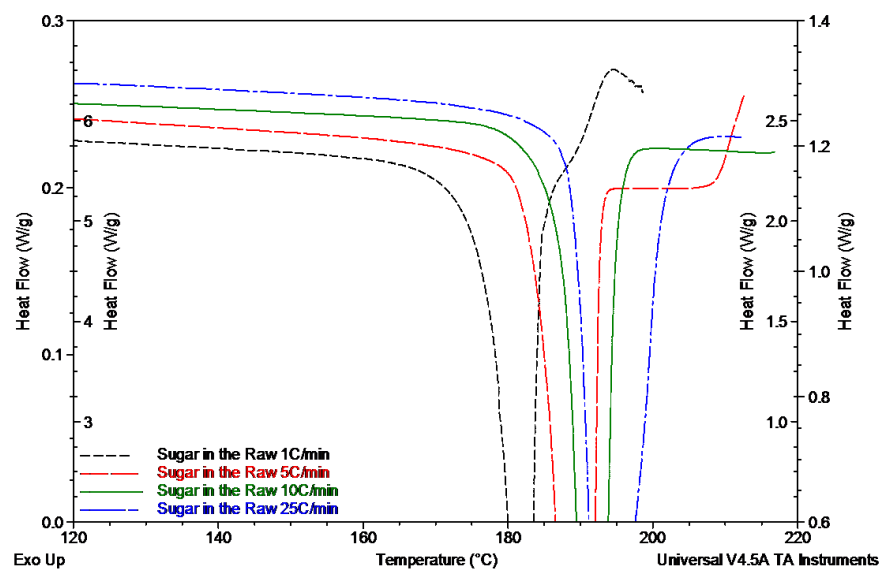
Figure 3.8 Example DSC thermograms of Sugar in the Raw cane at 1, 5, 10 and 25°C/min heating rates.
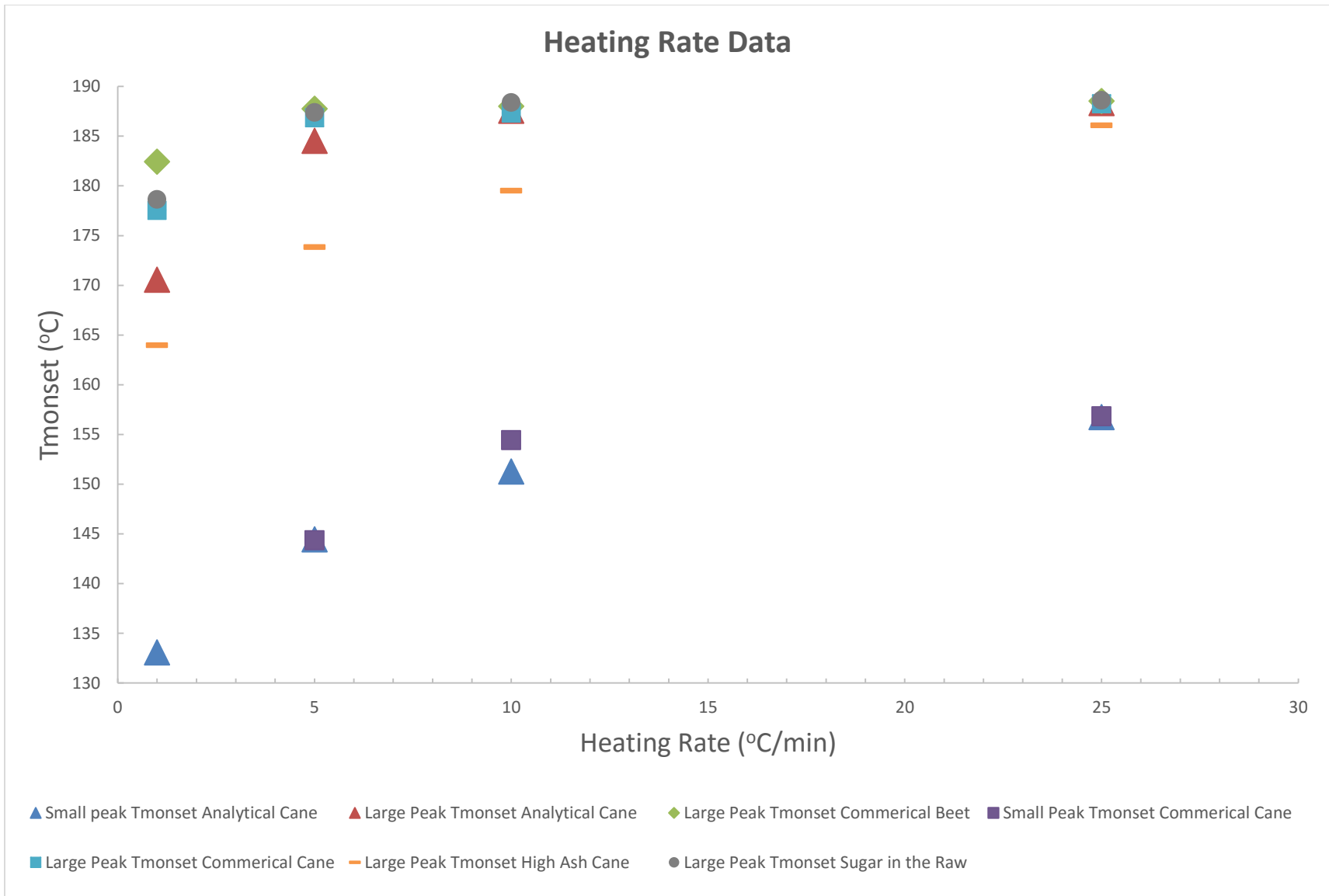
Figure 3.9 Small and large peak DSC Tmonset values as a function of heating rate for the 5 sucrose sample categories.
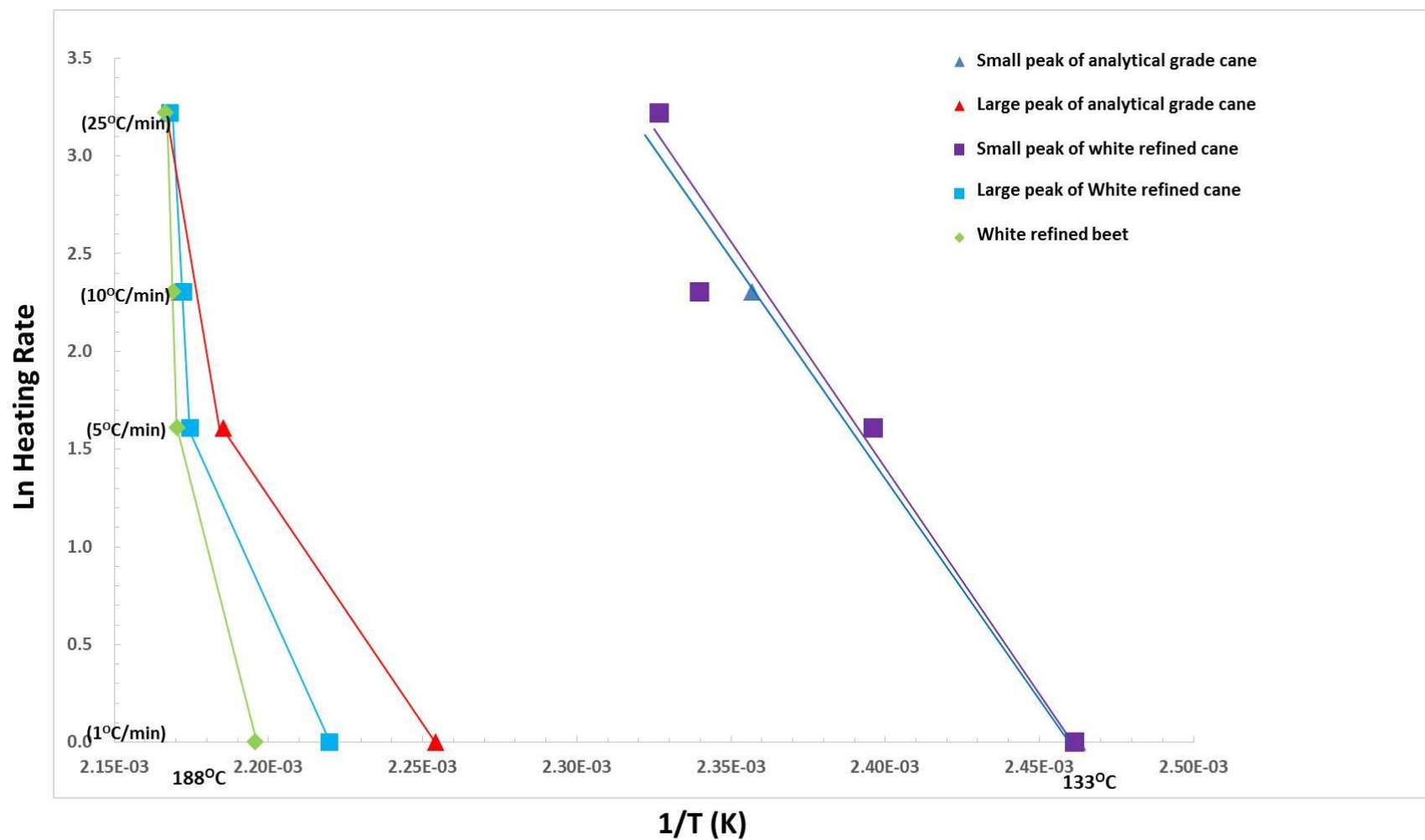
Figure 3.10 Heating rate dependency of sucrose samples from different sources.
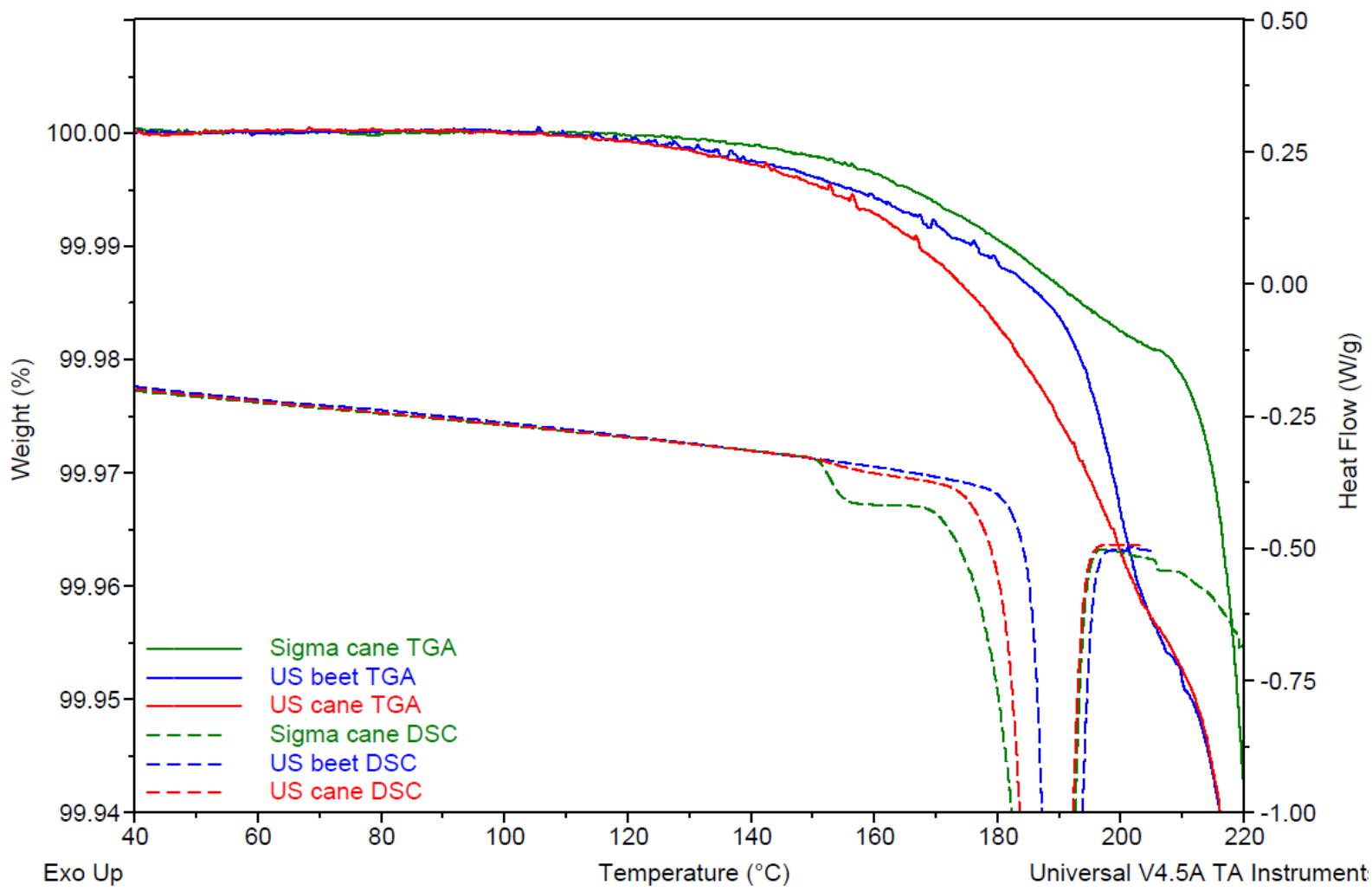
Figure 3.11 Comparison of the DSC thermal profiles and TGA weight loss profiles for analytical grade Sigma cane, US beet, and US cane sucrose samples at a 10°C/min heating rate.
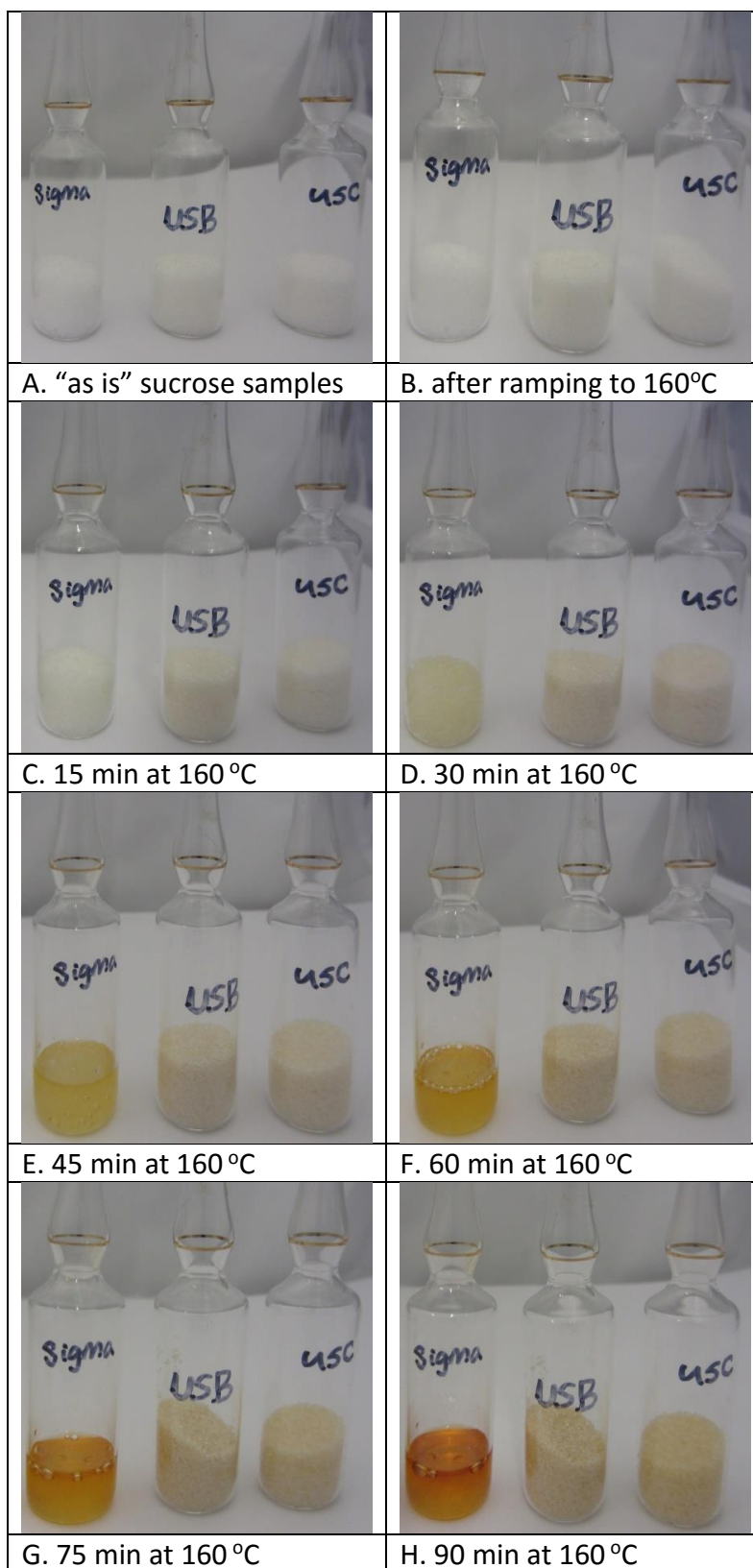
Figure 3.12 Observation of color and phase change, as a function of time, in analytical grade Sigma cane, US beet, and US cane samples held at 160°C in a GC oven for 180 minutes.

Figure 3.12 Continued.

I. 105 min at 160 °C	J. 120 min at 160 °C
K. 135 min at 160 °C	L. 150 min at 160 °C
M. 165 min at 160 °C	N. 180 min at 160 °C
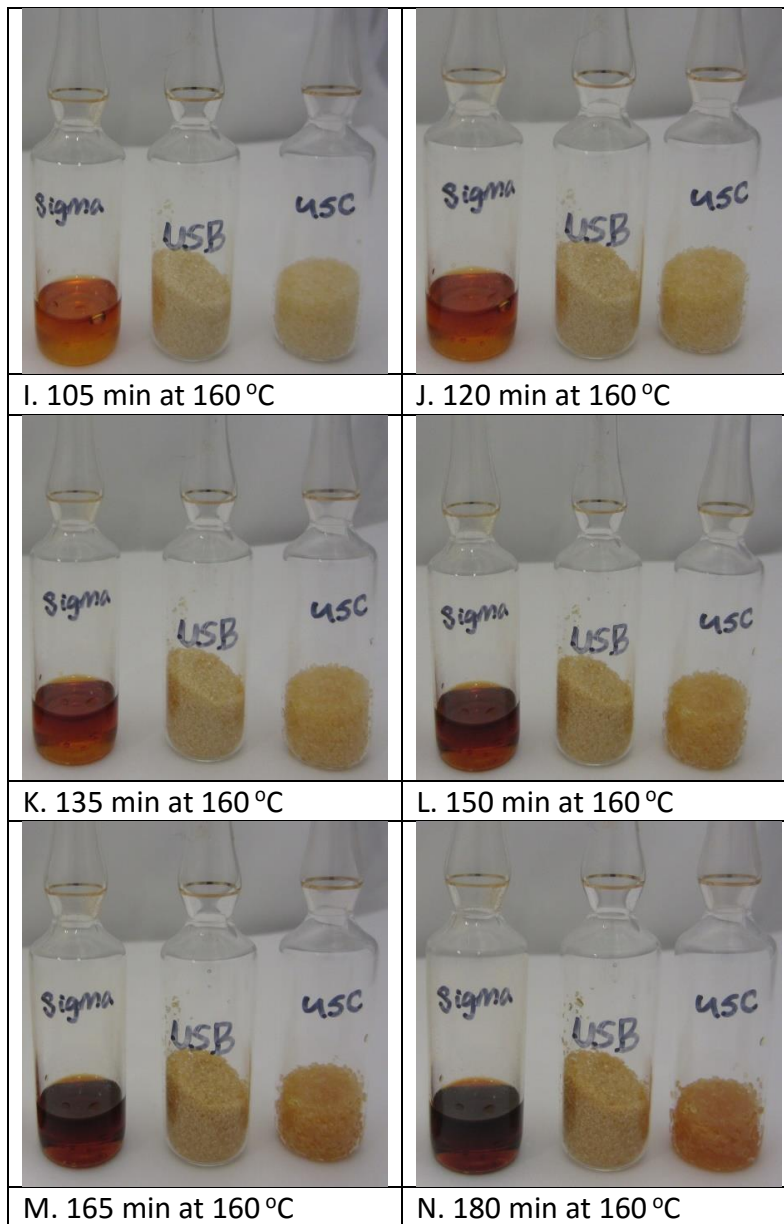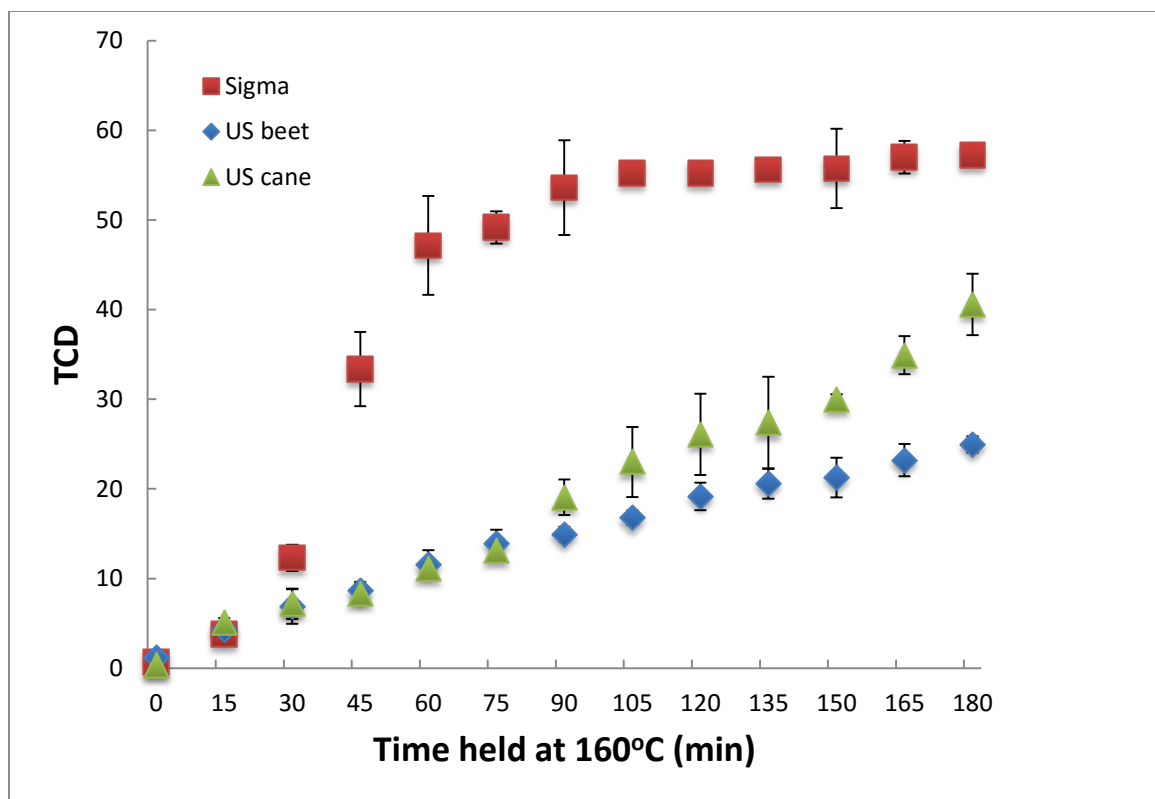
Figure 3.13 Average total color difference (TCD, Equation 3.1) values ± standard deviation, plotted as a function of time, for analytical grade Sigma cane, US beet, and US cane samples held at 160°C in a GC oven for 180 minutes. The zero time values in this plot correlate to image B in Figure 3.12, therefore all TCD measurements were obtained under isothermal conditions.

Chapter 4: Investigating the thermal decomposition differences between beet and cane sucrose sources using HPLC

4.1 Abstract

Sucrose, commonly termed sugar or table sugar, is an important commodity worldwide and is produced using mainly sugarbeet and sugarcane plants. Beet and cane sucrose sources are often used interchangeably by the food industry and in the home; however, despite their nearly identical chemical composition (usually >99% identical), differences in their instrumental aroma profile, sensory properties, product performance, and thermal behavior have been reported. In general, cane sucrose sources exhibit two endothermic DSC peaks, one small peak proceeded by one large peak; whereas, beet sucrose sources exhibit only one large endothermic DSC peak. Previous research studying analytical grade cane sucrose tied the small peak to the appearance of thermal decomposition components. However, no research was found exploring this relation for other sucrose samples, such as white refined cane or beet sources. Thus, the objective of this research was to investigate the relation between DSC thermogram differences and the appearance of thermal decomposition indicator components (glucose, fructose, and 5-HMF) in a variety of beet and cane sucrose sources, using high performance liquid chromatography (HPLC). Eleven sucrose samples, including analytical grade cane, commercial beet and cane, and laboratory-recrystallized beet, were heated at 10°C/min in a DSC to target temperatures, ranging from 140°C to 200°C at 10°C intervals. HPLC analysis was done on "as is" and heated sucrose samples using a lead form cation exchange column at 80°C, 0.6 ml/min flow rate, water mobile phase, equipped with RI and PDA detectors. In general, there was a strong, predictive relation between the DSC Tmonset value (for the small peak if

present or, if not present, for the large peak) and the temperature at which the initial thermal decomposition component(s) (TDConset) was detected using HPLC, for both beet and cane sucrose sources. However, in general, the temperature range over which these values occurred was substantially lower for cane compared to beet sucrose sources. In the case of analytical and white refined cane samples, the temperature range, at a heating rate of 10°C/min, was 150 (Tmonset of small DSC peak) to 170 (TDConset from HPLC analysis) °C; whereas, for white refined beet samples this temperature range was 188 (Tmonset of large DSC peak) to 200 (TDConset from HPLC analysis) °C. Thus, beet sucrose samples exhibited a greater thermal stability compared to cane sucrose samples. The cause of this wide variation in thermal stability is hypothesized to be related to differences in crystal composition and chemistry and is the subject of ongoing investigation in the Schmidt laboratory.

4.2 Introduction

Sucrose, commonly termed sugar, is an important commodity worldwide and is produced using mainly sugarbeet and sugarcane plant sources. Beet and cane sucrose sources are often used interchangeably by the food industry and in the home; however, despite their nearly identical chemical composition (usually >99% identical), differences in their instrumental aroma profile (Acree and others 1976; Parliment and others 1977; Monte and Maga 1982; Marsili and others 1994; Pihlsgard 1997; Magne and others 1998), sensory properties (Urbanus and others 2014a and b), product performance (Urbanus and others 2014a and b), and thermal behavior (Lu and others 2013) have been reported in the literature. In regards to the thermal behavior of sucrose, a number of interesting, as well as complicated, issues have been examined in the literature over a number of years, mainly using DSC, as summarized in Table 4.1. The issue of

focus in the present research is the thermal behavior differences between beet and cane sucrose sources.

Lu and others (2013) were the first to report that, in general, cane sucrose sources exhibited two endothermic DSC peaks, one small peak proceeded by one large peak; whereas, beet sucrose sources exhibited only one large endothermic peak. Example DSC thermograms for analytical grade Sigma cane, US cane, and US beet source samples are shown in Figure 4.1. Lu and others (2013) noted that four of thirty cane sucrose samples showed exception to this general observation, exhibiting only one endothermic DSC peak. The four cane sucrose sample exceptions contained either excess (high ash content cane and Sugar in the Raw samples) or processing added (residual sulfite in both Chinese cane samples) impurities, suggesting that the thermal behavior differences observed for these four cane samples are potentially associated with the presence of impurities and that perhaps the one large peak observed for the beet sucrose samples may also be related to the presence of impurities. The DSC thermogram for Sugar in the Raw, a cane sucrose source exception, is shown in Figure 4.1. As can be seen, the DSC thermogram for Sugar in the Raw is more similar to the DSC thermogram for US beet than for the cane sucrose thermograms.

Of interest to the research herein is to determine if the aforementioned thermal behavior differences between beet and cane sucrose sources are associated with the initial thermal decomposition component detection temperature. The predominant mechanism of sucrose thermal decomposition, in the presence (dashed arrow) and in the absence (solid arrow) of an aqueous solution, is provided in Figure 4.2. The different stages and products formed during the sucrose decomposition reaction, numbered in Figure 4.2, are briefly outlined below, according

to Lee and others (2011b). Once sucrose is broken down into glucose [1] and fructose

carbocation [1] via sucrose hydrolysis, glucose forms acidic and other decomposition

components through further reactions, which are not shown in Figure 4.1. Fructose carbocation,

due to its instability, immediately participates in subsequent, more complex reactions, resulting

in the formation of various decomposition components, including anhydrofructose [2a] by

cyclization; a wide range of products, such as 5-(hydroxymethyl)furfural (5-HMF) [2b], by

nonspecific degradation (e.g., condensation); oligosaccharides (kestoses) [2c] by combining

with the hydroxyl oxygen of another saccharide (mostly sucrose); and fructose [2d] by

accepting a hydroxyl ion (OH-) from water. These intermediate products are produced through

similar mechanisms in the presence and absence of an aqueous solution. However, in the

absence of an aqueous solution, minor products, such as anhydrous sucroses [3] and sucrose

isomers [4], are also produced through minor reaction pathways.

Previous research, studying analytical grade Sigma cane sucrose, tied the onset of the

small endothermic DSC peak to the appearance of three initial thermal decomposition indicator

components, glucose, fructose, and 5-(hydroxymethyl)furfural (5-HMF) (Lee and others 2011a

and b). However, no research was found exploring this type of relation for other sucrose

sources. Thus, the objective of the research herein was to investigate the possible association

between the DSC thermogram differences and the appearance of selected thermal

decomposition indicator components (glucose, fructose, and 5-HMF) in a variety of beet and

cane sucrose sources using high performance liquid chromatography (HPLC).

4.3 Materials and Methods

Materials

Eleven sucrose samples, representing a variety of sucrose types, were selected for study. These included two analytical grade cane (Sigma [S0389, ≥ 99.5%] and Fisher [S5-500, Certified ACS, purity not reported]), three white refined commercial beet (US beet, Pioneer beet, and Meijer beet), two white refined commercial cane (US cane, C&H cane), one commercial Turbinado cane (Sugar in the Raw), one high ash cane (sample number 11 in Appendix D from SPRI, New Orleans, LA), one commercially available granulated Chinese cane purchased from a market in Beijing, China, and one laboratory recrystallized US beet sample (recrystallization procedure is provide below). Detailed sample information for all commercially available sucrose samples is given in Appendix E. All sucrose samples were tested "as is," without further purification.

Standards used for HPLC analysis, including crystalline sucrose (S0389, ≥ 99.5%), D-(-)-fructose (F0127, ≥ 99.5%), D-(+)-glucose (G8270, ≥99.5%), and 5-(hydroxymethly)furfural (W501808, 5-HMF ≥ 99%) were purchased from Sigma-Aldrich Co. (St. Louis, MO) and used without further purification. HPLC grade water (Fisher Scientific Inc., Pittsburgh, PA) was used for the preparation of standard and sample solutions. Ethanol (Decon's Pure Ethanol 200 Proof) was purchased from Decon Labs (King of Prussia, PA).

Methods

Recrystallization of beet sucrose

A saturated sucrose solution was prepared by adding 78 g of US beet sucrose in 24 g of HPLC grade water, based on the reported sucrose saturation value of sucrose of 77.5g per 100 g of solution at 75°C (Taylor 1947). The recrystallization protocol used was adapted from Ouiazzane and others (2008). The saturated sucrose solution was heated to 75°C and gently

stirred in a 500mL glass beaker for 30 min to assist in the dissolving of all crystals. The temperature of the sucrose solution was then allowed to drop slowly to 40°C. The temperature was then held at 40°C to allow nucleation and subsequent crystals growth to occur. After holding at 40°C for approximately 3 hours, the temperature was cooled down to room temperature (approximately 25°C) in order to harvest the crystals. The solution containing the crystals was transferred to a Buchner funnel for filtration and crystals were rinsed with ethanol to remove the surrounding mother liquor solution. After rinsing, crystals were harvested and placed in a desiccator to continue drying for 48 hours before use.

DSC analysis and HPLC sample preparation

According to previous research work carried out in the Schmidt laboratory (Lee and others 2011b), thermal preparation of samples was done using a DSC Q2000 (TA Instruments, New Castle, DE), equipped with a refrigerated cooling system (RCS 90). The DSC was calibrated for enthalpy and temperature using a standard indium sample (Tmonset of 156.6 C, ΔH of 28.71 J/g, TA Instruments, New Castle, DE) prior to sample scanning. Hermetic aluminum Tzero pans and lids (TA Instruments, New Castle, DE) were used for all calibration and sample measurements, including an empty pan as the reference. Dry nitrogen, at a flow rate of 50 mL/min, was used as the purge gas. The eleven selected sucrose samples were heated at 10°C/min in the DSC to seven target temperatures (140°C, 150°C, 160°C, 170C, 180°C, 190°C and 200°C). Three sample pans of sucrose (approximately 9.0 mg each) were loaded in the DSC cell; one pan was placed on the sample platform and the others were placed on the bottom of the DSC cell. After the sample was heated (reaching, on average, a temperature approximately 1.5°C lower than target temperatures), the DSC was quickly equilibrated back to room temperature at approximately a

35°C/min cooling rate and, after removal from the cell chamber, the appearance of the sample inside the DSC pan was recorded using a Canon PowerShot ELPH 300 HS 12.1-Megapixel Digital Camera. Universal Analysis (UA) software was used to obtain the melting parameters (onset melting temperature, Tm onset; peak melting temperature, Tm peak; and enthalpy of melting, ΔH J/g) and plot the average heat flow signals.

HPLC analysis

Approximately 20 mg of each sucrose sample prepared in the DSC cell, as describe above, was dissolved in 2mL of HPLC water and then transferred to 2mL screw thread robovial with a silicane septa cap before injection (Fisher Scientific Inc., Pittsburgh, PA). HPLC analysis was conducted using a Waters 2695 Alliance HPLC system (Waters, Milford, MA), equipped with a Hewlett-Packard interface 35900E A/A converter. Analysis of both "as is" and heated sucrose samples prepared with HPLC water were carried out using the Aminex HPX-87C calcium form cation exchange resin based analytical column (300 $\times$ 7.8 mm) packed with sulfonated divinyl benzenestyrene copolymer with a particle size of 9 μm (Bio-Rad Lab., Richmond, CA). The guard column was a Carbo-C Refill cartridge (30 $\times$ 4.6 mm) (Bio-Rad Lab., Richmond, CA). HPLC grade water was used for the mobile phase. The analytical column temperature was maintained at 80°C and the guard column at 30°C. The flow rate was set to 0.6 mL/min. All samples were injected into the HPLC system using a 20 μm loop injector. A Waters 410 refractive index (RI) detector (Waters, Milford,MA) was connected to a Hewlett-Packard series 1050 photodiode array (PDA) detector (Hewlett-Packard, Palo Alto, CA) for the sucrose samples. While sucrose, glucose, and fructose were determined using the RI detector, 5-HMF was simultaneously measured using the PDA detector at a wavelength of 284 nm. Chromatographic peaks were

identified by comparing retention times and spectra to those of known standard solutions. A mixed standard solution, containing sucrose, glucose, fructose, and 5-HMF, was used for HPLC analysis of all sucrose samples. All computations were performed using an Agilent ChemStation (ChemStation for LC 3D Rev A. 08. 03, Agilent Technologies, Inc., Santa Clara, CA). For ease of comparison, the DSC heat flow signal and the HPLC sucrose, glucose, fructose and 5-HMF concentration results for each sample, were plotted on the same graph. Sucrose concentration was displayed as the average % ratio of sucrose remaining; whereas, glucose, fructose, and 5-HMF concentrations were displayed as the average % ratio of the decomposition component formed and plotted as a function of the target temperatures. HPLC analysis was done in duplicate for all three batches of sucrose samples. The limit of quantification (LOQ) of the HPLC analysis was 0.011 g/L for sucrose, 0.043 g/L for glucose, 0.032 g/L for fructose, and 0.0008 g/L for 5-HMF.

4.4 Results and Discussion

For ease of comparison, the DSC and HPLC results for each sucrose sample tested were plotted on the same graph, accompanied by the sample images taken "as is" and after heating to each temperature, using a Canon Digital Camera. Details of this graphing procedure are further explained, using Figure 4.3 as an example. As can be seen in Figure 4.3, the DSC heat flow signal for analytical grade Sigma cane sucrose at 10°C/min is plotted as a function of temperature and the HPLC concentration results (in %, w/w) of sucrose remaining and the selected thermal decomposition indicator components (glucose, fructose and 5-HMF) formed are also plotted, when detected, at each target temperature. The Figures are organized as follows: analytical grade cane sucrose (Sigma and Fisher) in Figures 4.3 and 4.4, respectively;

white refined cane sucrose (United Sugar [US], C&H, Sugar) in Figures 4.5 and 4.6, respectively; white refined beet sucrose (US, Pioneer, and Meijer) in Figures 4.7, 4.8, and 4.9, respectively; high ash cane in Figure 4.10; Sugar in the Raw (cane) in Figure 4.11; Chinese cane in Figure 4.12; and laboratory recrystallized US beet sucrose in Figure 4.13. DSC thermal behavior results are discussed individually below and then in combination with the HPLC results.

DSC Thermal Behavior

A difference in the number of endothermic peaks can be observed in the DSC thermograms for the various sucrose sources tested (Figures 4.3 to 4.13). As previously reported by Lu and others (2013; Chapter 3 herein) and discussed in the Introduction, the analytical and white refined cane sucrose samples exhibited two endothermic DSC peaks (at 10°C/min), one small (Tmonset approximately 151 to 154°C) and one large peak (Tmonset approximately 187°C); whereas the white refined beet samples exhibited only one large endothermic peak (Tmonset approximately 188°C). The high ash cane (0.107% ash compared to an average value of 0.02% for commercial sucrose, Tmonset approximately 180°C), Sugar in the Raw (cane, Tmonset at approximately 188°C), and Chinese granulated cane (Tmonset at approximately 188°C) sucrose samples exhibited one large endothermic peak, at an onset temperature similar to that of the white refined beet sucrose samples. However, unlike the white refined US beet sample, the laboratory recrystallized US beet sample exhibited two endothermic DSC peaks, one small peak, with a Tmonset of approximately 147°C, and one large endothermic peak, with a Tmonset of approximately 174°C. Recrystallizing the white refined US beet sucrose in HPLC grade water increased the purity of the sample, based on preliminary ICP measurements (Appendix G), but surprisingly decreased the DSC Tmonset value by

approximately 41°C (difference in Tmonset values, Figures 4.7 and 4.13). Preliminary ICP was done instead of conductivity ash, since the amount of sample required for conductivity ash analysis is much larger than can be reasonability obtained via laboratory recrystallization. The conductivity ash for "as is" US beet was 116.1 ± 4.8 ppm.

Becket and others (2006) reported a similar, but slightly more complicated, finding for a high ash beet sugar sample from Silver Spoon. Both the "as is" and recrystallized, without purification, beet sugar samples exhibited one endothermic peak (Tmpeak = 192.4±0.2°C and 190.0 ± 0.1°C, respectively). However, the recrystallized, with purification using ion-exchange, beet sugar exhibited two endothermic peaks, one small (Tmpeak = 151.9 ± 0.2°C) and one large (Tmpeak = 174.3 ± 0.6°C) peak. The complication in the Beckett and others (2006) study was that the recrystallized, without purification, beet sugar sample stilled exhibited only one large peak and it was not until purification using ion-exchange was employed that two peaks were observed. However, the conductivity values reported by Beckett and others (2006) help to resolve this complication – "as is" (17.98 ± 0.23 C [µS cm^{-1}] at 22°C), recrystallized, without purification (24.50 ± 0.55 C [µS cm^{-1}] at 24°C), and recrystallized, with purification using ion-exchange (9.32 ± 1.46 C [µS cm^{-1}] at 24°C) – thus, the recrystallized, without purification sample was actually less pure than the "as is" sample. Overall, Beckett and others (2006) concluded that the presence of the lower melting peak at approximately 150°C (termed herein the small peak) was highly dependent on the purity of the sucrose used, especially in terms of the mineral salt content, and was contradictory to expectations that the lower melting peak was observed for the purer sugars. The link between the presence of the small peak, sucrose

source, and purity is currently under further investigation in the Schmidt laboratory (Lu and others 2015; Chapter 5 herein).

In addition to considering the link between the presence of the small peak, sucrose source, and purity, it is also important to consider the link between the presence of the small peak, sucrose source, and crystal structure. No literature was found comparing the crystalline structure of beet and cane sucrose sources. However, as reviewed by Lee and others (2011a) and Lu and others (2013; Chapter 3 herein), a number of articles have hypothesized that the small peak in cane sucrose is due to polymorphism, that is, the presence of an additional crystal structure (e.g., Shallenberger and Birch 1975; Kishihara and others 2001; Okuno and others 2003; Lin 2007; Lee and Lin 2007; Lee and Chang 2009). On the other hand, other articles have concluded, based on X-ray diffraction data, that there is no evidence of polymorphism, despite the difference in the number of peaks observed in the DSC thermogram (e.g., Reynhardt 1990; Kawakami and others 2006). Thus, crystal structure studies, including crystal quality, are also underway in the Schmidt laboratory (Lu and others 2015; Chapter 5 herein).

DSC thermal behavior and HPLC detection of thermal decomposition components

Analyzing the connection between the DSC and HPLC measurements for all sucrose samples tested (Figures 4.3 to 4.13), reveals that there is a strong, predictive relation between the DSC Tmonset value (for the small peak if present or, if not present, for the large peak) and the temperature at which the initial thermal decomposition indicator component is detected (TDConset) using HPLC. For most samples, the TDConset value (°C) determined using HPLC is approximately 10°C higher than the DSC Tmonest value. For convenience, Table 4.2 summarizes the DSC Tmonset values and corresponding temperature at which the initial thermal

decomposition indicator component(s) was detected for each sucrose sample. Two exceptions

are noted in Table 4.2. First, the white refined cane samples, which exhibited a very shallow

small peak compared to the analytical cane samples, had approximately a 20°C difference.

Unfortunately, since the HPLC analyses were done at 10°C intervals, in an effort to screen the

thermal decomposition behavior of a large number of sucrose samples, it was not possible to

estimate the onset of thermal decomposition more precisely. Second, the high ash cane sample

had a lower temperature for detection of the first thermal decomposition indicator

components compared to the DSC Tmonset value.

Lee and others (2011b) reported a similar connection between DSC and HPLC

measurements for analytical grade Sigma cane sucrose as those observed for the majority of

the sucrose samples studied herein. In the Lee and others (2011b) study, the presence of the

first thermal decomposition indicator components, detected by HPLC analysis, was concomitant

with the Tmonset of the small endothermic DSC peak, both occurring at a target temperature of

151.0°C, at a 10°C/min heating rate (sample temperature 149.6°C). This initial thermal

decomposition component detection temperature reported by Lee and others (2011b) is

approximately 10°C lower than the one determined herein (160°C) for analytical grade Sigma

cane sucrose. Additionally, the amount of glucose detected herein at 160°C of 0.60 % was lower

than that reported by Lee and others (2011b) of 1.27%. These differences may be attributable

to the use of different lots of analytical grade Sigma cane sucrose purchased from Sigma-Aldrich,

which, according to Eggleston and others (1996), can vary in the amount of residual salts

present even between lots of the same analytical sucrose product and/or the slightly higher

HPLC column temperature used in Lee and others (2011b) of 85°C compared to 80°C used

herein.

Another significant observation from Table 4.2 is that there appears to be a large difference in thermal stability, both between and within sucrose sources. There seems to be no widely accepted definition for the term thermal stability in the literature, but rather the term seems to vary from a focus on the ability of a material to retain its useful properties (e.g., Papkov n.d.; Davis 1997) to a resistance to thermal decomposition (Doyle 1961). Thus, for clarity, the term thermal stability as used herein is defined as the resistance to the loss of crystalline structure at a given temperature, with or without the formation of thermal decomposition components. Three specific examples of between and within sucrose source thermal stability differences are discussed below. In the first example, analytical and white refined cane samples exhibited a DSC Tmonset of approximately 151°C and an initial thermal decomposition component detection temperature of 160°C and 170°C, respectively, whereas white refined beet sucrose samples exhibited a DSC Tmonset of approximately 188°C and an initial thermal decomposition component detection temperature of 200°C. Thus, in general, white refined beet sucrose, with a much higher DSC Tmonset and initial thermal decomposition component detection temperature, exhibited greater thermal stability than analytical and white refined cane sucrose.

In the second example (Table 4.2), white refined cane samples (US beet and C&H) exhibited a DSC Tmonset of approximately 151°C and a detection temperature of 170°C, whereas Sugar in the Raw (cane) exhibited a DSC Tmonset of approximately 188°C and a detection temperature of 200°C. Thus, despite being less pure, Sugar in the Raw exhibited greater thermal stability than the white refined cane sucrose. This observation points to the

potential protective role that some impurities may play in the thermal stability of sucrose discussed in the literature (Kamota 1960; Okuno and others 2002a and b and 2003; Maulny 2003; Beckett and others 2006; Lu and others 2013 [Chapter 3 herein]).

In the third example (Table 4.2), "as is" white refined beet exhibited a DSC Tmonset of approximately 188°C and an initial thermal decomposition component detection temperature of 200°C, whereas laboratory recrystallized beet exhibited a DSC Tmonset of approximately 147°C and a detection temperature of 150°C. As discussed in the DSC Thermal Behavior section, recrystallizing the white refined beet sucrose in HPLC grade water increased the purity of the sample, but decreased its thermal stability. Another possible explanation for the thermal behavior differences between the "as is" and laboratory recrystallized beet sample, in addition to purity, is a possible difference in crystal structure. Kawakami and others (2006), studying the melting behavior of intact (referred to as "as is" herein) and moisture induced recrystallized sucrose (source of sucrose was not identified), obtained DSC thermograms with both one and two peaks, but they reported that the X-ray diffraction measurements showed no crystal structure differences.

An additional aspect of this thermal stability discussion that deserves attention is the distinct difference in the appearance of the selected thermal decomposition components for cane and beet sucrose samples revealed by HPLC analysis. For the analytical and white refined cane sucrose sources exhibiting the small peak, glucose was the first thermal decomposition indicator component detected (Table 4.2); whereas for white refined beet, Sugar in the Raw, and Chinese cane sucrose sources, all three thermal decomposition indicator components (glucose, fructose, and 5-HMF) were detected at the same initial target temperature (Table 4.2).

The laboratory recrystallized US beet sample was unique in that both glucose and 5-HMF were observed at the same initial target temperature. This variation in appearance of the selected thermal decomposition components suggests a difference in the kinetics underlying the thermal decomposition (caramelization) reaction. Additional research on the comparison of the caramelization kinetics of beet and cane sucrose is already underway in the Schmidt Laboratory (Chapter 3 herein; Averill and Schmidt 2016). For future HLPC studies involving the detection of initial thermal decomposition components in sucrose, it is important to note that at the same target temperature as the appearance of glucose, an additional, measurable peak was also observed in the HPLC chromatogram, just prior to the peak for sucrose. This peak can be seen in the example HPLC chromatogram for analytical grade Sigma sucrose heated to 160°C, shown in Figure 4.14. This peak was observed at the same target temperature as that for the appearance of glucose in the HPLC chromatograms for all the sucrose samples studied herein. Though the absolute identification of this peak was beyond the scope of this study, based on the work of Richards (1986) and Manley-Harris and Richards (1991), we hypothesize this peak to be attributable to the formation of trisaccharides, specifically the kestoses (fructosylsucrose derivatives).

The underlying cause(s) of the difference in thermal stability between and within sucrose sources discussed above is hypothesized to be due to differences in crystal composition and chemistry and is under further investigation in the Schmidt laboratory. In order to obtain a complete picture of all potential factors, crystal structure and morphology measurements are also being carried out.

Two additional observations of significance can be made based on comparison of the DSC and HPLC results. First, the magnitude of the small endothermic DSC peak is related to the temperature at which the first thermal decomposition indicator component was detected. This observation can be seen by comparing the small endothermic DSC peak ΔH values and the temperature at which the first thermal decomposition indicator component was detected by HPLC for analytical grade cane sucrose (both Sigma and Fisher, Figures 4.3 and 4.4 respectively) to those for white refined cane sucrose (US cane and C&H, Figures 4.5 and 4.6, respectively). The average ΔH and temperature of component (glucose) detection for the analytical grade cane samples was 7.34 ± 0.85 J/g at 160°C; whereas the average ΔH and temperature of component (glucose) detection for the white refined cane samples was 4.52 ± 0.92 J/g and 170°C and the temperature of component (glucose) detection was 20°C higher than the Tmonset in the case of white refined cane compared to 10°C in the case of analytical grade cane samples. For the interested reader, the concentration of selected thermal decomposition indicator components (glucose, fructose and 5-HMF formation, % w/w), as well as the remaining sucrose concentration at "as is" and target temperatures are given in Appendix F. Based on the concentration data in Appendix F, the amount (concentration) of thermal decomposition indicator components detected is commensurate with the magnitude (ΔH) of the small endothermic DSC peak. At 180°C (last target temperature before the onset of the large endothermic peak), the concentration of glucose formed and the ΔH for analytical grade cane samples (1.2% and 7.34 J/g) are larger than those values for white refined cane samples (0.61% and 4.52 J/g). The ΔH values were obtained from Chapter 3 (Tables 3.4 and 3.6, respectively).

Second, there is a difference between beet and cane (both analytical and white refined)

sucrose sources in terms of crystal morphology retention, as observed visually, when the first

thermal decomposition indicator component(s) is detected via HPLC. Crystal morphology herein

refers to the external crystal structure or appearance. In the case of the cane samples (Figures

4.3 to 4.6), the external crystal morphology is still intact when the first thermal decomposition

indicator component (glucose) is detected via HPLC. Lee and others (2011b) reported no

obvious changes in the external crystal appearance, despite the detection of thermal

decomposition components at 150°C (10°C/min heating rate), in their investigation of the

thermal decomposition behavior of analytical grade Sigma cane sucrose. However, in the case

of the beet sucrose samples (Figures 4.7 to 4.9), the solid crystals are in the process of

transitioning to the liquid state when the first thermal decomposition components are detected

via HPLC. Interestingly, however, if heating of an analytical grade Sigma cane sample at

10°C/min is stopped at 165°C, cooled quickly, and rescanned, the resultant DSC thermogram

contains a glass transition temperature (Tg) with onset and midpoint values of 58.64 and

63.64°C and a Δcp value of 0.037 J/g, as well as a melting peak (Tmonset = 187.6°C and ΔH =

141.4 J/g). The appearance of the Tg in the DSC rescan (no Tg was observed in the original scan)

indicates that a loss of crystalline structure occurred in the cane sample during heating, but

since the crystal morphology was still intact at 165°C, loss of crystalline structure is

hypothesized to have occurred on the inside of the crystal, not on the outside as would be

expected based on the basic principle of conductive heat transfer. Additional research is

needed to further investigate this hypothesis.

To supplement these findings regarding possible changes on the inside of the sucrose

crystal, analytical grade Sigma cane sucrose was held isothermally at 120°C for 480 minutes in the DSC and then cooled quickly and rescanned. The 120°C holding temperature was selected based on TGA data reported by Schmidt and others (2012), which showed a very small initial weight loss beginning at 120°C, indicative of the onset of thermal decomposition. HPLC analysis, as describe in the Materials and Methods section, was carried out at the end of the 480 minutes. The DSC and HPLC results are shown in Figure 4.15. Glucose and 5-HMF were both detected after holding at 120°C for 480 minutes, indicating that thermal decomposition occurred at 120°C, a temperature well below the literature reported melting temperatures of sucrose (DSC values ranging from 160 to 192°C at a 10°C/min heating rate, Appendix B). The DSC rescan showed both a Tg (onset at approximately 50°C) and only one large endothermic DSC peak. The distinct small peak observed for "as is" analytical grade Sigma cane sucrose (Figure 4.3) was no long observed, though the baseline does slope steadily into the large endothermic peak. The crystal morphology after 480 minutes at 120°C was still intact, again suggesting that the loss of crystalline structure occurred on the inside of the crystal, not on the outside. For comparison purposes, Figure 4.16 shows the DSC thermograms for "as is" analytical grade Sigma cane sucrose, "as is" US beet sucrose, analytical grade Sigma cane sucrose that was heated to 165°C cooled quickly, and rescanned, and analytical grade Sigma cane sucrose that was held at 120°C for 480 mins cooled quickly, and rescanned. As discussed above, the DSC thermogram for the heated and rescanned Sigma cane samples no longer contained the distinct small peak as observed for the "as is" Sigma cane sample; however, the baseline now slopes steadily into the large endothermic peak. "Pre-heating" the Sigma cane resulted in tempering of the small peak, suggesting that the thermal event associated with the

small peak began during "preheating" at both 165°C and holding at 120°C for 480 mins.

Kawakami and others (2006) held moisture-induced recrystallized sucrose at 120°C for 60 and 180 minutes and reported that the "small peaks at lower temperatures disappeared to probably be integrated into the main peak." The authors attributed the small peak(s) to defects in the crystal structure (i.e., crystal quality), which were partially modified by the annealing procedure. However, the explanation offered herein is that holding the "as is" sucrose at 120°C for 480 minutes results in the loss of crystalline structure via the production of thermal decomposition components (as supported by HPLC analysis) inside the crystal structure, similar to the thermal decomposition process that produces the small peak at approximately 150°C in non-isothermal DSC experiments at a 10°C/min heating rate (Figure 4.3). This hypothesis is supported by the observation of a Tg and the lack of the usual small endothermic peak in the DSC rescan (Figure 4.15). The proposed location of the initial production of thermal decomposition components is within the crystal defects, specifically those associated with incorporation of water, such as mother liquor occlusions (i.e., saturated sucrose solution occlusions). Both occlusion and inclusion terms have been used in the literature to describe mother liquor entrapment within the crystal structure. However, based on the definitions given by Harvey (2000) [Inclusion - a coprecipitated impurity in which the interfering ion occupies a lattice site in the precipitate; Occlusion – a coprecipitated impurity trapped within a precipitate as it forms] the term occlusion was selected for use. Powers (1956 and 1958), using microscopic and vapor pressure measurements, appears to be the first to have provided evidence of the presence of water inside the sucrose crystal (in the form of a "relatively pure sucrose solution") and later implicated his finding as the explanation for the widely varying values given in the

literature for the melting point of sucrose. However, it was recognized, as far back as Richards (1903), "substances crystallizing from a solution enclose within their crystals small quantities of the mother-liquor" and that this entrapment was exceedingly common, "It is no careless exaggeration to state that in all my chemical experience I have never yet obtained crystals from any kind of solution entirely free from accidentally included mother-liquor; and, moreover, I have never found reason to believe that anyone else ever has" (Richards 1903). A number of researchers have studied mother liquor occlusions in sucrose, including Powers (1956, 1958, 1959, 1970), Thomas and Williams (1967), Mackintosh and White 1968, Eastmond (1970), Gou and White 1983, Grimsey and Herrington 1994, and Vaccari (2010). It follows that the composition and chemistry of these occlusions would play a significant role in the crystal's thermal stability.

Lastly, there appears to be connection between the thermal stability as measured by total color difference (TCD; isothermal holding at 160°C for 180 minutes) in Chapter 3, for analytical grade Sigma cane, US cane, and US beet sucrose samples, and the HPLC measurements (non-isothermal) herein. The order of thermal stability based on TCD and temperature at which the first thermal decomposition indicator component was detected using HPLC was the same, in order from least to most thermally stable: analytical grade Sigma cane << US cane < US beet.

4.5 Conclusions

This research reveals, based on the comparison of DSC and HPLC measurements for the sucrose samples studied herein, a wide variation in thermal stability behavior between and within sucrose sources. This wide variation in thermal stability is hypothesized to be due to differences in crystal composition and chemistry mainly associated with sugar processing

differences. By employing appropriate instrumental analyses, we plan to characterize the physicochemical beet and cane sucrose sample attributes and, thus, predict the thermal behavior of "as is" sucrose samples and control the thermal behavior of our own laboratory-recrystallized sucrose samples. Some of the main physicochemical attributes to be investigated include, crystal structure and morphology, impurity type and amount, pH, and moisture content (both surface and water within the crystal).

4.6 Acknowledgements

4.7 References

Acree TE, Lee CY, Butts RM, Barnard J. 1976. Geosmin, the earthy component of table beet odor. J Agric Food Chem 24(2):430–1.

Comparison of the Caramelization Kinetics of Beet and Cane Sucrose. 2016. 77th Annual Institute of Food Technologists, Chicago, IL, B. Averill and S.J. Schmidt, submitted for presentation.

Bhandari B, Hartel R. 2002. Co-crystallization of Sucrose at High Concentration in the Presence of Glucose and Fructose. J. of Food Sci, 67: 1797–1802.

Bonelli P, Schebor C, Cukierman AL, Buera MP, Chirife J. 1997. Residual moisture content as related to collapse of freeze-dried sugar matrices. Journal of Food Science 62(4):693-695.

Bonn G (1985). High-performance liquid chromatographic elution behavior of oligosaccharides, monosaccharides and sugar degradation products on series-connected ion-exchange resin columns using water as the mobile phase. Journal of Chromatography 332:411-424.

Davis JR. 1997. Heat-Resistant Materials. ASM International Handbook Committee, ASM International, Materials Park, OH, pp. 597.

Doyle CD. 1961. Estimating Thermal Stability of Experimental Polymers by Empirical Thermogravimetric Analysis. Analytical Chemistry, 33(1):77-79.

Eastmond GC. 1970. Solid-state polymerization. Progress in Polymer Science, 2:1–46.

Eggleston G, Trask-Morrell BJ, Vercellotti JR. 1996. Use of differential scanning calorimetry and thermogravimetric analysis to characterize the thermal degradation of crystalline sucrose and dried sucrose-salt residues. J. Agric. Food. Chem. 44, 3319-3325.

Gardiner D (1966). The pyrolysis of some hexoses and derived di-, tri-, and poly-saccharides. Journal of the Chemical Society C, 1473-1476.

Gloria H, Sievert D. 2001. Changes in the physical state of sucrose during dark chocolate processing. Journal of Agricultural and Food Chemistry 49:2433-2436.

Grimsey IM and Herrington TM. 1994. The formation of inclusions in sucrose crystals. International Sugar Journal, 96:504-514.

Gou SY and White ET. 1983. Measurement of inclusions in sugar crystals using a density gradient column. Proceedings of Australian Society of Sugar Cane Technologists. 219-224.

Hubbard WS, Mitchel WL. 1915. The hydrolysis of sugar solutions under pressure. The Journal of Industrial and Engineering Chemistry (7):609-610.

Hurtta M, Pitkänen I, Knuutinen J. 2004. Melting behaviour of D-sucrose, D-glucose and D-fructose. Carbohydrate Research 339:2267-2273.

Kamoda M. 1960. Proceedings of the Research Society of Japan Sugar Refineries' Technologists. 27, 158–238.

Kawakami K, Miyoshi K, Tamura N, Yamaguchi T, and Ida Y. 2006. Crystallization of sucrose glass under ambient conditions: Evaluation of crystallization rate and unusual melting behavior of resultant crystals. Journal of Pharmaceutical Sciences, 95(6): 1354-1363.

Kishihara S, Okuno M, Fujii S, Kawasaki K, Nishiura T. 2001. An opinion on structure of sucrose crystal. Proceedings of the Research Society of Japan Sugar Refineries' Technologists 49:1-8.

Lee JW (2010). Investigation of thermal decomposition as the cause of the loss of crystalline structure in sucrose, glucose, and fructose. PhD dissertation. University of Illinois at Urbana-Champaign.

Lee JW, Thomas LC, Schmidt SJ. 2011a. Investigation of the heating rate dependency associated with the loss of crystalline structure in sucrose, glucose, and fructose using a thermal analysis approach (Part I). Journal of Agricultural and Food Chemistry, (59):684-701.

Lee JW, Thomas LC, Jerrell J, Feng H, Cadwallader KR, Schmidt SJ. 2011b. Investigation of thermal decomposition as the kinetic process that causes the loss of crystalline structure in sucrose using a chemical analysis approach (Part II). Journal of Agricultural and Food Chemistry, (59):702-712.

Lee JW, Thomas, LC, Schmidt SJ. 2011c. Can the thermodynamic melting temperature of sucrose, glucose, and fructose be measured using rapid-scanning DSC? Journal of Agricultural and Food Chemistry, 59 (7): 3306–3310.

Lee JW, Thomas LC, Schmidt SJ. 2011d. Effects of heating conditions on the glass transition parameters of amorphous sucrose produced by melt-quenching. Journal of Agricultural and Food Chemistry, 59 (7): 3311–3319.

Lee T and Chang GD. 2009. Sucrose conformational polymorphism. Crystal Growth and Design, 9(8): 3551-3561.

Lee T and Lin YS. 2007. Dimorphs of sucrose. International Sugar Journal, 109 (1303):440-445. Levine H, Slade L. 1989. Interpreting the behavior of low-moisture foods. In: Hardman TM, editor. Water and Food Quality. London, UK: Elsevier Science. p 71-134.

Lin YS. 2007. Master thesis "Two Conformational Polymorphs of Sucrose". National Central University.

Lu Y, Lee JW, Thomas L, Schmidt SJ (2013). Proceedings of the 74th Annual Institute of Food Technologists on Differences in the Thermal Behavior of Beet and Cane Sugars. Chicago, IL.

Mackintosh DL and White ET. 1968. Enclave inclusions in sugar crystals. Proceedings of Queensland Society of Sugar Cane Technologists, 35th Conference, p.245-253.

Magne V, Mathlouthi M, Robilland B, Magne M, Mathlouthi B. 1998. Determination of some organic acids and inorganic anions in beet sugar by ionic HPLC. Food Chem 61(4):449–53.

Magoń A, Wurm A, Schick C, Pangloli P, Zivanovic S, Skotnicki M, Pyda M. 2014. Heat capacity and transition behavior of sucrose by standard, fast scanning and temperature-modulated calorimetry. Thermochimica Acta, 589: 183-196. Article reprinted in 2015, Thermochimica Acta, 603, 149-161.

Manley-Harris M and Richards GN. 1991. Formation of trisaccharides (kestoses) by pyrolysis of sucrose. Carbohydrate Research, 14 (219):101-13.

Marsili RT, Miller N, Kilmer GJ, Simmons RE. 1994. Identification and quantitation of the primary chemicals responsible for the characteristic malodor of beet sugar by purge-and-trap GC-MS-OD techniques. J Chromatogr Sci 32(5):165–71.

Mathlouthi M, Cholli AL, Koenig J. L. Spectroscopic study of the structure of sucrose in the amorphous state in aqueous solution. Carbohydr. Res. 1986, 147, 1-9.

Mauch, W. The chemical properties of sucrose. Sugar Technol. Rev. 1971, 1, 239-290.

Maulny A. 2003. Co-crystallisation of sugars. Ph.D. Thesis, Department of Chemistry, University of Hull, Hull, UK.

Monte WC, Maga JA. 1982. Flavor chemistry of sucrose. Sugar Technol Rev 8(3):181–204.

Okuno M, Kishihara S, Otsuka M, Fujii S, Kawasaki K. 2003. Variability of melting behavior of commercial granulated sugar measured by differential scanning calorimetry. International Sugar Journal 105:29-35.

Ouiazzane S, Messnaoui B, Abderafi ., Wouters J, and Bounahmidi T. (2008). Estimation of sucrose crystallization kinetics from batch crystallizer data. Journal of Crystal Growth, 310(4), 798-803.

Papkov VS. (n.d.). Heat resistance and thermal stability of polymers. The Great Soviet Encyclopedia, 3rd Edition (1970-1979).

Parliment T, Kolor M, Maing I. 1977. Identification of the major volatile components cooked beets. J Food Sci 42(6):1592–3.

Pihlsgard P. 1997. The properties of sugar focusing on odours and flavours—a literature review. SIK Rapport (634).

Powers HEC. 1956. Growth of sucrose crystals. Nature, 178:139-140.

Powers HEC. 1958. Sucrose crystal inclusions. Nature, 182:715-717.

Powers HEC. 1959. Inclusions. International Sugar Journal, 17-18:41-44.

Quintas M, Guimarães C, Baylina J, Brandão TRS, Silva, CLM. 2007. Multiresponse modelling of the caramelisation reaction. Innovative Food Science and Emerging Technologies, 8 (2), pp. 306-315.

Raemy, A.; Schweizer, T. F. Thermal behaviour of carbohydrates studied by heat flow calorimetry. J. Therm. Anal. 1983, 28, 95-108.

Reynhardt EC. 1990. An NMR, DSC and X-ray investigation of the disaccharides sucrose, maltose and lactose, Molecular Physics: An International Journal at the Interface Between Chemistry and Physics, 69:6, 1083-1097.

Richards GN, Shafizadeh F (1978). Mechanism of thermal degradation of sucrose: A preliminary study. Aust. J. Chem. 31, 1825-1832.

Richards GN (1986). Initial steps in thermal degradation of sucrose. Int. Sugar J. 88, 145-148.

Richards TW. 1903. The inclusion and occlusion of solvent in crystals: An insidious source of error in quantitative chemical investigation. Proceedings of the American Philosophical Society, 42(172): 28-36.

Roos YH, Karel M. 1990. Differential scanning calorimetry study of phase transitions affecting the quality of dehydrated materials. Biotechnology progress 6:159-163.

Roos YH, Karel M. 1991. Plasticizing effect of water on thermal behavior and crystallization of amorphous food models. Journal of Food Science 56(1):38-43.

Roos YH. 1995. Food components and polymers. In: Taylor SL, editor. Phase Transitions in Foods. 1st ed. San Diego, CA: Academic Press. p 109-156.

Saleki-Gerhardt A, Zografi G. 1994. Non-isothermal and isothermal crystallization of sucrose from the amorphous state. Pharmaceutical Research 11(8):1166-1173.

Saavedra-Leos MZ, Grajales-Lagunes A, González-García R, Toxqui-Terán A, Pérez-García SA, Abud-Archila MA, Ruiz-Cabrera MA. 2012. Glass Transition Study in Model Food Systems Prepared with Mixtures of Fructose, Glucose, and Sucrose. Journal of Food Science, 77:5, 118-126.

Schiweck H, Clarke M, Pollach G. 1994. Sugar. Ullmann's Encyclopedia of Industrial Chemistry 34:557-628.

Shah SV, Chakradeo YM. 1936. A note on the melting point of cane sugar.   Journal of Current Science. P652-3

Shallenberger RS, Birch GG. Sugar Chemistry, The Avi Publishing Company Inc., Westport, Connecticut 1975.

Slade L, Levine H. 1988. Non-equilibrium behavior of small carbohydrate-water systems. Pure and Applied Chemistry 60(12):1841-1864.

Slade L, Levine H. 1991. Beyond water activity: Recent advances based on an alternative approach to the assessment of food quality and safety. Critical Reviews in Food Science and Nutrition 30(2-3):115-360.

Smidova I, Copikova J, Maryska M, Coimbra MA. 2003. Crystals in hard candies. Czechoslovac Journal of Food Science 21:185-191.

Taylor M (1947). The solubility at high temperature of pure sucrose in water. Journal of the Chemical Society, 1, pp. 1678-1683.

Thomas JM and Williams JO. 1967. Lattice imperfections in organic solids. Part 2. Sucrose. Transactions of the Faraday Society, 63: 1922-1928.

Urbanus BL, Cox GO, Eklund EJ, et al (2014a) Sensory Differences Between Beet and Cane Sugar Sources. J. Food Sci. 79:1763–1768.

Urbanus BL, Schmidt SJ and Lee S (2014b) Sensory Differences between Product Matrices Made with Beet and Cane Sugar Sources. J. Food Sci. 79:2354-2361.

Vanhal I, Blond G. 1999. Impact of melting conditions of sucrose on its glass transition temperature. Journal of Agricultural and Food Chemistry 47:4285-4290.

Weitz, A.; Wunderlich, B. Thermal analysis and dilatometry of glasses formed under elevated pressure. J. Polym. Sci., Part B: Polym. Phys. 1974, 12, 2473.

Yuan JP, Guo SY, Li L (1996). Simultaneous determination of sugars and their degradation products 5-HMF by HPLC. Chinese Journal of Analytical Chemistry 24:57-60.

4.8 Figures and Tables
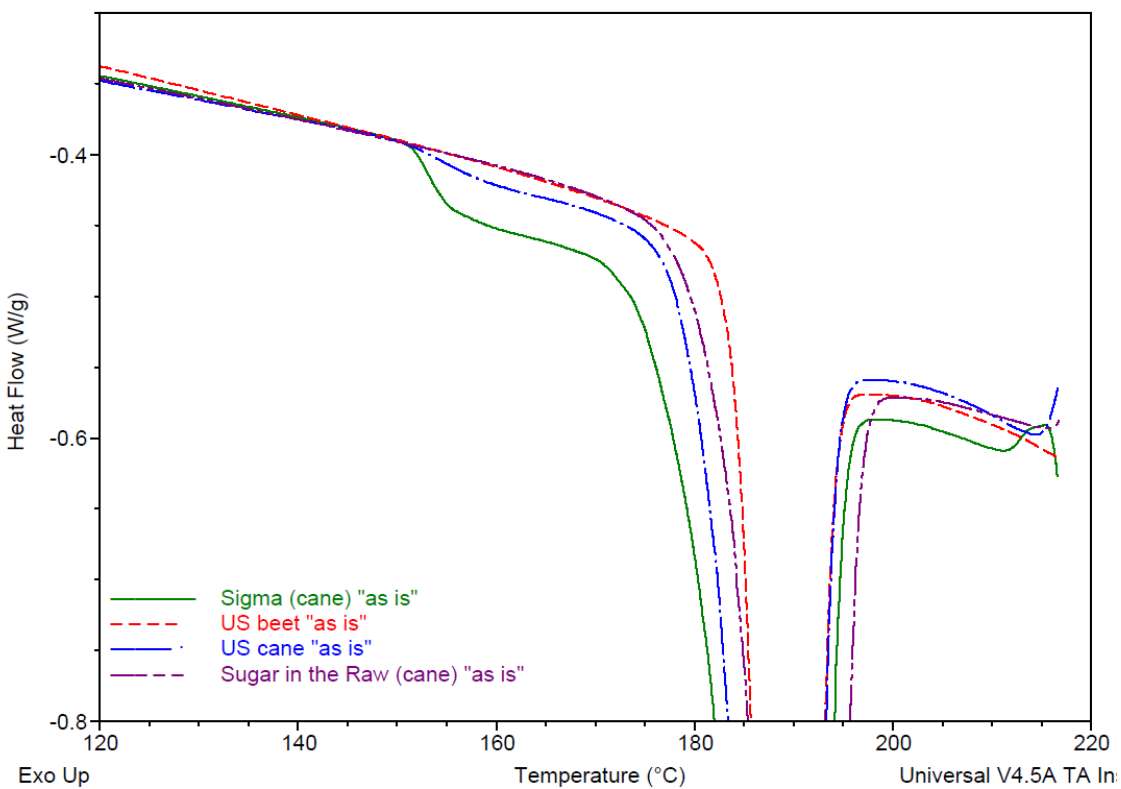
Figure 4.1 Example DSC thermograms of analytical grade Sigma cane, US beet, US cane, and Sugar in the Raw samples at a 10°C/min heating rate.
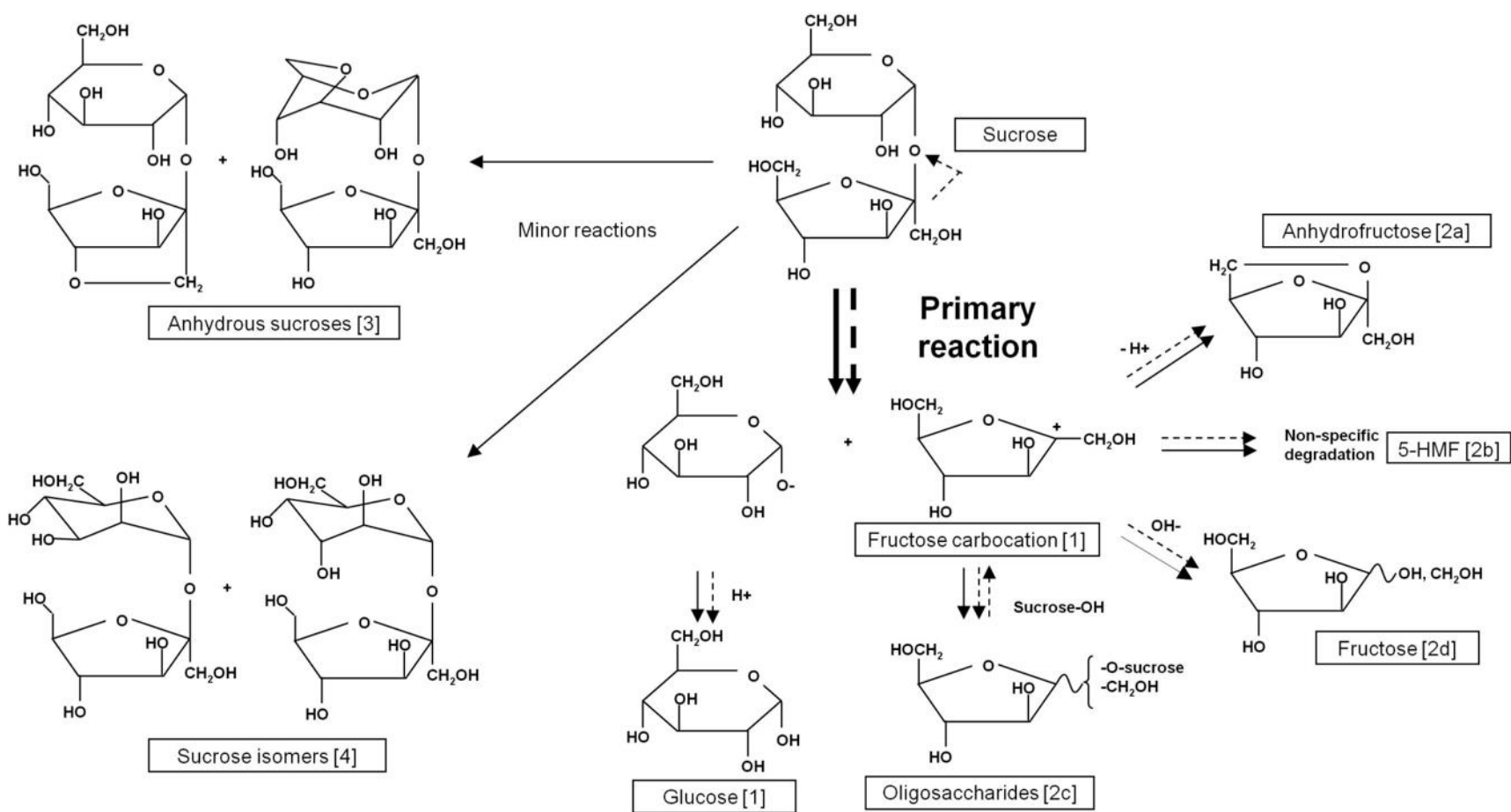
Figure 4.2 The predominant mechanism of sucrose thermal decomposition in the presence (dashed arrow) and in the absence (solid arrow) of an aqueous solution (excerpted from Lee and others 2011b). The numbers identify the different stages and products formed during the decomposition reaction and are discussed in more detail in the text.

Figure 4.3 Example DSC heat flow signal and associated Tmonset value at 10°C/min and HPLC concentration results (in %, w/w) for analytical grade Sigma cane sucrose remaining and indicator thermal decomposition components formed, plotted as a function of the target temperatures. The average small peak Tmonset ± standard deviation value is 151.60 ± 0.43 (Table 4.2). Images of "as is" and thermally processed sucrose samples at each temperature were recorded.
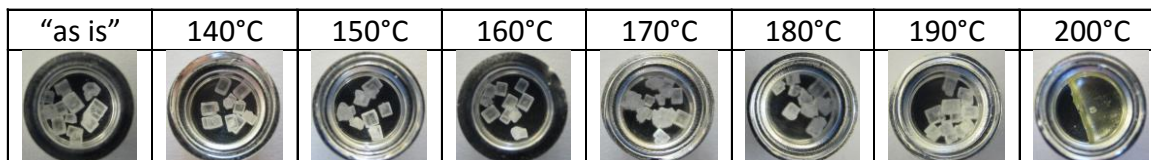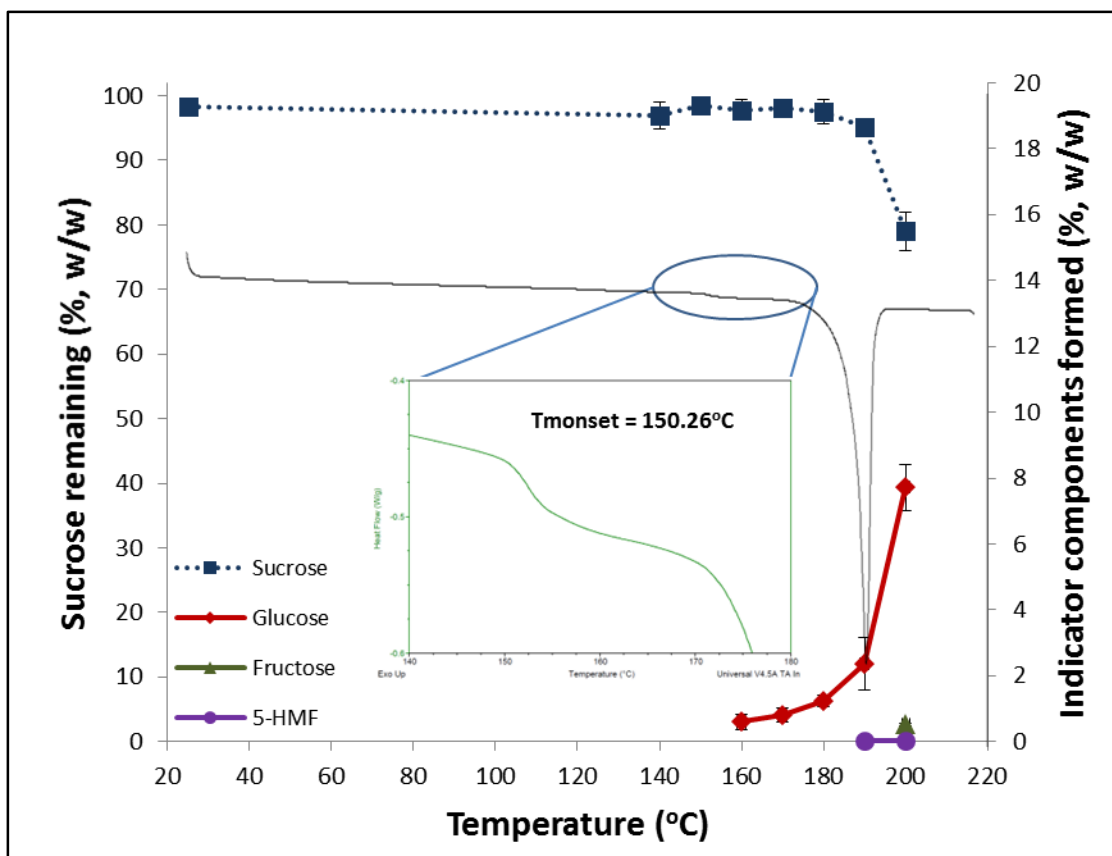
Figure 4.4 Example DSC heat flow signal and associated Tmonset value at 10°C/min and HPLC concentration results (in %, w/w) for analytical grade Fisher cane sucrose remaining and indicator thermal decomposition components formed, plotted as a function of the target temperatures. The average small Tmonset ± standard deviation value is 150.24 ± 0.23 (Table 4.2). Images of "as is" and thermally processed sucrose samples at each temperature were recorded.
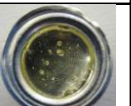
Figure 4.5 Example DSC heat flow signal and associated Tmonset value at 10°C/min and HPLC concentration results (in %, w/w) for US cane sucrose remaining and indicator thermal decomposition components formed, plotted as a function of the target temperatures. The average small Tmonset ± standard deviation value is 153.34 ± 3.03 (Table 4.2). Images of "as is" and thermally processed sucrose samples at each temperature were recorded.
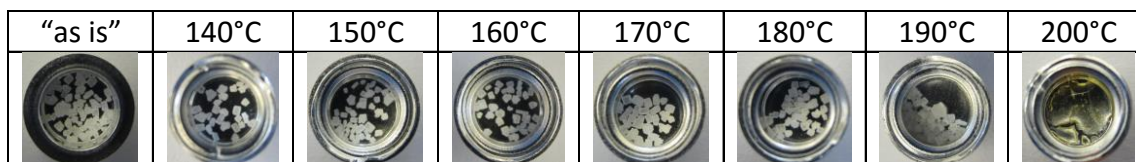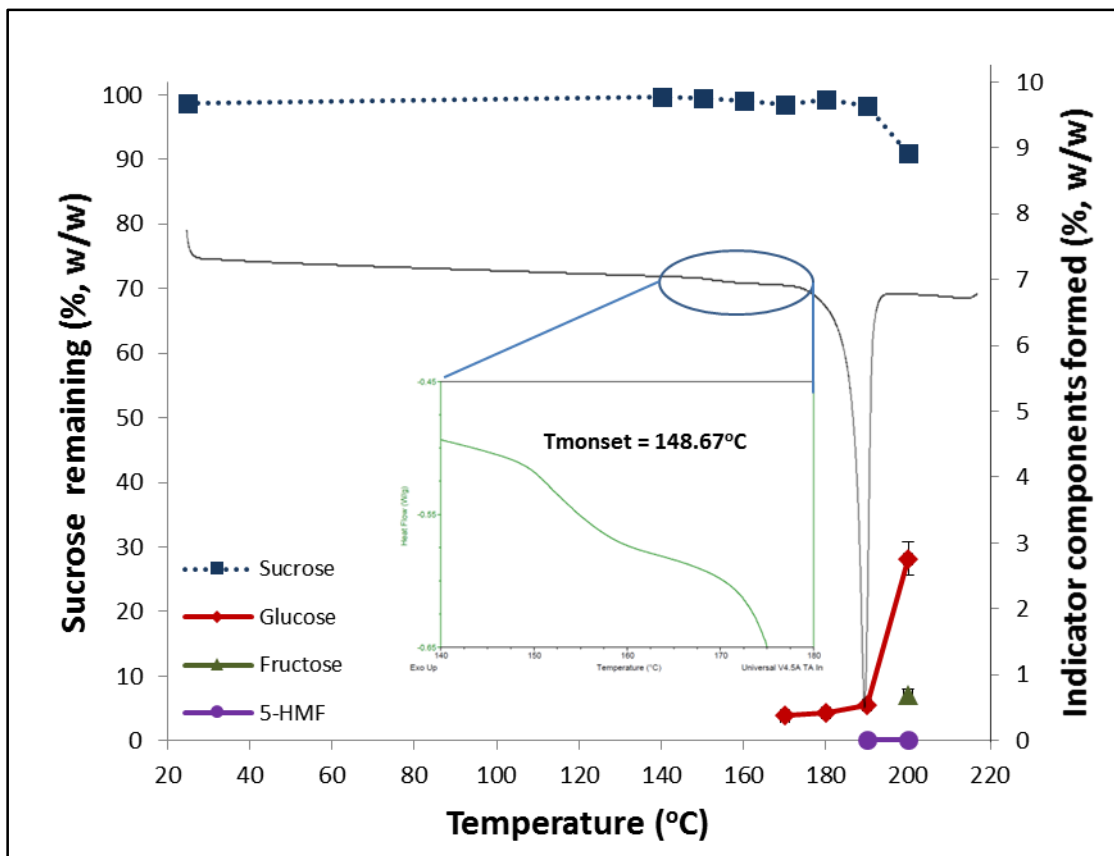
Figure 4.6 Example DSC heat flow signal and associated Tmonset value at 10°C/min and HPLC concentration results (in %, w/w) for C&H cane sucrose remaining and indicator thermal decomposition components formed, plotted as a function of the target temperatures. The average small Tmonset ± standard deviation value is 148.95 ± 0.40 (Table 4.2). Images of "as is" and thermally processed sucrose samples at each temperature were recorded.
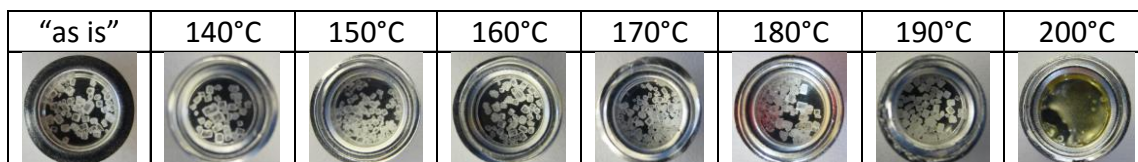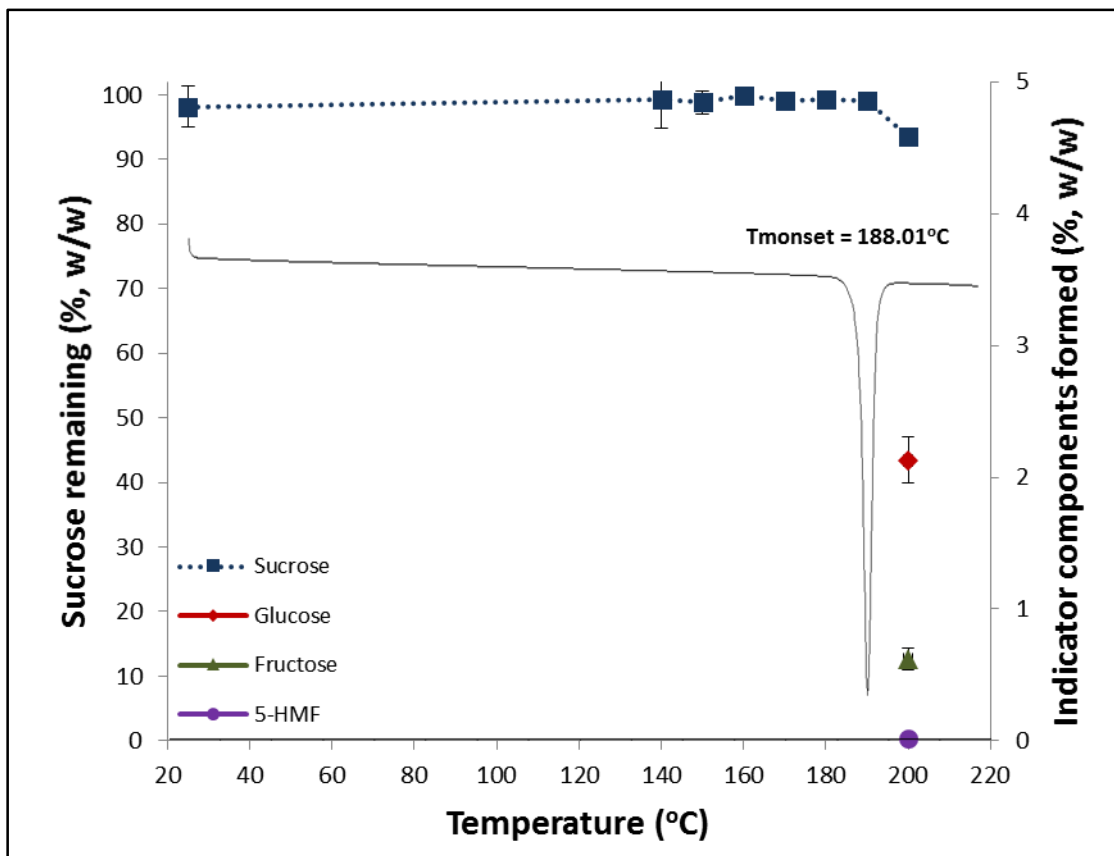
Figure 4.7 Example DSC heat flow signal and associated Tmonset value at 10°C/min and HPLC concentration results (in %, w/w) for US beet sucrose remaining and indicator thermal decomposition components formed, plotted as a function of the target temperatures. The average Tmonset ± standard deviation value is 188.01 ± 0.26 (Table 4.2). Images of "as is" and thermally processed sucrose samples at each temperature were recorded.
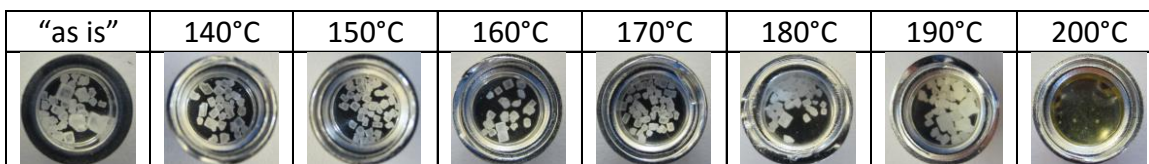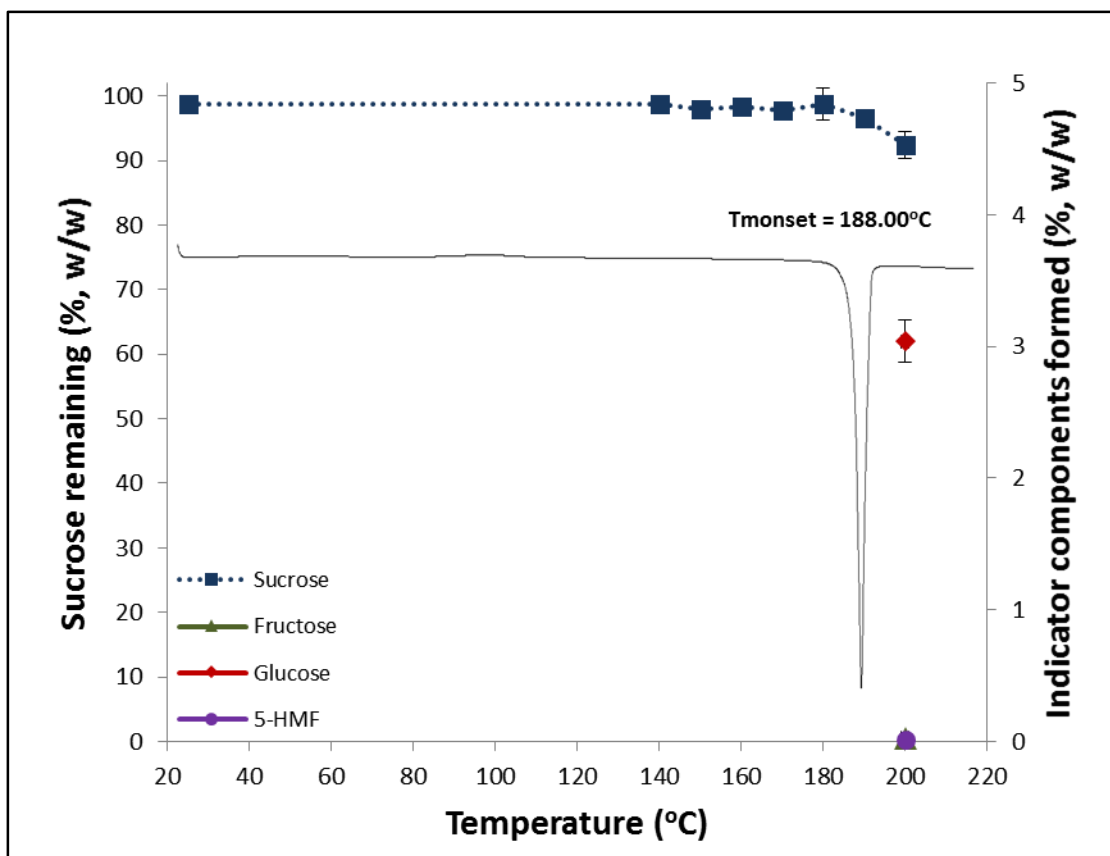
Figure 4.8 Example DSC heat flow signal and associated Tmonset value at 10°C/min and HPLC concentration results (in %, w/w) for Pioneer beet sucrose remaining and indicator thermal decomposition components formed, plotted as a function of the target temperatures. The average Tmonset ± standard deviation value is 187.65 ± 0.15 (Table 4.2). Images of "as is" and thermally processed sucrose samples at each temperature were recorded.

| "as is" | 140°C | 150°C | 160°C | 170°C | 180°C | 190°C | 200°C |
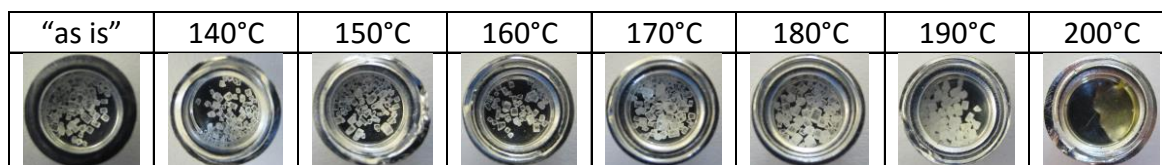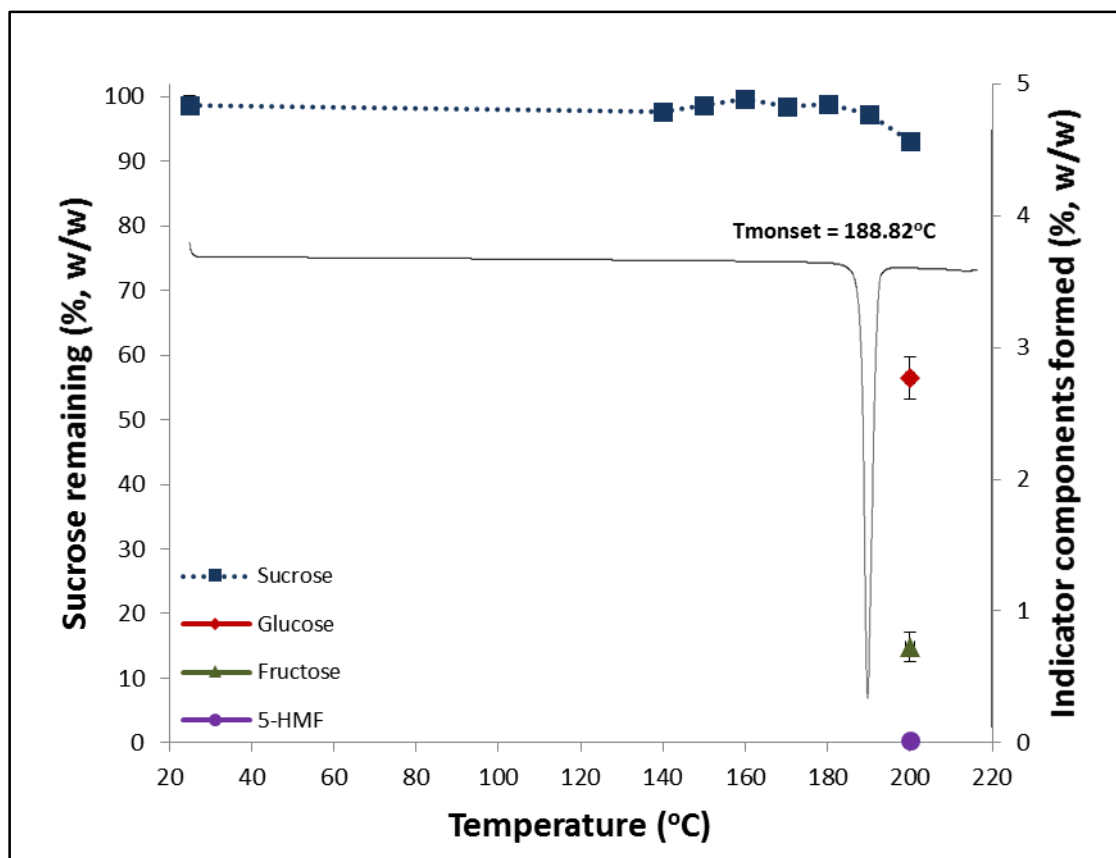
Figure 4.9 Example DSC heat flow signal and associated Tmonset value at 10°C/min and HPLC concentration results (in %, w/w) for Meijer beet sucrose remaining and indicator thermal decomposition components formed, plotted as a function of the target temperatures. The average Tmonset ± standard deviation value is 188.37 ± 0.03 (Table 4.2). Images of "as is" and thermally processed sucrose samples at each temperature were recorded.
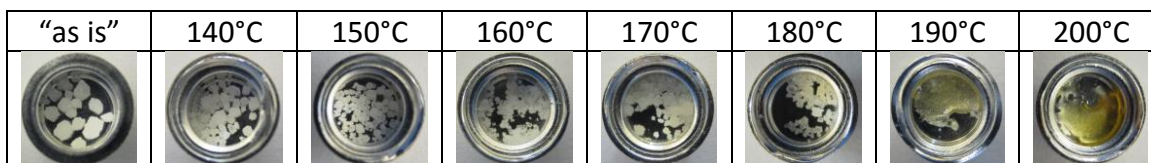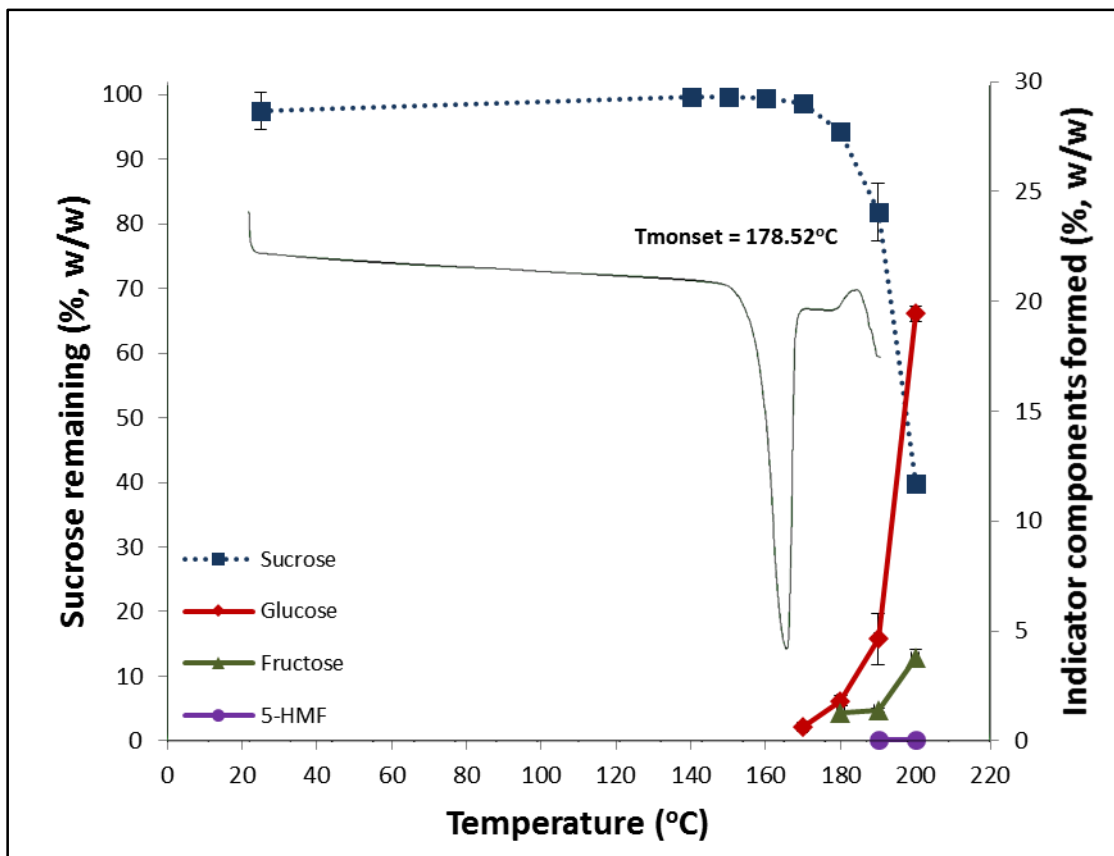
Figure 4.10 Example DSC heat flow signal and associated Tmonset value at 10°C/min and HPLC concentration results (in %, w/w) for High ash cane sucrose remaining and indicator thermal decomposition components formed, plotted as a function of the target temperatures. The average Tmonset ± standard deviation value is 179.54 ± 0.72 (Table 4.2). Images of "as is" and thermally processed sucrose samples at each temperature were recorded.
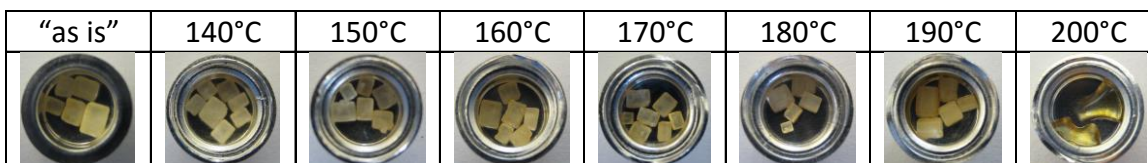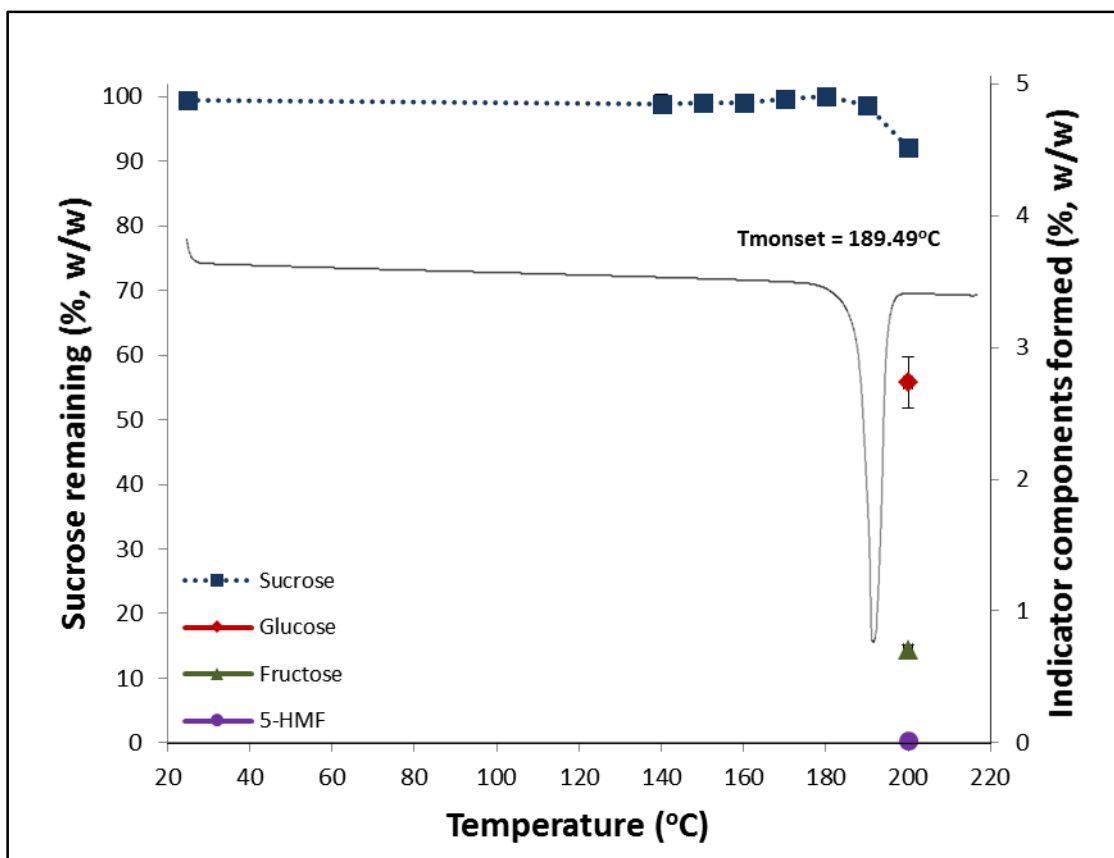
Figure 4.11 Example DSC heat flow signal and associated Tmonset value at 10°C/min and HPLC concentration results (in %, w/w) for Sugar in the Raw cane sucrose remaining and indicator thermal decomposition components formed, plotted as a function of the target temperatures. The average Tmonset ± standard deviation value is 188.34 ± 1.64 (Table 4.2). Images of "as is" and thermally processed sucrose samples at each temperature were recorded.

| "as is" | 140°C | 150°C | 160°C | 170°C | 180°C | 190°C | 200°C |
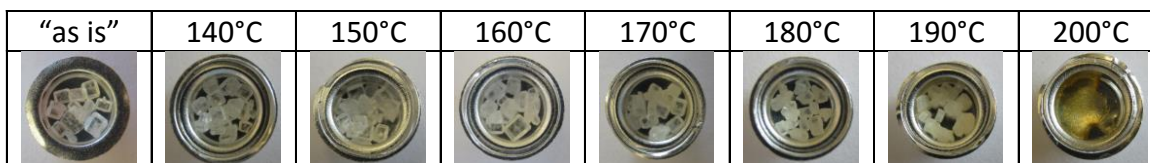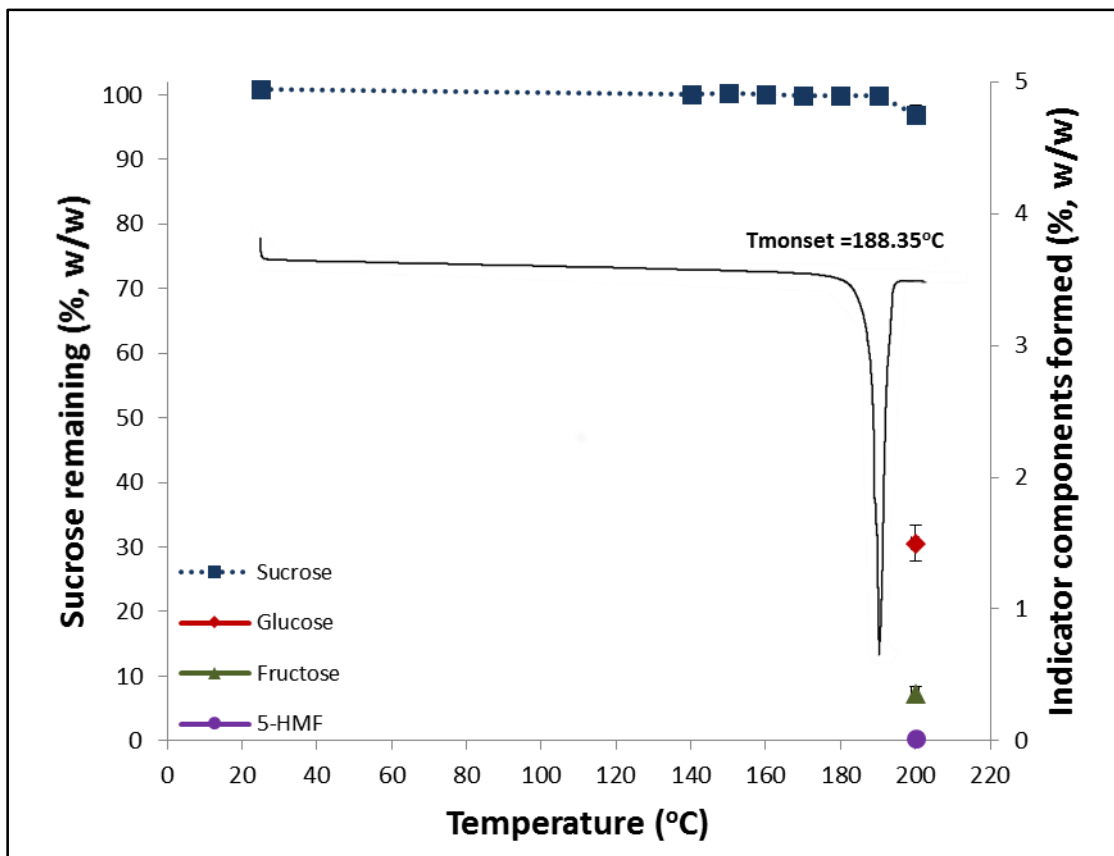
Figure 4.12 Example DSC heat flow signal and associated Tmonset value at 10°C/min and HPLC concentration results (in %, w/w) for Chinese cane sucrose remaining and indicator thermal decomposition components formed, plotted as a function of the target temperatures. The average Tmonset ± standard deviation value is 187.94 ± 0.58 (Table 4.2). Images of "as is" and thermally processed sucrose samples at each temperature were recorded.
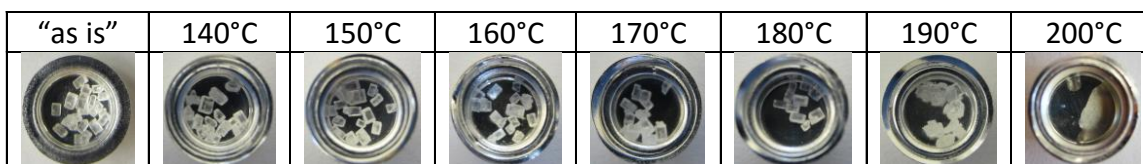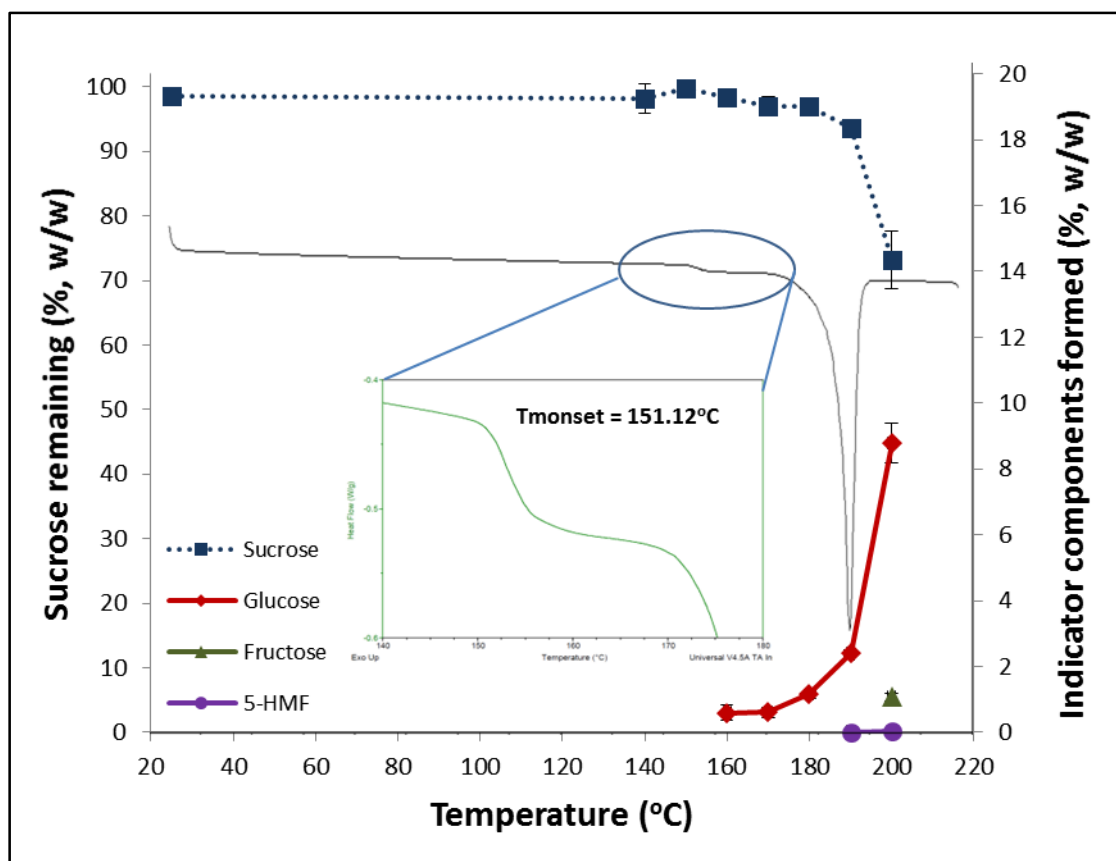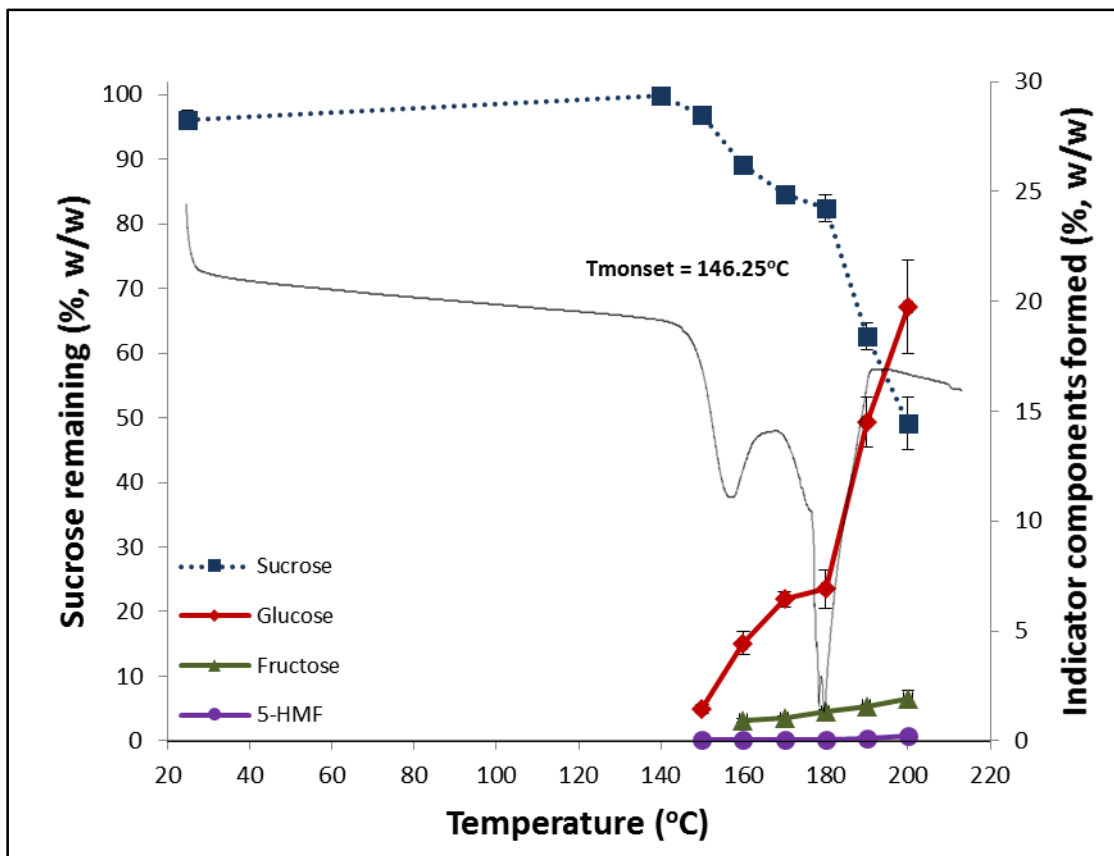
Figure 4.13 Example DSC heat flow signal and associated Tmonset value at 10°C/min and HPLC concentration results (in %, w/w) for Laboratory-recrystallized US beet sucrose remaining and indicator thermal decomposition components formed, plotted as a function of the target temperatures. The average small Tmonset ± standard deviation value is 147.13 ± 1.24 (Table 4.2). Images of "as is" and thermally processed sucrose samples at each temperature were recorded.
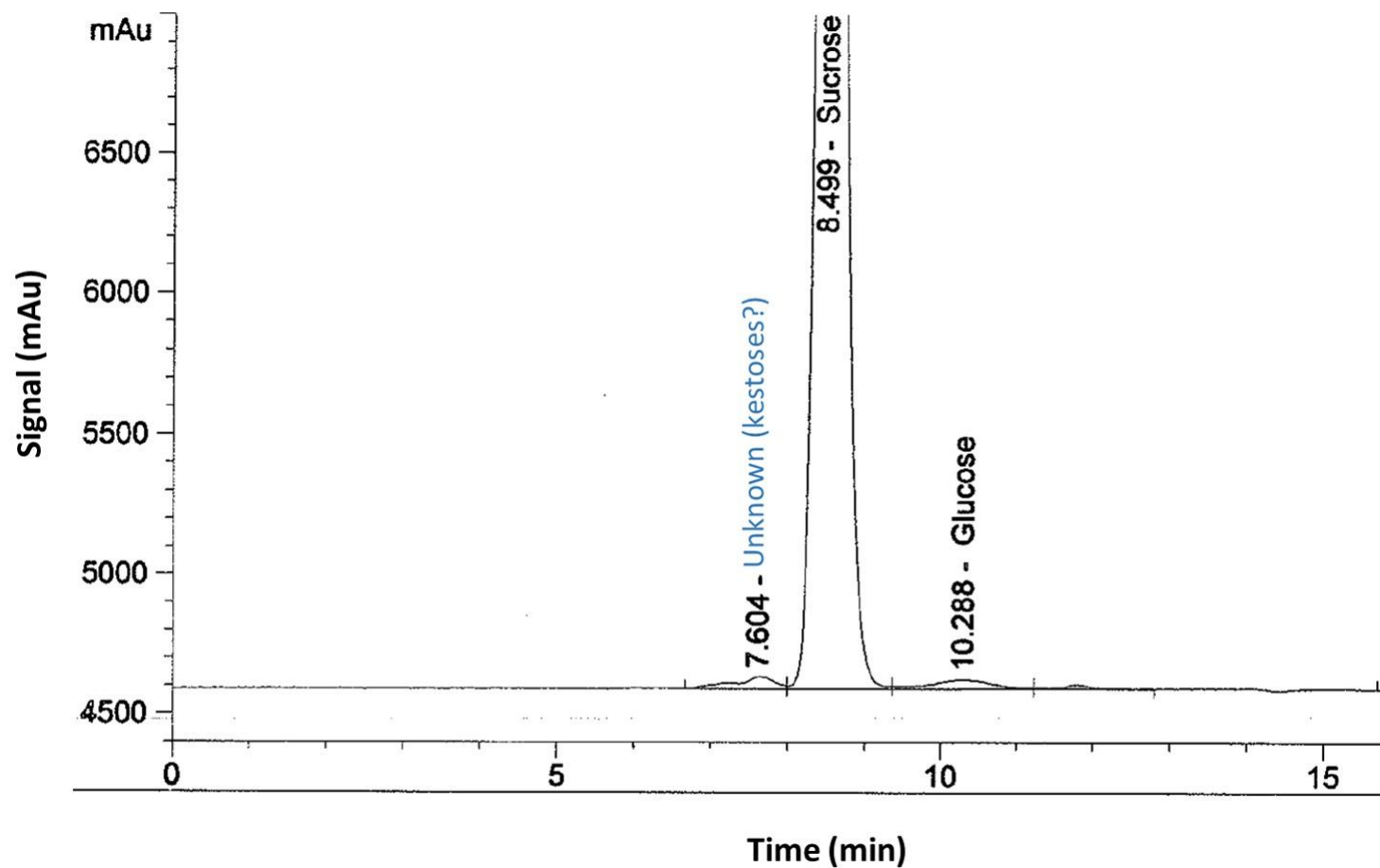
Figure 4.14 An example HPLC chromatogram (refractive index detector) for analytical grade Sigma sucrose heated to 160°C. An unidentified peak was observed at the same target temperature as that for the appearance of glucose and, based on the work of Richards and Shafizadeh (1986), was tentatively attributed to kestoses.
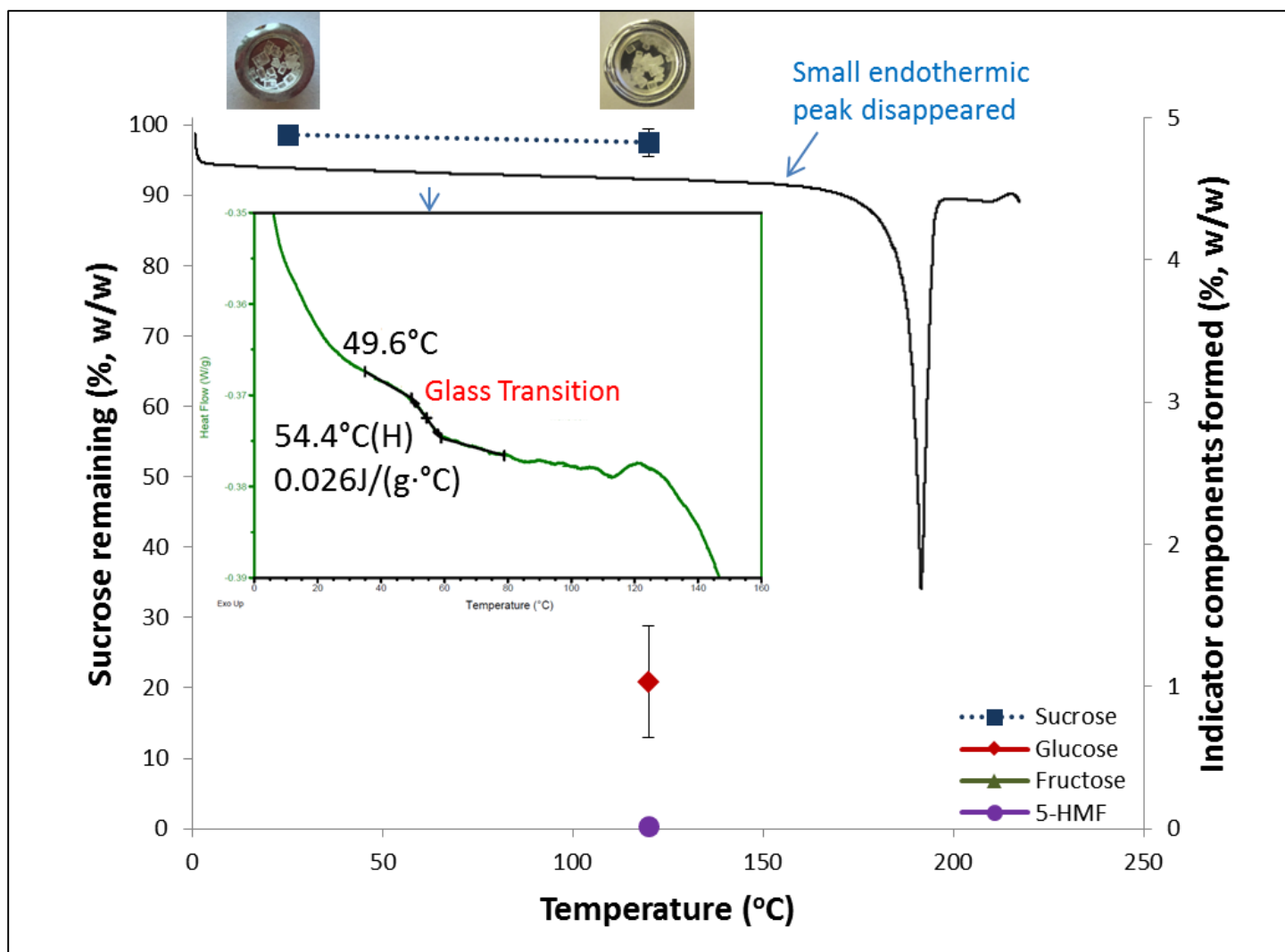
Figure 4.15 DSC heat flow scan at 10°C /min and HPLC results for 120°C isothermal 480 min Sigma sucrose and indicator thermal decomposition components. Images of "as is" and after 480 min isothermal at 120°C were recorded.
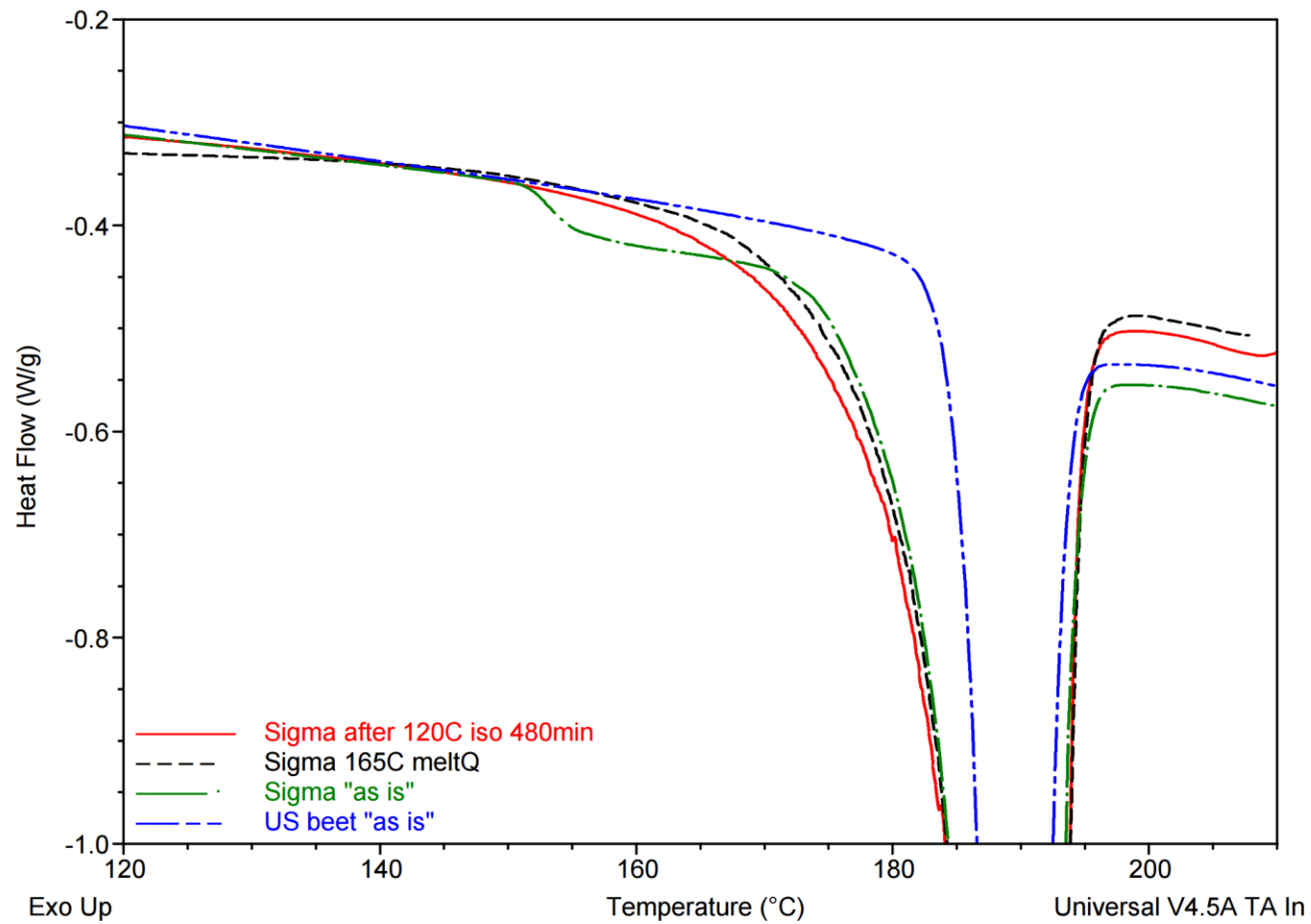
Figure 4.16 Comparison of the DSC thermograms for "as is" analytical grade Sigma cane sucrose, "as is" US beet sucrose, analytical grade Sigma cane sucrose that was heated to 165°C cooled quickly, and rescanned, and analytical grade Sigma cane sucrose that was held at 120°C for 480 mins cooled quickly, and rescanned.

Table 4.1 Summary of thermal behavior issues associated with sucrose reported in the literature, examined mainly using DSC.

Thermal Behavior Issues Associated with Sucrose	Example Associated References
Wide variation in literature reported melting temperature values. For example, 160 to 192°C for DSC obtained values at a 10°C/min heating rate, Appendix B.	Shah and Chakradeo 1936; Power 1958; Shallenberger and Birch, 1975; Lee and others 2011a
Variation in the number of endothermic DSC peaks obtained. Ranges from 1 to 3 peaks, with 1 or 2 peaks most commonly reported.	Reynhardt 1990; Okuno and others 2002a and b; Okuno and others 2003; Beckett and others 2006
Melting temperature exhibits heating rate dependency. The melting temperature increases as heating rate increases.	Okuno and others 2003; Hurtta and others 2004; Lee and others 2011a; Magoń and others 2014
Difference in thermal behavior between beet and cane sucrose sources. In general, cane sucrose sources exhibit 2 endothermic DSC peaks (1 small peaked followed by 1 large peak); whereas beet sources exhibit one large endothermic peak.	Kamoda 1960; Beckett and others 2006; Lu and others 2013

Table 4.2 Comparison of the average Tmonset (°C) at 10°C/min for the first (small) or only (large) peak measured in the DSC thermogram to the initial thermal decomposition component(s) detection temperature and associated initial component(s) detected for the eleven sucrose samples tested herein.

Sucrose Sample	DSC Tmonset (°C) at 10°C/min	Peak Measured	Initial Thermal Decomposition Component Detection Temperature (°C) and Initial Component(s) Detected
Analytical grade Sigma cane	151.60 ± 0.43	Small	160°C – Glucose
Analytical grade Fischer cane	150.24 ± 0.23	Small	160°C – Glucose
US cane	153.34 ± 3.03	Small	170°C – Glucose
C & H	148.95 ± 0.40	Small	170°C – Glucose
US beet	188.01 ± 0.26	Large	200°C – Glucose, Fructose, 5-HMF
Pioneer beet	187.65 ± 0.15	Large	200°C – Glucose, Fructose, 5-HMF
Meijer beet	188.37 ± 0.03	Large	200°C – Glucose, Fructose, 5-HMF
High ash cane	179.54 ± 0.72	Large	170°C – Glucose
Sugar in the Raw	188.34 ± 1.64	Large	200°C – Glucose, Fructose, 5-HMF
Chinese cane	187.94 ± 0.58	Large	200°C – Glucose, Fructose, 5-HMF
Laboratory recrystallized US beet	147.13 ± 1.24	Small	150°C – Glucose, 5-HMF

Chapter 5: Impact of sucrose crystal composition and chemistry on its thermal behavior

5.1 Abstract

For years, a wide variation in the thermal behavior of sucrose has been reported in the literature. However, the underlying mechanism(s) responsible for this variation are still under investigation. During our examination of a number of sucrose samples, a distinct difference was observed between the thermal profiles of beet and cane sucrose sources at 10°C/min heating rate using differential scanning calorimetry (DSC). In general, sucrose from beet sources exhibited only one large endothermic peak; whereas, sucrose from cane sources exhibited two endothermic peaks in the DSC thermogram, one small peak proceeded by one large peak. However, Sugar in the Raw (cane) and Chinese cane sugar, exhibited only one large endothermic peak. Previous studies also revealed that the formation of thermal decomposition components is associated with the appearance of the small endothermic DSC peak in cane sugar sources. We hypothesized that the presence of the small endothermic peak in most "as is" crystalline cane sucrose DSC thermograms is associated with the onset of thermal decomposition of sucrose within mother liquor occlusions, initiated by hydrolysis and mediated by the composition and chemistry of the sucrose crystal. Any factors that affect the composition and chemistry of the sucrose crystal will in turn influence the presence, location (Tmonset), and magnitude of the small peak. The specific objective of this research was to investigate the influence of the composition and chemistry of the sucrose crystal on its thermal behavior using a variety of beet and cane sucrose sources.

A variety of analytical methods and techniques were applied to approach this research objective, including moisture content analysis, pH, conductivity ash content, total sulfite

content measurements, single crystal X-ray diffraction (SXRD), X-ray Micro-Computed Tomography (Micro-CT), Differential Scanning Calorimetry (DSC), and High Performance Liquid Chromatography (HPLC). From this study we found that the pH, conductivity ash, and moisture content values varied widely within and between sugar sources, and were not able to explain the small peak difference between beet and cane sucrose sources. However, impurities in the mother liquor occlusion in beet, Chinese cane, and Sugar in the Raw appear to play a major role in thermally stabilizing the sucrose molecule. Beet and Chinese cane sucrose sources contained sulfite, whereas analytical and commercial cane sources were below the detection limit. Thus, sulfite content appears to explain the absence of the small endothermic DSC peak. Also, by addition of different concentrations of potassium sulfite, we can control the thermal behavior of laboratory-recrystallized Sigma sucrose, since the high concentration of sulfite can inhibit the small DSC peak in cane sources. In the case of Sugar in the Raw, the high conductivity ash and pH appear to be responsible for inhibition of the small peak. Overall, this research reveals that the composition and chemistry of the mother liquor occlusions entrapped within the sucrose crystal are instrumental in determining its thermal behavior.

5.2 Introduction

The crystallization and melting behavior of sucrose has been well studied over a long period of time (e.g., Shah and Chakradeo 1936). During our investigation of a variety of sucrose samples, a distinct difference has been observed between the DSC thermograms of beet and cane sucrose sources at a 10°C/min heating rate (Lu and others 2013; Chapter 3). In general, sucrose from beet sources exhibited only one large DSC endothermic peak, with an average onset temperature (Tmonset in °C) of 188.41 ± 0.37; whereas, sucrose from cane sources

exhibited two DSC endothermic peaks, one small peak proceeded by one large peak, yielding average Tmonset values of 153.80 ± 6.05 and 187.39 ± 1.72, respectively. Exceptions were found for three cane sucrose sources, Sugar in the Raw (cane), High ash cane, and Chinese cane sucrose, which exhibited only one large endothermic DSC peak, with Tmonset values of 188.34 ± 1.64, 179.54±0.72, and 187.94 ± 0.58, respectively (Lu and others 2013; Chapter 3). Representative DSC thermograms for selected sucrose samples, labeled with Tmonset values, are shown in Figure 5.1.

Previous research, coupling DSC and HPLC analyses, also revealed that the temperature at which thermal decomposition components were first detected differed between sucrose samples (Lu and others 2014; Chapter 4). For analytical grade cane and white refined cane sucrose samples, as well as laboratory-recrystallized beet, thermal decomposition components were first detected by HPLC analysis at temperatures ranging from 150 to 170°C (approximately 3 to 20°C after the onset temperature of the small endothermic DSC peak for these sucrose samples). Whereas, for white refined beet sucrose samples, Sugar in the Raw (cane), and Chinese cane, with no small endothermic DSC peak, thermal decomposition components were first detected at 200°C (approximately 10°C after the onset temperature of the large endothermic DSC peak for these sucrose samples). These results suggested that sucrose samples that do not exhibit a small endothermic DSC peak possess greater thermal stability than those that do exhibit a small endothermic DSC peak.

Several hypotheses have been suggested in the literature, which attempt to explain the cause of the small endothermic DSC peak. These hypotheses were previously grouped into six overarching categories by Lu and others (Chapter 3) and are summarized below. The

terminology used by the original author(s) was retained, where possible, in order to best capture the essence of their hypothesis and to avoid any inadvertent misinterpretation. Additionally, depending on the nature of the hypothesis, it may appear in more than one category. The presence of the small endothermic peak in crystalline sucrose is attributed to: 1) Amorphous content – presence of some amorphous fraction (highly concentrated mother liquor) in the granules, which produces a small devitrification peak (Bhandari and Hartel 2002); presence of partially amorphous, fine sucrose crystals (<50 μm), which produce a glass transition just prior to the melting peak (Mathlouthi 2012). 2) Water [hydrate, surface, or entrapped] – formation of a hydrate of sucrose (Miller 2001); solubilization (heat of solution) of the surface of the crystals by residual moisture (Bhandari and Hartel 2002); a non-stoichiometric entrapment of water in the crystal lattice and the affinity of added impurities for available water (Maulny 2004). 3) Impurities and defects – a non-stoichiometric entrapment of water in the crystal lattice and the affinity of added impurities for available water (Maulny 2004); formation of different crystal structures due to the type and amount of impurities present in the mother liquor (Okuno, 2003); defects in the lattice structure produced during crystallization (Kawakami and others 2006). 4) Polymorphism – formation of different crystal structures due to the type and amount of impurities present in the mother liquor (Okuno, 2003); conformational polymorphism about the glycosidic linkage (Lee and Lin 2007a and b; Lee and Chang, 2009). 5) Hydrogen bond breaking – breaking of some hydrogen bonds prior to the melting of the crystal structure (Reynhardt 1990). 6) Particle size – particle size differences within the sample (Magoń and others 2014).

In addition to these hypotheses, a variety of factors, also discussed in the literature, have been found to affect the presence and magnitude of the small peak. Researchers have tied the appearance of the small endothermic DSC peak to the amount and type(s) of impurities in sucrose (Maulny 2004; Beckett and others 2006), which can either inhibit or promote the existence of the small peak (Kamoda 1960; OKuno 2003). Beckett and others (2006) reported that the appearance of the small endothermic DSC peak is highly dependent on the purity of the sucrose. For example, the magnitude of the small peak decreased when the sucrose was recrystallized in the presence of KCl. They also observed that the appearance of the small peak was affected by the recrystallization conditions. For example, by introducing a stirring step or increasing the temperature of the recrystallization solution, the small peak decreased. Additionally, Kawakami and others (2006) found that by "annealing" recrystallized amorphous sucrose samples under a variety of relative humidity, temperature and time combinations, defects in the crystal structure were partially modified, which resulted in the alteration of melting behavior of sample (number and magnitude of peaks in the DSC thermograms).

Also of importance is the difference in processing between white refined beet and cane sucrose, where beet sugar processing routinely includes a sulfitation step, whereas sugar cane processing usually does not (Clarke and Godshall 1988; Asadi 2005). Among sugar cane processors worldwide, there is mixed interest in the use of sulfitation. In the United States, sulfitation has rarely been used in cane raw sugar factories since the 1950's (Andrews and Godshall 2002). However, in China, cane sugar refining routinely includes sulfitation steps for juice clarification (Huo 2008). Several product quality standards are in place for both white refined beet and cane sugars, including, when applicable, sulfur dioxide specification limits.

There are a number of standard setting organizations for sugar products, including the

European Economic Community, the Codex Alimentarius, and the Food Chemical Codex. In the

case of the Food Chemical Codex, the maximum permitted sulfur dioxide level for white sugar is

15 ppm and 20 ppm for raw sugar (Godshall 2013).

As a next step in attempting to tie the observed thermal behavior of the sucrose crystal

discussed above to its composition and chemistry, we drew a simple model of a sucrose crystal

(Figure 5.2). A key structural feature of the model, based on literature findings, is that during

crystallization, small quantities of saturated sucrose solution (termed mother liquor occlusions

or inclusions) are entrapped within the developing crystal lattice (Powers 1958 and 1970). This

entrapment of mother liquor was recognized, as far back as Richards (1903), "substances

crystallizing from a solution enclose within their crystals small quantities of the mother-liquor"

and that this entrapment was exceedingly common, "It is no careless exaggeration to state that

in all my chemical experience I have never yet obtained crystals from any kind of solution

entirely free from accidentally included mother-liquor; and, moreover, I have never found

reason to believe that anyone else ever has." We hypothesized that the presence of the small

endothermic peak in most "as is" crystalline cane sucrose DSC thermograms is associated with

the onset of thermal decomposition of sucrose within mother liquor occlusions, initiated by

hydrolysis and mediated by the composition and chemistry of the sucrose crystal. Any factors

that affect the composition and chemistry of the sucrose crystal will in turn influence the

presence, location (T_{monset}), and magnitude of the small peak. Thus, the objective of this

research was to investigate the influence of the composition and chemistry of the sucrose

crystal on its thermal behavior using a variety of beet and cane sucrose sources.

5.3 Materials and Methods

Materials

Two analytical grade crystalline sucrose samples were purchased from Sigma-Aldrich Co. (St. Louis, MO; #S0389, ≥ 99.5%) and Fisher Scientific Inc. (Pittsburgh, PA; S5-500; Certified ACS, purity not reported). One beet (US beet) and one cane (US cane) sucrose sample were obtained directly from United Sugar (US) Corporation (Clewiston, FL). Other beet (Pioneer beet) and cane (C&H cane) sucrose samples were obtained from local stores in the Champaign-Urbana, IL area. One commercially available granulated Chinese cane sucrose sample was purchased from a market in Beijing, China. Sample information for all commercially available sucrose samples is given in Appendix E. All sucrose samples were tested "as is" without further purification. Potassium sulfite (≥ 97%), anhydrous citric acid (≥ 99.5%), and sodium chloride (≥ 99.5%) were purchased from Sigma-Aldrich Co. (St. Louis, MO). Polyvinylpyrrolidone, cross-linked was purchased from ACROS Organics™ (Thermo Fisher Scientific Inc. Waltham, MA). HPLC grade water (Fisher Scientific Inc., Pittsburgh, PA) was used for the preparation of standard and sample solutions. Ultrapure water was collected through successive steps of resin filtration and deionization using Milli-Q water system (EMD Millipore Corporation, Temecula, CA), which dispenses the water via a 0.22 μm membrane filter.

Methods

Moisture content measurement

The total moisture content of the crystalline sucrose samples were determined using volumetric Karl Fisher titration (EMD, Aquastar AQV21) with a 50:50 formamide/methanol solvent system, under ambient temperature and relative humidity conditions. Measurements

were done in duplicate for each sucrose sample by DonLevy Laboratories (Crown Point, IN). The

moisture content (wet basis) of each sugar sample was reported by DonLevy Laboratories in

Appendix H. Approximately 0.5g of each sucrose sample was dissolved in the two-solvent

system by continuous stirring for 5 minutes, and then titrated to reach the end point of drift,

approximately 10 minutes. The moisture content of the sucrose samples was reported on the %

wet basis (g water/g sample x 100%) and since crystalline materials are known to quickly adsorb

water from the atmosphere (Schmidt 2012), relative humidity (%RH) and the temperature (°C)

of the lab were also reported for Karl Fisher each moisture content measurement.

pH measurement

Sample preparation and pH measurements were based on the International Commission

for Uniform Methods of Sugar Analysis (ICUMSA) Method 2011 (The Determination of pH by a

Direct Method in Raw Sugar, Molasses, Juices and Syrups – Official; in White Sugar, Specialty

Sugars and Plantation White Sugars - Tentative). 10g of each sucrose sample was dissolved in

10 g of HPLC grade water (a ratio 50:50 of sucrose:water) in a 50mL disposable polyethylene

tube with a screw cap. In order to completely dissolve the solute, capped sample tubes were

warmed in an 80°C water bath and vortexed at maximum speed at 5 minutes intervals, until no

crystalline sucrose remained. Approximately 30 minutes was required for complete dissolution.

Then, the sample tubes were cooled to room temperature (22 to 25°C) before measuring the

pH using an Orion VERSA STAR Multiparameter Benchtop Meter (Thermo Fisher Scientific Inc.

Waltham, MA) equipped with an Orion™ ROSS Ultra™ Refillable pH/ATC Triode™ Combination

Electrodes with a built-in temperature sensor. Orion™ pH 4.01 (pink), 7.00 (yellow), and 10.01

(blue) buffer standards were used for instrumental calibration before sample testing. pH

measurements were done in triplicate for all three batches of prepared sucrose solution. The pH of pure HPLC grade water was also recorded. All pH readings were converted to the temperature at 25°C.

Conductivity ash measurement

Sample preparation and conductivity ash measurements were based on the International Commission for Uniform Methods of Sugar Analysis (ICUMSA) Method 2011 (The Determination of Conductivity Ash in Refined Sugar Products and in Plantation White Sugar-Official). The conductivity ash in solution (at a ratio of 28g solids/100g solution concentration) gives a measure of the concentration of ionized soluble salts in solution of low conductivity (Schneider 1979). For sample preparation, 7g of sucrose was dissolved in 18 g of ultrapure water (a ratio 28:100 of sucrose:sucrose solution) in a 50mL disposable polyethylene tube with a screw cap. In order to completely dissolve the solute, capped sample tubes were warmed in an 80°C water bath and vortexed at maximum speed at 5 minutes intervals, until no crystalline sucrose remained. Approximately 20 minutes was required for complete dissolution. Then, the sample tubes were allowed to cool down to room temperature (22-25°C) before measurement. The conductivity probe (Orion DuraProbe 4-Electrode Conductivity Cells 013005MD) connected to an Orion VERSA STAR Multiparameter Benchtop Meter (Thermo Fisher Scientific Inc. Waltham, MA) was calibrated using freshly prepared sodium chloride solutions at three concentration: 47 ppm (100 μS/cm conductivity standard), 692 ppm (1413 μS/cm conductivity standard), and 7230 ppm (12.9 mS/cm conductivity standard). The conductivity of ultrapure water was also recorded. All conductivity values were converted to

the temperature at 20°C. The method for converting conductivity values to conductivity ash % content were calculated using Equation 5.1,

$$\text{Conductivity ash \%} = 6 \times 10^{-4} \times (C_{soln} - 0.35 C_{water}) \qquad \text{Equation 5.1}$$

where C_{soln} is the measured conductivity of sucrose solution and the ultrapure water, respectively, in μS/cm at 20°C. The conductivity measurement was done in triplicates for all three batches of prepared sucrose solutions and results were displayed in average ppm values.

Total sulfite measurement

Total sulfite (TSO_2) in the sucrose samples was measured using a total sulfite assay microplate format (Megazyme, Wicklow, Ireland), which is based on the reaction principle between thiol groups and Ellman's reagent (Ellman 1958; Riddles and others 1983; Thannhauser and others 1987; Chan and Wassernan 1992). Analytical grade sodium sulfite provided in the test kit was dissolved into 1g/L freshly prepared citric acid solution to prepare a serial of standard solutions (5ppm to 400 ppm). For sample preparation, 2.5 g of each sucrose sample was dissolved in 2 mL of ultrapure water in a 15mL disposable polyethylene tube with screwed cap. In order to completely dissolve the solute, capped sample tubes were warmed in an 80°C water bath and vortexed at maximum speed at 5 minutes intervals, until no crystalline sucrose remained. Approximately 30 minutes was required for complete dissolution. Then the sample tubes were allowed to cool down to the room temperature (22 to 25°C). For the Sugar in the Raw sample, a clarification step was carried out by addition of 0.2g of polyvinylpolypyrollidone (PVPP) into the sugar solution. After the addition of PVPP, the tube was shaken vigorously for 5 min and then filtered through Whatman No.1 filter paper to collect the clarified sucrose solution. Standard solutions and 100μL of each sample were added into a

96 wells microplate and mixed with 100µL of TSO_2 Reagent I. The microplate was placed on a plate shaker and mixed for 3 minutes at room temperature. The background absorbance (A_1) for each standard and sample at 405 nm was then recorded using a µQuant™ microplate spectrophotometer with wavelengths ranging from 200 nm to 999 nm (BioTek® Instruments, Inc. Winooski, VT). Next, 50 µL of TSO_2 Reagent II was added into each standard and sample solution well. After 3 minutes of mixing on a plate shaker at room temperature, the absorbance (A_2), which reflected the concentration of the total sulfite content, was recorded at 405 nm using the µQuant™ microplate spectrophotometer. The TSO_2 content in each sucrose sample was calculated from the generated linear standard curve (Absolute absorbance against sulfite concentration). The sulfite detection limit for this method is 5.28 ppm (Megazyme 2011).

DSC analysis of "as is" and ground beet and cane sucrose samples

Experiments were carried out using a DSC Q2000 (TA Instruments, New Castle, DE), equipped with a RCS 90 refrigerated cooling system. The DSC was calibrated for enthalpy and temperature using a standard indium sample (Tmonset of 156.6°C, ΔH of 28.71 J/g, TA Instruments, New Castle, DE) prior to sample measurements. Hermetic aluminum Tzero pans and lids (TA Instruments, New Castle, DE) were used for all calibration and sample measurements, including an empty pan as the reference. Dry nitrogen, at a flow rate of 50 mL/min, was used as the purge gas. Hermetically sealed "as is" (crystals larger than a No. 45 U.S.A. standard testing sieve with 42 mesh and 0.355 µm opening size) and ground sucrose (needs to pass through a No.100 U.S.A. standard testing sieve with 100 mesh and 0.15 µm opening size) from beet and cane sucrose sources (analytical grade Sigma cane, US beet, and US cane), approximately 3 mg, were equilibrated at 25°C and then heated at rate of 10°C/min to

220°C. The end temperature was selected so as to ensure coverage of the entire endothermic peak for all samples tested. For laboratory recrystallized Sigma samples, due to the relatively large crystal size and weight, a single crystal of each sample (3 to 9 mg) was hermetically sealed in a Tzero sample pan and scanning using the same DSC conditions as described above. All experiments were conducted in at least duplicate. The selected experimental conditions were based on previous research carried out in the Schmidt laboratory (Lee and others 2011a). Universal Analysis (UA) software was used to obtain the melting parameters (onset melting temperature Tm onset; peak melting temperature, Tm peak; and enthalpy of melting, ΔH J/g) and plot the average heat flow signals.

HPLC analysis

The "as is" and ground Sigma cane, US beet, and US cane sucrose samples were prepared using a DSC Q2000 (TA Instruments, New Castle, DE), equipped with a refrigerated cooling system (RCS 90). Each sample was heated to target temperatures of 140°C, 150°C, 160°C, 170°C, 180°C, 190°C and 200°C at 10°C/min using DSC. Each sucrose sample (approximately 9.0 mg) was hermetically sealed in a Tzero DSC pan. Three sample pans of sucrose were loaded in the DSC cell; one pan was placed on the sample platform and the others were placed on the bottom of the DSC cell. After the samples reached each target temperature (approximately sample temperature was 1.5°C lower than the target temperature due to thermal lag), the system was quickly equilibrated back to room temperature. Approximately 20 mg of each sucrose sample was then dissolved into 2mL of HPLC water and transferred to 2mL screw thread robovial with silicone septa caps before injection (Fisher Scientific Inc., Pittsburgh, PA). HPLC analyses were conducted using a Waters 2695 Alliance HPLC system (Waters, Milford,

MA), equipped with a Hewlett-Packard interface 35900E A/A converter. HPLC analysis of "as is" and DSC heated sucrose solutions were carried out using the Aminex HPX-87C calcium form cation exchange resin based analytical column (300 × 7.8 mm) packed with sulfonated divinyl benzenestyrene copolymer with a particle size of 9 μm (Bio-Rad Lab., Richmond, CA). The guard column was a Carbo-C Refill cartridge (30 × 4.6 mm) (Bio-Rad Lab., Richmond, CA). HPLC grade water was used as the mobile phase. The analytical column temperature was maintained at 80°C and the guard column at 30°C. The flow rate was set to 0.6 mL/min. All samples were injected into the HPLC system using a 20 μm loop injector. A Waters 410 refractive index (RI) detector (Waters, Milford,MA) was connected to a Hewlett-Packard series 1050 photodiode array (PDA) detector (Hewlett-Packard, Palo Alto, CA) for sample detection. While sucrose, glucose, and fructose were determined using the RI detector, 5-HMF was simultaneously measured using the PDA detector at a wavelength of 284 nm. Chromatographic peaks were identified by comparing retention times and spectra to those of known standard solutions. A mixed standard solution, containing sucrose, glucose, fructose, and 5-HMF, was used for HPLC analysis of all sucrose samples. All computations were performed using an Agilent ChemStation (ChemStation for LC 3D Rev A. 08. 03, Agilent Technologies, Inc., Santa Clara, CA). The earliest and most abundant selected thermal decomposition indicator component (glucose; detected using HPLC and its corresponded decomposition temperature, Donset, was labeled on the DSC thermogram). HPLC analysis was carried out in duplicate for all three batches of sucrose samples. The limit of quantification (LOQ) of the HPLC analysis was 0.011 g/L for sucrose, 0.043 g/L for glucose, 0.032 g/L for fructose, and 0.0008 g/L for 5-HMF.

Powder and Single Crystal X-ray Diffraction (PXRD & SXRD)

Both the PXRD and SXRD measurements of sucrose samples were conducted in the George L. Clark X-ray Facility and 3M Materials Laboratory at University of Illinois at Urbana-Champaign.

Powder X-ray diffraction was applied to determine structural properties, such as lattice parameters, strain, grain size, preferred orientation, and to determine atomic arrangement. If the sucrose sample contains some amorphous material, the disorder of the structure will result in amorphous scattering. For example, if the sample is completely amorphous no peaks will be visible (Suryanarayana and Norton 1998). A Rigaku MiniFlex 600 (MiniFlex, Rigaku Corporation, The Woodlands, TX), benchtop powder X-ray diffractometer was used to collect PXRD in the Bragg-Brentano configuration using Cu Kα radiation. A 2θ scan range of 3° to 60° was collected in continuous mode at a scan rate 1°/min with increments measured ever 0.02°. Sucrose samples were well ground before PXRD scanning to avoid the preferred orientations. Single crystal X-ray diffraction (SXRD) is used to determine single crystal repeating unit cell structure, which provides the best structural evidence for polymorphism. For selected sucrose samples (analytical grade Sigma cane, US beet, US cane, Sugar in the Raw, and HPLC recrystallized samples), the unit cell parameters were collected using a Bruker X8Apexll (APEX) and a Bruker D8 Venture systems, then compared to sucrose parameters contained in the Cambridge Crystallographic Data Centre (CCDC), specifically Brown and Levy (1973) (CSD# SUCROS). The Bruker X8ApexII (APEX) system (utilizes Mo radiation) is equipped with a four-circle kappa-axis diffractometer and motorized ApexII CCD detector. The dual source system, Bruker D8 Venture Duo (utilizes Cu or Mo radiation), is equipped with a four-circle kappa-axis diffractometer and motorized Photon 100 CMOS detector capable of shutter-less data collection. Selected single

crystals were mounted on a 0.3mm Hampton Research Cryoloop using Paraton oil (Hampton Research). A short series of omga scans were collected. Data were harvested and the unit cell was indexed and refined using APEX II software (Bruker AXS, Inc., Madison, WI). Both APEX and Bruker D8 Venture systems primarily used for variable temperature, single crystal experiments on samples with a minimum dimension of 0.01mm.

Micro-CT measurements

X-ray computerized microtomography (CT) is a combination of imaging and computing methods, which are used to produce 3D images to reveal the internal structure of a sample. The X-ray microscope takes multiple projection images at different viewing angles to provide the original 2D images. A computer then utilizes these 2D projection images to reconstruct 3D volumetric data to reveal the internal structure without destructing the sample (Yin 2012). The Xradia Bio Micro-CT (MicroXCT-400) is a high-resolution 3D X-ray imaging system, which is optimized for non-destructive imaging of complex internal structures (from: LOT-QuantumDesign GmbH). The Xradia MicroXCT-400 provides the unique ability to reveal the internal structure with full 3D imaging of features down to <1.0 micron resolution, which can be utilized to investigate the internal structure of the sucrose crystal before and after thermal treatment. Based on the crystal size, pixel size from 1 or 2 μm, and optical magnification 20X or 10X were selected for CT scanning. There were 901 2D projecting images in total, which were collected for each crystal, and usually the large the sample, the more informative images (images including sample information) will be obtained.

For this study, selected analytical grade Sigma cane, US beet, and US cane crystals were first scanned in the Micro-CT in the "as is" state, then heated to 165°C at 10°C/min using the

DSC. After heating, the same crystal was scanned again in the Micro-CT. The morphology of each selected crystal before and after heating was also recorded using a Leica M205C Microsystem (Leica, Heidelberg Germany) equipped with both reflected bright field and polarized light.

Laboratory recrystallization method

The recrystallization protocol mention in Chapter 4 for producing laboratory-recrystallized sucrose was based on the method reported by Ouiazzane (2008) with midifications. In order to improve the quality (better size, appearance, and other morphological properties) of our own laboratory-recrystallized sucrose samples, the method of cooling crystallization with undisturbed solution (leaving solution in a location where it will be undisturbed by vibrations or movement) was applied. This slow crystallization method is available from the website of University of Florida Center for X-ray Crystallography. In order to have large size, nice surface appearance, and fewer defects of grown crystals, shaking should be avoided to minimize the nucleation sites during recrystallization.

<u>Preparation of saturated sugar solutions</u>

The saturation solubility of sucrose at 75°C is 77.5g per 100 g of solution (Taylor 1947). Saturated sucrose solutions were prepared by adding 19 g of Sigma cane sucrose and 6 g of HPLC grade water into a 50mL disposable polyethylene tube with a screwed cap. Capped tubes were then warmed for about 1 hour using an 85°C water bath and periodically shaken gently by hand until no crystalline sucrose remained. The temperature of the saturated solution was then allowed to decrease under room temperature conditions and subsequently incubated at 25°C to allow nucleation to occur. All unnecessary movement was avoided during cooling and

incubation. After approximately 24 to 48 hours, the new crystals, with the desired size and shape, were harvested. Addition of potassium sulfite at levels of 0.1%, 0.2%, 0.5%, 0.8% and 1% (weight percentage of sucrose) was also applied in this study to produce new laboratory-recrystallized Sigma cane samples. The specified amount of potassium sulfite was added to the sucrose sample and dissolved together in HPLC water during heating.

<u>Centrifugal filtration</u>

The newly-grown crystals, with the desired morphology, were placed into the Vivaspin® 20ml centrifugal concentrators (Vivaproducts, Inc. Littleton, MA) and filtered using centrifugal filtration (Eppendorf Centrifuge 5810R, Hamburg, Germany) at 3600 RPM for 25 min to remove the mother liquor on the crystal surface. The harvested crystals were then put onto a petri dish with a cover and conditioned at ambient environment (20-30 %RH, 20-25°C) for 48 hours before use. The laboratory-recrystallized samples were then transferred to 15mL glass vials with a screwcap and covered with parafilm for additional protection from moisture sorption during storage.

5.4 Results and Discussion

An evidence-assertion approach will be used in this section, where the results (evidence) for each analytical method will be presented and discussed individually and then assembled into a hypothesis (assertion) that holistically addresses our original research objective to investigate the influence of the composition and chemistry of the sucrose crystal on its thermal behavior, specifically the origin of the small endothermic peak in some sucrose DSC thermograms.

Evidence

Moisture content, pH, conductivity ash, and total sulfite content measurements

The moisture content, pH, conductivity ash, and total sulfite content measurements are given in Table 5.1 and will be discussed in order below.

Moisture content

As can be observed from Table 5.1, there is no clear trend in moisture content values between beet and cane sucrose sources. For example, analytical grade Sigma cane sucrose, which exhibited the largest magnitude (ΔH J/g) small endothermic DSC peak and generated the largest amount of thermal decomposition components, had the lowest moisture content of all samples tested ($0.025\pm0.007\%$ w.b.); whereas, US beet and Sugar in the Raw samples, which did not exhibit a small endothermic DSC peak, had relatively high moisture content values ($0.060\pm0.014\%$ and $0.140\pm0.014\%$ w.b, respectively). Contrary to our expectations, the appearance and magnitude of the small endothermic DSC peak does not appear to be directly related to the sample moisture content as determined by Karl Fisher titration. However, it is possible that this result may be related to the Karl Fisher titration moisture content measurement method, as discussed in detail below.

In the literature, the water content of sugar is divided into three types of water: 1) free moisture, which is on the surface of the crystal and is easily and quickly removed by oven drying; 2) bound moisture, which is water located in the amorphous layer on the surface of the crystal and in the reentrant angles and is only released slowly as the amorphous sucrose crystallizes; and 3) inherent moisture, which is the water included within the crystal structure and is only released when the crystal is dissolved, e.g. during Karl Fischer titration measurements (Rodger and Lewis 1962).

As previously mentioned the moisture content determined using Karl Fischer volumetric titration method did not show higher values in cane source compared to beet sucrose sources. This could be due to a number of reasons. First, total water content may not be directly related to the appearance and magnitude of the small endothermic DSC peak, since the surface water is also counted into this value, but is hypothesized not to be a significant player in the hydrolysis reactions taking place within the mother liquor occlusions inside the crystal (further discussed in DSC and HPLC section below). Second, the amount of surface water is related to particle size and relative humidity. The smaller the size of the crystals in a sucrose sample, the more surface water can be adsorbed, due to the larger surface area compared to that of a sample of large crystals (Roge and Mathlouthi 2000). Lastly, some limitations of Karl Fischer volumetric titration method itself could also affect the moisture content result, such as sample dissolving and titrating times, initial residual moisture content of the solvent reagents, as well as the relative humidity of the lab during sample preparation.

The official method for measurement of moisture content in sugar is oven drying (ICUMSA GS2/1/3/9-15, The Determination of Sugar Moisture by Loss on Drying – Official). According to ICUMSA (2007) Loss on Drying method, the sugar sample (25 to 30 g) is held isothermally at 105°C for 3 hours at atmospheric pressure, followed by standardized cooling conditions. However, this oven drying based method mainly in the case of crystalline sugar only measures free (or surface) water, not total water. Theoretically, oven drying would underestimate the total amount of water present. However, preliminary research carried out in the Schmidt lab (Burnside and others 2011) showed that glucose was detected by HPCL analysis in analytical grade Sigma cane sucrose after 3 hours at 105°C, the conditions specified by the ICUMSA (2007)

Loss on Drying method. These preliminary results suggest that thermal decomposition is initiated in sucrose samples under the low temperature, long time oven drying conditions, potentially resulting in an overestimate of the surface water content. The possibility of thermal decomposition is a common caution associated with the use of oven drying of carbohydrate materials, as weight loss may not only be due to the water loss, but also caused by the formation of volatile decomposition components, such as 5-HMF (Bradley 2010).

Additional efforts to calculate the surface water content and the inherent water content were made by subtracting the surface water content, determined by isotherm adsorption studies, from Karl Fisher Titration measurements. However, these efforts proved unsuccessful. Rogé and Mathlouthi (2000) calculated the internal water content of sucrose by subtracting the surface water, measured using a modified Karl Fischer Titration method, from the total water content, measured using the traditional Karl Fischer Titration method. They reported that the internal water content remained constant, while the surface water increased as a function of % relative humidity. Lastly, an attempt was made to determine the inherent (or internal) water content of the beet and cane sucrose crystals using proton NMR spectroscopy at 500.07 MHz (Varian aquired by Agilent, Santa Clara, CA) (Hausch and others 2015). The sucrose was dissolved in DMSO-d_6. However, despite packing the samples in a dry glove box (humidity is less than 1 ppm), unexpected trends were obtained, also renduring this attempt unsuccessful.

pH and Conductivity Ash

As can be observed from Table 5.1, both pH and conductivity ash values varied widely within and between sucrose sources. White refined beet and cane sucrose sources have overlapping pH and conductivity value. However, it is interesting to note that the analytical

grade cane (Sigma and Fisher) sucrose samples have the lowest pH values and conductivity ash

content (pH = 5.32±0.34, 5.40±0.27 and conductivity ash = 9.0±0.1, 9.8±0.6 ppm for Sigma and

Fisher, respectively) compared to all other sucrose samples; whereas, Sugar in the Raw, a cane

sugar without a small endothermic DSC peak, had the highest pH and conductivity ash values

(pH = 7.73 ± 0.07 and conductivity ash content = 1576.7 ± 5.5 ppm).

It is widely recognized that the glycosidic linkage between D-glucose and D-fructose of the

sucrose molecule is remarkably more stable in an alkaline aqueous solution compared to an

acid medium (Mauch 1971; Lowary and Richards 1988). The hydrolysis of sucrose is highly

affected by the presence of acids, since the velocity constant (k in min^{-1}) of the hydrolysis

reaction (a first order reaction), is influenced by the activity of the hydrogen ions, which can be

described as the acid function, temperature, as well as concentration of sucrose and

electrolytes (Dawber and others 1966; Hollo and Szejtli 1961; Mauch 1971). In the literature,

several researchers have reported that impurities play an important role in the thermal

behavior of crystalline sucrose (Kamoda 1960; Eggleston and others 1996; Kishihara and others

2001; Okuno and others 2002a and b and 2003; Maulny 2003; Beckett and others 2006). For

example, Okuno's group summarized that the existence of Na$^+$, K$^+$ or hydrogen carbonate ions

(HCO3$^-$) will increase the melting point of recrystallized sucrose; whereas, the addition of Ca2$^+$

or Mg2$^+$ will lower the melting point of recrystallized sucrose. The higher ash content of raw

sugar compared to white refined sugar has been reported by Gillett (1949a and b). Gillett found

that the total ash content in raw sugars (ranged from 0.35% to 0.61% for 29 different

plantations) was much higher than in white sugars (about 0.001% in confectioners' sugar

samples and about 0.01% in granulated sugar samples) measured using the conductometric

method. These results support our hypothesis that the high conductivity ash content and pH values for Sugar in the Raw are related to the disappearance of the small endothermic DSC peak, which as predicted, the higher the ash content and/or the pH condition could inhibit the thermal induced hydrolysis in sucrose crystals.

These results support our hypothesis that the high pH and conductivity ash content values for Sugar in the Raw are related to the absence of a small endothermic peak in the DSC thermogram, where the higher pH conditions and/or ash content serve to inhibit the proposed thermal induced hydrolysis within the mother liquor occlusions.

Total Sulfite Content

There is a substantial difference in the total sulfite content between sucrose sugar sources (Table 5.1). Beet and Chinese cane sucrose sources contained sulfite (ranging from 6.5 to 11.2 ppm); whereas analytical and white refined cane sucrose sources were below the detection limit. "As is" Sugar in the Raw, a cane sucrose source, has a light brown color. Even after employing a clarification step to remove the color, a slight yellow color remained in the sugar solution and could have resulted in either an overestimation of the total sulfite content in this sample or the reading was in error and the sample actually does not contain sulfite. According to the Standard for Sugars (Alimentarius Commission Codex STAN 212-1999), the maximum levels of sulfites content within white refined sugar (beet and cane sucrose sources) and raw cane sugar are 15mg/kg and 20mg/kg, respectively. Therefore, the total sulfite content determined for selected sugar samples determined in this study (not including our laboratory recrystallized samples with higher levels of potassium sulfite addition) were all below the maximum levels established by the Codex Standard for Sugars. The total sulfite content in beet

sucrose sources is attributed to the sulfitation treatment employed during beet sugar

processing. It is well known that sulfites can inhibit browning reactions caused by ascorbic acid,

lipid, Maillard and enzymatic browning reactions (Wedzicha and others 1991). Thus, the

presence of sulfite may explain the absence of a small endothermic DSC peak in beet sucrose

sources; however the underlying mechanism of how sulfite increases the thermal stability of

crystalline sucrose requires further investigation.

Powder and Single Crystal X-ray Diffraction

The powder X-ray diffraction (PXRD) of all selected sucrose samples matched the reported

sucrose pattern of Brown and Levy (1973). As an example, a 2θ overlay plot of analytical grade

Sigma sucrose and a theoretical sucrose pattern calculated from Brown and Levy (1973) is given

in Figure 5.3. Further evidence collected from single crystal X-ray diffraction (SXRD) shows that

the unit cell parameters for all sucrose crystals measured are consistent with the known unit

cell of sucrose reported by Brown and Levy in 1973 (Table 5.2). Since PXRD and SXRD provide

the best structural evidence for polymorphism and unit cell parameters for all crystals match

the known reference unit cell of sucrose, therefore, the appearance of the small endothermic

DSC peak in cane sucrose samples is not attributable to polymorphism of crystalline sucrose, a

hypothesis suggested by Okuno and others (2003), Lee and Lin (2007a and b), and Lee and

Chang (2009). A search of the literature did yield a high-pressure polymorph of sucrose, sucrose

II (Patyk and others 2012), formed at a critical pressure of 4.80 GPa at 295K. However, sucrose II

is not stable at ambient conditions.

Micro-CT measurements

According to Micro-CT verification experiments (color histogram between crystalline sucrose and its surrounded saturated sugar solution), the entrapped mother liquor occlusions (viscous liquid) could not be clearly differentiated from the crystalline matrix (solid) due to their similar densities. Therefore, the small dark areas in the "as is" and heated crystals were identified as internal gas filled cavities (Figure 5.4 A thru D). A small number of internal gas filled cavities can be observed for both "as is" analytical grade Sigma cane and "as is" US beet sucrose sources as shown in Figures 5.4 A and B).

Based on our review of literature, it appears that Powers (1958) was the first to report observing both mother liquor and gaseous inclusions in sucrose under the microscope. By observing select crystal specimens in the act of dissolving, Powers (1958) reported that "when an inclusion of syrup is breached, the heavy syrup may be seen streaming downward, whereas when a gaseous inclusion is breached a bubble may be seen to strain like a balloon, and then to break away and rapidly rise to the surface." As to the origin of the bubbles, Powers (1958) states "The probable origin is that air dissolved in the original crystallizing syrup became supersaturated and formed as bubbles on the growing face. These were then overgrown by the layers." Gas bubble incorporation in growing crystals was also studied by Wilcox and Kuo (1973), who mentioned the work of Powers (1958 and 1959). It may also be possible that some cavities were formed within the mother liquor occlusions as sucrose crystallized from within the supersaturated entrapped mother liquor occlusions, as temperature decreased during the crystallization process. It may also be possible that some cavities were formed within the mother liquor occlusions as sucrose crystallized from within the supersaturated entrapped mother liquor occlusions, as temperature decreased during the crystallization process.

After heating to 165°C, a temperature 10°C higher than the onset temperature of the small

endothermic DSC peak, many more internal cavities were generated in analytical grade Sigma

cane sucrose compared to US beet (Figures 5.4 C and D). The generation of numerous cavities

resulted in a "Swiss cheese-like" internal structure for analytical grade Sigma cane sucrose. Yet,

analytical grade Sigma cane sucrose maintained its original external morphology and

appearance (see inset polarized light microscope images), similar to that of US beet, in which

numerous cavities did not develop upon heating to 165°C. Heat generated cavity formation

within the analytical grade Sigma cane sucrose crystal is associated with the presence of the

small endothermic DSC peak and in turn is associated with thermal induced hydrolysis, the

beginning of thermal decomposition, within the mother liquor occlusions. The ability of the

crystal to accommodate cavity formation without cracking is most likely associated with the

thermal expansion of the crystal lattice, which occurs during heating. The linear thermal

expansion of a sucrose crystal was reported as 0.0028%, 0.005%, and 0.0029% for the longest,

widest, and shortest axis per °C. The calculated cubical expansion is approximately 1.1×10^{-4}

per °C (Honig 1953). Upon rescanning in the DSC, a glass transition was detected at 68°C for

analytical grade Sigma cane sucrose, but no glass transition was detected for US beet. This

observation supports our hydrolysis hypothesis in analytical grade Sigma cane sucrose. Our

future research goal is to quantify the total cavity volume (% porosity) in different sucrose

sources before and after heating, based on 3-D image reconstruction, and to further explain the

mechanism of hydrolysis inhibition in beet sucrose sources.

Cavity formation during the heating of sucrose, observed using electron microscopy, was

reported by Thomas and Williams (1967). When sucrose crystals were heated for a prolonged

period (6 hours) under vacuum at 120°C, decomposition "volcanoes" were produced. The authors reasoned that perhaps, as in the thermal decomposition of some inorganic solids, such as calcite and the hydrates of nickel sulphate, preferential decomposition of the sucrose occurred at dislocations (a specific type of lattice defect). Thomas and Williams (1967) did observe dislocations in the sucrose crystal and, of special interest to the research herein, reported that "The cores of these dislocations consist of a column of water impurity which may be liberated on heating and by mechanical means." Thomas and Williams (1967) were not able to decide conclusively whether the observed decomposition "volcanoes" coincided with dislocations or not. However, upon further heating of the crystal after the occurance of the decomposition "volcanoes," caramelization took place and tended to occur preferentially within the area of enhanced imperfection.

DSC and HPLC analyses of "as is" and ground beet and cane sucrose sources

Application of physical grinding in the case of analytical grade Sigma and white refined US cane sucrose samples resulted in the loss of the small endothermic DSC peak without the appearance of a glass transition (Tg) (Figures 5.5). In addition to elimination of the small endothermic DSC peak, the onset temperature of the large peak in analytical grade Sigma cane sucrose shifted to a slightly lower temperature (about 4°C lower than the "as is" sample) when scanned at 10°C/min. Grinding not only released the water from the mother liquor occlusions, eliminating the small endothermic DSC peak in analytical and white refined cane sucrose samples, but also resulted in a 20°C increase in the decomposition onset temperature (Donset) for these samples as determined by HPLC analysis (as labeled in Figure 5.5). Unlike the analytical and white refined cane sucrose samples, grinding did not alter the DSC thermogram,

nor the HPLC analysis results, of the US beet sucrose sample. It is specifically worthy noting that decreasing the US beet particle size did not affect its onset temperature, supporting the conclusion that the effect of grinding is due to the release of the water from the mother liquor occlusions, not a result of the decrease in particle size. Also as it has been discussed in the literature, the melting temperature of a bulk material is not dependent on its size, only until the dimensions of a material decrease towards the atomic scale. Then, the melting point depression can be observed for materials, such as metals, in nanometer scale dimensions (Takagi 1954; Lopeandia and Rodriguez-Viejo, 2007; Sun and Simon 2007). Therefore, the observed thermal behavior differences between "as is" and ground cane samples cannot be explained by particle size decreases as proposed by Magoń and others (2014), but rather due to the easier release of water from the mother liquor occlusions after sample grinding (Richards 1903). For the interest reader, the HPLC data, at each temperature for both "as is" and ground sucrose samples, are located in Appendix F and I.

Even though the "as is" US beet sucrose contains mother liquor occlusions, it does not appear to undergo thermal induced hydrolysis, since there is no small endothermic peak in its DSC thermogram. The underlying cause of the thermal stability in beet sucrose samples is hypothesized to be due to the chemistry of the mother liquor occlusion, specifically the residual sulfite remaining from the use of SO_2 during beet sugar processing. The specific mechanism of action of the sulfite in the mother liquor occlusions requires further study.

The release of water due to grinding was discussed in the literature many years ago by Richards (1903): "It is usually considered as a sufficient precaution to powder the material finely and expose it to the air for a short time, in order to allow the undesirable water to

evaporate." For example, baric chloride samples containing crystal water of four different degrees of fineness were thoroughly air-dried before moisture measurement. The results show a steady decrease in the amount of water as the powder becomes finer; hence each successive powdering must have opened new cells.

More recently and more specific to sucrose, Beckett and others (2006) believed that the appearance of the peak at 150°C was mainly attributed to impurities in sucrose, especially as related to the mineral salt content. Based on the recrystallization work done by Bhandari and Hartel (2002), Beckett and others (2006) recrystallized sucrose with inorganic salts, such as KCl and K_2SO_4, which resulted in inhibition of the small endothermic DSC peak. However, after harvesting the recrystallized sucrose with inorganic impurities, the newly-grown crystals were ground before DSC analysis. Elimination of the small endothermic DSC peak was attributed to the presence of the inorganic impurities, however, based on the effect of sample grinding discussed above, elimination of the small peak cannot be solely attributed to the presence of inorganic impurities, but rather is confounded with the effects of sample grinding. Thus, based on literature findings, as well as our own research results, the presence of the small endothermic DSC peak can be removed either through thorough removal of the water from mother liquor occlusions (e.g., via grinding) or by mediation of the chemistry of the occlusion (e.g., via addition of specific type(s) of impurities, such as sulfite).

One additional question is in regards to the type of water mainly involved in the presence of the small endothermic DSC peak. To assess the effect of surface water versus occluded mother liquor water on the thermal behavior of sucrose, DSC thermograms, at a 10°C/min heating rate, from three sucrose samples were plotted and are shown in Figure 5.6 - "as is"

analytical grade Sigma cane sucrose under room %RH and temperature conditions (22 %RH and 24°C), "as is" analytical grade Sigma cane sucrose that was held for 48 hours and packed into a DSC pan in a 0%RH glove box, and ground "as is" analytical grade Sigma cane sucrose under room %RH and temperature conditions. This data illustrates that the main type of water associated with the presence of the small endothermic DSC peak is occluded water, since the 0%RH glove box analytical grade Sigma cane sucrose sample yield similar DSC thermograms containing the small endothermic DSC peak, whereas only when the occluded mother liquor water was removed via grinding did the small endothermic DSC peak disappear.

Previous research carried out in the Schmidt laboratory (Lee 2011) explored the effect of increasing the surface water content on the magnitude of the small endothermic DSC peak. To carry out this comparison, "as is" analytical grade Sigma cane sucrose was equilibrated to various % relative humidity values using for saturated salt slurries (11.3 [LiCl], 43.2 [K_2CO_3], 75.3 [NaCl], and 84.3 [KCl] %RH for 5 days at 25°C). An "as is" analytical grade Sigma cane sucrose sample was also included, with a relative humidity of 14%, as measured using an AquaLab 4TE (Decagon Devices, Pullman, WA) water activity meter. The resulting DSC thermograms, at a 10°C/min heating rate, are shown in Figure 5.7. The magnitude of the small endothermic DSC peak increased slightly at 75%RH and more substantially at 84.3 %RH, but remained quite similar for the lower %RH values. The increase in the magnitude of the small peak at the higher %RH values can be attributed to increasing amounts of water due to the onset of capillary condensation (compared to mainly surface water at the lower %RH values), which actually begins to dissolve the sucrose at the surface of the crystal (Billings and others 2006; Scholl and Schmidt 2014).

Recrystallization study

By applying our own laboratory recrystallization method, though we did not have high yield of crystals, the newly-grown sucrose crystals were large in size and clear in appearance, with less defects (dislocation, crystal twinning along the grain boundaries) compared to white refined sucrose crystals, which also was reported by Thomas and Williams (1967) and Vaccari and Mantovani (1995). The low crystal yield is attributed to the method we selected for use in this study - cooling crystallization. In cooling crystallization, a different solubility as a function of temperature is utilized. In a closed container, crystallization occurs without water evaporation. Thus, the maximum amount of crystals grown highly depends on the solubility difference between the temperatures at the start and end of crystallization (Vaccari and Mantovani 1995).

Interestingly, when analytical grade Sigma cane sucrose was recrystallized in pure HPLC water using this protocol, the DSC thermal profile exhibited only one large endothermic DSC peak, with the Tmonset close to the temperature of the small peak in "as is" Sigma sucrose (Figure 5.8). However, the single crystal X-ray diffraction results (Table 5.2) indicate that the unit cell parameters of this newly recrystallized Sigma sucrose are the same as the structure recorded in the Cambridge Crystallographic Data Centre (CCDC) and is, thus, not a polymorph of sucrose. Addition of potassium sulfite (K_2SO_3), at concentrations of 0.5% or higher, can eliminate the small DSC peak (Figure 5.6), but do not change the crystalline structure (Table 5.2). Thermal profiles for all recrystallized Sigma samples collected using DSC at 10°C/min are provided in Table 5.3. The concentrations of total sulfite in the laboratory-recrystallized Sigma sucrose with potassium sulfite are given in Table 5.4. A clear trend can be observed in which crystallizing Sigma sucrose with higher amounts of potassium sulfite content results in a more

effective inhibition effect on small endothermic DSC peak. The potential mechanism to explain the thermal influence of sulfite found in the literature is that SO_2 will react with carbonyl groups in sugar molecule to form a sugar bisulfite adduct, which in turn suppresses the degradation of the monosaccharide (Shi 2014). Our future research will be focused on confirming the increased thermal stability of our own laboratory-recrystallized Sigma sucrose samples with potassium sulfite using HPLC analysis. It will also be interesting to determine whether other impurities reported in the literature, such as potassium sulfate (K_2SO_4) reported by Beckett and others 2006), will show the same impact on the thermal behavior of sucrose.

Assertion

The results of this study suggest that mother liquor occlusions within the sucrose crystal are essential to the presence of the small endothermic DSC peak, where the mother liquor occlusions are associated with thermal induced hydrolysis and subsequent thermal decomposition. However, the occlusions alone are not sufficient to explain the presence of the small endothermic DSC peak, since the white refined beet, Sugar in the Raw, and Chinese cane sucrose samples also contain occlusions, but do not exhibit the small endothermic DSC peak. The laboratory-recrystallization investigation further proved that the appearance of the small endothermic DSC peak in analytical grade Sigma cane sucrose can be inhibited by sulfite contained in the mother liquor occlusions, which explains the lack of a small endothermic DSC peak in white refined beet, Sugar in the Raw, and Chinese cane sucrose samples. This research reveals that the sucrose crystal composition and chemistry is instrument in determining its thermal behavior.

5.5 Conclusions

For years, a wide variation in the thermal behavior of sucrose has been reported in the literature. However, the underlying mechanism(s) responsible for this variation are still under investigation. As discussed in the assertion, this study suggests that mother liquor occlusions within the sucrose crystal are essential to the presence of the small endothermic DSC peak, where the mother liquor occlusions are associated with thermal induced hydrolysis and subsequent thermal decomposition. However, the occlusions alone are not sufficient to explain the presence of the small endothermic DSC peak, since the white refined beet, Sugar in the Raw, and Chinese cane sucrose samples also contain occlusions, but do not exhibit the small endothermic DSC peak. The laboratory-recrystallization investigation further proved that the appearance of the small endothermic DSC peak in analytical grade Sigma cane sucrose can be inhibited by sulfite contained in the mother liquor occlusions, which explains the lack of a small endothermic DSC peak in white refined beet, Sugar in the Raw, and Chinese cane sucrose samples. This research reveals that the sucrose crystal composition and chemistry is instrument in determining its thermal behavior, which in turn, is important to thermal processing and reactions of sucrose and sucrose containing foods, such as baking and caramelization.

Our future research will focus on confirming the increased thermal stability of our own laboratory-recrystallized Sigma sucrose samples containing potassium sulfite using HPLC analysis. We are also interested in determining whether other impurities reported in the literature, such as potassium sulfate (K_2SO_4), will exhibit the same impact on the thermal behavior of sucrose.

5.6 Acknowledgements

5.7 References

Andrews LS, Godshall MA. 2002. Comparing the Effects of Sulphur Dioxide on Model Sucrose and Cane Juice Systems. Journal American Society of Sugarcane Technologists. 22: 90-101.

Asadi M. ed. 2007. Beet-sugar handbook. John Wiley & Sons, Inc., Hoboken, New Jersey, USA.

Beckett ST, Francesconi, MG, Geary PM, MacKenzie G, Maulny APE. 2006. DSC study of sucrose melting. Carbohydrate Research 341: 2591-2599.

Bhandari B, Hartel R. 2002. Co-crystallization of Sucrose at High Concentration in the Presence of Glucose and Fructose. J. of Food Sci, 67: 1797–1802.

Billings SW, Bronlund JE, Paterson AHJ. 2006. Effects of capillary condensation on the caking of bulk sucrose. J. Food Eng. 77: 887–895 and the Corrigendum in 2008. J. Food Eng. 84:180.

Bradley RL. 2010. Moisture and total solids analysis, Chapter 6. In "Food Analysis, 4th Edition." S. Suzanne Nielsen (Ed.). Springer, NY, NY. p. 602.

Brown GM, Levy HA. 1973. Further refinement of the structure of sucrose based on neutron-diffraction data. Acta Cryst. B29, 790-797.

Burnside E, Lee JW, Schmidt SJ. 2011. Does the ICUMSA Standard Method for moisture content determination in sugars result in thermal decomposition in sucrose? Research Project in FSHN 595 Water Relations in Foods, Spring 2011.

Chan KY, Wasserman BP (1993) Direct Colorimetric Assay of Free Thiol-Groups and Disulfide Bonds in Suspensions of Solubilized and Particulate Cereal Proteins. Cereal Chem 70:22–26.

Clarke MA, Godshall MA. eds. 1988. Chemistry and Processing of Sugarbeet and Sugarcane. Chapter 13, The nature of colorants in sugarcane and beet sugar manufacture. Elsevier Science Publishers, Amsterdam.

Codex Alimentarius Commission, Standard for sugars. CODEX STAN 212-1999 (Updated up to the 38th Session of the Codex Alimentarius Commission 2015). Available from GSFA Online: http://www.codexalimentarius.net/gsfaonline/groups/details.html?id=161&lang=en.

Dawber JG, Brown DR, Reed RA. 1966. Acid-catalyzed hydrolysis of sucrose: A student study of a reaction mechanism. J Chem Educ 43:34.

Eggleston G, Trask-Morrell BJ, Vercellotti JR. 1996. Use of differential scanning calorimetry and thermogravimetric analysis to characterize the thermal degradation of crystalline sucrose and dried sucrose-salt residues. J. Agric. Food. Chem. 44, 3319-3325.

Ellman GL. 1958. A colorimetric method for determining low concentrations of mercaptans. Arch. Biochem. Biophys. 74:443-450.

Gillett TR. 1949a. Conductometric Measurement of Ash in White. Sugars Analytical Chemistry 21(9): 1081-1084.

Gillett TR. 1949b. Conductometric Determination of Ash in Raw Sugars. Sugars Analytical Chemistry 21(9): 1084-1086.

Hausch BJ, Lu Y, Shi Y and Zhan Z. 2015. Investigating the moisture content difference in mother liquor occlusion between beet and cane sucrose sources. FSHN 595 Water Relations in Foods Course Reseacrh Project, Spring 2015, University of Illinois at Urbana-Champaign, IL.

Hollo J, Szejtli J. 1961. Acid hydrolysis of the glycosidic bond. IV. The influence of the nature and concentration of different acides on the hydrolysis of starch. Staerke 13, 327-331.

How to Grow Crystals. The University of Florida Center for X-ray Crystallography. Available from: https://xray.chem.ufl.edu/how-to-grow-crystals/. Last accessed Nov.30, 2015.

Huo H. 2008. 1st ed. Modern chemistry and technology of Chinese sugar refinery. Chemical Industry Press. Total page 324.

ICUMSA 2011. Official and Tentative Methods Recommended by the International Commission for Uniform Methods of Sugar Analysis.

Kamoda M. 1960. Proceedings of the Research Society of Japan Sugar Refineries' Technologists. 27, 158–238.

Kawakami K, Miyoshi K, Tamura N, Yamaguchi T, and Ida Y. 2006. Crystallization of sucrose glass under ambient conditions: Evaluation of crystallization rate and unusual melting behavior of resultant crystals. Journal of Pharmaceutical Sciences, 95(6): 1354-1363.

Kishihara S, Okuno M, Fujii S, Kawasaki K, Nishiura T. 2001. An opinion on structure of sucrose crystal. Proceedings of the Research Society of Japan Sugar Refineries' Technologists 49:1-8.

Lee JW. 2011. Data collected during post-doctoral research carried out at the University of Illinois at Urbana-Champaign, IL.

Lee JW, Thomas LC, Jerrell J, Feng H, Cadwallader KR, Schmidt SJ. 2011b. Investigation of thermal decomposition as the kinetic process that causes the loss of crystalline structure in sucrose using a chemical analysis approach (Part II). Journal of Agricultural and Food Chemistry, (59):702-712.

Lee JW, Thomas LC, Schmidt SJ. 2011a. Investigation of the heating rate dependency associated with the loss of crystalline structure in sucrose, glucose, and fructose using a thermal analysis approach (Part I). Journal of Agricultural and Food Chemistry, (59):684-701.

Lee T and Chang GD. 2009. Sucrose conformational polymorphism. Crystal Growth and Design, 9(8): 3551-3561.

Lee T and Lin YS. 2007a. Dimorphs of sucrose. International Sugar Journal, 109 (1303):440-445.

Lee T and Lin YS. 2007b. Two Conformational Polymorphs of Sucrose. National Central University.

Lopeandia AF, Rodriguez-Viejo J (2007). Size-dependent melting and supercooling of Ge nanoparticles embedded in a SiO2 thin film. Thermochimica Acta 461: 82-87.

LOT-QuantumDesign GmbH. Available from: http://www.lao.cz/data/ke-stazeni/MicroXCT_200_eu_1_.pdf. Last accessed Nov,30 2015.

Lowary TL, Richards GN (1988) Effects of impurities on hydrolysis of sucrose in concentrated aqueous solutions. Int Sugar J 90(1077):164–167.

Lu Y, Lee JW, Thomas L, Schmidt SJ. 2013. Proceedings of the 74th Annual Institute of Food Technologists on Differences in the Thermal Behavior of Beet and Cane Sugars. Chicago, IL.

Lu Y. Lee JW, Thomas L, Jerrell JJ, Cadwallader KR, Schmidt SJ. 2014. Proceedings of the 75th Annual Institute of Food Technologists on Investigating Thermal Decomposition Differences between Beet and Cane Sugars Using HPLC. New Orleans, LA.

Mathlouthi M and Roge B. 2012. Melting And Crystallization of Sugars: a structural approach. 2012 IFT Annual Meeting presentation. Las Vegas, NV.

Mauch W (1971) Chemical properties of sucrose. Sugar Technol. Rev 1:239–290.

Maulny A. 2003. Co-crystallisation of sugars. Ph.D. Thesis, Department of Chemistry, University of Hull, Hull, UK.

Megazyme Total Sulphite (TSO2) & Free Sulphite (FSO2) Assay procedure. Mannual & Auto-Analyser Liquid Stable, Rapid, Format. K-SULPH, September, 2011.   Megazyme Inc, Wicklow, Ireland.

Magoń A, Wurm A, Schick C, Pangloli P, Zivanovic S, Skotnicki M, Pyda M. 2014. Heat capacity and transition behavior of sucrose by standard, fast scanning and temperature-modulated calorimetry. Thermochimica Acta, 589: 183-196. Article reprinted in 2015, Thermochimica Acta, 603, 149-161.

Miller, MM. 2001. The effect of applied fields on crystallisation. Brunel University.

Okuno M, Nakai N, and Kishihara S. 2003. Melting Point of Sucrose Crystals Prepared in Various Solvents. Proceedings of research Society of Japan Sugar Refineries' Technologists, (51):1-6.

Okuno, M.; Kishihara, S.; Fujii, S.; Kawasaki, K. Analysis of structure of sucrose crystal by differential scanning calorimetry. Proc. Res. Soc. Jpn. Sugar Refin. Technol. 2002a, 50, 11-18.

Okuno, M.; Kishihara, S.; Fujii, S.; Kawasaki, K. Melting point of sucrose crystal prepared in sucrose solution containing various impurities. Proc. Res. Soc. Jpn. Sugar Refin. Technol. 2002b, 50, 19-27.

Ouiazzane S, Messnaoui B, Abderafi ., Wouters J, and Bounahmidi T. (2008). Estimation of sucrose crystallization kinetics from batch crystallizer data. Journal of Crystal Growth, 310(4), 798-803.

Patyk E, Skumiel J, Podsiadto M, and Katrusiak A. 2012. High-pressure (+)-sucrose polymorph. Angewandte Communications, International Additions, 51:2146-2150.

Powers HEC. 1958. Sucrose crystal inclusions. Nature, 182:715-717.

Powers HEC. 1959. Inclusions. International Sugar Journal, 17-18:41-44.

Reynhardt EC. 1990. An NMR, DSC and X-ray investigation of the disaccharides sucrose, maltose and lactose, Molecular Physics: An International Journal at the Interface Between Chemistry and Physics, 69:6, 1083-1097.

Richards TW. 1903. The Inclusion and Occlusion of Solvent in Crystals. An Insidious Source of Error in Quantitative Chemical Investigation. Proceedings of the American Philosophical Society Vol. 42, No. 172 (Jan. - Apr., 1903), pp. 28-36.

Riddles, P. W., Blakelye, R. L., and Zerner, B. 1983. Reassessment of Ellman's reagent. Methods Enzymol. 91:49-60.

Rizzi GP (2010) Control of Color Formation by Ionic Species in Non-Enzymic Browning Reactions.

Rodgers, T and Lewis, CL (1962-1963). The drying of white sugar and its effect on bulk handling. Int Sug J 64: 359-362; 65: 12-16,43-45,80-83.

Rogé, B. Mathlouthi, M. (2000). Caking of sucrose crystals: effect of water content and crystal size. Zuckerindustrie, 125(5), 336-340.

Scholl, S.K. and Schmidt, S.J. 2014. Determining the physical stability and water-solid interactions responsible for caking during storage of alpha anhydrous glucose. Journal of Food Measurement and Characterization, 8:326-335.

Shah SV, Chakradeo YM. 1936. A note on the melting point of cane sugar. Journal of Current Science. P652-3.

Shi Y (2014) Existence of the sugar-bisulfite adducts and its inhibiting effect on degradation of monosaccharide in acid system. Appl Biochem Biotechnol 172:1612–1622.

Schmidt S.J. 2012. Exploring the sucrose-water state diagram: Applications to hard candy cooking and confection quality and stability. Manufacturing Confectioner, January: 79-89.

Schneider F 1979. Sugar Analysis: ICUMSA Methods. International Commission for Uniform Methods of Sugar Analysis. Norwich 265pp.

Sun J, Simon SL (2007). The melting behavior of aluminum nanoparticles. Thermochimica Acta 463: 32-40.

Suryanarayana C, Norton MG. 1998. X-ray Diffraction: A Practical Approach. New York NY: Plenum Press. 281 p.

Takagi M (1954). Electron-Diffraction Study of Liquid-Solid Transition of Thin Metal Films. J Phys. Soc. Jpn. 9: 359-363.

Taylor M (1947). The solubility at high temperature of pure sucrose in water. Journal of the Chemical Society, 1, pp. 1678-1683.

Thannhauser, T. W., Konishi, Y., and Scheraga, H. A. 1987. Analysis for disulfide bonds in peptides and proteins. Methods Enzymol. 143:115-119.

Thomas JM and Williams JO. 1967. Lattice imperfections in organic solids. Part 2. Sucrose. Transactions of the Faraday Society, 63: 1922-1928.

Vaccari G, Mantovani G. 1995. Sucrose crystallization. In: Mathlouthi M, Reiser P, editors. Sucrose properties and applications. 1st ed. Bishopbriggs: Blackie Academic and Professional. p 33-72.

Wedzicha BL, Bellion, Goddard SJ. 1991. Inhibition of browning by sulfites. Adv Exp Med Biol. 289:217-36.

Yin L (2012) 12 X-ray computerized microtomography. In: Graciela PW, Wang Q (eds) nonotechnology research methods for foods and bioproducts, 1st ed. John Wilwy & Sons, Inc., pp 215–23.

5.8 Figures and Tables
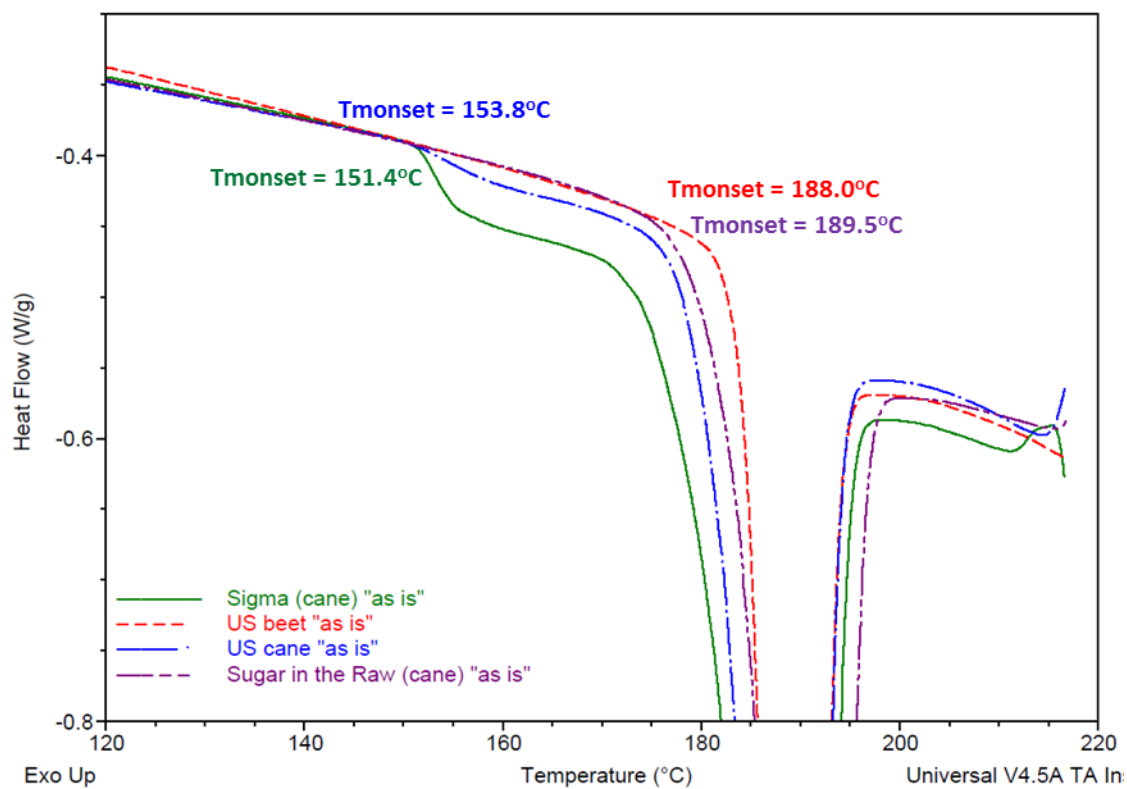
Figure 5.1 DSC thermograms of analytical grade Sigma cane, US beet, US cane, and Sugar in the Raw (cane) samples at 10°C/min heating rate.
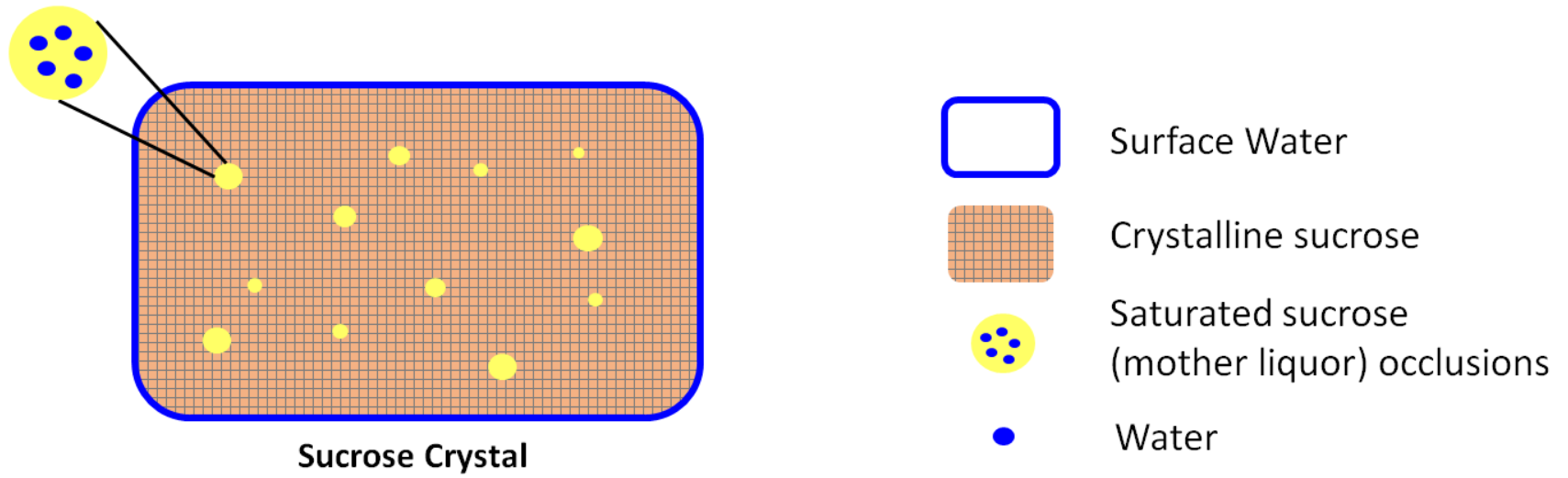
Figure 5.2 Model of a sucrose crystal containing mother liquor occlusions.
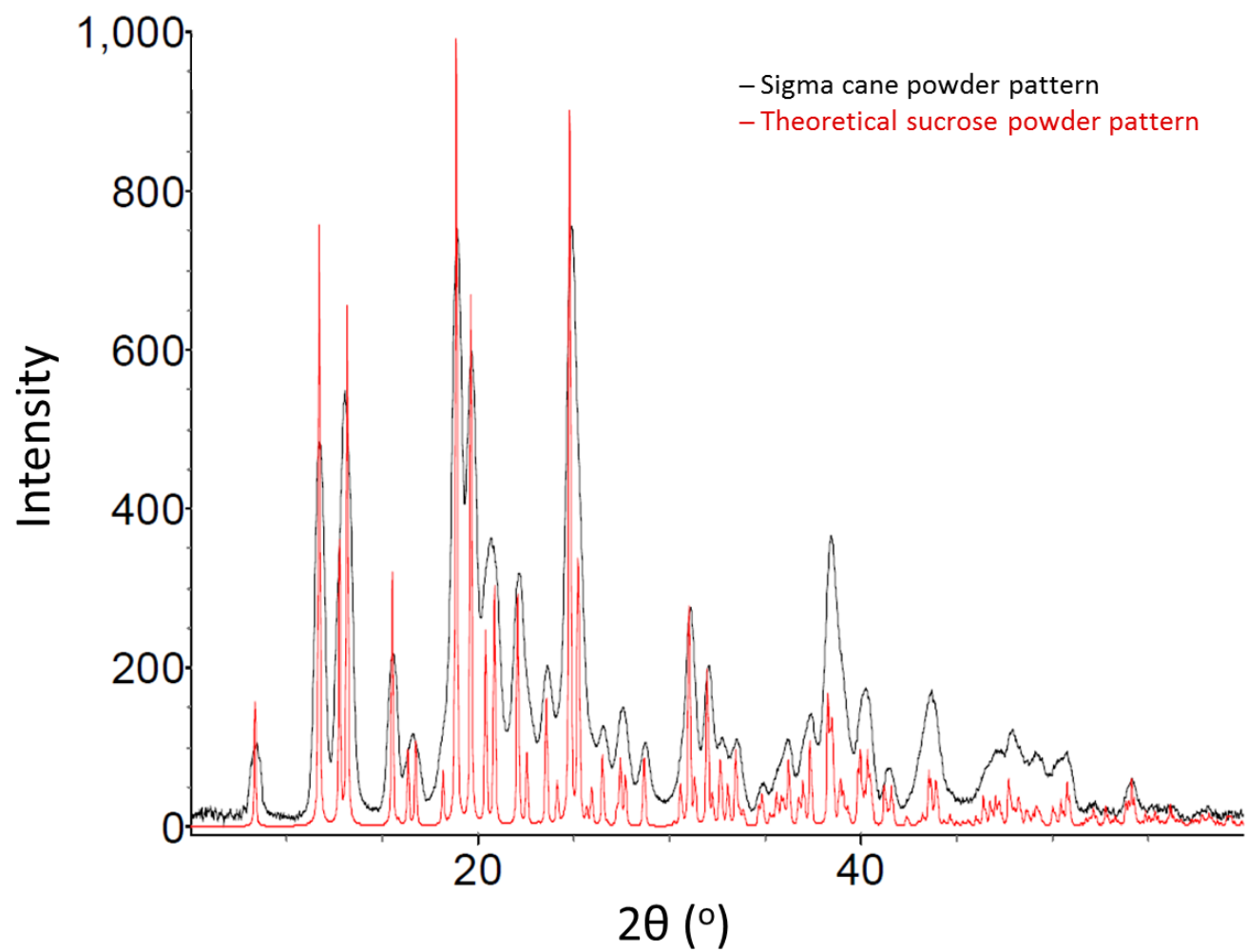
Figure 5.3   Powder X-ray diffraction patterns of analytical grade Sigma cane sucrose plotted with a theroretical sucrose pattern calculated from Brown and Levy (1973).
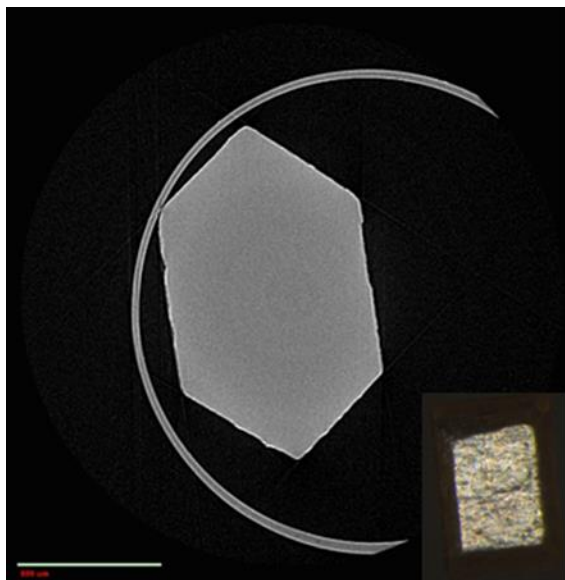
A. Sigma "as is"
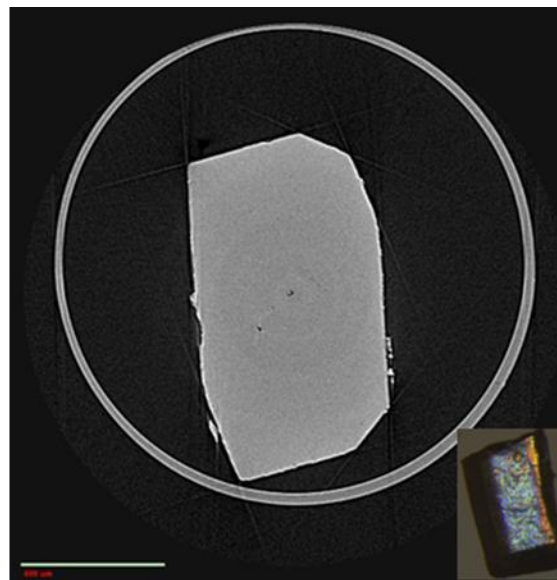
B. US beet "as is"
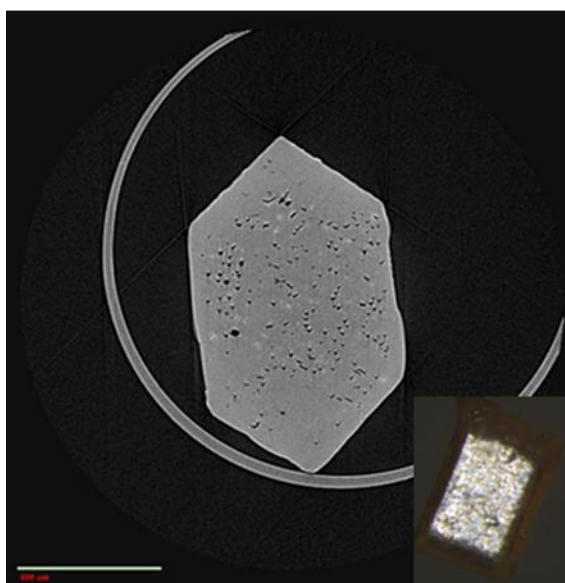
C. Sigma after heating to 165° C
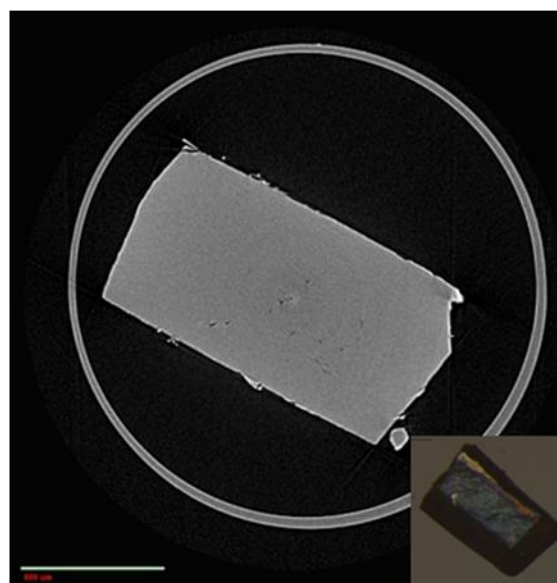
D. US beet after heating to 165° C

Figure 5.4 Micro-CT radiographs of the internal structure of analytical grade Sigma cane sucrose and US beet sucrose sources "as is" and after heating to 165°C. Grey scale intensity differences are due to differences in material density and atomic number. Inset polarized light microscope images of "as is" crystals and crystals after heating to 165°C showing the surface morphology of crystals.
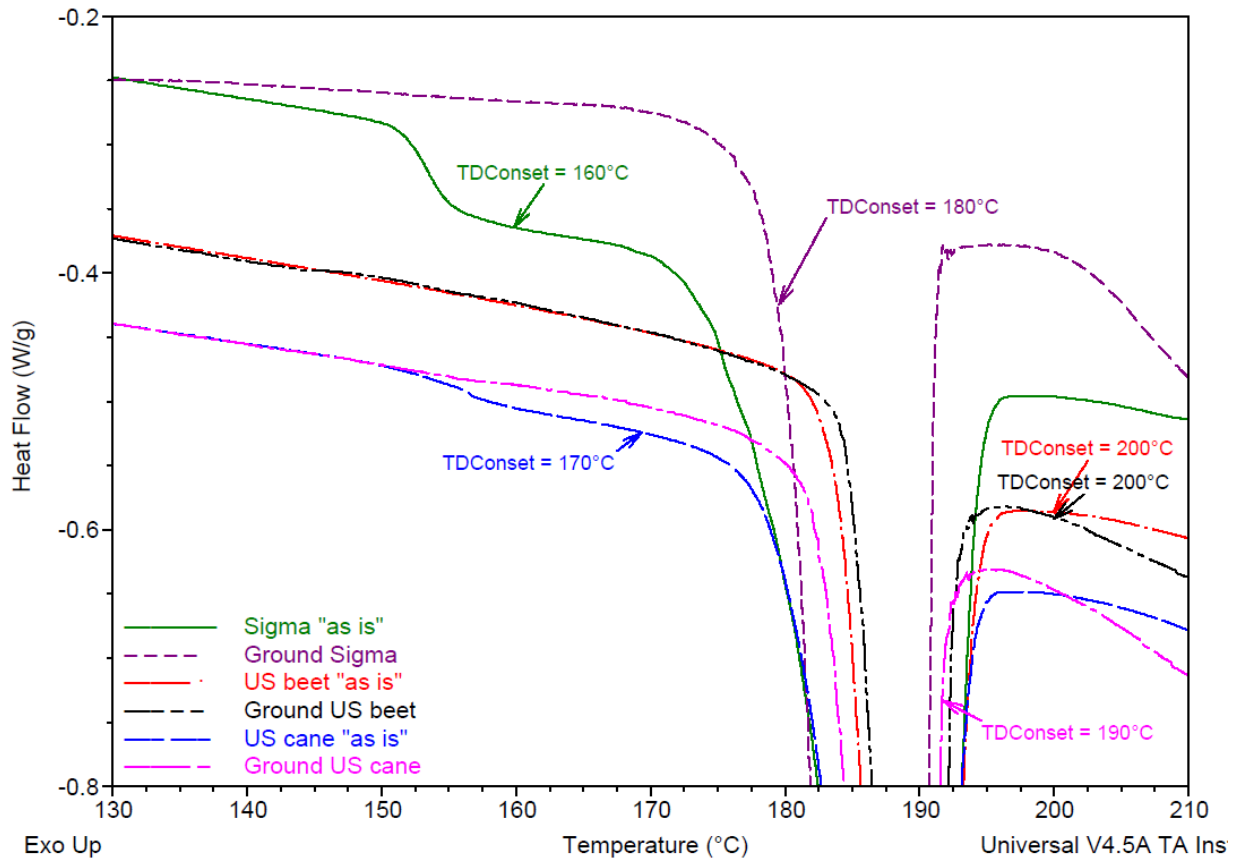
Figure 5.5 DSC thermograms of "as is" and ground analytical grade Sigma cane sucrose, US beet, and US cane samples at 10°C/min labeled with the temperature at which the earliest decomposition indicator component (glucose; Donset) was detected using HPLC.
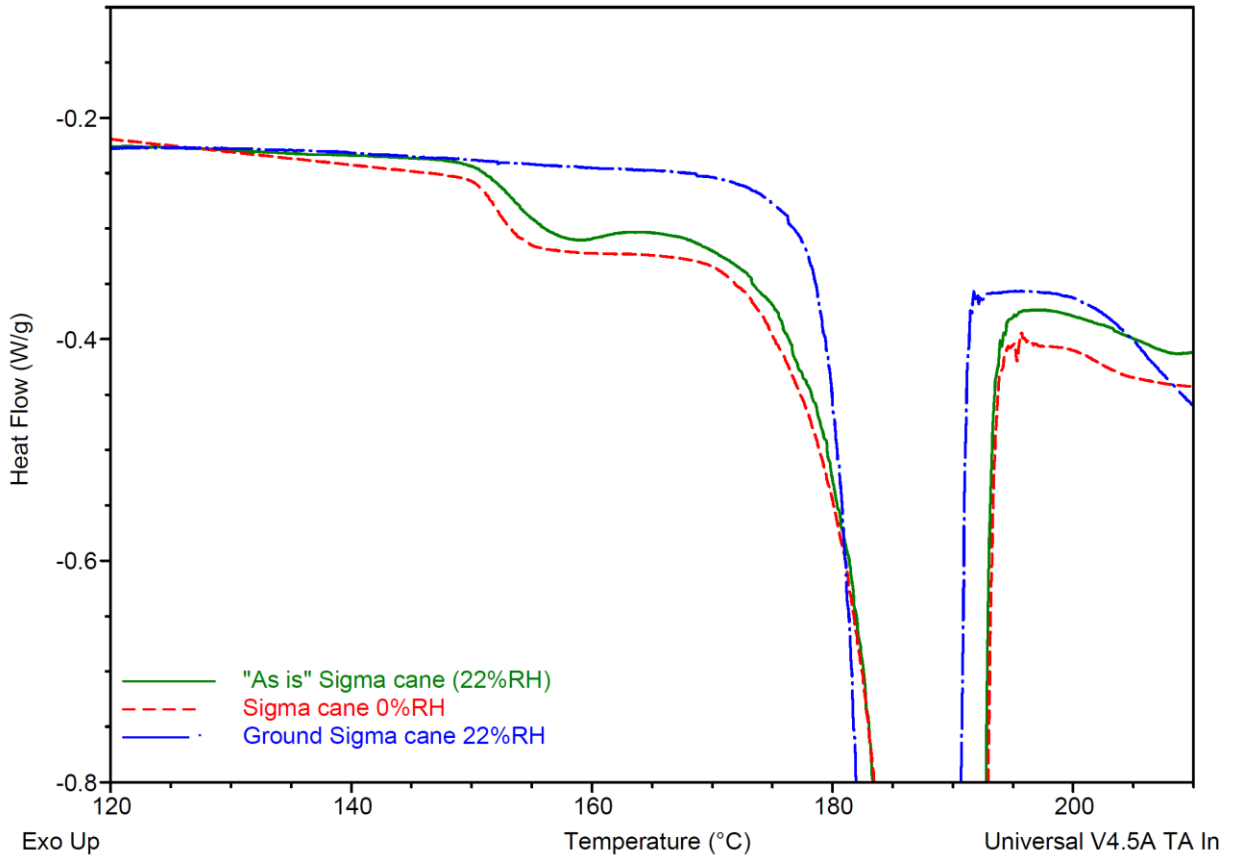
Figure 5.6 DSC thermograms, at 10°C/min heating rate, of "as is" and ground analytical grade Sigma cane sucrose samples at 22 %RH and "as is" analytical grade Sigma cane sucrose at 0%RH.
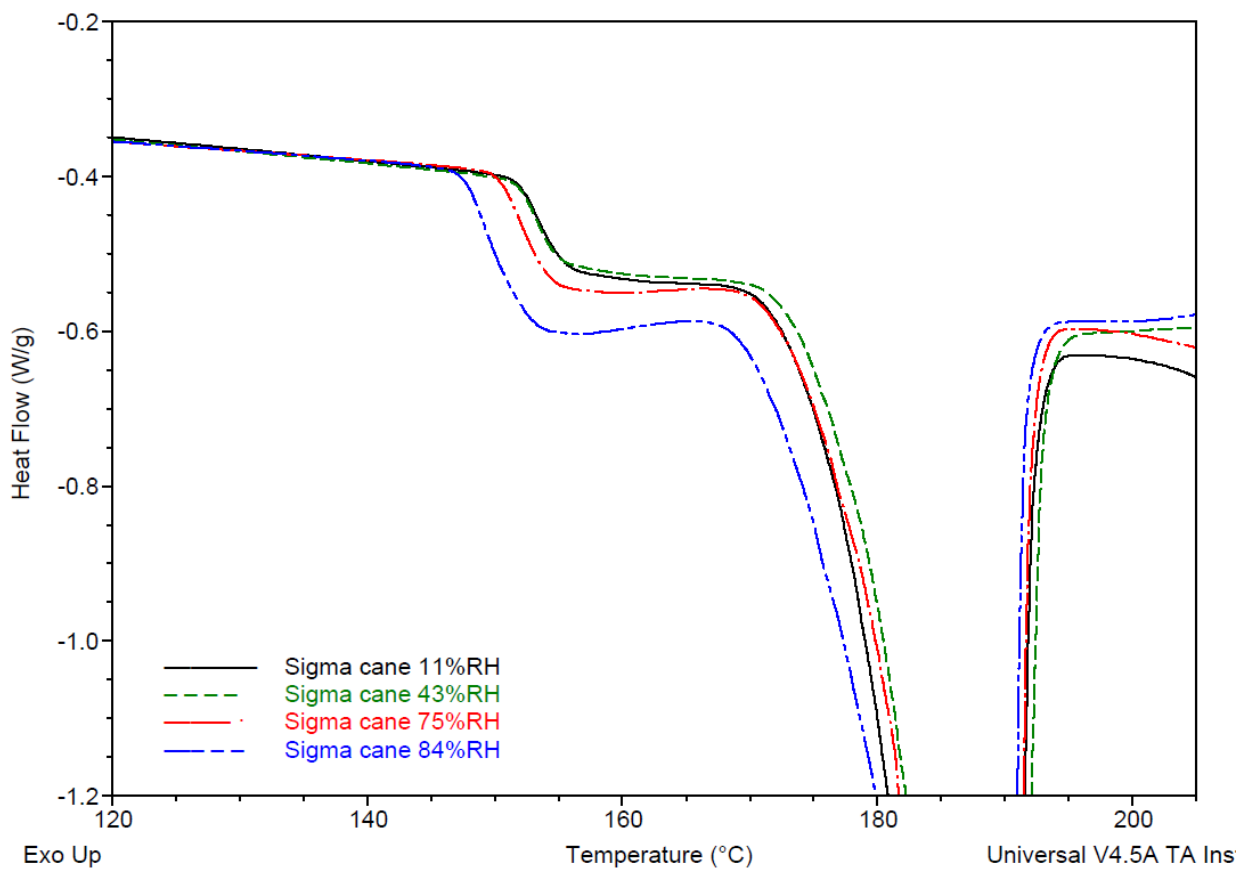
Figure 5.7 DSC thermograms of "as is" analytical grade Sigma cane sucrose equilibrated to various %RH values (0, 11, 43, 75, and 84%) at a 10°C/min heating rate.
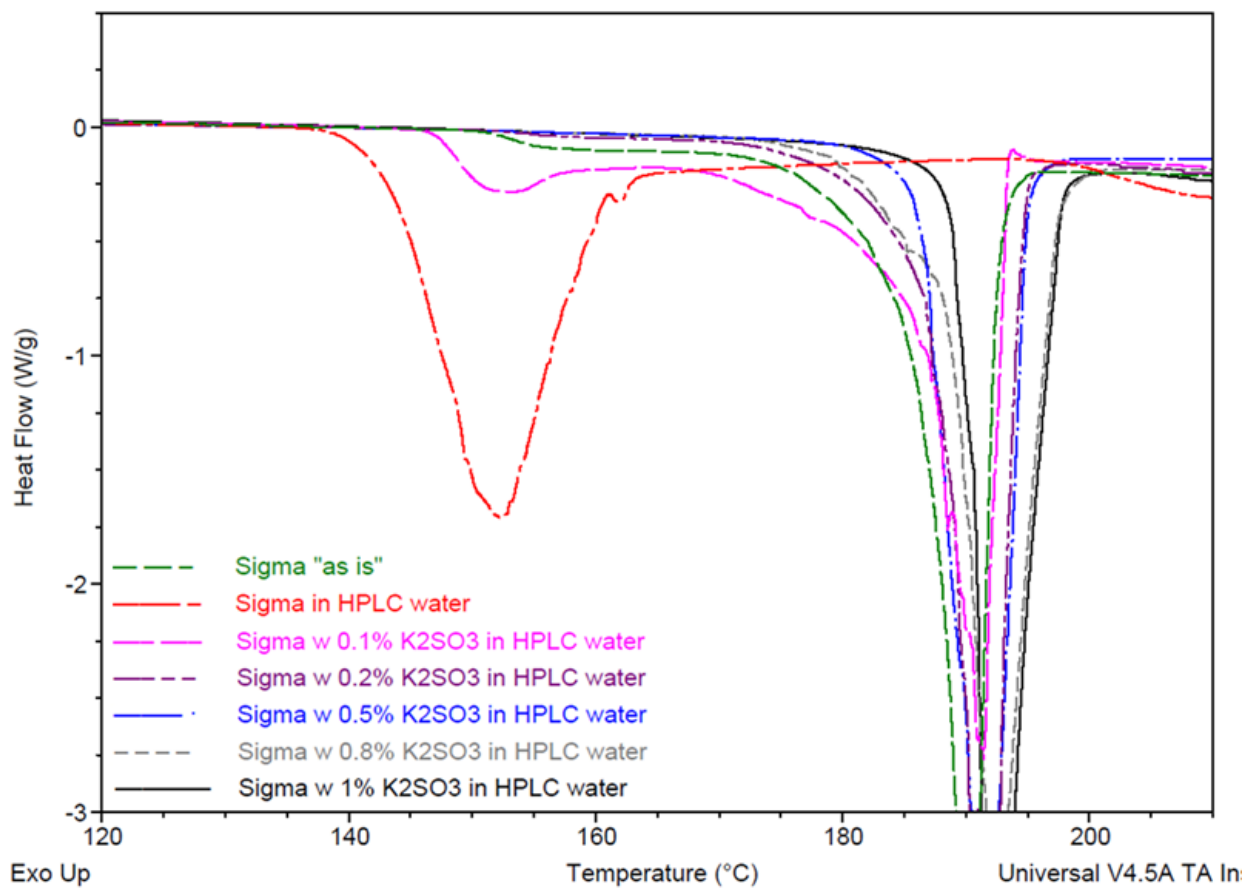
Figure 5.8 DSC thermograms of Laboratory-recrystallized Sigma cane sucrose with 0 to 1% of potassium sulfite percentage in HPLC water at 10°C/min.

Table 5.1 Average moisture content, pH, and conductivity ash values for beet and cane sucrose sources

Sample ID	Source	Karl Fischer titration			pH[a]	Conductivity Ash (ppm)	Total sulfite[b] (ppm)
		MC % (w.b.)	Temperature (°C)	%RH			
Sigma Sucrose	Cane	0.025±0.007	24.5	21.8	5.32 ± 0.34	9.0 ± 0 .1	<DL
Fisher Sucrose	Cane	0.070±0.014	21.4	24.6	5.40 ± 0.27	9.8 ± 0.6	<DL
US cane	Cane	0.030±0.000	24.5	21.8	5.86 ± 0.15	193.5 ± 12.3	<DL
C&H	Cane	0.090±0.014	21.4	24.6	5.65 ± 0.11	120.4 ± 11.6	<DL
Dixie crystal	Cane	0.040±0.014	23.1	24.5	6.30 ± 0.05	131.0 ± 3.0	<DL
Domino	Cane	0.035±0.007	23.1	24.5	6.80 ± 0.07	298.1 ± 13.7	<DL
Sugar in the Raw	Cane	0.140±0.014	21.4	24.6	7.73 ± 0.07	1576.7 ± 5.5	8.64±5.54
Chinese sugar	Cane	0.140±0.000	21.4	24.6	6.10 ± 0.06	243.5 ± 0.3	6.53±2.22
US beet	Beet	0.060±0.014	24.5	21.8	5.95 ± 0.19	116.1 ± 4.8	11.16±4.85
Pioneer	Beet	0.115±0.007	21.4	24.6	7.02 ± 0.07	72.1 ± 0.8	10.16±3.51
Meijer	Beet	0.090±0.000	21.4	24.6	6.77 ± 0.21	78.1 ± 0.9	7.39±2.08
Market pantry	Beet	0.055±0.021	23.1	24.5	6.23 ± 0.18	133.9 ± 2.6	8.66±2.34

[a]The pH of HPLC grade water = 5.83 ± 0.34
[b]Detection Limits (DL) = 5.28 ppm (Megazyme 2011)

Table 5.2 Unit cell parameter (average value (standard deviation)) of selected beet and cane sucrose samples obtained using single crystal X-ray diffraction.

Sample ID	a(Å)	b(Å)	c(Å)	α(°)	β (°)	γ(°)	Volume (Å^3)	Space group	Exp. Temp (°C)
Sucrose Ref[a].	7.7585(4)	8.7050(4)	10.8633(5)	90	102.945	90	715.04	P2$_1$	22.5±1.5
Sigma (cane)	7.7277(10)	8.6776(11)	10.8341(13)	90	102.9640(10)	90	707.99(15)	P2$_1$	-91.0
US beet	7.741(2)	8.691(2)	10.853(3)	90	102.981(3)	90	711.5(3)	P2$_1$	-91.0
US cane	7.7376(15)	8.6930(16)	10.833(2)	90	102.991(2)	90	710.0(2)	P2$_1$	-100.0
Chinese cane	7.755(2)	8.695(4)	10.864(4)	90	102.955(14)	90	713.9(7)	P2$_1$	23.2
Sugar in the Raw	7.7213(15)	8.6654(17)	10.8168(22)	90	103.069(30)	90	704.99(35)	P2$_1$	23.2
Sigma rec. in HPLC water	7.740(6)	8.668(7)	10.829(8)	90	103.01(2)	90	707.90(15)	P2$_1$	23.5
Sigma rec. w/ 0.5% K$_2$SO$_3$	7.7667(14)	8.7026(11)	10.850(2)	90	102.839(16)	90	715.0(3)	P2$_1$	23.2

[a] Unit cell parameters of sucrose reported by Brown and Levy (1973)

Table 5.3 Average DSC parameters (Tm onset, Tm peak, ΔH) and associated standard deviations for " as is" and laboratory-recrystallized Sigma cane samples ramped from 25 to 220°C at 10°C/min. Dash indicates that the small/large peak was not observed.

Sample ID	Small Tm onset °C	Small Tm peak °C	Small ΔH (J/g)	Tm onset °C	Tm peak °C	ΔH (J/g)
Sigma "as is"	151.60±0.43	172.42±1.50	7.64±0.64	187.51±0.27	190.72±0.29	126.92±1.89
Recrystallized in HPLC water	144.40±1.24	151.01±1.69	105.85±3.32	—	—	—
Recrystallized w/ 0.1% K_2SO_3	147.47±0.55	153.21±0.52	25.48±6.89	187.43±1.60	191.34±0.12	106.18±12.33
Recrystallized w/ 0.2% K_2SO_3	151.99±0.11	166.83±2.28	2.47±0.46	188.83±0.09	191.63±0.79	133.80±1.27
Recrystallized w/ 0.5% K_2SO_3	—	—	—	190.13±1.02	192.07±0.59	132.00±6.25
Recrystallized w/ 0.8% K_2SO_3	—	—	—	189.06±0.51	191.90±0.39	136.8±1.84
Recrystallized w/ 1.0% K_2SO_3	—	—	—	189.93±0.91	191.72±0.91	133.35±2.62

Table 5.4 Total sulfite content in laboratory-recrystallized Sigma cane samples.

Sample ID	Total sulfite content (ppm)
Sigma cane "as is"	<DL
Sigma Recrystallized in HPLC water	<DL
Sigma Recrystallized w/ 0.1% K_2SO_3	<DL
Sigma Recrystallized w/ 0.2% K_2SO_3	<DL (4.57 ± 0.06)
Sigma Recrystallized w/ 0.5% K_2SO_3	12.93 ± 3.61
Sigma Recrystallized w/ 0.8% K_2SO_3	24.09 ±9.30
Sigma Recrystallized w/ 1.0% K_2SO_3	40.51 ± 9.24

[*]Detection Limits (DL) = 5.28 ppm

Chapter 6: Unraveling the wide varation in the thermal behavior of crystalline sucrose using an enhanced recrystallization protocol

6.1 Abstract

For years, a wide variation in the thermal behavior of sucrose has been reported in the literature. During our investigation of a number of sucrose samples, a distinct difference was observed between the thermal profiles of beet and cane sucrose sources at 10°C/min heating rate. In general, sucrose from beet sources exhibited only one large endothermic peak; whereas, sucrose from cane sources exhibited two endothermic peaks in the differential scanning calorimetry (DSC) thermogram, one small peak proceededly by one large peak. Previous studies also revealed that the formation of thermal decomposition components is associated with the appearance of the small endothermic DSC peak in cane sugar sources. By applying our own laboratory-recrystallized method (recrystallized in pure HPLC water with and without the addition of K_2SO_3), we could alter the thermal behavior of sucrose, which only exhibted one DSC peak with the Tmonset either at lower temperature (~144°C) or at higher temperature (~190°C) at a 10°C/min DSC heating rate. We hypothesized that the presence of the small endothermic peak in most "as is" crystalline cane sucrose DSC thermograms is associated with the onset of thermal decomposition of sucrose within mother liquor occlusions, initiated by hydrolysis and mediated by the composition and chemistry of the sucrose crystal. The purpose of this research was to investigate the crystalline structure and internal morphology of a variety of "as is" and thermal treated sucrose samples. In accordance with previous research, the sucrose samples selected were analytical grade cane, commercially available white refined beet and cane, and laboratory-recrystallized cane (with and without K_2SO_3). A variety of analytical

techniques were applied to approach this research objective, including Differential Scanning

Calorimetry (DSC), High Performance Liquid Chromatography (HPLC), Powder and Single crystal

X-ray Diffraction (PXRD and SXRD), and X-ray Micro-Computed Tomography (Micro-CT) analyses.

We found that the earliest decomposition indicator component (glucose) could be detected at

different temperatures among sucrose samples, which was dependent on the sample sources,

recrystallization methods carried out, and associated with the Tmonset in DSC thermogram for

each sucrose sample. The PXRD and unit cell parameters collected for all sucrose crystals

studied herein (before and after heating) are consistent with the known unit cell of sucrose,

therefore, the appearance of the small endothermic DSC peak within our cane sucrose sources

and laboratory-recrystallized samples are not due to a polymorph of sucrose. The smallest

number of internal gas filled cavities was observed in "as is" analytical grade Sigma cane as

compared to "as is" US beet, "as is" US cane sucrose, and "as is" recrystallized Sigma cane with

0.5% K_2SO_3, with the porosity values 0.00588 ± 0.00002%, 0.02039 ± 0.00316%, 0.07451 ±

0.07300% and 0.17519 ± 0.00634%, respectively. After heating crystals to 165°C, a temperature

10°C higher than the onset of the small peak, Sigma cane (2.67347 ± 0.06747% of porosity) and

US cane (2.14628 ± 0.11490% of porosity) exhibited the formation of many, many more internal

cavities with large sizes compared to US beet (0.04851 ± 0.00462% of porosity) and

recrystallized Sigma cane with 0.5% K_2SO_3 (0.16861 ± 0.01544% of porosity). We believed that

the residual sulfite in the mother liquor occlusions inhibits the formation of large number of

cavities, which are attributed to the thermal induced hydrolysis reactions.

6.2 Introduction

The crystallization and melting behavior of sucrose has been well studied over a long period of time. During our investigation of a number of sucrose samples, a distinct difference was observed between the thermal profiles of beet and cane sucrose sources at 10°C/min heating rate. In general, sucrose from beet sources exhibited only one large endothermic peak with an average onset temperature (Tmonset in °C) of 188.41±0.37; whereas, sucrose from cane sources exhibited two endothermic peaks in the differential scanning calorimetry (DSC) thermogram, one small and one large peak, yielding average Tmonset values of 153.80±6.05 and 187.39±1.72, respectively (Lu and others 2013). An example of thermograms with labeled Tmonset values between each sugar sources was given in Figure 6.1. Previous studies also revealed that the formation of thermal decomposition components was associated with the appearance of the small endothermic DSC peak in cane sugar sources (Lu and others 2014).

It was recognized, as far back as Richards (1903), "substances crystallizing from a solution enclose within their crystals small quantities of the mother-liquor" and that this entrapment was exceedingly common, "It is no careless exaggeration to state that in all my chemical experience I have never yet obtained crystals from any kind of solution entirely free from accidentally included mother-liquor; and, moreover, I have never found reason to believe that anyone else ever has". The presence of water inside the sucrose crystal, observed by light microscopy, was reported earlier by Powers (1956, 1958). Powers (1958) also linked the amount of water in the crystal to the size of the crystal, with large crystals (approaching an inch in length) containing more water (0.1 to 0.4%) compared to smaller crystals (0.01 to 0.04%). It is interesting to note that Powers (1956, 1958) explained the widely variation in specific gravity and melting point values for sucrose given in the literature, 1.58 to 1.60 gram/cm^3 and 160 to

186°C, respectively, to the presence of these water inclusions. The presence of inclusions was further studied by Powers (1970), where the mother liquor (small quantities of saturated sucrose solutions) contains the impurities with particular color substance could be visualized and affect crystal quality. Powers (1970) also mentioned that during crystallization, due to stirring and higher temperature (near heating surfaces), where the solution is undersaturated, crystals tend to dissolve, thus creating on their surface small or big cavities, which are filled with mother liquor. The phenomenon of trapping mother liquor in crystals was also demonstrated by Vaccari (2010). The mother liquor solution entrapped in sucrose crystal is related to the instability of the surface structure, which is due to the high growth rate of the various faces. This high growth rate can be reached through specific conditions of supersaturation, temperature and stirring. Also, there is another cause, which should be responsible for particular disturbance of the surface of the crystal and, consequently, to promote the trapping of mother liquor occlusions that is the boiling of the solution during the crystallization. This technology is usually utilized in traditional sugar technology to keep the planned conditions of supersaturation and, consequences on the quality of the crystal. During boiling, vapor bubbles tend to form mainly on the crystal surface, thus promotes inclusion of mother liquor. This could be explained by the rapid evaporation of the solution on the surface of the crystals results in a local increase of the supersaturation, as well as causes a local increase of the growth rate and an increase of the surface instability. The formation of cavities could promote the trapping of solution. To avoid this phenomenon, it would be necessary to crystallize at low supersaturation (with very long times) and without boiling (cooling crystallization) conditions, which are in contrast with normal practices utilized in the sugar

refining industry. In addition, we realized in the literature, that the terminology of "inclusion" and "occlusion" are used interchangeably. According to the definitions given by Harvey (2000), inclusions form by the potential interfering ions whose size and charge are similar to a lattice ion and may substitute into the lattice structure by chemical adsorption, provided that the interferent precipitates with the same crystal structure; whereas, occlusions form when rapid precipitation traps a pocket of solution within the growing precipitate. Thus, we will use the term "occlusion" herein to accurately discribe the penomenon of trapping mother liquor solutions.

Another important area to explore is the role of crystal defects in the loss of crystalline structure in sucrose and the presence of the small peak in cane sucrose. Thomas and Williams (1967), studying lattice imperfections in sucrose, showed that water is located in dislocation cores within the sucrose crystal structure, which can be liberated on heating. Thomas and Williams (1967) also demonstrated that prolonged heating at 120°C under vacuum gave rise to decomposition volcanoes on the surface of the crystal, again likely situated at dislocation sites. Thomas and Williams (1967) was also noted that regions of higher imperfection density undergo preferential caramelization when sucrose crystals were heated. Eastmond (1970) reviewed the result of Thomas and Williams (1967), and stated that these results demonstrate that lattice imperfections are important as reaction sites. Further evidence arises from the sensitivity of many of these reactions to the presence of very small concentrations of chemically inert impurities and from the general irreproducibility of reaction rates.

The morphology of sucrose grown in aqueous solution has been studied by a number of researchers (Ubbelohde 1965; Hartel and Shastry 1991; Bubnik and others 1992; Mullin 2001;

Vaccari 2010; Roos and others 2013; Vaccari and Mantovani 1995, 1999ab; Sgualdino and

others 2005, 2007). When sucrose crystals are grown in a pure aqueous solution, there may be

15 possible faces, in which 8 most important faces were shown in Figure 6.2 (Vavrinecz 1965).

The missing of some faces is due to that the faster growing phases will become smaller and

smaller until they disappear; whereas the slower growing phases will gradually become larger

and larger. Thus, in the final external morphology, the crystal will be composed of only the

slower growing faces (Vaccari 2010). Pure crystalline sucrose should always be the same

regardless of plant source, since the molecular structure of the sucrose crystal is determined by

physical constrains (Hartel and Shastry 1991). However, mother liquor solution can remain on

the crystals even after centrifugation, thus, the entrapped impurities can further impact the

chemistry, composition and morphology of crystals. There are some differences between beet

and cane sucrose that are sensitive to small levels of impurities present during processing. Since

these impurities can play a large role in the crystallization process, these differences may

become quite important in controlling the formation of sugar crystals in a food product. Also, it

is known that raffinose as a trisaccharide is always present in beet sugar processing. In the

presence of quite low concentration of raffinose in sucrose growing solution could result in a

very simple morphology, particularly elongated on the b axis.

Additionally, an important difference between white refined beet and cane sugar

processing is that beet sugar processing routinely includes a sulfitation step, whereas cane

sugar processing usually does not (Clarke and Godshall, 1988; Asadi 2005). Among sugar cane

processors worldwide, there is mixed interest in the use of sulfitation. In the United States,

sulfitation has rarely been used in cane raw sugar factories since the 1950's (Andrews and

Godshall 2002). However, in China, cane sugar refinery routinely includes sulfitation steps for

juice clarification (Huo 2007). We hypothesized that the presence of the small endothermic

peak in most "as is" crystalline cane sugar DSC thermograms is associated with the onset of

thermal decomposition of sucrose within mother liquor occlusions, initiated by hydrolysis and

mediated by the composition and chemistry of the sucrose crystal (Lu and others 2015). Thus,

the objective of this study was to characterize the physical properties and chemistry of the "as

is" sucrose crystal from beet and cane sources, as well as our own laboratory-recrystallized

sucrose samples. A variety of analytical techniques were applied to approach this research

objective, including Differential Scanning Calorimetry (DSC), High Performance Liquid

Chromatography (HPLC), powder and Single Crystal X-ray Diffraction (PXRD and SXRD), and

X-ray Micro-Computed Tomography (Micro-CT) analyses.

Powder X-ray diffraction was applied to determine structure properties, such as lattice

parameters, strain, grain size, preferred orientation, thermal expansion, and measure thickness

of thin films and multi-layers and to determine atomic arrangement. If the sucrose sample

contains some amorphous material, the disorder of the structure will result in amorphous

scattering. For example, if the sample is completely amorphous, no peaks will be visible

(Suryanarayana and Norton 1998). Single crystal X-ray Diffraction (SXRD) is used to determine

single crystal repeating unit cell structure, which provides the best structural evidence for

polymorphism. Polymorphism indicates the phenomenon that the same chemical compound

exhibits different crystal forms (Authier and Chapuis 2014). X-ray computerized

microtomography (Micro-CT) is a combination of imaging and computing methods, which can

be applied to acquire 3D images to reveal the internal structures of sample. The sample absorbs

a certain amount of X-ray photons as determined by sample density, atomic number, thickness and linear attenuation coefficient. The X-ray photons, which escape from the sample are captured by the detector and the intensity measure creating a radiograph, or "projection" (Hsieh 2012). X-ray microscope takes multiple projection images at different viewing angles to provide the original 2D images. A computer then utilizes these 2D projecting images to reconstructs 3D volumetric data to reveal the internal structure without destructing the sample (Yin 2012). The Xradia Bio Micro-CT (MicroXCT-400) is a high-resolution 3D X-ray imaging system, which is optimized for non-destructive imaging of complex internal structures (from: LOT-QuantumDesign GmbH). The Xradia MicroXCT-400 provides the unique ability to reveal the internal structure with full 3D imaging of features down to <1.0 micron resolution, which can be utilized to investigate the internal morphology of the sucrose crystal before and after thermal treatment.

6.3 Materials and Methods

Materials

Analytical grade crystalline sucrose (≥ 99.5%) was purchased from Sigma-Aldrich Co. #S0389 (St. Louis, MO). White refined beet (US beet) and white refined cane (US cane) samples were obtained directly from U.S. Sugar Corporation (Clewiston, FL). All sugars were tested "as is" without further purification. Potassium sulfite (K_2SO_3 ≥ 97%), potassium sulfate (K_2SO_4 ≥99%), and potassium iodide (KI anhydrate, ≥ 99%) were purchased from Sigma-Aldrich Co. (St. Louis, MO). HPLC grade water (Fisher Scientific Inc., Pittsburgh, PA) was used for the preparation of standard and sample solutions.

Methods

Sucrose recrystallization

Preliminary sucrose recrystallization experiments were carried out based on the general method reported in the literature (Maulny 2003; Beckett and others 2006). 100 g of Sigma sucrose, 1% of K_2SO_4 (percentage to the weight of sugar), and HPLC grade water (25 mL) were mixed and heated to 128°C. Once the temperature was reached, the solution was removed from the heating source. At this point the solution was vigorously hard stirred for 30 sec using a spatula to initiate crystallization. The temperature of the solution was allowed to drop to room temperature. The crystals were dried over P_2O_5 overnight before use. Appearance of the recrystallized sample was recorded using a Canon PowerShot Digital Camera.

In order to improve the quality (better size, appearance, and other morphological properties) of our own laboratory-recrystallized sucrose samples, the method of cooling crystallization with undisturbed solution (leaving solution in a location where it will be undisturbed by vibrations or movement) was applied. The modified slow crystallization method was carried out according to the crystallization principles provided by University of Florida Center for X-ray Crystallography. Our enhanced recrystallization protocol was optimal for growing large size sucrose crystals with less surface defects. Shaking should be avoided during recrystallization to minimize the nucleation sites.

Preparation of saturated sugar solutions

The reported saturation values at 70°C and 75°C of sucrose are approximately 76g and 77.5g per 100 g of solution, respectively (Taylor 1947). Saturated sucrose solutions were prepared by adding 19 g of analytical grade Sigma cane sucrose and 6 g of HPLC grade water into a 50mL disposable polyethylene tube with a screw cap. Sample tubes were then warmed to

85°C using water bath for about 1 hour, and was slightly shaken by hand in between to help dissolve sample until no crystalline sucrose remained. The temperature of the saturated solution was then allowed to drop spontaneously and continually in a 25°C incubator to allow nucleation occuring in that closed system (avoid any shaking or unnecessary moving over temperature drop or incubation). After approximately 24-48 hours, the recrystallized crystals with desired size and shape were harvested. For the addition of potassium sulfite at 0.5% or potassium sulfate at 1% (weight of dry matter) laboratory-recrystallized Sigma samples, the K_2SO_3 or K_2SO_4 was added together with sucrose and HPLC water into the tube before heating.

Centrifugal filtration

The newly-grown crystals with desired morphology were placed into the Vivaspin® 20ml centrifugal concentrators (Vivaproducts, Inc. Littleton, MA) and filtered using centrifugal filtration (Eppendorf Centrifuge 5810R, Hamburg, Germany) at 3600 RPM for 25 min. The harvested crystals with minimized mother liquor occlusions surrounded were then placed onto a petri dish with a cover and conditioned under ambient environmental conditions (20-30 %RH, 20-25°C) for 48 hours before being used. The laboratory-recrystallized samples were then transferred to 15mL glass vials and sealed with parafilm for storage. The morphology information for commercial and laboratory-recrystallized sucrose from different sources was recorded using Leica M205C Microsystem (Leica, Heidelberg Germany) equipped with polarized light. To obtain the full melting profile of recrystallized Sigma samples, DSC analysis was applied according to previous work carried out in the Schmidt laboratory (Lu and others 2013, 2015).

DSC sample preparation and HPLC analysis

Based on previous research work carried out in the Schmidt laboratory (Lee and others 2011a and b), thermal analysis of sucrose samples were carried out using a DSC Q2000 (TA Instruments, New Castle, DE), equipped with a refrigerated cooling system (RCS 90). The DSC was calibrated for enthalpy and temperature using a standard indium sample (Tmonset of 156.6 C, ΔH of 28.71 J/g, TA Instruments, New Castle, DE) prior to sample scanning. Hermetic aluminum Tzero pans and lids (TA Instruments, New Castle, DE) were used for all calibration and sample measurements, including an empty pan as the reference. Dry nitrogen, at a flow rate of 50 mL/min, was used as the purge gas. Selected sucrose samples, including analytical grade Sigma cane, US beet, Sigma cane recrystallized in pure HPLC water, and Sigma cane recrystallized with 0.5% K_2SO_3 in HPLC water were heated to target temperatures at 140°C, 150°C, 160°C, 170°C, 180°C, 190°C and 200°C at 10°C/min using DSC. Commercial sucrose samples, as well as large single crystal from laboratory-recrystallized Sigma sucrose (approximately 5.0 mg), were hermetically sealed in T-zero DSC pans. When reaching each target temperature (approximately 1.5°C lower than target temperatures), the system was quickly equilibrated back to room temperature at approximated 35°C/min cooling rate. Approximately 5 mg of each "as is" and heated sucrose sample was dissolved into 100 mL of HPLC water and then transferred to a 2mL screw thread robovial with silicane septa caps before injection (Fisher Scientific Inc., Pittsburgh, PA). Detection of sucrose and the thermal decomposition components (glucose and fructose) was carried out based on AOAC Official Method 996.04. Carbohydrates were separated by anion exchange chromatography and detected by pulsed amperometric detection at a gold working electrode. A Dionex IC3000 HPLC equipped with a gradient pump, Dionex Carbopac PA1 guard and analytical columns, as well as

an electrochemical detector with disposable carbohydrate-certified gold electrodes was used. A 150mM solution of sodium hydroxide was used as the eluent at a flow rate of 1.0 mL/min. The temperature of column was set 30°C. The flow rate was 1 mL/min with 10% acetonitrile/0.1% acidified water solution. The water was acidified with 85% phosphoric acid. The limit of detection (LOD) for sucrose, glucose, and fructose was 0.5 ppm. The earliest decomposition component (glucose) and its corresponded decomposition temperature (TDConset) were labeled onto the corresponding DSC thermograms. HPLC analysis was carried out in duplicates for all samples.

Powder and Single Crystal X-ray Diffraction (PXRD & SXRD)

A Rigaku MiniFlex 600 (MiniFlex, Rigaku Corporation, The Woodlands, TX), benchtop powder X-ray diffractometer was used to collect PXRD in the Bragg-Brentano configuration using Cu Kα radiation. A 2θ scan range of 3° to 60° was collected in continuous mode at 1°/min scan rate, with increments measured every 0.02°. Sucrose samples were well ground before PXRD scanning to minimize the preferred orientations. For selected sucrose samples (Sigma, US beet, US cane, and laboratory-recrystallized analytical grade Sigma cane sucrose samples), the single crystal unit cell parameters were collected using a Bruker D8 Venture system. The unit cell parameters were then compared to sucrose parameters contained in the Cambridge Crystallographic Data Centre (CCDC), specifically Brown and Levy (1973) (This sample does not have a CCDC # but has a reference as SUCROS). Each crystal for SXRD unit cell collection was selected using Leica M205C Microsystem (Leica, Heidelberg Germany) under polarized light and morphology information of each sugar sources was recorded. Bruker D8 Venture Duo (utilizes Cu or Mo radiation), and is equipped with a four-circle kappa-axis diffractometer and motorized

Photon 100 CMOS detector collecting shutter-less data. Selected single crystals were mounted on a 0.3mm Hampton Research Cryoloop using Paraton oil (Hampton Research). A short series of ω scans were collected. Data were harvested and the unit cell was indexed and refined using APEX II software (Bruker AXS, Inc., Madison, WI).

Micro-CT measurements

Pixel size and optical magnification of CT scans were selected based on the crystal size. A total of 901, 2D projecting, images were collected for each sample scan. Based on the original size of sample, the number of informative images was varied. Preliminary experiments were carried out to collect images of recrystallized analytical grade Sigma cane sucrose grown in saturated sucrose solution with Xradia Bio Micro-CT (MicroXCT-400), in order to differentiate the crystalline phase from the surrounded saturated sucrose solution. In addition, to visualize the mother liquor occlusions entrapped in sucrose, 10% KI (weigh of dry matter), which has much higher density compared to crystalline sucrose (3.12 g/cm³ vs. 1.59 g/cm³) and serves as a contrast agent for Micro-CT scan, was recrystallized with analytical grade Sigma cane sucrose using our enhanced recrystallization protocol mentioned previously. For Micro-CT analysis, Sigma cane, US beet, US cane, and Sigma cane crystallized with 0.5% K_2SO_3 crystals were first scanned in their "as is" states using Xradia Bio Micro-CT. Then each crystal was scanned to 165°C at 10°C/min using the DSC. After reaching the target temperature (approximately 1.5°C lower than 165°C), the system was quickly equilibrated back to room temperature at approximated 35°C/min cooling rate. After which, the same crystal was scanned again using Micro-CT under the same experimental conditions.

Image analysis and reconstruction was carried out using FEI Avizo 9.0.1 (Visualization Sciences Group, Mérignac cedex, France). The analysis were summerized as following steps: The raw tiff images with pixel size information recorded were imported.The image segmentation was set with a new label field was created. The segmentation editor provided different tools to help differentiate the materials based on the histogram of the color peaks. Then the brush tool was used to mask crystal area and interpolated next 5 to 10 images if the crystal position was fixed during CT scanning. This highlighted region was then created as new material and magic wand was used to select the crystalline solid. After added crystalline part to new material (named as "crystal"), holes were filled for all slides and add as new material named "pore". The threshold tool was then applied to separate the pore from crystalline solid. If there were small outliers or alien particles need to be filtered from focus, remove island function will be applied. The volume statistics and other calculations could be approached using label analysis functions. 3D structure of sucrose samples could be visualized by reconstructing all selected 2D images using volume rendering functions. In the study herein, the porosity% value, which indicates as ratio of the pore volume (gas filled cavities) to the total volume of sample, of each "as is" and heated sucrose sample was calculated using Equation 6.1,

$$Porosity\% = (Vp \ / \ Vt) \ \text{x} \ 100\% \qquad \text{Equation 6.1}$$

where Vp is the volume of void space (gas filled cavities), and Vt is the total/bulk volume of material, including the void components.

6.4 Results and Discussion

Sucrose recrystallization

The appearance of recrystallized Sigma cane sucrose with 1% K_2SO_4 according to the

general method reported in the literature (Maulny 2003; Beckett and others 2006) is recorded

in Figure 6.3. Instead of harvesting the grown single crystals with ideal morphology (nice shape

and faces as illustrated in Figure 6.2), by using this method we only obtained several large mass

of agglomerated crystals (Figure 6.3). This recrystallized sample needs to be cut into small

pieces, in order to seal into DSC pans for thermal analysis.

The appearance for our laboratory recrystallized samples: analytical grade Sigma cane

recrystallized in HPLC water, analytical grade Sigma cane recrystallized with 0.5% of K_2SO_3, "as

is" analytical grade Sigma cane, US beet, and US cane were recorded using Leica M205C

Microsystem (Figure 6.4 to 6.8). More recrystallized sucrose samples using our enhanced

recrystallization protocol, other commercial sucrose samples from beet and cane sources, were

also observed using Leica M205C Microsystem and recorded in Appendix J. By applying our

enhanced recrystallization protocol (modified cooling crystallization method) with undisturbed

solution and centrifugal filtration step, the substantial large size of single crystals with less

surface defects were obtained (Figure 6.4 and 6.5). Among three commercial sucrose samples

(analytical grade Sigma cane, US beet, and US cane), though they all exhibited smaller size

comparing to our own laboratory-recrystallized sucrose samples, the analytical grade Sigma

cane (Figure 6.6) has relatively large size compared to US beet (Figure 6.7) and US cane (Figure

6.8) sucrose crystals. In addition, more defects (cracks, twins) were found in commercial

sucrose samples compared to our laboratory recrystallized sucrose crystals. Another interesting

observation is that the white refined beet sugar sucrose samples are always shiner compared to

cane sucrose samples. It is known that in general, dull appearance relates to defects within the

crystalline structure of a material. For example, the single crystal aluminum oxide specimen is very transparent, whereas the polycrystalline and porous (~5% porosity) aluminum oxide are translucent and opaque, respectively (Callister and Rethwisch 2012).

By applying our enhanced recrystallization protocol, though we did not have a high yield number of crystals or fast growth rate, our lab-grown sucrose crystals have larger size with less defects. In general, the faster crystal growth rates and higher growing steps will result in rougher surfaces and deeper cavities (Vaccari 2010). The low yield of recrystallization method developed for this study is predictable. In cooling crystallization, a different solubility as a function of temperature is utilized. In a closed container, crystallization occurs without water evaporation. Thus, the maximum amount of grown crystals will be highly dependent on the difference of solubility between the starting and the end temperatures of crystallization (Vaccari and Mantovani 1995). However, by applying our enhanced recrystallization method, we did not obtain the large mess of agglomerated crystals as when using the method reported by Maulny (2003), Beckett and others (2006); nor did we harvest the large conglomerates, which represent of a collection of crystals joined together randomly as the recrystallized sucrose published by Lee and Chang (2009)

Instead, we were be able to grow and harvest nice and large single crystals. In addition to the crystal growing method, the enhanced morphology and quality of our laboratory recrystallized sucrose samples, which are relied on the critical centrifugal conditions that has been developed in this study. It is known that in both beet and cane sugar refining, the crystals in massecuite are separated from the surrounding molasses or syrup by centrifugal machines (Meade and Chen 1977; McGinnis 1982; Asadi 2007). The centrifugal machine is the device

used to separate the crystalline sugar from mother liquor based on the difference in weight and viscosity between the liquid and solid, thus prevent a fast gradation by sedimentation. In sugar refineries, water is sometimes used to filter through to rinse the crystals to improve the quality of sugar (McGinnis 1982). In order to mimic the procedure in sugar refineries, the new grown crystals were transferred into centrifugal concentrators and filtered using centrifugal filtration at 3600 RPM for 25 min in this study. To avoid any dissolution effect, no rinsing step was included. However, compared to centrifugal conditions where the sugar industrial usually selected: speed limit was 1000 rpm (standardized) or 1600 to 2200 rpm (high speed), a much higher speed (3600 rpm) and relatively longer time (less than 10 minutes vs 25 minutes) were selected in our protocol for centrifugal filtration, in order to obtain the better separation effects. In addition, our lab-grown crystals were always harvest when they had relatively large sizes, which present less surface area for mother liquor contact as compared to smaller crystals, thus resulted in purging with greater ease in the centrifugal apparatus and better purging efficiency (Meade and Chen 1977).

DSC sample preparation and HPLC analysis

The DSC thermograms of "as is" analytical grade Sigma cane sucrose, recrystallized Sigma cane sucrose with 1% K_2SO_4 using the general recrystallization method reported in the literature (Maulny 2003; Beckett and others 2006) and its ground sample, as well as Recrystallized Sigma cane sucrose with 1% K_2SO_4 using our modified method are plotted in Figure 6.9. The small endothermic was not inhibited by addition of 1% K_2SO_4 as reported by others (Maulny 2003; Beckett and others 2006), when using both the general method and our own-laboratory recrystallized method, unless a grinding step was included before DSC scanning.

The blue DSC thermogram indicates that after overnight drying of recrystallized Sigma cane sucrose with 1% K_2SO_4 using the general method, sample was ground into fine powder and the small DSC peak around 150°C was no longer present at 10°C/min heating rate. Grinding was a sample preparation step for DSC measurement as reported by Beckett and others (2006); however, as Lu and others (2015) investigated that just inducing the grinding step could make the DSC small endothermic peak in cane sucrose sources disappear.

It is usually considered as a sufficient precaution to powder the material finely and expose it to the air for a short time, in order to allow the undesirable water to evaporate (Richards, 1903). Beckett and others (2006), whom believed that the appearance of the peak at 150°C was mainly attributed to impurities in sucrose (i.e. KCl and K_2SO_4), especially dependent on the mineral salt content; however, they disregard the impact of sample grinding. Therefore, by repeating Beckett's work, it will be difficult to differentiate which aspect (grinding versus impurities) had a significantly impact on the appearance of the small endothermic DSC peak around 150°C. In particular, from Figure 6.9, it is showing that Sigma cane sucrose recrystallized with 1% K_2SO_4 without grinding, resulted in an even larger small DSC peak compared to "as is" Sigma cane sucrose. However, after grinding, the small peak in Sigma cane sucrose recrystallized with 1% K_2SO_4 was completely eliminated. This result is mainly attributed to a much easier releasing of mother liquor occlusion in sucrose crystals after grinding (shorten the distance of water molecules diffuse to the surface), thus inhibits the thermal induced hydrolysis process in sucrose crystals during heating (Lu and others 2015)

The thermograms of "as is" analytical grade Sigma cane sucrose, "as is" US beet sucrose, Sigma cane sucrose recrystallized in HPLC water, and Sigma cane sucrose recrystallized with 0.5%

K$_2$SO$_3$ using our own laboratory-recrystallized method were plotted in Figure 6.10. The blue

curve indicates the DSC heat flow of recrystallized Sigma cane sucrose in HPLC water as a

function of temperature. By using this enhanced recrystallization protocol, we successfully

removed the large endothermic peak (second peak in cane sucrose sources), with only one

relatively large size of endothermic peak with Tmonset around 144°C as compared to Sigma

cane "as is" thermogram (green curve). However, recrystallizing Sigma cane sucrose with

addition of potassium sulfite at concentrations of 0.5% using our own laboratory-recrystallized

method, the small DSC peak can be eliminated, thus only the large endothermic DSC peak was

exhibited with Tmonset around 190°C. This unique observation is against the common principle,

since Sigma cane sucrose recrystallized in very pure HPLC grade water, due to partitioning

effect, the new-grown crystals will have less impurities as compared to "as is" Sigma crystals,

but exhibited the lowest Tmonset value; whereas Sigma recrystallized with impurities (0.5%

K$_2$SO$_3$) exhibited the highest Tmonset value. It is known that for most crystalline materials, the

presence of even a small quantity of impurities will lower the melting point by a few degrees

and broaden the melting transition temperature range. Because impurities cause defects in the

crystalline lattice, it is easier to overcome the intermolecular interactions between the

molecules (Callister and Rethwisch 2012), and consequently, a lower temperature is required

for melting in the presence of impurities.

HPLC analysis indicates that the earliest decomposition indicator component, glucose, was

first detected at 160, 200, 150 and 200°C for "as is" Sigma cane, "as is" US beet, recrystallized

Sigma cane in HPLC water, and recrystallized Sigma cane with 0.5% K$_2$SO$_3$ respectively at

10°C/min DSC heating rate (Appendix K). Overall, the initial thermal decomposition

temperature (TDConset) of each sucrose sample was close to its own Tmonset, which is about

151, 188, 144 and 190°C for "as is" Sigma cane, "as is" US beet, recrystallized Sigma cane in

HPLC water, and recrystallized Sigma cane with 0.5% K_2SO_3 respectively at 10°C/min DSC

heating rate as reported by Lu and others (2013 and 2015). This difference in thermal behavior

of each sucrose source could be attributed to the different refining or crystallization process. In

the US, an important difference between white refined beet and cane sugar processing is that

beet sugar process routinely includes a sulfitation step, whereas the cane sugar process does

not (Clarke and Godshall, 1988; Asadi 2005). Sulfitation has rarely been used in cane sugar

factories since the 1950's (Andrews and Godshall 2002). The thermal decomposition resistance

in commercial beet sugar (US beet) and laboratory-crystallized sucrose sample with addition of

K_2SO_3 is hypothesized to the sulfite content within the mother liquor occlusions. SO_2, which

used in sulfitation step, will first converted to sulfurous acid (or sulfite) after dissolving into an

aqueous solution (neither sulfuric acid nor sulfate). The hypothesized mechanism to explain the

thermal influence of sulfite based on research carried out by Shi (2014) is that SO_2 will react

with carbonyl group in sugar molecule to form a sugar bisulfite adduct, which suppresses the

degradation of the monosaccharide. Thus, for our laboratory recrystallized Sigma cane with 0.5%

K_2SO_3 sucrose sample, the addition of sulfite can help inhibit the thermal induced hydrolysis in

the mother liquor occlusions and enhance the thermal stability of the sucrose crystal.

Powder and Single Crystal X-ray Diffraction (PXRD & SXRD)

To avoid preferred orientation effects of sucrose crystals in the PXRD, each sugar sample

was ground to a fine powder before PXRD was carried out. The ring pattern collected using D8

venture diffractometer system in Figure 6.11 indicates that "as is" sucrose (top) has strong

preferred orientation, which shows as sharp spots on the rings; whereas, after grinding

(bottom), the preferred orientation has been eliminated. The PXRD of all selected sucrose

samples matched the theoretical sucrose pattern calculated from the work of Brown and Levy

(1973). An example of the calculated pattern overlaid on the Sigma cane sucrose pattern is

given in Figure 6.12. The calculated pattern matches well with the peak locations of the Sigma

sucrose. Further evidence shows that unit cell parameters for all sucrose crystals from different

sources before or after heat treatment (scanned using DSC at 10°C/min to target temperatures)

determined using SXRD are consistent with the known unit cell parameters of sucrose reported

by Brown and Levy in 1973 (Table 6.1). The full crystal structures of "as is" analytical grade

Sigma cane, US beet, and US cane collected using SXRD were refined and deposited to the

Cambridge Crystallographic Data Centre (CCDC) database (Lu and others 2016). Structural

parameters and metrical data of analytical grade Sigma cane, US beet and US cane were

recorded in Appendix L to M. Though there is a small DSC endothermic peak in Sigma and US

cane samples (Figure 6.1), the average structure and electron density shows no evidence in

SXRD results to support the "metastable sucrose polymorphs" theory, which is explained by the

conformational disorders of the -CH2-OH functional groups of the fructofuranose ring that

results in the misalignment of intramolecular hydrogen bonds between the hydroxyl groups and

the glucopyranose ring oxygen (Lee and Chang 2009). This theory, is therefore not responsible

for the low-melting DSC peak observed in sucrose. It is known that PXRD combined with SXRD

provides the best structural evidence for polymorphism. The powder pattern and unit cell

parameters for all crystals examined are consistent with the known unit cell of sucrose,

therefore, the appearance of small DSC peak within our cane sucrose sources or

laboratory-recrystallized Sigma cane in HPLC water sample is not attributed to a new form of crystalline structure (polymorphism) as suggested by Okuno and others (2003), Lee and Lin (2007a and b) and Lee and Chang (2009). A search of the literature did yield a high-pressure polymorph of sucrose, sucrose II (Patyk and others 2012), formed at a critical pressure of 4.80 GPa at 295K. However, sucrose II is not stable at ambient conditions.

Micro-CT measurements

The preliminary Micro-CT scan of newly-grown Sigma sucrose crystals surrounded by sucrose saturated solution was recorded in Figure 6.13. From Figure 6.13 we could hardly differentiate the crystalline sucrose from the surrounded saturated mother liquor solutions based on the color differences. In another word, even though there is mother occlusion in sucrose crystal, it won't be distinguishable from the crystalline solid using Micro-CT scanning. The trapped air bubble in the solution, however, has a much darker color as compared to the saturated solution and solid phases, which thus should also be distinguishable from sucrose crystal samples. In order to visualize the mother liquor occlusions entrapped in sucrose crystals, 10% of KI (weigh of dry matter), which has much higher density compared to crystalline sucrose (3.12 g/cm³ vs 1.59 g/cm³), was added to the mother liquor as a contrast agent during Sigma sucrose recrystallization. Interestingly, based on the density difference, we were able to observe the high dense KI (bright spot in 2D image and yellow dot in 3D volume rendering) entrapped in the sucrose crystalline solid (Figure 6.14). Therefore, compared to the traditional visualizing method by addition of colored substances during sucrose crystallization (Power 1958; Vaccari 2010), this study successfully developed a new method using the contrast agent (KI),

while sucrose crystallization to prove the existence of mother liquor occlusion within sucrose crystal by Micro-CT scanning.

2D images of each sugar samples scanned using Micro-CT were reconstructed into 3D images with porosity information using FEI Avizo 9.0.1 software (Figure 6.15 and Appendix O). The blue matrix indicates the bulk part of crystalline sucrose and the red spots are gas filled cavities observed in both "as is" and 165°C heated sucrose samples. Based on Micro-CT verification study mentioned above (Figure 6.13), the entrapped mother liquor occlusions (viscous liquid) could not be clearly differentiated from the crystalline matrix (solid) owing to the similar densities. The small dark areas in 2D images were, therefore, identified as internal gas filled cavities and rendered with red color in 3D images for better visualization. The smallest number of internal gas filled cavities were observed in "as is" Sigma cane as compared to "as is" US beet, "as is" US cane, and "as is" analytical grade Sigma cane recrystallized with 0.5% K_2SO_3 sucrose crystals, with the porosity values 0.00588 ± 0.00002%, 0.02039 ± 0.00316%, 0.07451 ± 0.07300% and 0.17519 ± 0.00634% respectively. After heated to 165°C, a temperature 10°C higher than the onset of the small peak, the crystal was immediately cooled back to room temperature and re-scaned using Micro-CT. Sigma cane (2.67347 ± 0.06747% of porosity) and US cane (2.14628 ± 0.11490% of porosity) exhibited the generation of many, many more internal cavities with large sizes compared to US beet (0.04851 ± 0.00462% of porosity) and Sigma cane recrystallized with 0.5% K_2SO_3 (0.16861 ± 0.01544% of porosity). Yet, Sigma and US cane maintained their original external morphology as can be observed in the 3D images after heating to 165°C, similar to that of US beet and Sigma cane recrystallized with 0.5% K_2SO_3, which did not form numerous cavities upon heating. A slight decrease in porosity for Sigma

recrystallized with 0.5% K_2SO_3 cane crystal after heating to 165°C was observed. This could be due to the large size of the recrystallized crystal, and in order to maintain the high resolution of image, only partial of the crystal was scanned. Therefore, it appears as a cylindrical shape after 3D reconstruction (Figure 6.15) and the region of CT scanning cannot be focused on exactly the same location after heating as before heating. Another important point that needs to be mentioned is that the potential mechanisms of the existence/formation of cavities in "as is" sucrose samples compared to the heated samples are varied.

A well-established theory of cavity formation within crystals and its related trapping of mother solution was illustrated by Vaccari (2010). During crystal growth, the higher growth rate resulted in rougher surface, higher growing steps and deeper cavities, which is demonstrated in Figure 6.16(a). At the growing surface, the solution is changed because of the relative movement between crystal and solution; whereas, at the bottom of the dip cavities, the solution cannot be changed, where the degree of supersaturation decreases and the steps at the steps at the bottom of the cavities stop their movement. Consequently, the mother liquor could be entrapped within the cavities (Figure 6.16b). Also, the bigger the crystals the faster the growing rate and, as a consequence, the high possibility of trapping much more mother solution. While, heat generated cavity formation (i.e. in the cases of Sigma and US cane heating to 165°C), on the contrary, is associated with the presence of the small DSC peak and is attributed to thermal induced hydrolysis within the mother liquor occlusions. Upon rescanning in the DSC, a glass transition was detected at 68°C for Sigma cane, but not for US beet. This observation supports the hydrolysis hypothesis in Sigma and US cane samples. However, the occlusions alone are not sufficient to explain the presence of the small peak, since the US beet

and Sigma cane recrystallized with 0.5% K$_2$SO$_3$ also contains mother liquor occlusions (cavities in "as is" state), but do not exhibit the small peak or form large size of cavity areas after heated to 165°C. This result could be explained by the relative high amount of sulfite in beet sources and Sigma recrystallized cane with 0.5% K$_2$SO$_3$ (Lu and others 2015), which is attributable to the sulfitation steps during beet sugar refining process or the addition of sulfite during recrystallization. It is known that the sulfites can inhibit browning reactions caused by ascorbic acid, lipid, Maillard and enzymatic browning reactions (Wedzicha and others 1991). As mentioned previously that SO$_2$ will react with carbonyl group in sugar molecule to sugar bisulfite adduct, which suppressed the degradation of monosaccharides (Shi 2014), thus could inhibit the formation of large sizes of cavities due to thermal induced hydrolysis in sugar beet sources and recrystallized Sigma sucrose with addition of 0.5% K$_2$SO$_3$.

6.5 Conclusions

By applying our enhanced laboratory-recrystallization method (recrystallized in pure HPLC water or with addition of K$_2$SO$_3$), we were be able to alter the thermal behavior of sucrose, allowing Sigma cane sucrose to have only one endothermic DSC peak, with a Tmonset either around 144°C or around 190°C at a 10°C/min DSC heating rate. We also found that the thermal decomposition of each sucrose source was directly related to the Tmonset values using DSC. The PXRD and unit cell parameters collected for all crystals examined (before or after heating) are consistent with the known unit cell of sucrose, therefore, the appearance of small DSC peak within our cane sucrose sources or laboratory-recrystallized sample is not attributed to polymorphism of sucrose. A smallest number of internal gas filled cavities were observed in "as is" Sigma cane as compared to "as is" US beet, "as is" US cane sucrose and "as is" Sigma cane

recrystallized with 0.5% K_2SO_3 crystals; whereas after heating to 165°C, a temperature 10°C higher than the onset of the small peak, Sigma cane and US cane exhibited the generation of many, many more internal cavities with large sizes compared to US beet and Sigma cane recrystallized with 0.5% K_2SO_3. We concluded that the relatively high sulfite content in mother liquor occlusions could inhibit the formation of large sizes of cavities due to thermal induced hydrolysis in sugar beet sources and recrystallized Sigma sucrose with addition of 0.5% K_2SO_3. This research reveals that the sucrose crystal composition and chemistry influences its thermal behavior, which in turn, is important to thermal processing and reactions of sucrose and sucrose containing foods, such as baking and caramelization.

6.6 Acknowledgements

6.7 References

Andrews LS, Godshall MA. 2002. Comparing the Effects of Sulphur Dioxide on Model Sucrose and Cane Juice Systems. Journal American Society of Sugarcane Technologists. 22: 90-101.

Asadi M. ed. 2007. Beet-sugar handbook. John Wiley & Sons, Inc., Hoboken, New Jersey, USA.

Authier A, Chapuis G. ed. 2014. A Little Dictionary of Crystallography. By IUCr Commission on Crystallographic Nomenclature. Chester, International Union of Crystallography. 238pp.

Beckett ST, Francesconi, MG, Geary PM, MacKenzie G, Maulny APE. 2006. DSC study of sucrose melting. Carbohydrate Research 341: 2591-2599.

Beevers, C. A.; McDonald, T. R. R.; Robertson, J. H.; Stern, F. The crystal structure of sucrose. Acta Crystallogr. 1952, 5, 689–690.

Brown GM, Levy HA. 1973. Further refinement of the structure of sucrose based on neutron-diffraction data. Acta Cryst. B29, 790-797.

Bubnik Z, Vaccari G, Mantovani G, Sgualdino G, Kadlec P. 1992 Effect of dextran, glucose and fructose on sucrose crystal elongation and morphology. Zuckerindustrie. 117(7): 557-561.

Callister WD, Rethwisch DG. 2012. Fundamentals of materials science and engineering: an integrated approach. 4th ed. Hoboken, N.J.: Wiley.

Clarke MA, Godshall MA. eds. 1988. Chemistry and Processing of Sugarbeet and Sugarcane. Chapter 13, The nature of colorants in sugarcane and beet sugar manufacture. Elsevier Science Publishers, Amsterdam.

Eastmond GC. 1970. Solid-state polymerization. Progress in Polymer Science, 2:1–46.

Hartel R.W., Shastry A.V. Sugar crystallization in food products. (1991) Critical reviews in food science and nutrition, 30 (1), pp. 49-112.

Harvey, D. 2000. Modern Analytical Chemistry. 1st edn. McGraw-Hill. 861 pages.

How to Grow Crystals. The University of Florida Center for X-ray Crystallography. Available from: https://xray.chem.ufl.edu/how-to-grow-crystals/. Last accessed Nov 30, 2015

Hsieh CH. May, 2012. Master thesis "Procedure and analysis of mineral samples using high resolution X-ray micro tomography". The University of Utah, Department of Metallurgical Engineering. Available from http://content.lib.utah.edu/cdm/singleitem/collection/etd3/id/1973/rec/1715. Last accessed 25thFeb, 2016.

Huo H. 2008. 1sted. Modern chemistry and technology of Chinese sugar refinery. Chemical Industry Press.

Lee JW, Thomas LC, Schmidt SJ. 2011d. Effects of heating conditions on the glass transition parameters of amorphous sucrose produced by melt-quenching. Journal of Agricultural and Food Chemistry, 59 (7): 3311–3319.

Lee JW, Thomas, LC, Schmidt SJ. 2011c. Can the thermodynamic melting temperature of sucrose, glucose, and fructose be measured using rapid-scanning DSC? Journal of Agricultural and Food Chemistry, 59 (7): 3306–3310.

Lee T and Chang GD. 2009. Sucrose conformational polymorphism. Crystal Growth and Design, 9(8): 3551-3561.

Lee T and Lin YS. 2007a. Dimorphs of sucrose. International Sugar Journal, 109 (1303):440-445.

Lee T and Lin YS. 2007b. Master thesis. Two Conformational Polymorphs of Sucrose. National Central University.

LOT-QuantumDesign GmbH. Available from: http://www.lao.cz/data/ke-stazeni/MicroXCT_200_eu_1_.pdf. Last accessed Nov,30 2015

Lu Y, Lee JW, Thomas L, Schmidt SJ. 2013. Proceedings of the 74th Annual Institute of Food Technologists on Differences in the Thermal Behavior of Beet and Cane Sugars. Chicago, IL.

Lu Y, Thomas L, Yin L, Gray D, Jerrell JJ, Cadwallader KR, Schmidt SJ. 2015. Proceedings of the 76th Annual Institute of Food Technologists on Impact of sucrose crystal composition and chemistry on its thermal behavior. Chicago, IL.

Lu Y, Gray DL, Schmidt SJ. 2016. CCDC 1473968, 1473969 and 1473970 contain the supplementary crystallographic data of analytical grade Sigma cane sucrose, US beet sucrose, and US cane sucrose, respectively. The data can be obtained free of charge from The Cambridge Crystallographic Data Centre via www.ccdc.cam.ac.uk/structures.

Maulny A. 2003. Co-crystallisation of sugars. Ph.D. Thesis, Department of Chemistry, University of Hull, Hull, UK.

McGinnis, R. A. ed. 1982. Beet-sugar technology. Beet Sugar Development Foundation; 3rd edition. Fort Collins, Colorado, USA.

Meade, George Peterkin,Chen, James C. P.(1977) Cane sugar handbook :a manual for cane sugar manufacturers and their chemists New York : Wiley,

Mullin, J. W. Crystallization, 4th ed.; Elsevier Butterworth-Heinemann: Oxford, UK, 2001; 594 pp.

Okuno M, Kishihara S, Otsuka M, Fujii S, Kawasaki K. 2003. Variability of melting behavior of commercial granulated sugar measured by differential scanning calorimetry. International Sugar Journal 105:29-35.

Patyk E, Skumiel J, Podsiadto M, and Katrusiak A. 2012. High-pressure (+)-sucrose polymorph. Angewandte Communications, International Additions, 51:2146-2150.

Powers HEC. 1956. Growth of sucrose crystals. Nature, 178:139-140.

Powers HEC. 1958. Sucrose crystal inclusions. Nature, 182:715-717.

Powers HEC. 1970. Sucrose crystal: inclusion and structure. Sugar Technol. Rev., 1, 85-190.

Richards TW. 1903. The Inclusion and Occlusion of Solvent in Crystals. An Insidious Source of Error in Quantitative Chemical Investigation. Proceedings of the American Philosophical Society Vol. 42, No. 172 (Jan. - Apr., 1903), pp. 28-36.

Roos YH., Karel M., Labuza T.P., Levine H., Mathlouthi M., Reid D., Shalaev E., Slade L. Melting and crystallization of sugars in high-solids systems (2013) Journal of Agricultural and Food Chemistry, 61 (13), pp. 3167-3178.

Sgualdino G., Aquilano D., Vaccari G., Mantovani G., Salamone A. Growth morphology of sucrose crystals the role of glucose and fructose as habit-modifiers(1998).Journal of Crystal Growth, 192 (1-2), pp. 290-299.

Sgualdino G., Aquilano D., Fioravanti R., Vaccari G., Pastero L. Growth kinetics, adsorption and morphology of sucrose crystals from aqueous solutions in the presence of raffinose(2005). Crystal Research and Technology, 40 (10-11), pp. 1087-1093.

Sgualdino, G.; Aquilano, D.; Pastero, L.; Vaccari, G. Face-by-face growth of sucrose crystals from aqueous solutions in the presence of raffinose II: growth morphology and segregation. J. Cryst. Growth 2007, 308, 141–150.

Shi Y (2014) Existence of the sugar-bisulfite adducts and its inhibiting effect on degradation of monosaccharide in acid system. Appl Biochem Biotechnol 172:1612–1622.

Suryanarayana C, Norton MG. 1998. X-ray Diffraction: A Practical Approach. New York NY: Plenum Press. 281 p.

Taylor M (1947). The solubility at high temperature of pure sucrose in water. Journal of the Chemical Society, 1, pp. 1678-1683.

Thomas JM and Williams JO. 1967. Lattice imperfections in organic solids. Part 2. Sucrose. Transactions of the Faraday Society, 63: 1922-1928.

Ubbelohde, A. R. Melting and Crystal Structure; Clarendon Press: Oxford, UK, 1965; 325 pp.

Vaccari G, Mantovani G. 1995. Sucrose crystallization. In: Mathlouthi M, Reiser P, editors. Sucrose properties and applications. 1st ed. Bishopbriggs: Blackie Academic and Professional. p 33-72

Vaccari G., Mantovani G., Sgualdino G., Tamburini E., Aquilano D. Fructo-oligosaccharides and sucrose crystal growth morphology I. Experimental growth habits.(1999) Zuckerindustrie, 124 (1), pp. 34-39.

Vaccari G., Sgualdino G., Tamburini E., Lodi G., Aquilano D., Mantovani G. Fructo-oligosaccharides and sucrose crystal growth morphology II. Verification of nonsucrose absorption through chromatographic analysis and X-ray diffractometry (1999) Zuckerindustrie, 124 (7), pp. 536-540.

Vaccari G. 2010 The Sugar Crystal: A Chameleon. 2010 SPRI Award Presentation. Proc. of the SPRI 2010 Conference on Sugar Processing, New Orleans, LA.

Vavrinecz, G. (1965) Atlas of Sugar Crystals. Verlag Dr. A. Bartens, Berlin, Germany.

Wedzicha BL, Bellion, Goddard SJ. 1991. Inhibition of browning by sulfites. Adv Exp Med Biol. 289:217-36.

Yin L (2012) 12 X-ray computerized microtomography. In: Graciela PW, Wang Q (eds) nonotechnology research methods for foods and bioproducts, 1st ed. John Wilwy & Sons, Inc., pp 215–234.

6.8 Figures and Tables
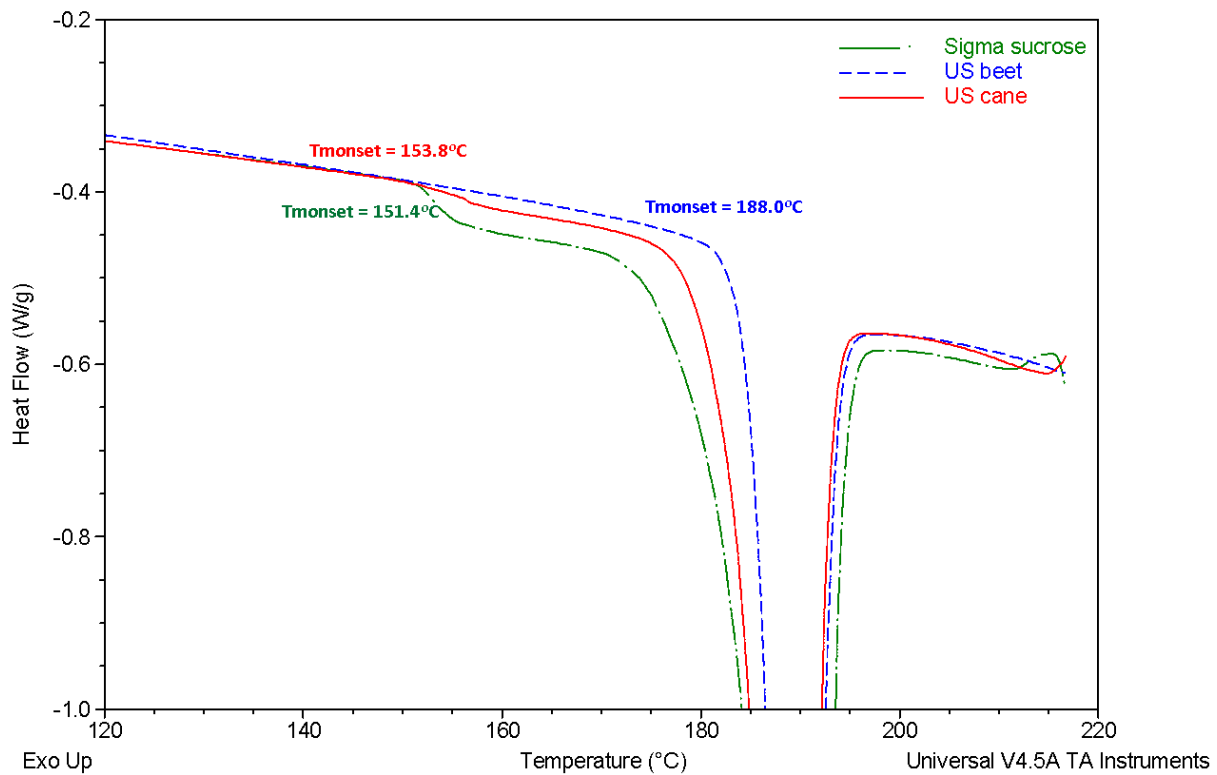
Figure 6.1 DSC thermograms of analytical grade Sigma cane, US beet, and US cane samples at 10°C/min.
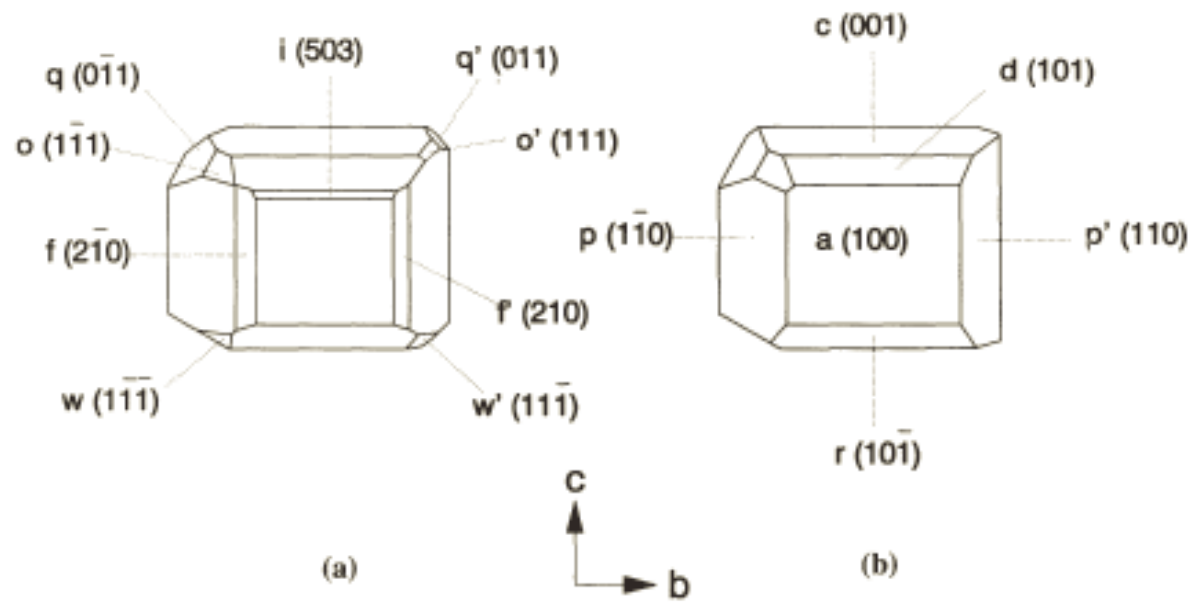
Figure 6.2 Classic sucrose crystal with all 15 possible faces (a) and the most common/important faces labeled with Miller's indexes (Vavrinecz 1965).
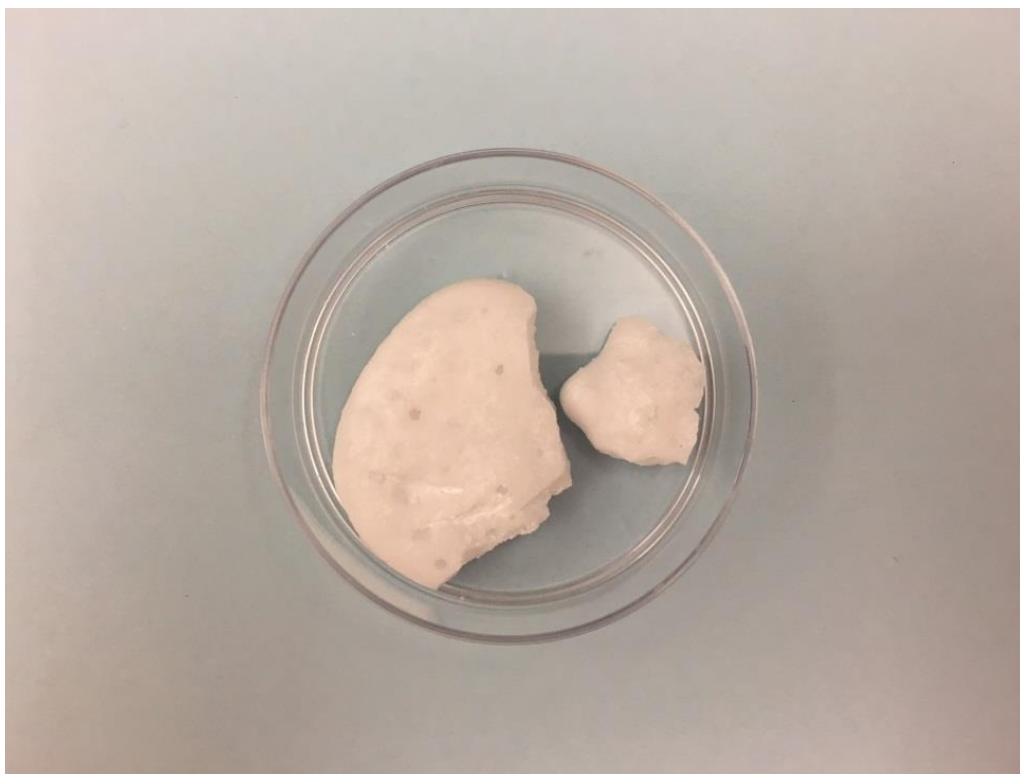
Figure 6.3 Appearance of recrystallized Sigma cane sucrose with 1% K_2SO_4 produced in the Schmidt lab according to the general method reported in the literature (Maulny 2003; Beckett and others 2006).
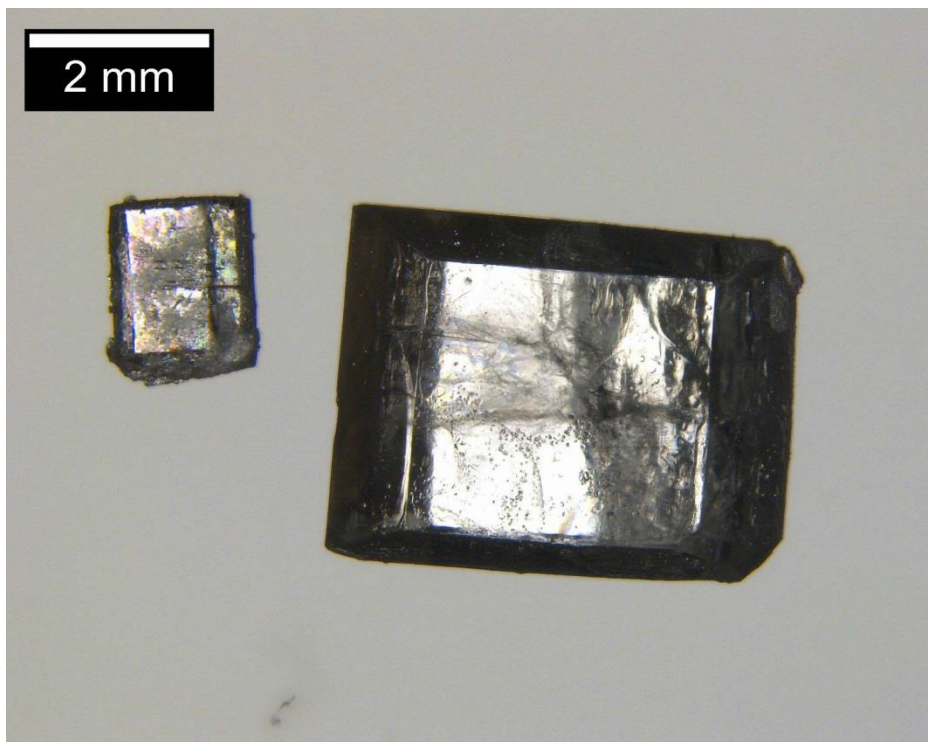
Figure 6.4 Appearance of Sigma sucrose recrystallized in HPLC water.
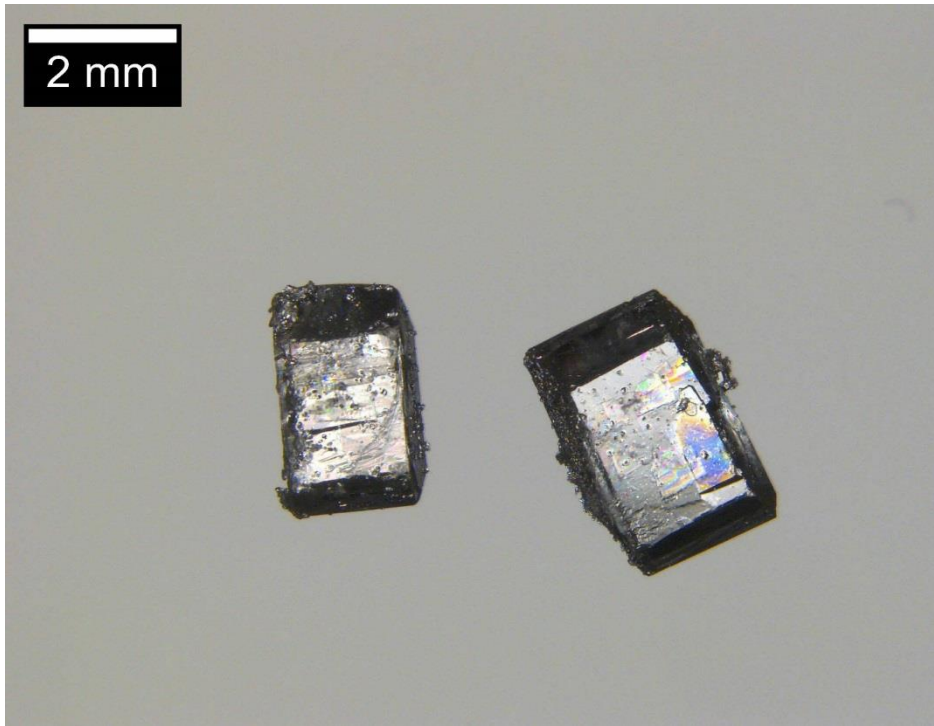
Figure 6.5 Appearance of Sigma cane sucrose recrystallized with 0.5% K_2SO_3 in HPLC water.
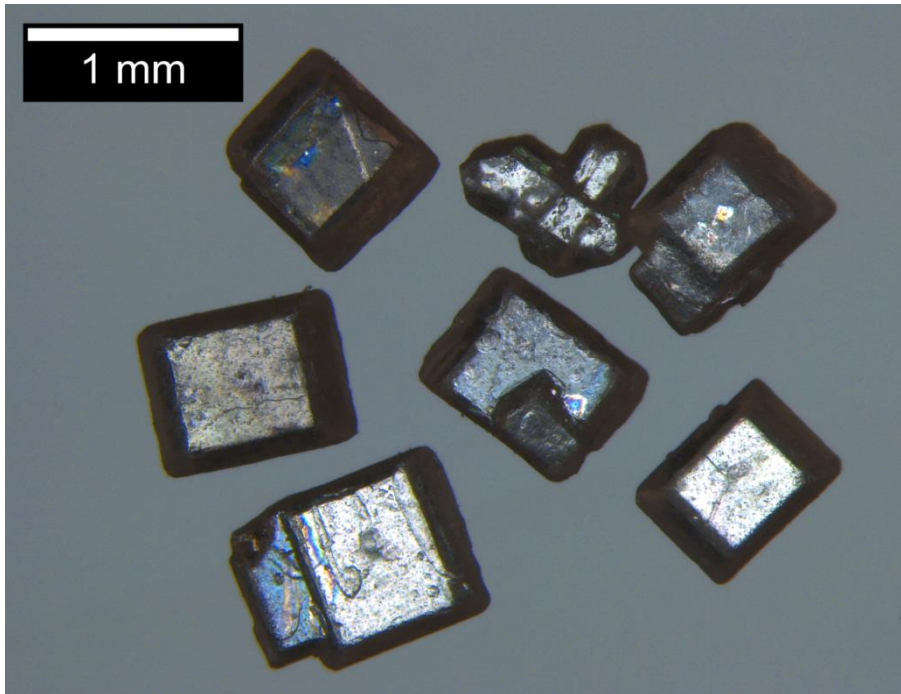
Figure 6.6 Appearance of "as is" Sigma cane sucrose.
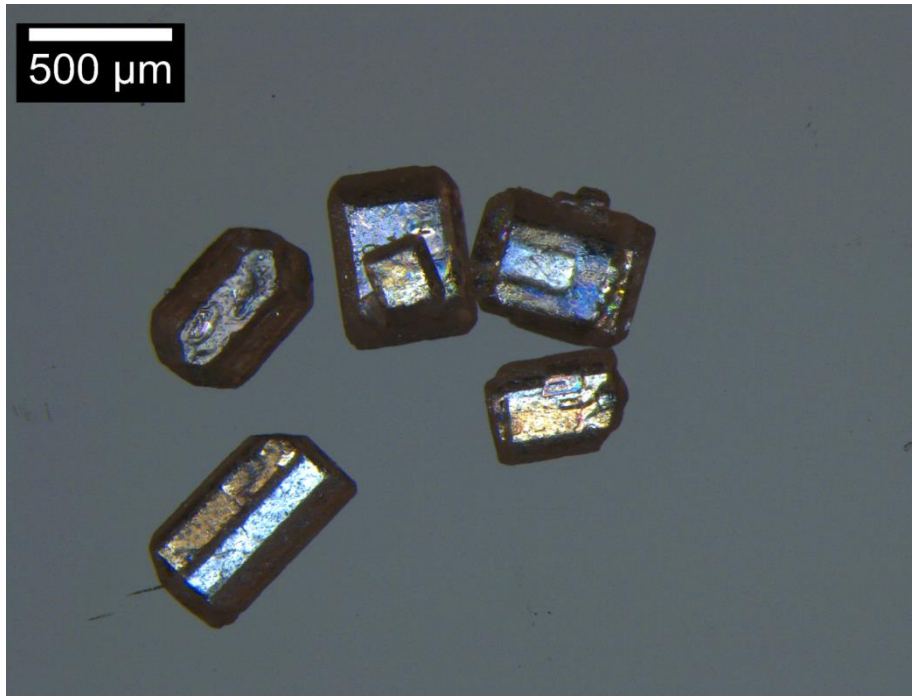
Figure 6.7 Appearance of "as is" US beet sucrose.
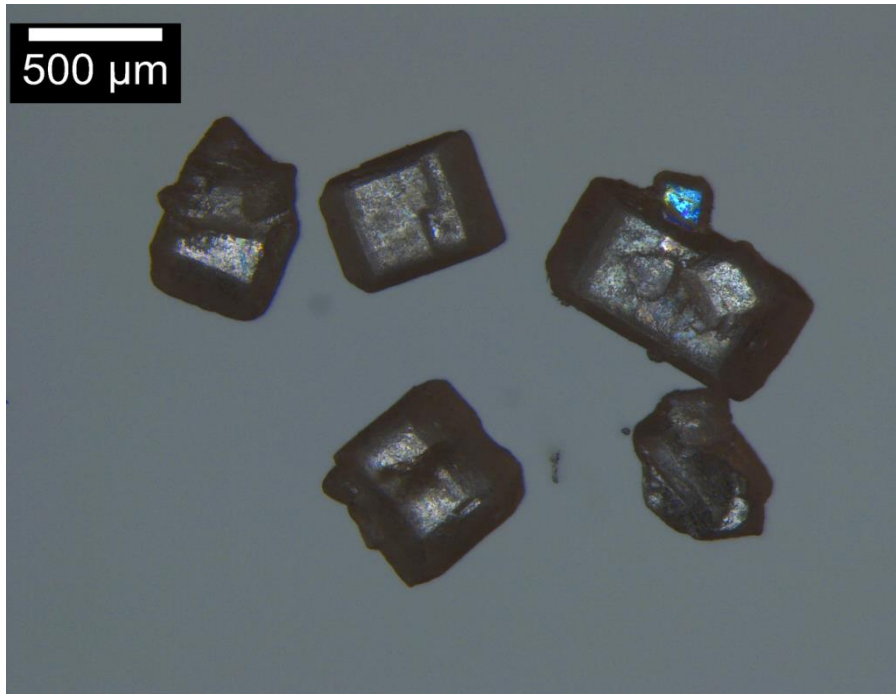
Figure 6.8 Appearance of "as is" US cane sucrose.
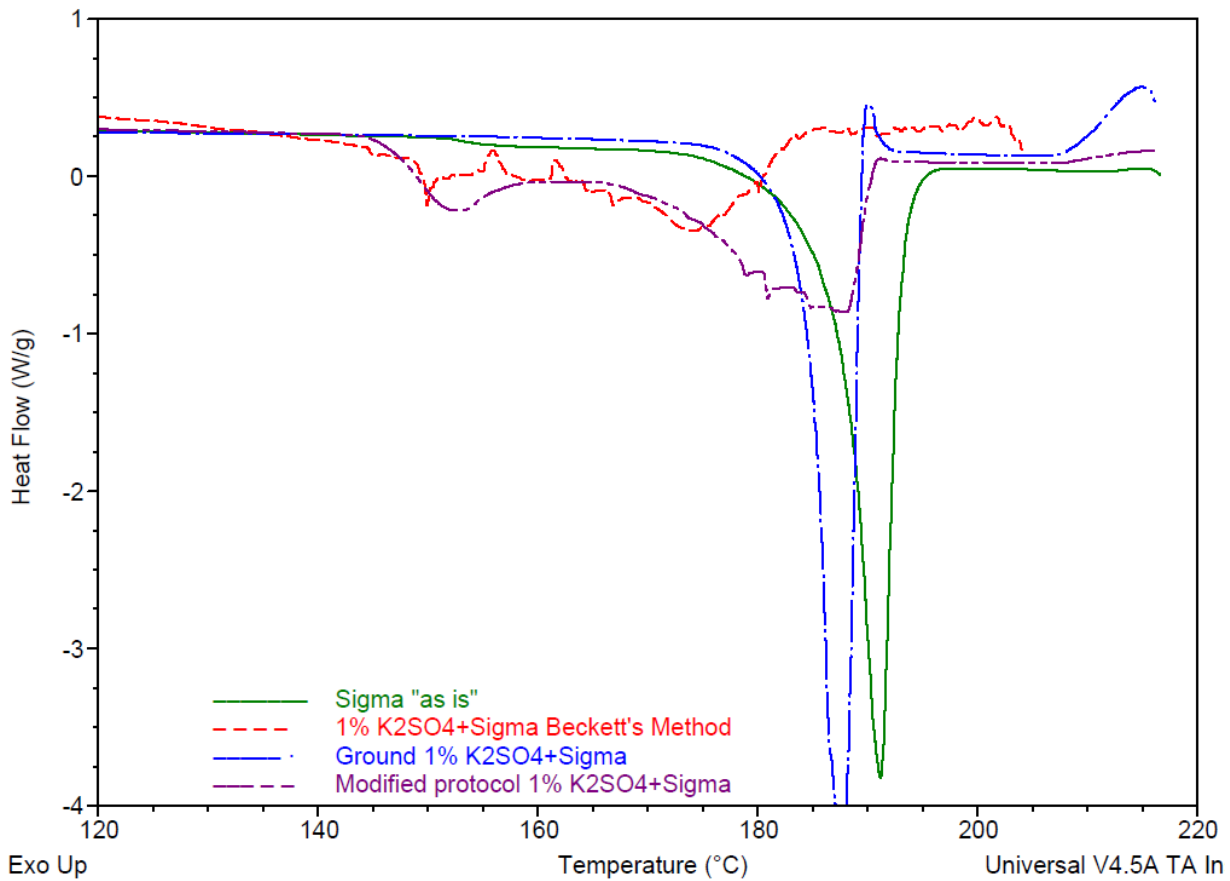
Figure 6.9 DSC thermograms of Sigma cane "as is", and Sigma cane recrystallized with 1% K_2SO_4 using different recrystallization methods at 10°C/min heating rate.
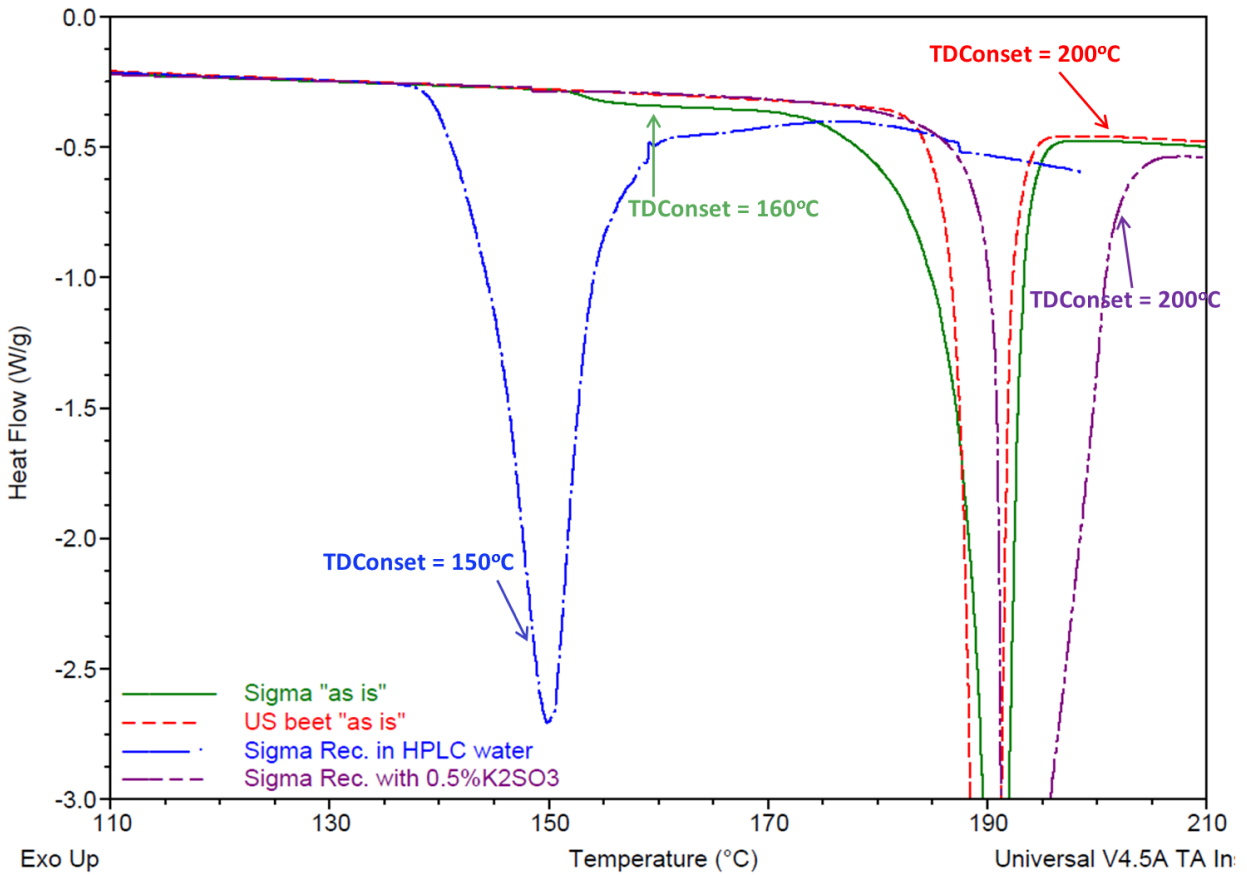
Figure 6.10 DSC thermograms of "as is" Sigma cane, "as is" US beet, Sigma cane recrystallized in HPLC water, and Sigma cane recrystallized with 0.5% K_2SO_3 at 10°C/min labeled with the temperature at which the earliest thermal decomposition component (TDConset: glucose) was detected using HPLC.
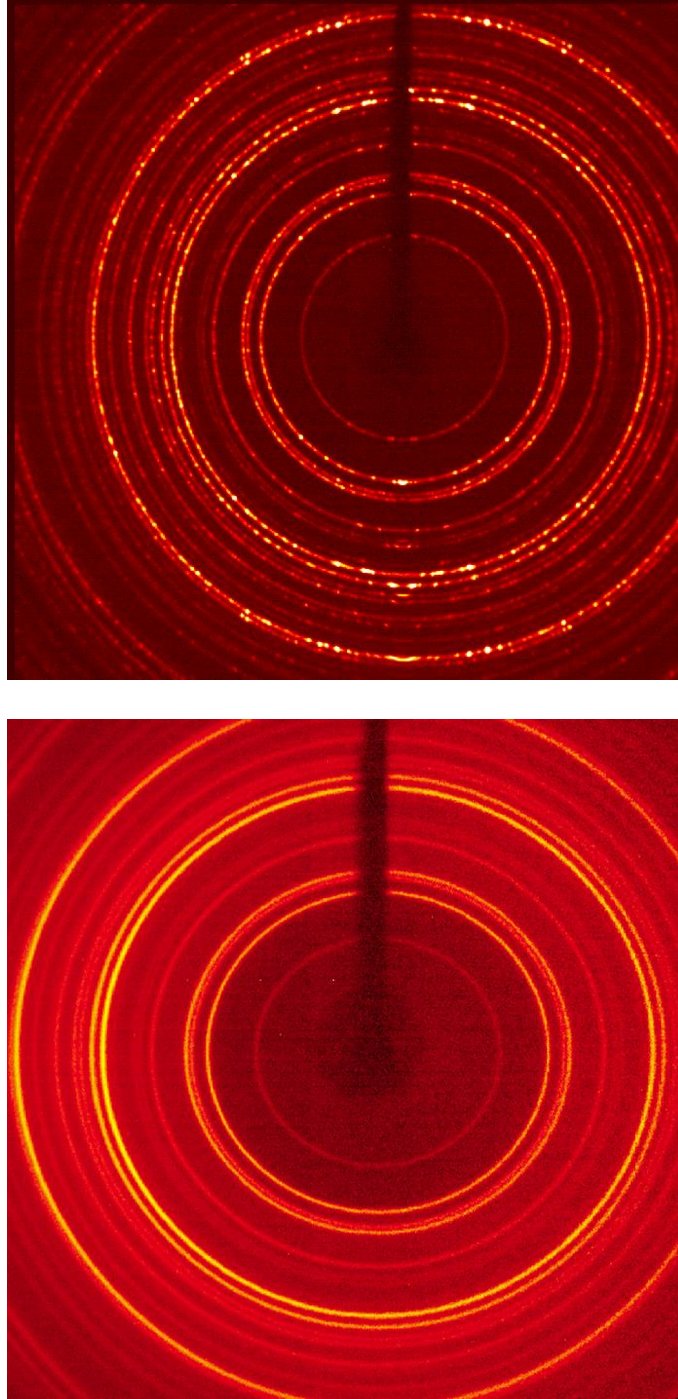
Figure 6.11 Rings diffraction patterns of "as is" Sigma cane (top) with preferred orientation effects and ground Sigma cane sucrose (bottom) with random ordered pattern using D8 Venture diffractometer system.
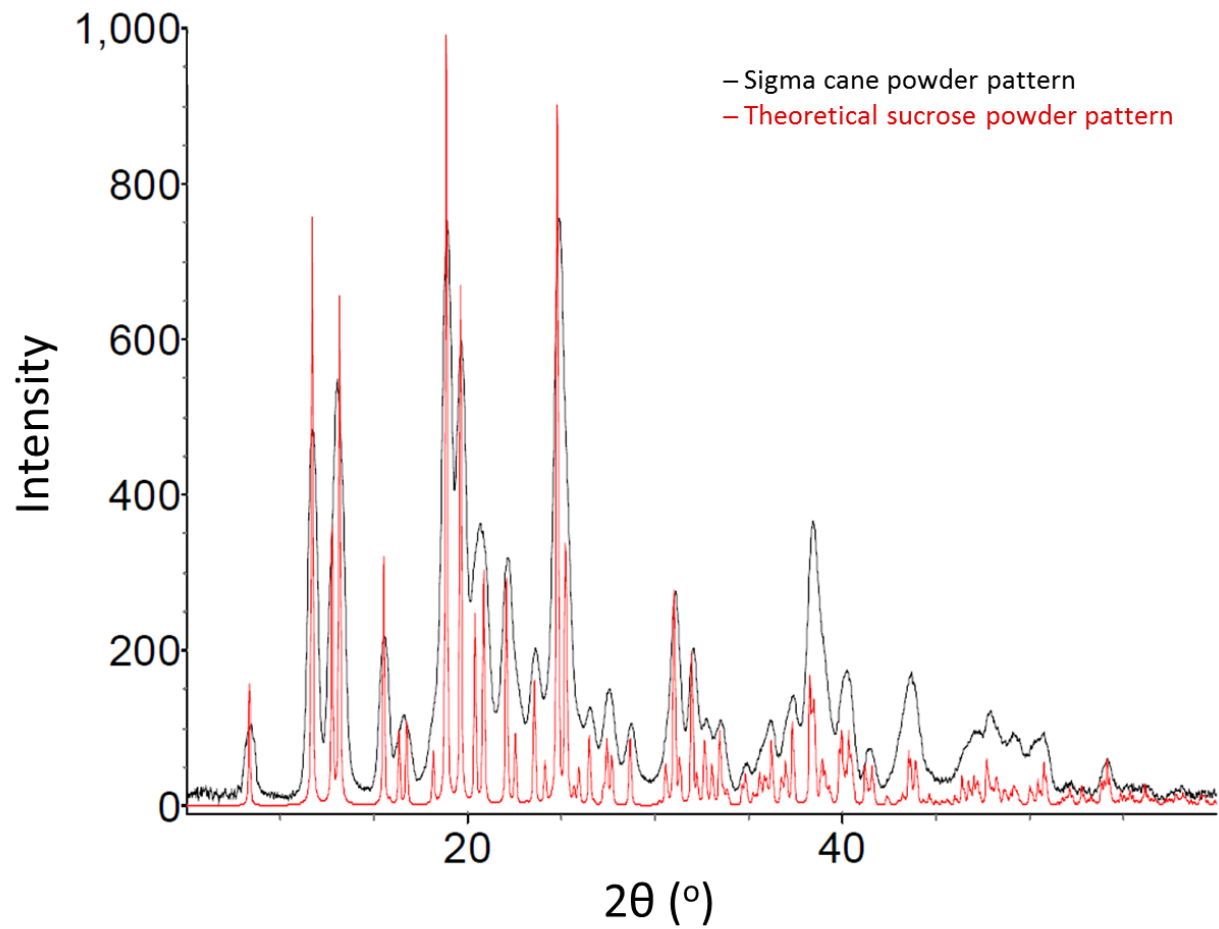
Figure 6.12 Powder X-ray diffraction patterns for Sigma cane sucrose overlaid with theoretical sucrose pattern (Brown and Levy 1973).
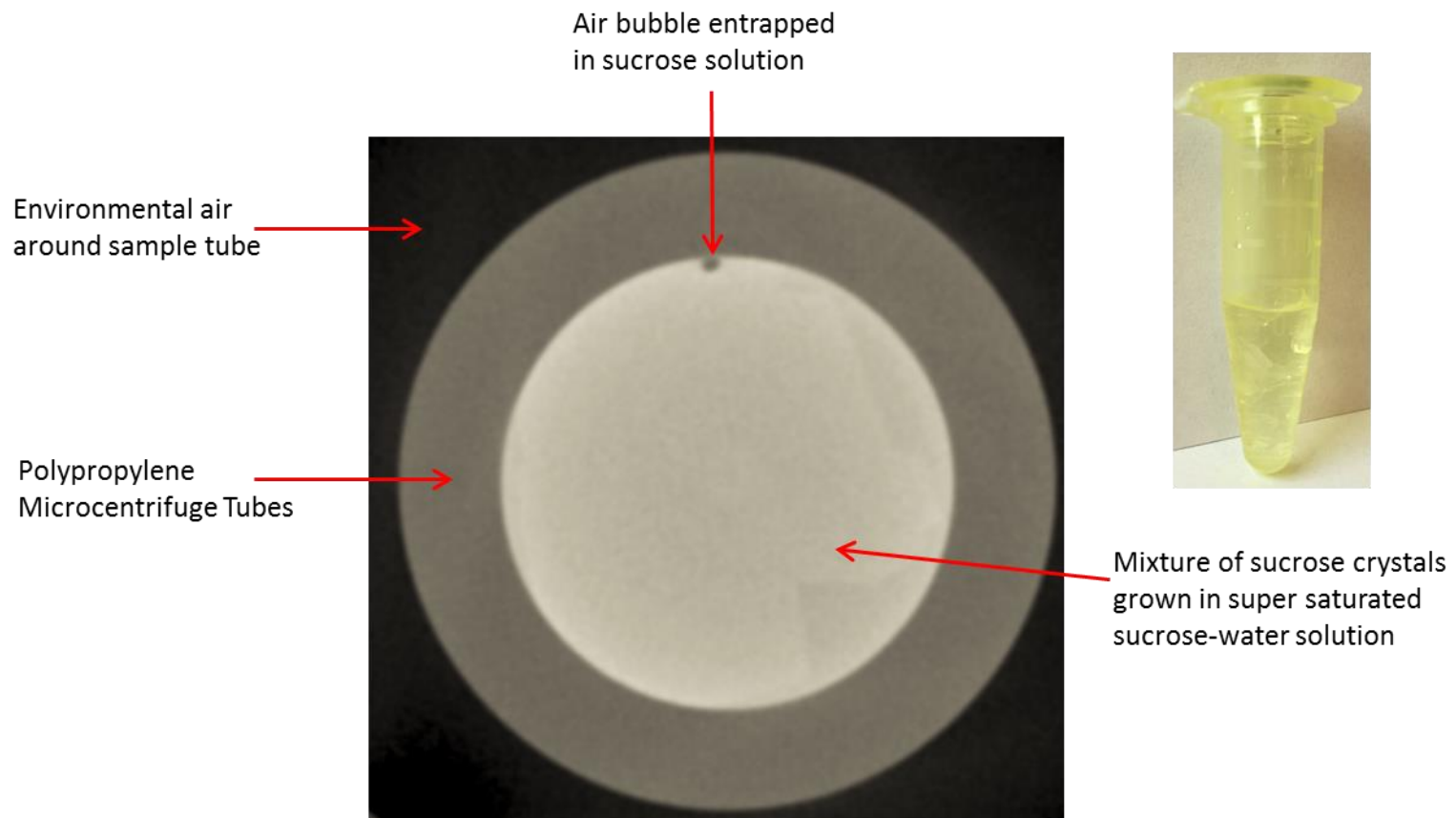
Figure 6.13 Micro-CT scanned 2D image of Sigma sucrose crystal grown in saturated sucrose solution.
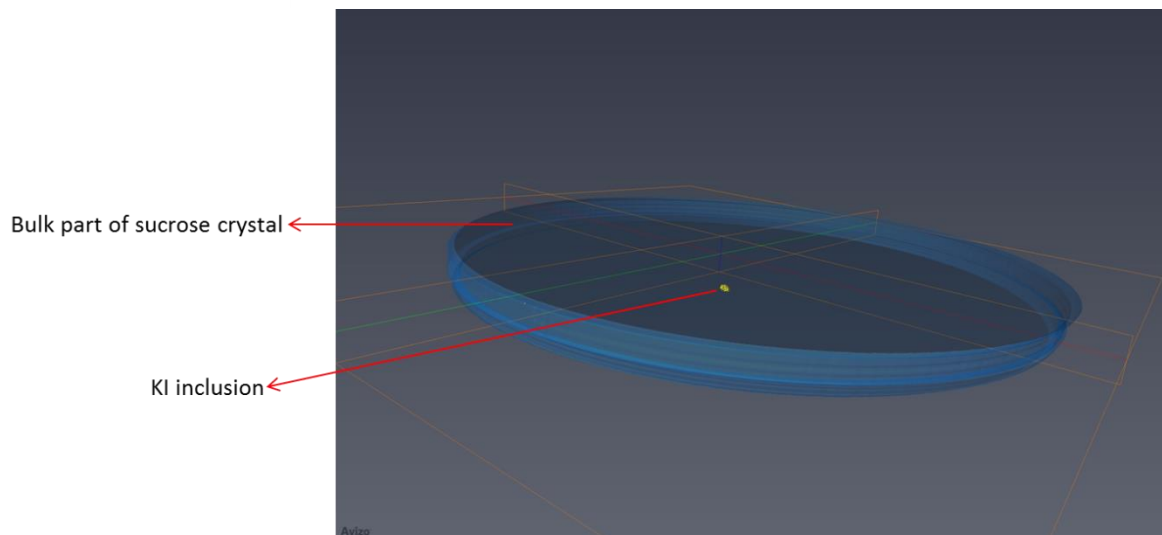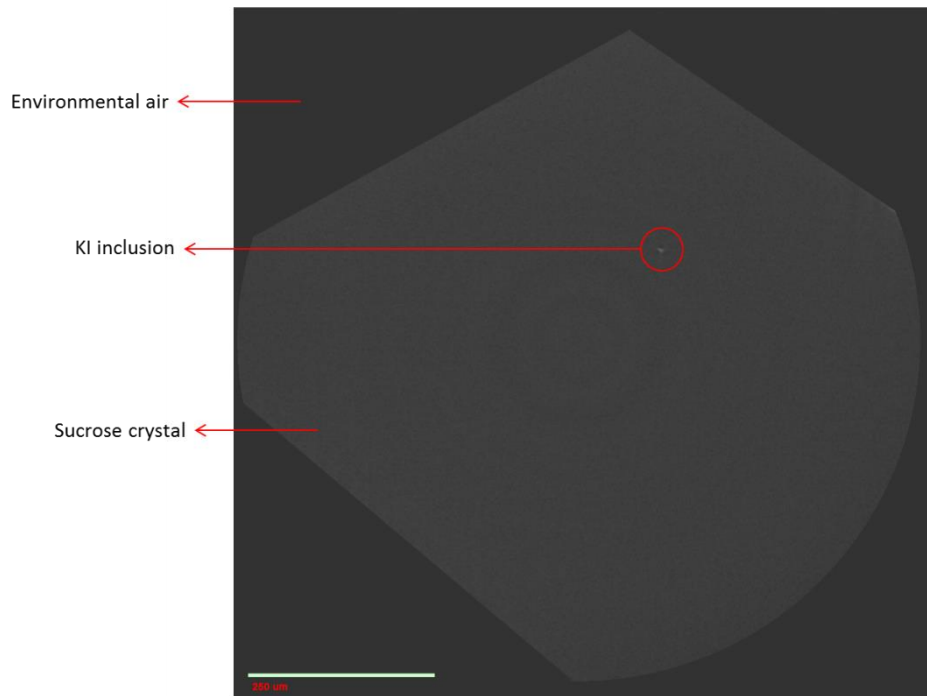
Figure 6.14 Micro-CT scanned 2D image (top) of Sigma sucrose recrystallized with 10% KI and 3D volume rendering (bottom).
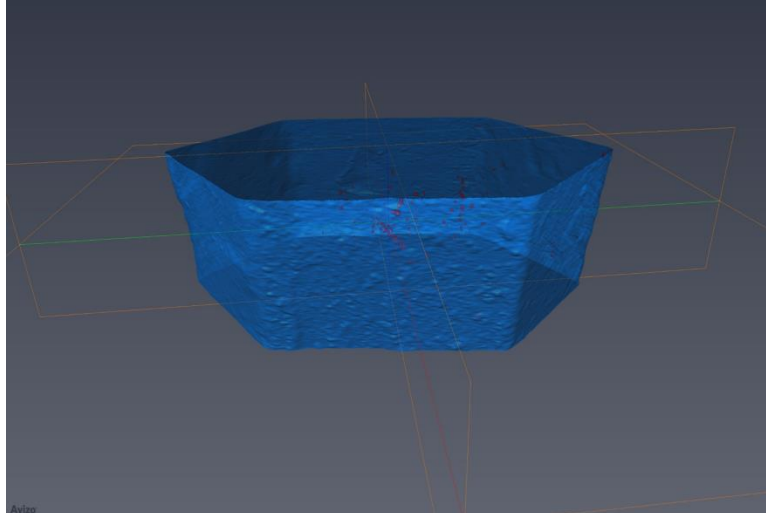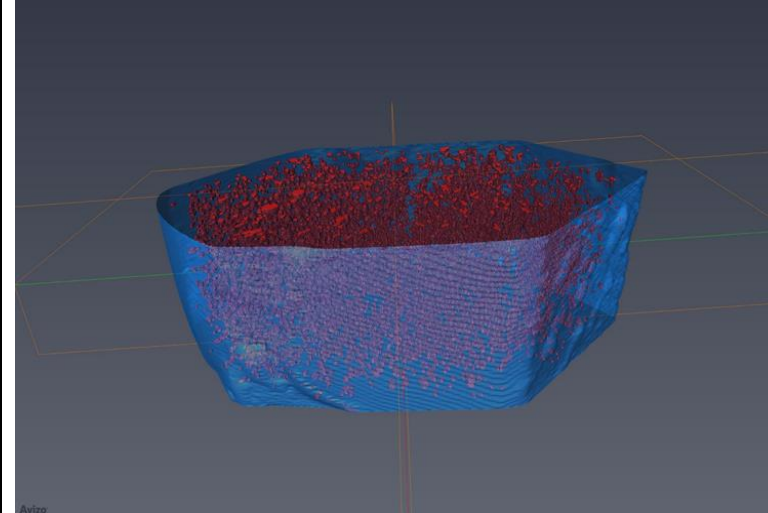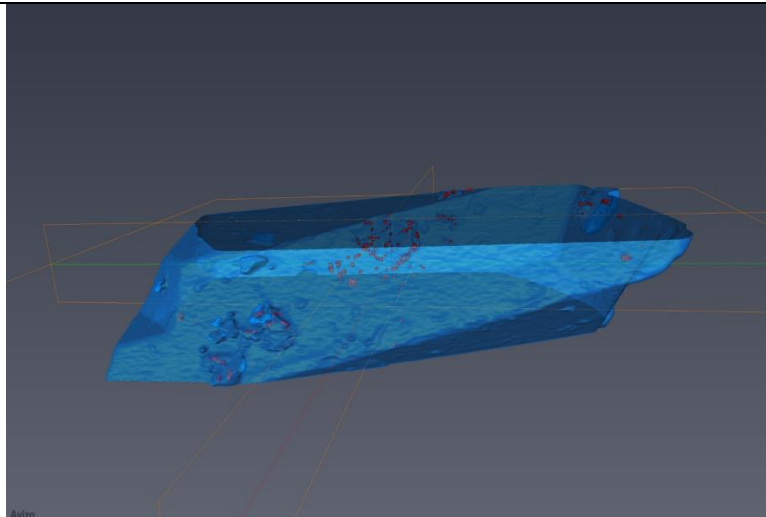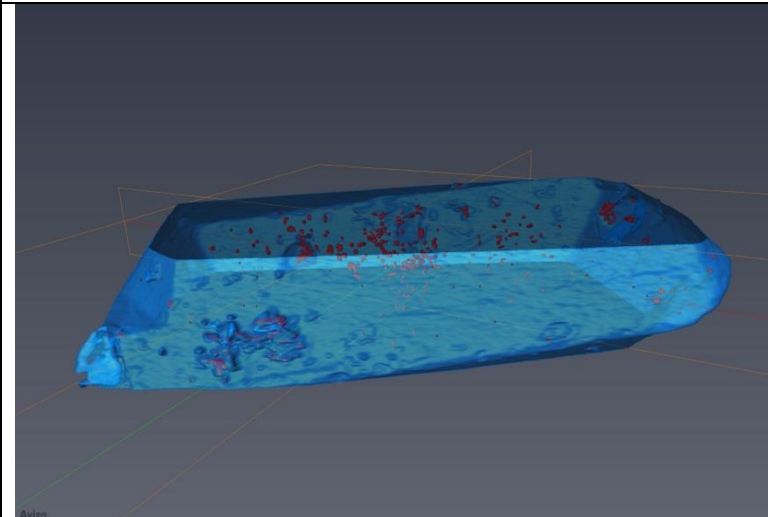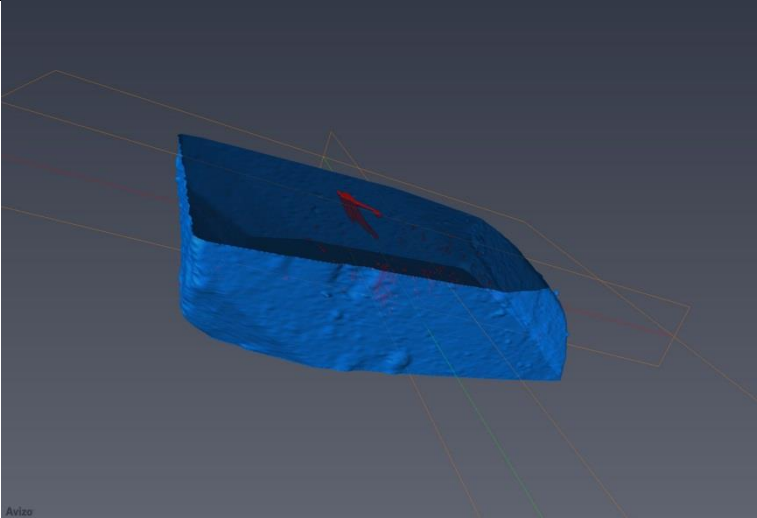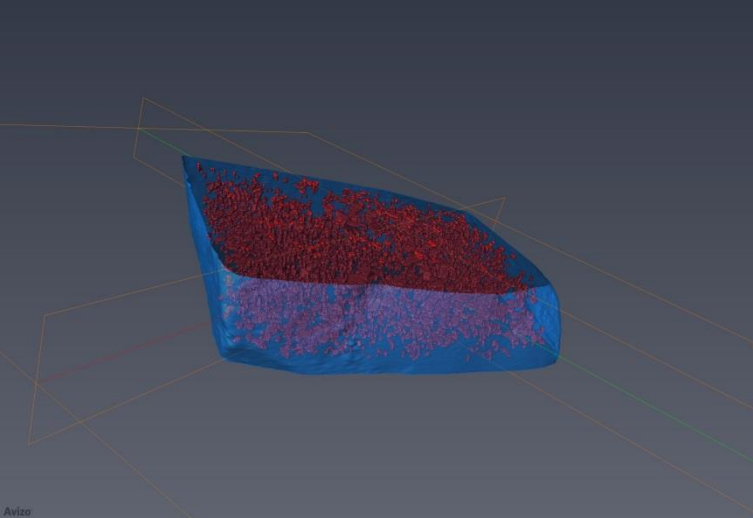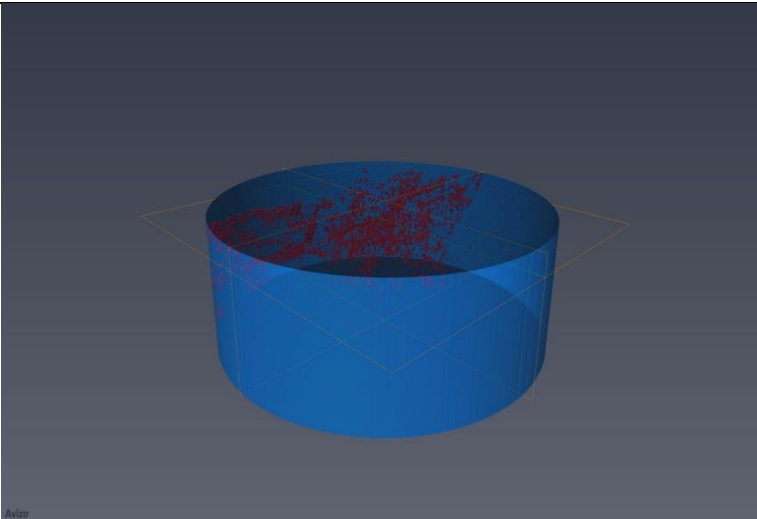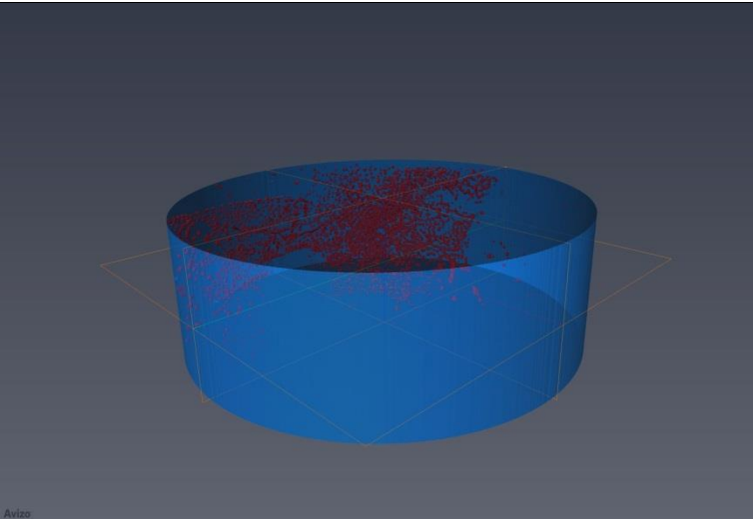
Sample ID	"as is"	165°C
Sigma	Porosity%: 0.00588 ± 0.00002	Porosity%: 2.67347 ± 0.06747
US beet	Porosity%: 0.02039 ± 0.00316	Porosity%: 0.04851 ± 0.00462

Figure 6.15 3D Micro-CT images for "as is" and 165°C Sigma cane, US beet, US cane, and Sigma crystallized with 0.5% K_2SO_3 crystals.

Figure 6.15 continued.

Sample ID	"as is"	165°C
US cane	Porosity%: 0.07451 ± 0.07300	Porosity%: 2.14628 ± 0.11490
Sigma cane recrystallized with 0.5% K_2SO_3	Porosity%: 0.17519 ± 0.00634	Porosity%: 0.16861 ± 0.01544
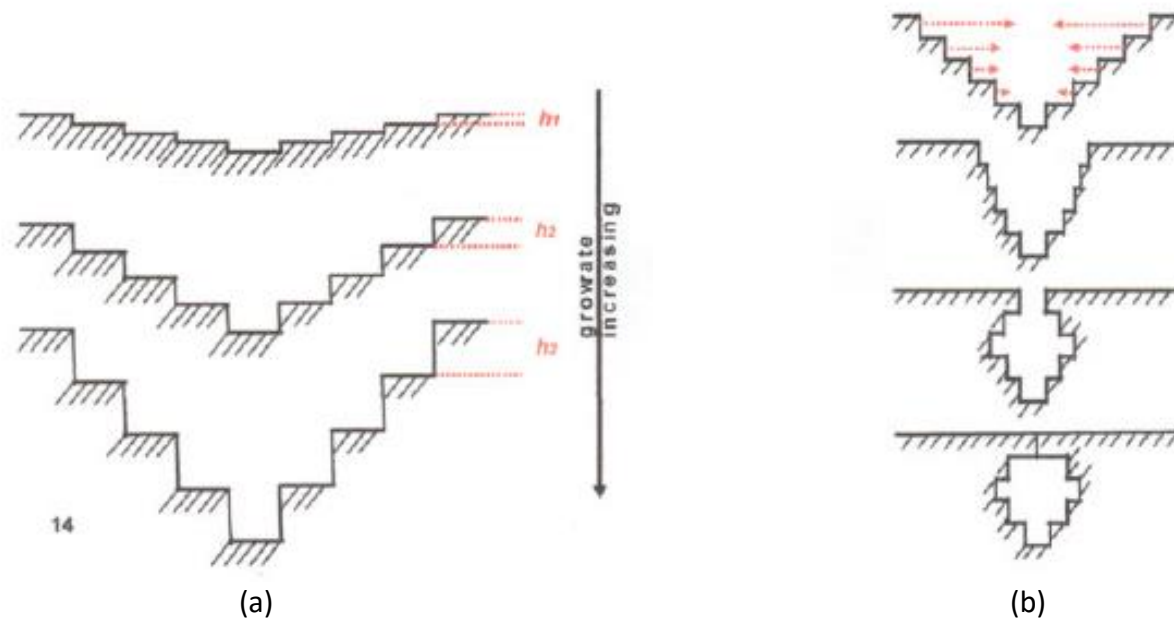
Figure 6.16 Higher growith rates result in rougher surfaces, higher growing steps, and deeper cavities (a), as well as entrappment of mother liquor occlusions (b)

Table 6.1 Unit cell parameters of selected beet and cane sucrose samples obtained using single crystal X-ray diffraction. Each parameter was reported as average value (standard deviation).

Sample ID	a(Å)	b(Å)	c(Å)	α(°)	β (°)	γ(°)	Volume (Å³)	Space group	Temp (°C)
Sucrose Reference[a]	7.7585(4)	8.7050(4)	10.8633(5)	90	102.945	90	715.04	P2$_1$	22.5±1.5
Sigma cane "as is"	7.763(3)	8.703(4)	10.858 (6)	90	103.042(19)	90	714.6(9)	P2$_1$	23.5
Sigma cane 165°C	7.770(4)	8.689(5)	10.878(6)	90	103.072(20)	90	715.3(1.1)	P2$_1$	23.5
US beet "as is"	7.766(6)	8.690(7)	10.848(8)	90	103.1(4)	90	713.3(14)	P2$_1$	23.5
US beet 165°C	7.752(3)	8.692(3)	10.844(5)	90	103.019(17)	90	711.9(7)	P2$_1$	23.5
US cane "as is"	7.741 (3)	8.686(4)	10.834(5)	90	102.887(17)	90	710.1(9)	P2$_1$	23.5
US cane 165°C	7.749(4)	8.700(4)	10.861(6)	90	103.01(2)	90	713.3(1.0)	P2$_1$	23.5
Sigma rec. in HPLC water	7.740(6)	8.668(7)	10.829(8)	90	103.01(2)	90	707.90(15)	P2$_1$	23.5
Sigma rec. in HPLC water 140°C	7.741(5)	8.685(6)	10.821(9)	90	103.05(3)	90	708.6(1.5)	P2$_1$	23.5
Sigma rec. w/ 0.5% K$_2$SO$_3$	7.7667(14)	8.7026(11)	10.850(2)	90	102.839(16)	90	715.0(3)	P2$_1$	23.2
Sigma rec. w/ 0.5% K$_2$SO$_3$ 165°C	7.7595 (10)	8.7092(8)	10.856(2)	90	103.046(15)	90	714.7(2)	P2$_1$	23.2

[a]Sucrose reference is from Brown and Levy (1973)

Chapter 7: Investigating the vibrational modes of sucrose crystals from different sources as a function of temperature

7.1 Abstract

Thermal behavior differences between beet and cane sugars have been reported. In general, cane sucrose sources exhibit two endothermic DSC peaks, one small and one large peak; whereas, beet sucrose sources exhibit only one large endothermic peak. Previous research revealed that beet sucrose samples exhibited a greater thermal stability compared to cane sucrose samples, using HPLC analysis. In this study, the vibrational modes (Glycosidic bond, CH and CH2, as well as OH groups) of sucrose crystals, as a function of temperature, were determined using confocal Raman imaging microscope for analytical grade Sigma cane, US beet, US cane, laboratory-recrystallized analytical grade Sigma cane sucrose with 0.5% K_2SO_3, and ground analytical grade Sigma cane sucrose samples. From this research we found that the thermal decomposition in cane sucrose sources was related to the decrease in relative Raman intensity of glycosidic bond deformation during heating. Also the missing/merging of v O11-H15…O9 (Intramolecular) band could result in the breaking/weakening of intramolecular hydrogen bonds in crystalline sucrose, thus making the glycosidic bond vulnerable and easy to be attacked, since the relative orientation of the glucose and fructose moieties is fixed by intramolecular hydrogen bonds. In addition, the observed difference of v (Non-bonded OH) in Raman spectra among sucrose sources was associated with thermal induced hydrolysis, which occurs more rapidly in cane sucrose sources than beet. Therefore, this study makes a substantial impact on investigating the thermal behavior of crystalline sucrose at the molecular level, since

no previous research was found to explore these three vibrational modes, as a function of temperature, between beet and cane sucrose sources.

7.2 Introduction

Recently, thermal behavior differences between beet and cane sugars have been reported (Lu and others 2013). In general, cane sucrose sources exhibit two endothermic DSC peaks, one small peak proceeded by one large peak; whereas, beet sucrose sources exhibit only one large endothermic peak (Figure 7.1). Previous research revealed that beet sucrose samples exhibited a greater thermal stability compared to cane sucrose samples, using HPLC analysis (Lu and others 2014). HPLC analysis results indicated that temperature of the apperance of the initial thermal decomposition component(s) (TDConset) is associated with the onset temperature (Tmonset) of the small endothermic DSC peak in cane samples; whereas, thermal decomposition resistance was observed in commercial beet, Sugar in the Raw, and Chinese cane samples. Lu and others (2015) found that mother liquor occlusions within sucrose crystals are essential to the presence of the small endothermic DSC peak, since the mother liquor occlusions are the cite of crystal defects where thermal induced hydrolysis and subsequent thermal decomposition is initiated. However, the occlusions alone are not sufficient to explain the presence of the small DSC peak, since the commercial beet and Chinese cane samples also contain occlusions, but do not exhibit the small endothermic DSC peak. The laboratory-recrystallization investigation further proved that the appearance of the small endothermic DSC peak in analytical grade Sigma cane sucrose can be inhibited by sulfite contained in the mother liquor occlusions, which explains the lack of a small endothermic DSC peak in white refined beet and Chinese cane sucrose samples. Beet and Chinese cane sucrose

sources contained sulfite, ranging from 6.5 to 11.2 ppm, whereas, analytical and white refined

cane sucrose sources were below the detection limit. In addition, physically grinding cystalline

"as is" sucrose alone resulted in the disappearance of the small endothermic DSC peak in cane

sucrose sources without exhibiting a glass transition (Tg) at lower temperatures. Thus, Lu and

others (2015) concluded that the presence of the small endothermic DSC peak in most "as is"

crystalline cane sugar DSC thermograms is associated with the onset of thermal decomposition

of sucrose occurring in mother liquor occlusions, initiated by hydrolysis and mediated by the

composition and chemistry of the sucrose crystal. A model of a sucrose crystal containing

entrapped mother liquor occlusions was also proposed in their study (Lu and others 2015). Any

factors that affect the composition and chemistry of the sucrose crystal will, in turn, influence

the presence, location (Tmonset), and magnitude of the small endothermic DSC peak.

The cause of the small endothermic DSC peak in the DSC thermogram of sucrose has been

well investigated by the Schmidt laboratory (Lee and others 2011 a and b; Lu and others 2013,

2014 and 2015), as well as other research groups (Reynhardt 1990; Miller 2001; Bhandari and

Hartel 2002; Okuno, 2003; Maulny 2004; Kawakami and others 2006; Beckett and others 2006;

Lee and Lin 2007a and b; Lee and Chang, 2009; Mathlouthi 2012) in the past few years, however,

there are remaining questions that need to be investigated. For example, the decomposition

mechanism of the sucrose crystal at the molecular level still needs to be further explored.

Therefore, in this study, the vibrational modes of sucrose crystals as a function of temperature

were determined using confocal Raman imaging and spectroscopy for analytical grade Sigma

cane, commercial beet and cane, laboratory recrystallized cane sucrose, as well as ground cane

sucrose samples. Raman spectroscopy has been proved as an effective tool for investigating

molecular structures and interactions (Mathlouthi 1986), which is sensitive, reliable,

non-destructive and can be used in situ (Castro and others 2005).

In the literature, more research groups have been devoted into characterizing the

vibrational modes and interactions of sucrose in water solution (Mathlouthi and others 1980;

Immel and Lichtenthaler 1995; Lescure 1995; Kačuráková and Mathlouthi 1996; Max and

Chapados 2001 and 2007; Paranjpe and Deb 2001; Lerbret and others 2005; Te and others 2010;

Brizuela and others 2014) compared to in crystalline state. A sucrose molecule contains eight

OH groups and the bands corresponding to the eight OH stretching vibrations in crystalline

sucrose were identified and assigned by Giermanska and Szostak (1991), using polarized

Infrared (IR) and Raman spectra. More recently, a complete characterization of the vibrational

spectra of sucrose in the solid state was reported by Brizuela and others (2012). Later on, the

same research group also published a complete assignment of vibrational spectra of sucrose in

aqueous medium (Brizuela and others 2014). Based on research carried out by Brizuela and

others (2012), a further investigation was performed using IR, Raman and Inelastic Neutron

Scattering (INS) spectroscopies in order to complete the assignments of bands observed in

sucrose crystals (Szostak and others 2014). In addition, the temperature dependent vibrational

modes of the glycosidic bond in crystalline trehalose and sucrose were investigated by Seo and

others (2008).

In order to explore the cause of the appearance of the small endothermic peak in cane

sucrose samples in the DSC thermograms at molecular level, the main objective of this study

was to investigate three selected vibrational modes in sucrose crystals from different sources as

a function of temperature. According to the information provided in the literature, as well as

our own research observation, the difference in thermal behavior among analytical grade cane, white refined beet and cane, ground analytical grade cane, as well as laboratory-recrystallized analytical grade cane with 0.5% of K_2SO_3 sucrose samples in solid state was further investigated in this study using a Raman confocal imaging microscope equipped with a temperature programmed hotstage.

7.3 Materials and Methods

Materials

Analytical grade crystalline cane sucrose ($\geq$ 99.5%) was purchased from Sigma-Aldrich Co. (St. Louis, MO. #S0389). White refined beet (US beet) and cane (US cane) samples were obtained directly from United Sugar Corporation (Clewiston, FL). Ground sucrose (passed a standard testing sieve with 100 mesh and 0.15 µm opening size) and laboratory-recrystallized sucrose with addition of 0.5% of K_2SO_3 (potassium sulfite $\geq$ 97% was purchased from Sigma-Aldrich Co.) were made originally from analytical grade Sigma cane sucrose (recrystallization method is discussed in detail in Chapter 5 and 6). All sucrose crystals were tested "as is" without further purification. A Silicon wafer was used as a reference material and measured using the same experimental settings as the crystalline sucrose samples.

Methods

Raman Spectrometer

The Raman system used was the Horiba LabRAM HR confocal Raman imaging microscope with a Olympus LMPlanFL 50X objective in the Imaging Technology Group at the Beckman Institute, University of Illinois at Urbana-Champaign. In the Horiba LabRAM HR confocal-Raman microscopy system, the grating was 300 lines/mm the slit was 100 µm and the hole was 200 µm.

The laser was selected at 532 nm and the focus was set at 0.4 μm for all selected XY points. Acquisition time was set at 5 seconds for all measurements. The Raman spectra were collected in the wavenumber ranged from 100 to 4000 cm^{-1}. A Linkam THMS600 hot stage was used in this study, to obtain the spectra at increased temperatures for each sucrose samples. The Linksys32 temperature software was used to control the heating protocol. The standby temperature was set at 23.6^{o}C and the heating rate was 10°C/min. The spectra were collected from 25°C to 195°C at 10°C intervals for all sucrose samples.

Peak identification

In order to eliminate the noise in a Raman spectrum that arises from fluorescence or background radiation, baseline correction was applied during spectra analysis. This step was carried out using the peaks and baseline function in OriginPro 9.0 (OriginLab, Northampton, MA). An example of baseline subtraction for the "as is" analytical grade Sigma sucrose spectrum from 3100-3700 cm^{-1} is given in Figure 7.2, which clearly shows a substantial improvement in the Raman spectrum baseline after the background subtraction. Therefore, even though we collected the full spectra for each sample (100 to 4000 cm^{-1}), which is shown in Figure 7.3, to improve the baseline correcting performance, three spectra regions of interest were analyzed separately. The maximum height of the peak was then calculated using the same software to find the local max after baseline correction. To better interpret the data, the relative Raman intensity and Raman shift were plotted as function of temperature using excel. The Raman intensity of each band measured at 25°C was set as 100% relative Raman intensity.

7.4 Results and Discussion

The full spectrum (100 to 4000 cm^{-1}) of each sucrose samples was collected from 25°C to 195°C at 10°C intervals. The full Raman spectrum of crystals from each sucrose source at 0.4 μm excitation laser focus is given in Figure 7.3. The structural formula of a sucrose molecule with numbering of each atom is illustrated in Figure 7.4. To better assign the target bands, as well as investigate the vibrational modes at each temperature within and between sucrose crystals from each source, the full spectrum was divided into 3 regions: Region I: 790 to 1200, Region 2: 2850 to 3050, and Region 3: 3100 to 3700 cm^{-1} for further study. Additionally, at high temepratures (>185°C), the phase transition and caramelization reactions have already begun, which resulted in a very high interference in Raman signals. This phenomenon has also been reported by Seo and others (2008). They explained that when heated close to the melting temperature of sugar, it rapidly changed into caramel, causing no informative Raman Signals to be obtained. Thus, in this study, the results were presented and discussed within the temperature range from 25 to 185°C.

Glycosidic bond modes δ(O1–C1–C4) (Region 1: 790-1200 cm^{-1})

The vibrational modes in this spectral region are typically due to torsions of the endocyclic and exocyclic of C-O, coupled with other vibrations, such as the deformations of C-O-C, C-C-H and C-O-H (Gafour and others 2011), which is known as an area (Susi and Scheker 1969) or fingerprint (Tul'chinsky and others 1976) of crystallinity. According to the vibrational modes of crystalline sucrose characterized by Brizuela and others (2012, Appendix K), an example Raman spectrum of the glycosidic bond deformation (δ(O1–C1–C4) in Figure 7.4) assigned for Sigma sucrose at 25°C using OriginPro 9.0, as well as the Raman spectra of five sucrose samples plotted together at 25°C using Excel, are recorded in Figure 7.5. The results of Raman shift and

relative Raman intensity of glycosidic bond deformation δ(O1–C1–C4) as a function of temperature in analytical grade Sigma cane, US beet, US cane, analytical grade Sigma cane recrystallized with 0.5% K_2SO_3, and ground analytical grade Sigma cane sucrose samples were plotted in Figure 7.6 and 7.7, respectively.

The glycosidic bond deformation (δ(O1–C1–C4) of most sucrose samples, except for Laboratory-recrystallized Sigma sucrose with addition of 0.5% K_2SO_3, exhibited a slight decrease in Raman shift (Figure 7.6) with increased temperatures. For ground Sigma cane sample, the Raman shift went up and down as a function of temperature and finally decreased after 155°C. In general, the Stokes shift (red shift) in Raman spectrum is due to energy absorption, which is accompanied with lattice expansion. Similar research was published by Seo and others (2008), whom investigated the temperature dependent vibrational modes of glycosidic bond in trehalose, sucrose (from Sigma, which is a cane sugar source), and maltose. They reported that the slope of Raman shift of the glycosidic bond in trehalose and sucrose changed at temperature around 120°C (reflected as a bond length or bond angle change), but not in maltose. They explained that when maltose was heated close to its melting temperature, it rapidly changed into a caramel.

In the literature, the temperature dependence of the glycosidic bond vibrations can simply be related to the thermal expansion of the crystal, which was reported by Alers and others (1995), as they reported that the Raman shift decreased with increasing thermal expansion. However, Seo and others (2008) pointed out that if the temperature dependence of the glycosidic bond vibration in disaccharides is solely due to the thermal expansion, there should not be a step changes in slope at a temperature of 120°C (for sucrose and trehalose). In addition,

Seo and others (2008) also found that the slope changed only in glycosidic bond vibrations, not in the other vibrations. The Raman shift usually decreases with increasing temperature due to thermal expansion of a material; however, Seo and others (2008) found an increased Raman shift in C-O stretching and Ring type of vibration during heating. Therefore, Seo and others (2008) proposed several possibilities to explain the changes happened at the glycosidic bond structure, including a broken linkage structure, a bond length change, or a bond angle change. However they disregard the idea of broken linkage occuring in the sucrose structure, because they believed that 120°C is much lower than the reported melting temperature of trehlose (213°C) and sucrose (185-187°C). Nevertheless, as discussed in Chapter 3, by using high sensitivity TGA analysis, all three sucrose samples from different sources (Sigma cane, US beet and US cane) began to lose weight at essentially the same temperature, near 120°C at a heating rate of 10°C/min, which suggests perhaps that some bond breaking is associated with the initial stage of thermal decompsition. More research is need to determine the cause of the changes occurring at 120°C as observed by both Raman spectroscoy and TGA.

Compared to the Raman shift, the relative Raman intensity, as a function of temperature, provided more information to explore. From Figure 7.7, a trend of continual decrease in relative Raman intensity of the glycosidic bond deformation (δ(O1–C1–C4), between 25 to 165°C, was observed in analytical grade Sigma cane and US cane. A slight increased relative Raman intensity at higher temperatures (175 to 185°C) within these two samples could possibly due to the rapidly forming thermal decomposition components, thus creating more baseline fluctuation. However, US beet and laboratory-recrystallized Sigma sucrose with 0.5% K_2SO_3 sucrose crystal exhibited relatively constant relative Raman intensity values during heating, then

an increasing trend begining at 165°C. In addition, the ground Sigma cane sample was found to initially decrease in relative Raman intensity until 75°C, which followed by a continuous increase in relative Raman intensity from 75 to 155°C, then the relative Raman intensity began to decrease again when the temperature increased above 155°C. The unusual pattern of relative Raman intensity as a function of temperature found in ground sucrose sample is most likely related to the particle size, since the sensitivity of the confocal Raman measurement may influence by the very small particle sizes.

From this study, as well as the thermal behavior investigation of sucrose reported by Lu and others (2013, 2014 and 2015), we believed that the decrease in relative Raman intensity of the glycosidic bond deformation as a function of temperature in most cane sucrose sources is an indicator of initial thermal decomposition, involving the glycosidic bond. The decomposition mechanism of crystalline sucrose reported in the literature proposed that the first step of thermal decomposition is the protonation of the glycosidic oxygen and yields initial products: α-D-glucopyranose and fructose carbocation (Richards and Shafizadeh 1986). Šimkovic and others (2003) also reported that the primary reaction of thermal degradation of sucrose is the splitting of the glycosidic bond. Thus, this study supports our previous research findings (Lu and others 2014) that thermal decomposition is associated with the small endothermic DSC peak in cane sucrose sources, which could also be observed as a decrease in relative Raman intensity of glycosidic bond deformation by the function of temperature in cane sucrose sources.

CH$_2$ and CH Modes (Region 2 2850-3050 cm^{-1})

According to the vibrational modes of crystalline sucrose characterized by Brizuela and others (2012, Appendix K) and Szostak and others (2014 Appendix L), example Raman spectrum

of –CH2 and –CH stretching vibration assigned for analytical grade Sigma sucrose at 25°C (~3000 cm-1) using OriginPro 9.0 and Raman spectra of all five sucrose samples plotted together at 25°C in Excel are recorded in Figure 7.8. The results of Raman shift and relative Raman intensity of –CH_2 and –CH stretching vibration ($v$$CH_2$ + vCH) as a function of temperature in analytical grade Sigma cane, US beet, US cane, Sigma cane recrystallized with 0.5% K_2SO_3, and ground Sigma cane sucrose samples were plotted in Figure 7.9 and 7.10.

The Raman shift of –CH_2 and –CH stretching decreased as a function of temperature for all five sucrose samples (Figure 7.9). As the most abundant groups in sucrose, as well as other carbohydrates, –CH_2 and –CH stretching modes exhibit high intense in Raman spectra compared to the glycosidic bond (O1–C1–C4) vibration. The Raman shift occurred in this region (2850-3050 cm^{-1}) during heating could possibly be more related to the thermal expansion of the sucrose crystal or the thermal induced hydrolysis occurred at cites of mother liquor occlusion within crystal. The resistance of decrease in relative Raman intensity of ($v$$CH_2$ + vCH) as a function of temperature (from 25°C to 185°C) exhibited a trend (Figure 7.10) as US beet (64.0%) > laboratory-recrystallized Sigma cane with 0.5% K_2SO_3 (47.9%) > Ground Sigma cane (37.2%) > US cane (24.5%) > Sigma cane (19.4%) at the end temperature of 185°C, though all sucrose samples exhibited a decrease in relative Raman intensity. In this selected region, the C-H stretching bands are very intense in Raman spectra compared to the other regions; however, as reported by Gafour and others (2011), this mode is highly affected by the various orientations of hydroxyl group and the intermolecular hydrogen bonds, in particular, contribute enormously to these frequencies. Thus, in order to understand more about the thermal decomposition mechanisms

of crystalline sucrose at molecular level, special attention must be paid to the investigation of O-H vibrational modes as a function of temperature between sucrose sources.

O-H Modes (Region 3 3100-3700 cm^{-1})

Silicon wafer was used as a reference material and measured using the same experimental settings as the sucrose samples. However, no –OH vibrational mode was found in the Raman spectrum for the silicon wafer at 25°C (Figure 7.11), which excluded the possibility that the surface adsorbed water or the moisture from the environment interfere with the Confocal Raman measurements. According to the vibrational modes of crystalline sucrose characterized by Brizuela and others (2012, Appendix K) and Szostak and others (2014 Appendix L), example Raman spectrum of OH groups stretching modes (*v* O8-H14---O2 Intermolecular; *v* O11-H15---O9 Intramolecular; *v* O3-H7---O11 Intermolecular; *v* Non-bonded OH) assigned for Sigma sucrose crystal at 25°C (3100-3500 cm^{-1}) using OriginPro 9.0 and Raman spectra of all five sucrose samples plotted together at 25°C in Excel were recorded in Figure 7.12. The results of Raman shift and relative Raman intensity of these four –OH stretching vibration modes, as a function of temperature in analytical grade Sigma cane, US beet, US cane, Sigma cane recrystallized with 0.5% K$_2$SO$_3$, and ground Sigma cane sucrose samples, were plotted in Figures 7.13 to 7.17, respectively.

From Figures 7.13 to 7.17, a slight increase in Raman Shift (~3245 cm^{-1}) of the first OH stretching (*v* O8-H14---O2 Intermolecular) band was observed in all sucrose samples, except for ground Sigma cane. This band was no longer observed starting at 135 °C in ground Sigma cane sucrose crystal (Figure 7.17). The decrease in the relative Raman intensity of *v* (O8-H14---O2), as a function of temperature, was observed in all sucrose samples, with a final relative Raman

intensity at 185°C of 17.4, 43.9, 30.7, 23.8% for analytical grade Sigma cane, US beet, US cane, Sigma cane recrystallized 0.5% K_2SO_3 respectively, and 53.5% for ground Sigma cane at 125°C.

From Figures 7.13 to 7.17, the disappearance of Raman Shift (~3340 cm^{-1}) of the second band of –OH stretching (v O11-H15---O9 Intramolecular) started at 115, 125, 125, 115, and 95°C with corresponded final relative Raman intensity of 40.1, 89.0, 34.4, 43.0 and 70.6% in analytical grade Sigma cane, US beet, US cane, Sigma cane recrystallized with 0.5% K_2SO_3, and ground Sigma cane sucrose, respectively.

It is known that the conformation of crystalline sucrose revealed the glucose and fructose moieties are fixed in their relative orientation by two intramolecular hydrogen bonds between O2-H11---O3 and O11-H15---O9 (Figure 7.4 dash lines), respectively (Pérez 1995). In the literature, one of the possibilities of the presence of the small DSC endothermic peak in crystalline sucrose is attributed to the breaking of some hydrogen bonds prior to the melting of the crystal structure (Reynhardt 1990); however, these researchers did not specify which type(s) of hydrogen bonds were actually broken during heating. From our own investigation, the disappearance of v O11-H15---O9 (Intramolecular) band in crystalline sucrose has been observed. Though the disappearance of this band may not result in the thermal decomposition of sucrose molecule directly; however, the breaking/weakening of intramolecular hydrogen bonds in crystalline sucrose could cause the glycosidic bonds to become vulnerable and easy to attack, since the relative orientation of glucose and fructose residues is fixed by these two intramolecular hydrogen bonds.

From Figures 7.13 to 7.17, the Raman Shift (~3390-3420 cm^{-1}) of the third band of –OH stretching (v O3-H7---O11 Intermolecular) exhibited a slightly increase in all sucrose samples,

except for ground Sigma cane. The decreased trend in the relative Raman intensity of v

(O3-H7---O11) as a function of temperature was observed in all sucrose samples, with a final

relative Raman intensity at 185°C: 24.3, 54.3, 29.8, 46.6, and 31.8% for analytical grade Sigma

cane, US beet, US cane, Sigma cane recrystallized 0.5% K_2SO_3, and ground analytical grade Sigma

cane, respectively.

Last, but not least, a relatively constant v (Non-bonded OH) Raman shift (3560-3570 cm^{-1},

band 4 in Figure 7.12) as a function of temperature was observed in most sucrose crystals,

except for ground analytical grade Sigma cane (Figure 7.13 to 7.17). The relative Raman

intensity of v (Non-bonded OH) band at 185°C was 21.3, 72.5, 26.2, 61.3, and 19.0% for

analytical grade Sigma cane, US beet, US cane, Sigma recrystallized with 0.5% K_2SO_3, and

ground Sigma sucrose, respectively. A substantial decrease in relative Raman intensity was also

observed at relatively low temperatures, 105 and 95°C for analytical grade Sigma cane and US

cane, respectively. Therefore, we hypothesized that the substantiated drop of relative Raman

intensity of v (Non-bonded OH) in cane sucrose samples at low temperatures could be related

to the thermal induced hydrolysis occuring in the mother liquor occlusions (a model was

illustrated by Lu and others in 2015), resulting in the loss of entrapped water due to the

hydrolysis reaction, which is reflected as a decrease in relative Raman intensity of v

(Non-bonded OH). Based on the vibrational modes of –OH groups assigned by Szostak and

others (2014 Appendix L), the band located around 3560 cm^{-1} in sucrose crystal was

characterized as stretching vibration of non-bonded –OH group (O4–H, O7–H9). However, the

complication has been found in characterization of –OH stretching modes in Raman and IR

spectra in the literature, which is not limited to carbohydrate research. Shallenberger and Birch

(1975) proposed that the narrow band is due to free OH groups at 3600 cm^{-1} and the broad one

at 3400 is due to OH group linked by hydrogen bonds around 3400 cm^{-1}. Giermanska and

Szostak (1991) proposed that a sucrose molecule contains eight OH groups, two of them are

embodied in the intramolecular and another five OH groups in the intermolecular hydrogen

bonds (OH…O). The remaining OH group may be considered as "free" ones. All these hydrogen

bonds are weak and significantly distorted from linearity. Giermanska and Szostak (1991) also

gave a table to show assignment of the OH group stretching vibrations in the sucrose crystal. A

number of theoretical studies (Dauchez and others 1992 and 1994 a and b; Derreumaux and

Vergoten 1995; Benbrahim and others 2002; Taleb-Mokhtari and others 2003; Sekkal and others

2003; Reguieg and others 2007; Mahdad-Benzerdjeb and others 2007) have been conducted in

order to obtain the normal modes of vibration of mono- and di-saccharides. The vibrational

frequencies of the isomaltulose, a disaccharide, in the solid state were calculated and assigned

to the experimentally observed vibrational frequencies by Gafour and others (2014).

Isomaltulose is a monohydrate sugar. The stretching vibrational mode of water is calculated at

3570 cm^{-1}. The same mode was calculated at 3569 cm^{-1} for α-melibiose and 3552 cm^{-1} for

D-turanose. Additionally, based on their previous research (Gafour and others 2011), several

observed bands in the 3000-3700 cm^{-1} region are all attributed to the stretching vibrational

modes of O-H bonds; however, they confirmed that for lactose monohydrate, a stretching

vibrational modes of OH from water is calculated at 3553 cm^{-1}, and the same mode was

calculated at 3569 cm^{-1} for α-D-melibiose and 3552 cm^{-1} for D-turanose, according to research

carried out by Mahdad-Benzerdjeb and Taleb-Mokhtari (2007). Therefore, we have more

evidence to believe that the observed OH stretching at higher frequencies in our sucrose samples (3560-3570 cm^{-1}) is associated with entrapped water molecules within sucrose crystal.

In addition, the sensitivity of Raman spectrometer in terms of detecting water vibration can be very high, as reported by Thomas (2000). Chabiron and others (1999), developed a quantitation application of confocal micro-Raman spectrometry in order to measure the water content of individual melt inclusions in a rapid and non-destructive method. Based on their work, Thomas (2000) conducted a research study to show that water concentrations in quenched melt inclusions can be determined using confocal laser Raman microprobe spectroscopy over the entire concentration range of interest (0 to 20% H_2O). They reported that the high-frequency region (3000-4000 cm^{-1}) of the spectrum is characterized by an asymmetric OH stretching centered at 3550 cm^{-1} with a shoulder-like tail to lower frequencies near 3290 cm^{-1} and a typically sharp band at 3630 cm^{-1}. The breadth and asymmetry of the band at 3550 cm^{-1} reflects contribution from both molecular water and other OH-containing species (Pandya and others 1992). The presence of a week 3640 cm^{-1} band was confirmed in spectra from a high water content silica glasses (>10 wt%). At even high bulk water content (>20 wt%), molecular H_2O becomes the dominated species and results in a shift of the very strong main band from high frequencies (centered around 3550 cm^{-1}) to 3450 cm^{-1}. Osawa and others (2008) investigated the structure of water at electrified platinum using Surface-Enhanced Infrared Absorption Spectroscopy. The structure of water on a polycrystlline Pt electrode in H_2SO_4 and $HClO_4$, as a function of applied potential, was examined. They found that interfacial water exhibited a relatively sharp v(OH) band at 3500-3550 cm^{-1}. The frequency is between those for free water on top of the adsorbed CO (3656 cm^{-1}) and for hydrogen-bonded water in the bulk

(3400cm^{-1}), indicating that interfacial water molecules are weakly hydrogen-bonded. The emergence of the very broad band at ~3000 cm^{-1}, is characteristic of very strongly hydrogen-bonded water molecules (Scherer 1978; Coker and others 1985; Thiel and Madey 1987; Miranda and Shen 1999; Henderson 2002; Richmond 2002). Sharp v(OH) band observed at 3500-3560 cm^{-1} in H_2SO_4 and at 3560-3590 cm^{-1} in $HClO_4$ indicates the presence of almost free OH bonds in ice-like structured water layer.

Therefore, based on a through reivew of the literature, as well as our own experimental observations, we hypothesize that the observed difference of v (Non-bonded OH) in Raman spectra (band 4 in Figure 7.12) among sucrose sources is associated with thermal induced hydrolysis, which occurs more rapidly in cane sucrose sources at a lower temperature compared to beet sucrose sources and Sigma cane recrystallized with 0.5% K_2SO_3. As mentioned in previous chapters, in the U.S., an important difference between white refined beet and cane sugar processing is that the beet sugar process routinely includes a sulfitation step, whereas cane sugar usually does not (Clarke and Godshall, 1988; Asadi 2007), because sulfitation has rarely been used in cane raw sugar factories since the 1950's (Andrews and Godshall 2002). Thus, thermal decomposition resistance in commercial beet sugar (US beet) and laboratory-crystallized Sigma cane with addition of sulfite content is due to the residual sulfite contained within the mother liquor occlusion, which resulted in less decrease in relative Raman intensity of v (Non-bonded OH) observed in these two sucrose samples during heating. Based on the literature, SO_2 will react with carbonyl group in sugar molecule to form sugar bisulfite adduct (Shi 2014), which suppressed the decomposition in monosaccharides.

7.5 Conclusions

In this study, the vibrational modes of beet, cane, laboratory-recrystallized sucrose crystals from 25°C to 195°C at 10°C intervals were investigated in 100 to 4000 cm^{-1} Raman spectra region. The vibrational modes of the glycosidic bond, CH_2 and CH, and O-H groups were measured as a function of temperature for each sucrose sample. Research herein makes a substantial impact on investigating the thermal behavior of crystalline sucrose at the molecular level, since no previous research was found to explore these three vibrational modes, as a function of temperature, between different sources of sucrose crystals.

Some key results summarized from this study are: i) thermal decomposition, which is associated with the appearance of the small endothermic DSC peak in cane sucrose sources, could also be observed as a significant decrease in the relative Raman intensity of glycosidic bond deformation during heating in cane sucrose sources, but not in beet sucrose sources; ii) the disappearance of v O11-H15---O9 (Intramolecular) band in sucrose crystals may not result in the thermal decomposition of sucrose molecule directly; however, breaking/weakening of intramolecular hydrogen bonds in crystalline sucrose makes the glycosidic bonds more vulnerable and easy to attack, since the relative orientation of glucose and fructose moieties is fixed by intramolecular hydrogen bonds; iii) the observed difference of v (Non-bonded OH) in Raman spectra among sucrose sources was associated with the thermal induced hydrolysis which occurs more easily and rapidly in cane sucrose sources than beet or Sigma cane recrystallized with 0.5% K_2SO_3 sucrose samples.

7.6 Acknowledgements

7.7 References

Alers P, Hintermanna HE, Haywardb I. Correlations between Raman scattering and thermal expansion behavior for CVD and natural diamond. Thin Solid Films 1995, 259, 14–17.

Andrews LS, Godshall MA. 2002. Comparing the Effects of Sulphur Dioxide on Model Sucrose and Cane Juice Systems. Journal American Society of Sugarcane Technologists. 22: 90-101.

Asadi M. ed. 2007. Beet-sugar handbook. John Wiley & Sons, Inc., Hoboken, New Jersey, USA.

Beckett ST, Francesconi, MG, Geary PM, MacKenzie G, Maulny APE. 2006. DSC study of sucrose melting. Carbohydrate Research 341: 2591-2599.

Benbrahim N, Sekkal-Rahal M and Vergoten G. Spectrochim. Acta A, 58, 3021–3031 (2002).

Bhandari B, Hartel R. 2002. Co-crystallization of Sucrose at High Concentration in the Presence of Glucose and Fructose. J. of Food Sci, 67: 1797–1802.

Brizuela AB, Bichara LC, Romano E, et al (2012) A complete characterization of the vibrational spectra of sucrose. Carbohydr Res 361:212–218. doi: 10.1016/j.carres.2012.07.009.

Brizuela AB, Castillo MV, Raschi AB, et al (2014) A complete assignment of the vibrational spectra of sucrose in aqueous medium based on the SQM methodology and SCRF calculations. Carbohydr Res 388:112–124. doi: 10.1016/j.carres.2013.12.011.

Castro K, Pérez-Alonso M, Rodríguez-Laso MD, et al (2005) On-line FT-Raman and dispersive Raman spectra database of artists' materials (e-VISART database). Anal Bioanal Chem 382:248–258. doi: 10.1007/s00216-005-3072-0.

Chabiron, A., Pfeifert, C., Pironon, J., and Cuney, M. (1999) Determination of wa- ter content in melt inclusions by Raman spectrometry. In : H. Ristedt, Manag- ing Editor; V. Lüders, R. Thomas, and A. Schmidt-Mumm, Guest Editors, Terra Nostra–Schriften der Alfred-Wegner-Stiftung 99/6; ECROFI XV (European Current Research On Fluid Inclusions), Abstracts and Program, June 21–24, 1999, p. 68–69. GeoForschungsZentrum Potsdam.

Clarke MA, Godshall MA. eds. 1988. Chemistry and Processing of Sugarbeet and Sugarcane. Chapter 13, The nature of colorants in sugarcane and beet sugar manufacture. Elsevier Science Publishers, Amsterdam.

Coker DF, Miller RE, Watts RO. The infrared predissociation spectra of water clusters. J. Chem. Phys. 1985, 82, 3554-3562.

Dauchez M, Derreumaux P and Vergoten G. Vibrational molecular force field of model compounds with biologic interest. II. Harmonic dynamics of both anomers of glucose in the crystalline stateJ. Comput. Chem., 14, 263–277 (1992).

Dauchez M, Derreumaux P, Lagant P, et al (1994a) Force-field and vibrational spectra of oligosaccharides with different glycosidic linkages-Part I. Trehalose dihydrate, sophorose monohydrate and laminaribiose. Spectrochim Acta Part A Mol Spectrosc 50:87–104.

Dauchez M, Lagant P, Derreumaux P (1994b) Force field and vibrational spectra of oligosaccharides with different glycosidic linkages—Part II. Maltose monohydrate, cellobiose and gentiobiose in Spectrochimica Acta - Part A: Molecular Spectroscopy. 50:105–118.

Derreumaux P and Vergoten G. A new spectroscopic molecular mechanics force field. Parameters for proteins. J. Chem. Phys., 102, 8586–8605 (1995).

Gafour HM, Bouterfas M, Bekhti N, Derrar SN, Sekkal Rahal M (2011). Harmonic Dynamics of a-D-Lactose in the Crystalline State. J Mol Imag Dynamic 1:102. doi:10.4172/2155-9937.1000102.

Gafour HM, Sail K (2014). Application of the Modified Urey–Bradley–Shimanouchi Force field of α-D-Glucopyranose and β-D-Fructopyranose to Predict the Vibrational Spectra of Disaccharides. Journal of applied spectroscopy. 80(6): 962-970.

Giermanska J, Szostak MM (1991) Polarized Raman and Infrared Spectra of OH Stretching Vibrations in the Sucrose Crystal. Journal of Raman Spectroscopy. 22:107–109.

Henderson, M. A. The interaction of water with solid surfaces: Fundamental aspects revisited. Surf. Sci. Rep. 2002, 46, 5-308.

Immel S, Lichtenthaler FW (1995) The Conformation of Sucrose in Water: A Molecular Dynamics Approach. Liebigs Annalen. 1925–1937.

Kačuráková M, Mathlouthi M (1996) FTIR and laser-Raman spectra of oligosaccharides in water: Characterization of the glycosidic bond. Carbohydr Res 284:145–157. doi: 10.1016/0008-6215(95)00412-2.

Kawakami K, Miyoshi K, Tamura N, Yamaguchi T, and Ida Y. 2006. Crystallization of sucrose glass under ambient conditions: Evaluation of crystallization rate and unusual melting behavior of resultant crystals. Journal of Pharmaceutical Sciences, 95(6): 1354-1363.

Lee JW, Thomas LC, Jerrell J, Feng H, Cadwallader KR, Schmidt SJ. 2011b. Investigation of thermal decomposition as the kinetic process that causes the loss of crystalline structure in sucrose using a chemical analysis approach (Part II). Journal of Agricultural and Food Chemistry, (59):702-712.

Lee JW, Thomas LC, Schmidt SJ. 2011a. Investigation of the heating rate dependency associated with the loss of crystalline structure in sucrose, glucose, and fructose using a thermal analysis approach (Part I). Journal of Agricultural and Food Chemistry, (59):684-701.

Lee T and Chang GD. 2009. Sucrose conformational polymorphism. Crystal Growth and Design, 9(8): 3551-3561.

Lee T and Lin YS. 2007a. Dimorphs of sucrose. International Sugar Journal, 109 (1303):440-445.

Lee T and Lin YS. 2007b. Two Conformational Polymorphs of Sucrose. National Central University.

Lerbret, A.; Bordat, P.; Affouard, F.; Descamps, M.; Migliardom, F. How homogeneous are the trehalose, maltose, and sucrose water solutions? An insight from molecular dynamics simulations. J. Phys. Chem. B 2005, 109, 11046– 11057.

Lescure JP. Analysis of sucrose solutions. 1995:155-185. In: Mathlouthi M, Reiser P, editors. Sucrose properties and applications. 1st ed. Bishopbriggs: Blackie Academic and Professional.

Lu Y, Lee JW, Thomas L, Schmidt SJ. 2013. Proceedings of the 74th Annual Institute of Food Technologists on Differences in the Thermal Behavior of Beet and Cane Sugars. Chicago, IL.

Lu Y, Thomas L, Yin L, Gray D, Jerrell JJ, Cadwallader KR, Schmidt SJ. 2015. Proceedings of the 76th Annual Institute of Food Technologists on Impact of sucrose crystal composition and chemistry on its thermal behavior. Chicago, IL.

Lu Y. Lee JW, Thomas L, Jerrell JJ, Cadwallader KR, Schmidt SJ. 2014. Proceedings of the 75th Annual Institute of Food Technologists on Investigating Thermal Decomposition Differences between Beet and Cane Sugars Using HPLC. New Orleans, LA.

Mahdad-Benzerdjeb A, Taleb-Mokhtari IN, Sekkal-Rahal M (2007) Normal coordinates analyses of disaccharides constituted by d-glucose, d-galactose and d-fructose units. Spectrochimica Acta Part A: Molecular and Biomolecular Spectroscopy 68: 284-299.

Mathlouthi M and Koenig JL. 1986. Vibrational spectra of carbohydrates. Adv Carbohydr Chem Biochem. 44:7-89.

Mathlouthi M and Roge B. 2012. Melting And Crystallization of Sugars: a structural approach. 2012 IFT Annual Meeting presentation. Las Vegas, NV.

Mathlouthi M, Luu C, Meffroy-Biget AM and Luu DV. Carbohydr. Laser-raman study of solute-solvent interactions in aqueous solutions of D-fructose, D -glucose, and sucrose. Res. 81,213 (1980).

Maulny A. 2003. Co-crystallisation of sugars. Ph.D. Thesis, Department of Chemistry, University of Hull, Hull, UK.

Max J-J and Chapados C. Sucrose Hydrates in Aqueous Solution by IR Spectroscopy. The Journal of Physical Chemistry A 2001 105 (47), 10681-10688. DOI: 10.1021/jp012809j.

Max J-J, Chapados C (2007) Glucose and fructose hydrates in aqueous solution by IR spectroscopy. J Phys Chem A 111:2679–2689.

Miller, MM. 2001. The effect of applied fields on crystallisation. Brunel University.

Miranda, P. B.; Shen, Y. R. Liquid interfaces: A study by sum-frequency vibrational spectroscopy J. Phys. Chem. B 1999, 103, 3292-3307.

Okuno M, Kishihara S, Otsuka M, Fujii S, Kawasaki K. 2003. Variability of melting behavior of commercial granulated sugar measured by differential scanning calorimetry. International Sugar Journal 105:29-35.

Osawa M, Tsushima M (2008) Structure of Water at the Electrified Platinum - Water Interface : A Study by Surface-Enhanced Infrared Absorption Spectroscopy. J Phys Chem C 112:4248–4256.

Pandya, N., Muenow, D.W., and Sharma, S.K. (1992) The effect of bulk composition on the speciation of water in submarine volcanic glasses. Geochimica et Cosmochimica Acta, 56, 1875–1883.

Paranjpe AS and Deb SK. Low frequency Raman scattering from aqueous sucrose solution. Journal of Non-Crystalline Solids, 2001, 296(1-2):115-122.

Pérez S. 1995. The structure of sucrose in the crystal and in solution. In: Mathlouthi M, Reiser P, editors. Sucrose properties and applications. 1st ed. Bishopbriggs: Blackie Academic and Professional. p 11-30.

Reguieg C, Yousfi N and Sekkal-Rahal M. Spectrochim (2007). Normal coordinates analyses of β-D-allose and α-D-talose in the crystalline state Acta A, 67, 966–975.

Reynhardt EC. 1990. An NMR, DSC and X-ray investigation of the disaccharides sucrose, maltose and lactose, Molecular Physics: An International Journal at the Interface Between Chemistry and Physics, 69:6, 1083-1097.

Richards GN, Shafizadeh F (1978). Mechanism of thermal degradation of sucrose: Apreliminary study. Aust. J. Chem. 31, 1825-1832.

Richmond, G. L. Molecular Bonding and Interactions at Aqueous Surfaces as Probed by Vibrational Sum Frequency Spectroscopy. Chem. ReV. 2002, 102, 2693-2724.

Scherer, J. R., The vibrational spectroscopy of water. In Advances in Infrared and Raman Spectroscopy, Clark, R. J. H., Hester, R. E., Eds.; Heyden: Philadelphia, PA, 1978; Vol. 5, Chapter 3.

Sekkal M, Legrand P, Vergoten G and Dauchez M. Spectrochim. A vibrational molecular force field of model compounds with biological interest—III. Harmonic dynamics of α- and β-D-galactose in the crystalline state. Acta A, 48, 959–973 (1992).

Sekkal N, Taleb-Mokhtari IN, Sekkal-Rahal M, Bleckmann P and Vergoten G. Harmonic dynamics of α- and β-methyl-D-galactopyranoside in the crystalline state. In: Spectrochimica Acta. A: Molecular and Biomolecular Spectroscopy 59 (2003), S. 2883 – 2896.

Seo Takahashi H, Kuzume A, Ito M (2009) Water at interfaces. J Environ Sci 21:S7–S12. doi: 10.1016/S1001-0742(09)60025-5.

Shallenberger RS and Birch GG. 1975. Sugar chemistry. Westport, Connecticut AVI.

Shi Y (2014) Existence of the sugar-bisulfite adducts and its inhibiting effect on degradation of monosaccharide in acid system. Appl Biochem Biotechnol 172:1612–1622.

Šimkovic I, Šurina I, Vričan, M (2003). Primary reactions of sucrose thermal degradation. Journal of Analytical and Applied Pyrolysis, 70 (2), pp. 493-504.

Susi H, Scheker JR (1969) The normal vibrations of formic acid and methyl formate. Spectrochimica Acta Part A: Molecular Spectroscopy Spectrochim 25: 1243-1263.

Szostak MM, Piela K, Hołderna -Natkaniec K, et al (2014) Optical nonlinearity and electric conductivity origin study on sucrose crystal by using IR, Raman, INS, NMR, and EPR spectroscopies. Carbohydr Res 395:29–37. doi: 10.1016/j.carres.2014.05.015.

Taleb-Mokhtari IN, Sekkal-Rahal M, Vergoten G (2003) Modified UBFF calculations of the α-L-fucopyranose molecule in the crystalline state. Spectrochimica Acta Part A: Molecular and Biomolecular Spectroscopy 59:607-616.

Te JA, Tan ML, Ichiye T. Solvation of glucose, trehalose, and sucrose by the soft-sticky dipole–quadrupole–octupole water model. Chem. Phys. Lett. (2010) 491, 218–223.

Thiel PA, Madey TE. The interaction of water with solid-surfaces: Fundamental aspects. Surf. Sci. Rep. 1987, 7, 211-385.

Thomas R. 2000. Determination of water contents of granite melt inclusions by confocal laser Raman microprobe spectroscopy. American Mineralogist, 85, 868–872.

Tul'chinsky VM, Zurabyan SE, Asankoshoev KA, Kogan GA, Khorlin YY (1976). Study of the infrared spectra of oligosaccharides in the region 1,000-40 cm^{-1}. Carbohydrate Research 51: 1-8.

7.8 Figures and Tables
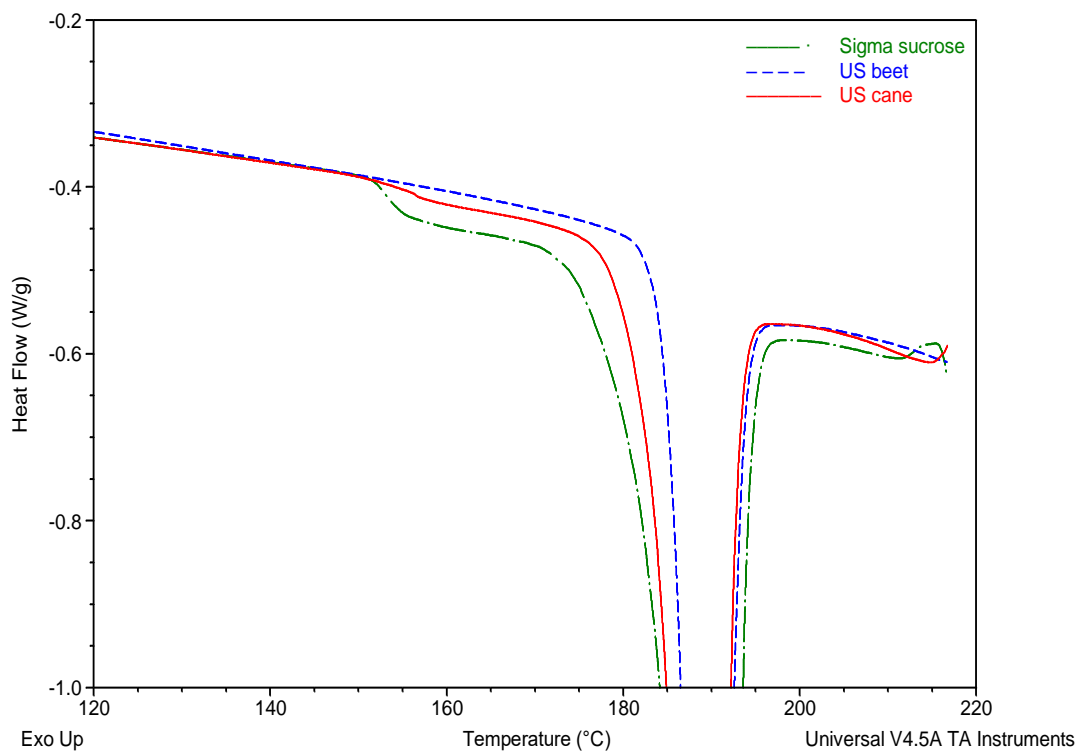
Figure 7.1 DSC thermograms of analytical grade Sigma cane, US beet, and US cane samples at 10°C/min.
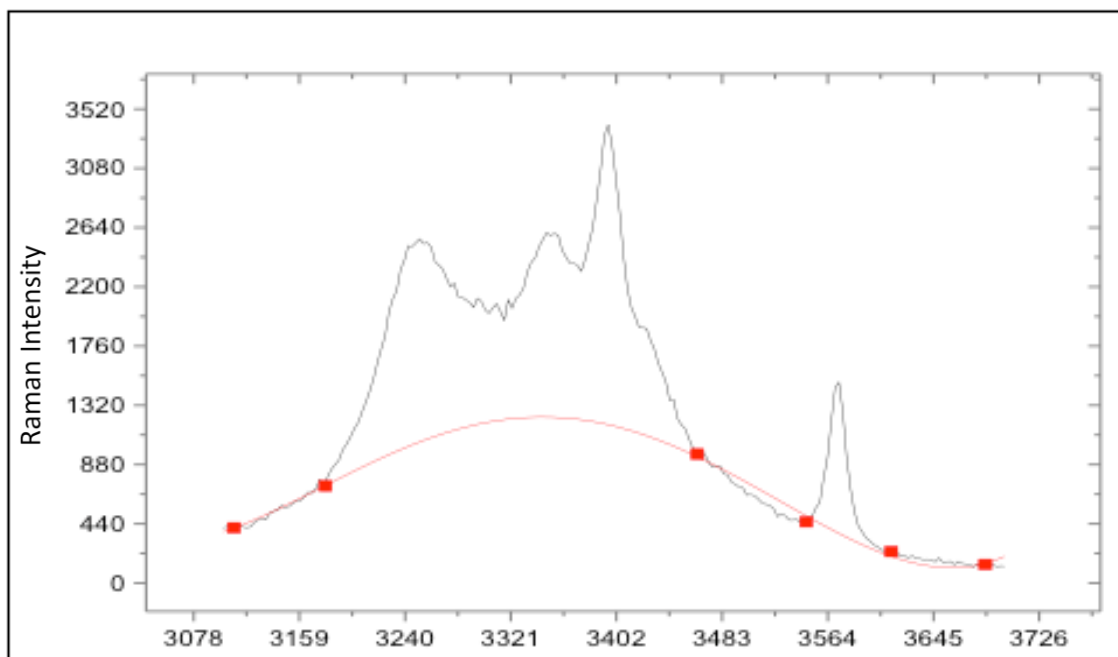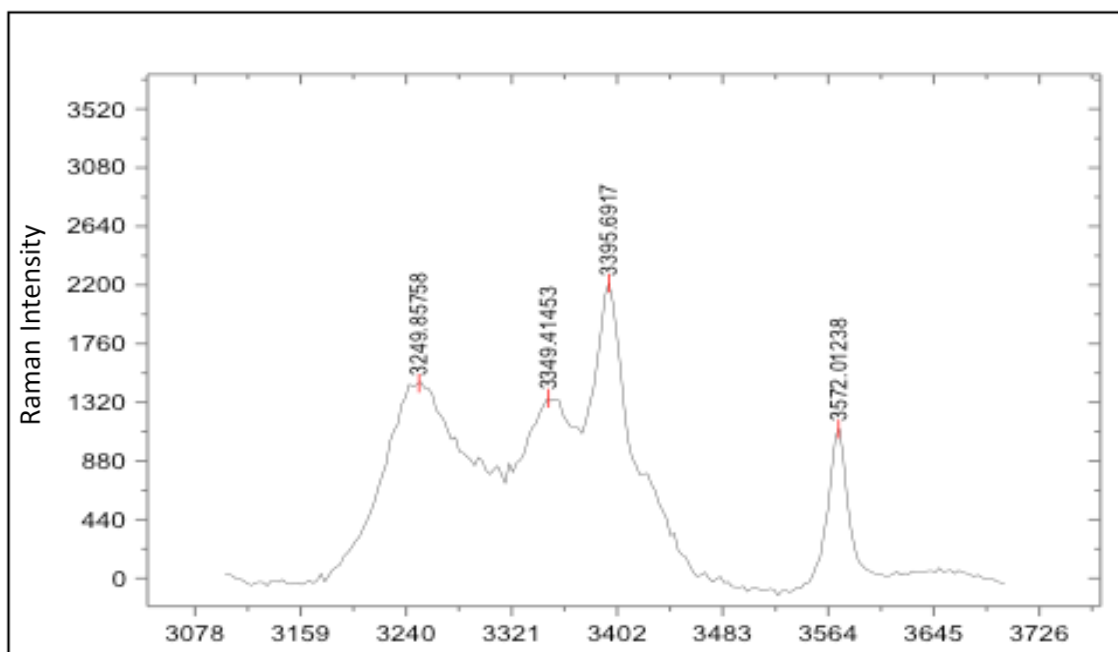
Figure 7.2 Analytical grade Sigma cane sucrose before (top) and after (bottom) baseline correction and peak identification at 25°C in the 3100-3700 cm^{-1} range.
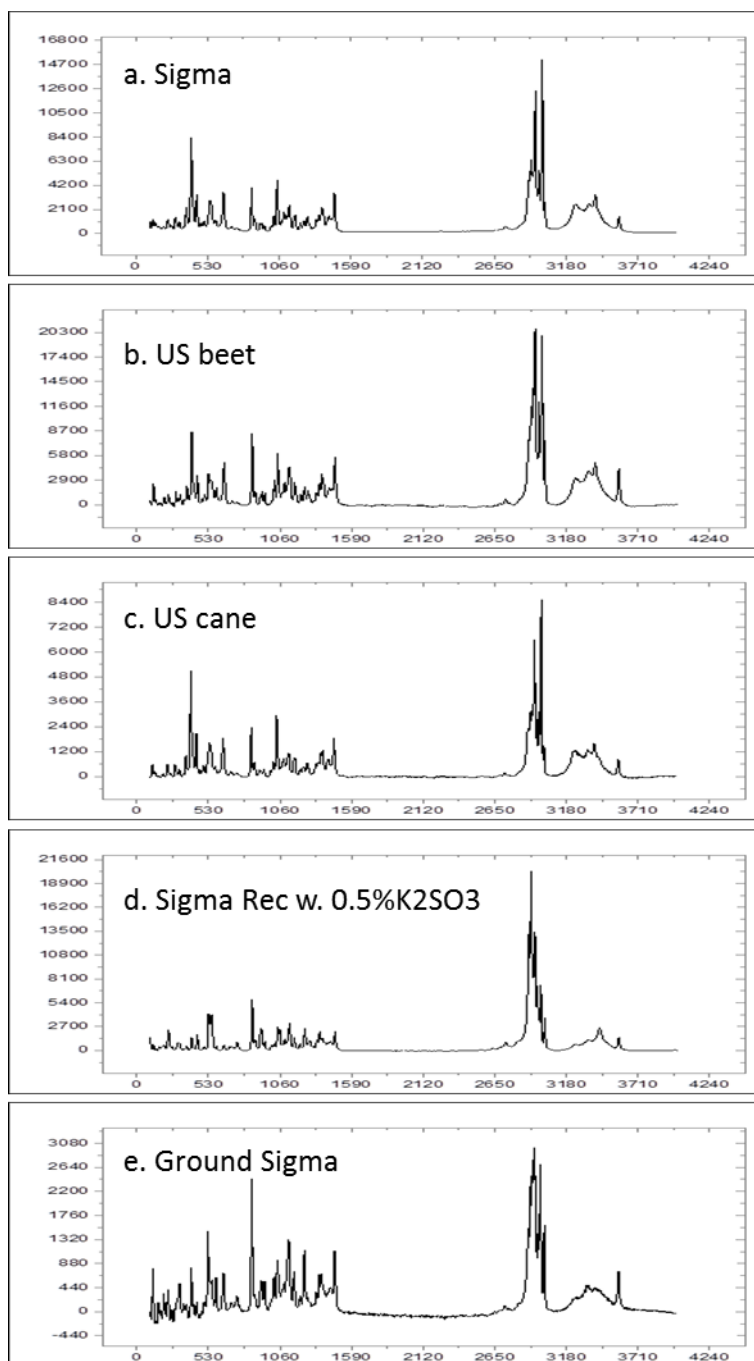
Figure 7.3 Raman Spectra of the crystalline sucrose in the 100 – 4000 cm-1 range at 25°C. From top to the bottom are "as is": a. analytical grade Sigma cane; b. US beet; c. US cane; d. Sigma cane recrystallized with 0.5% K_2SO_3; e. Ground Sigma cane.
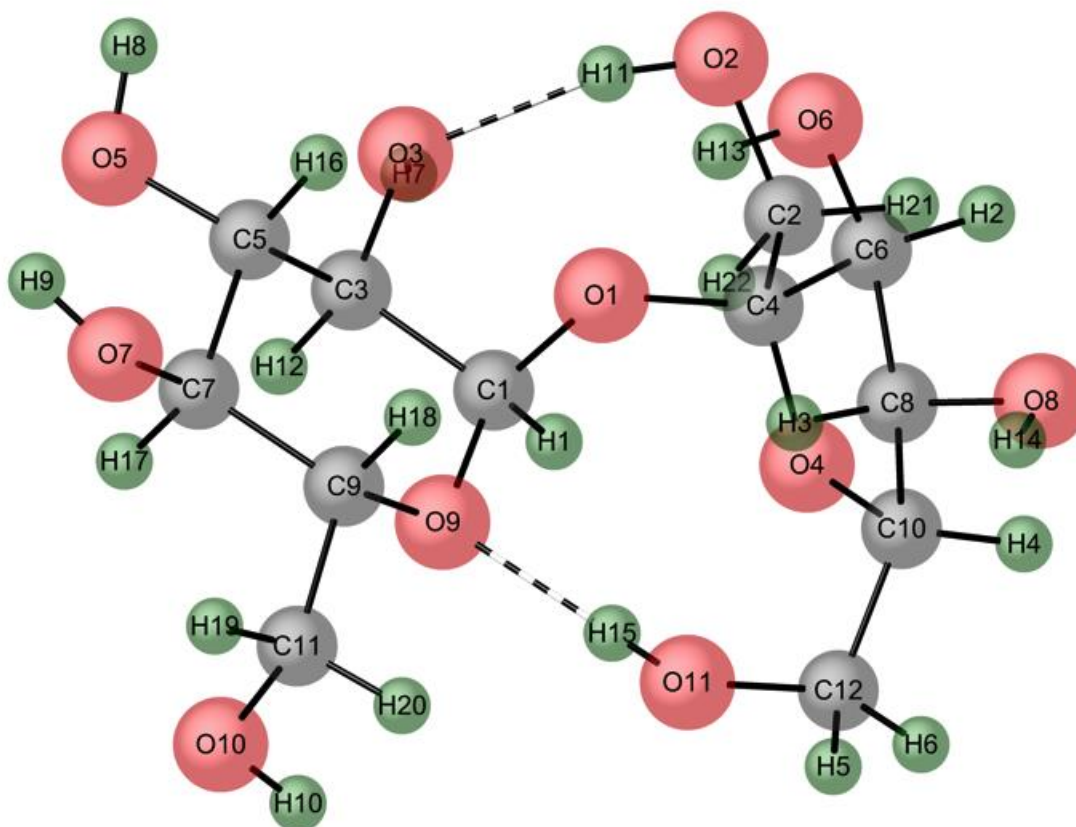
Figure 7.4 Molecular structure of sucrose with the labeled atoms according to IUCr A09963 from Cambridge Crystal Data Center.
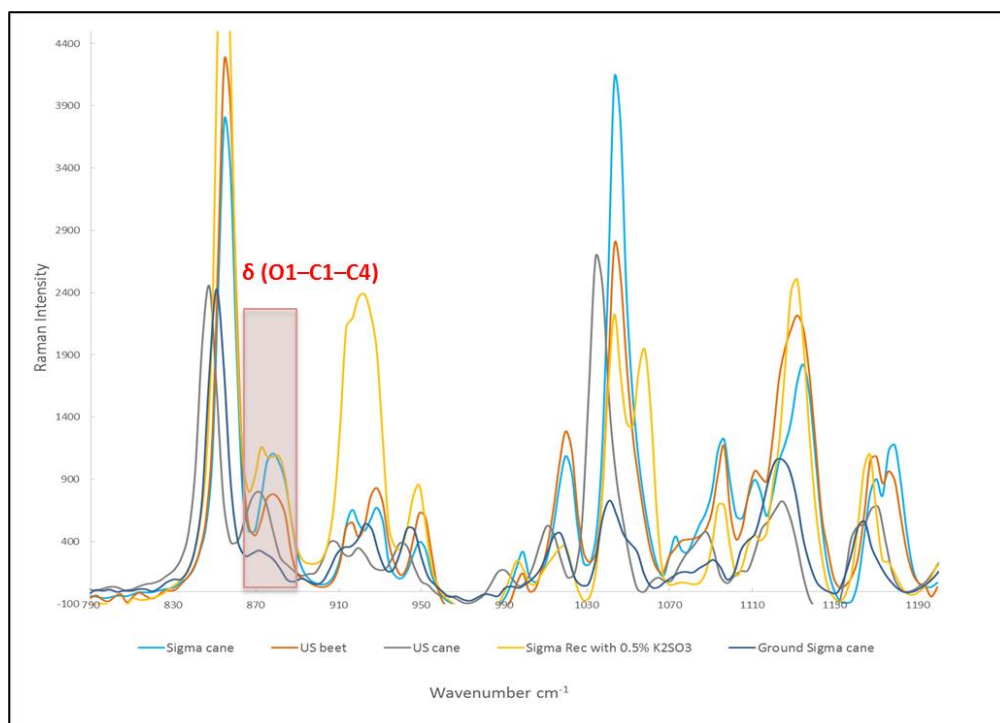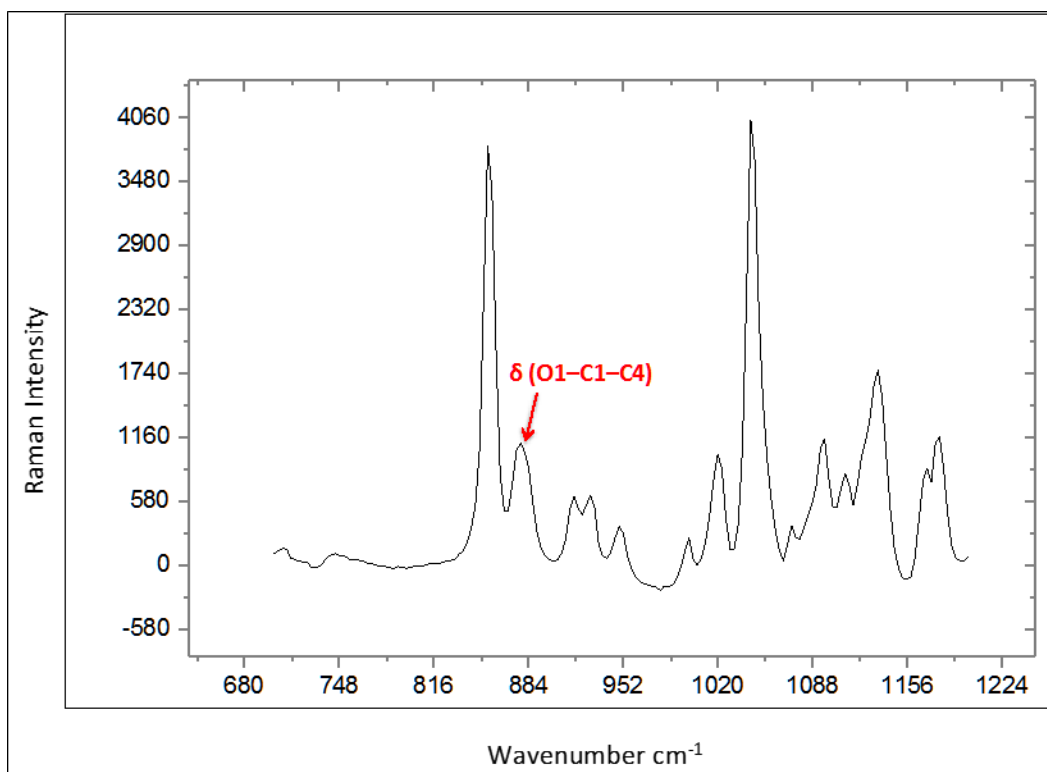
Figure 7.5 Example Raman spectrum of glycosidic bond deformation δ(O1–C1–C4) assigned for analytical grade Sigma cane sucrose at 25°C using OriginPro 9.0 (top) and Raman spectra of all five sucrose samples plotted together at 25°C in Excel (bottom).
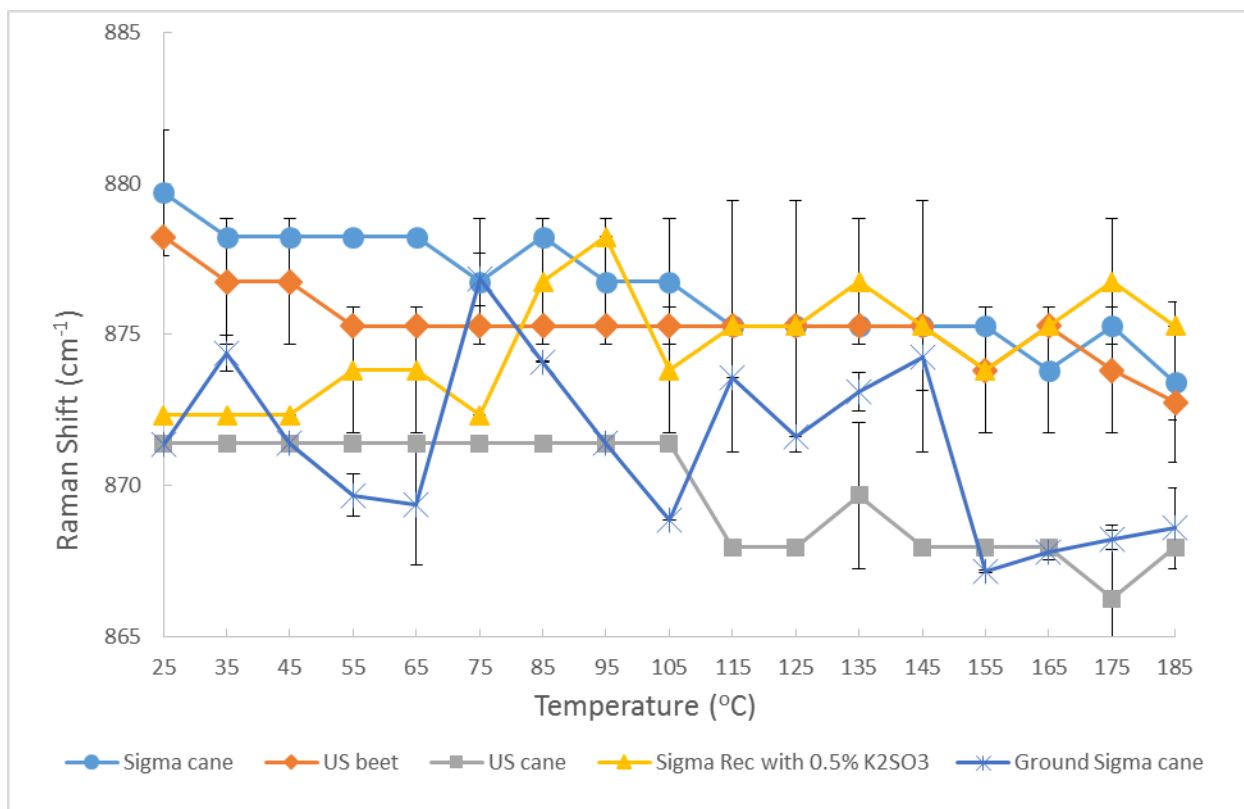
Figure 7.6 The Raman shift of glycosidic bond deformation δ(O1–C1–C4) as a function of temperature in analytical grade Sigma cane, US beet, US cane, Sigma cane recrystallized with 0.5% K_2SO_3, and ground Sigma cane sucrose samples.
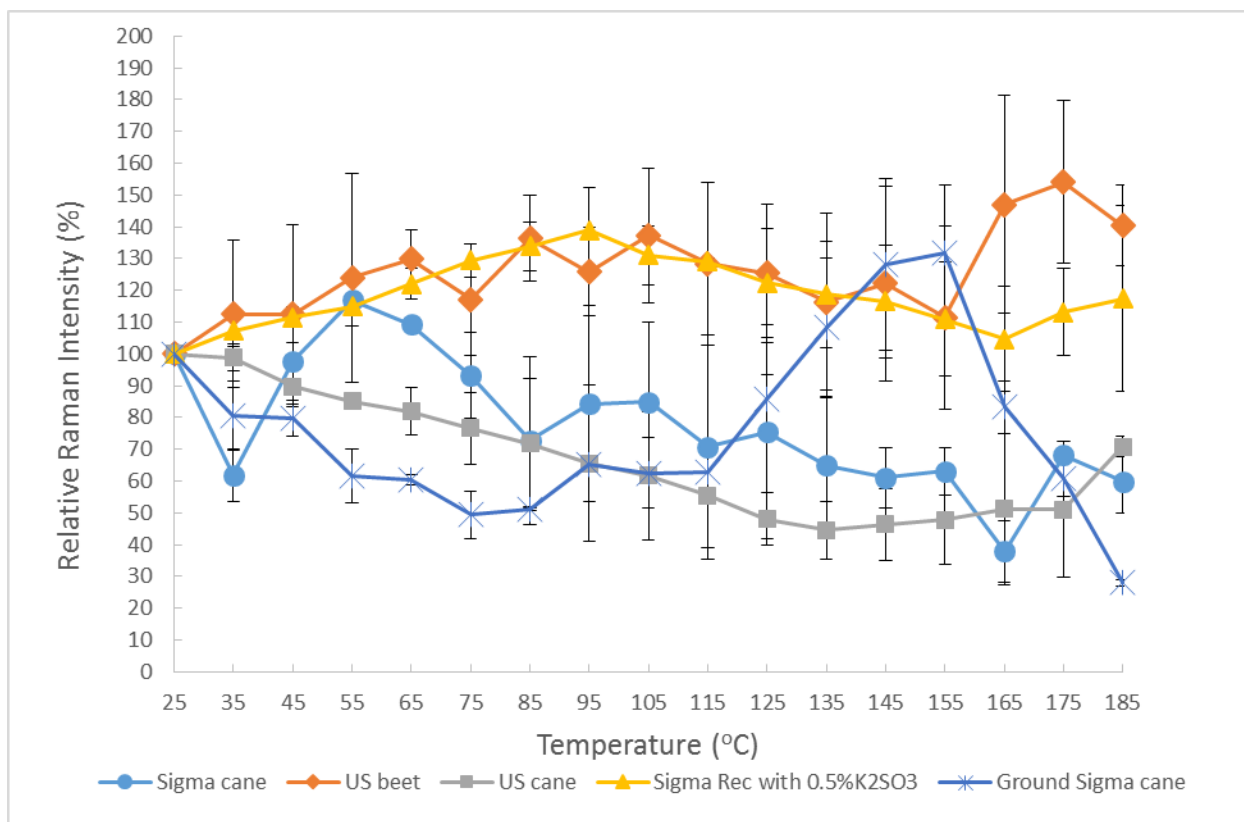
Figure 7.7 The relative Raman intensity of glycosidic bond deformation δ(O1–C1–C4) as a function of temperature in analytical grade Sigma cane, US beet, US cane, Sigma cane recrystallized with 0.5% K_2SO_3, and ground Sigma cane sucrose samples.
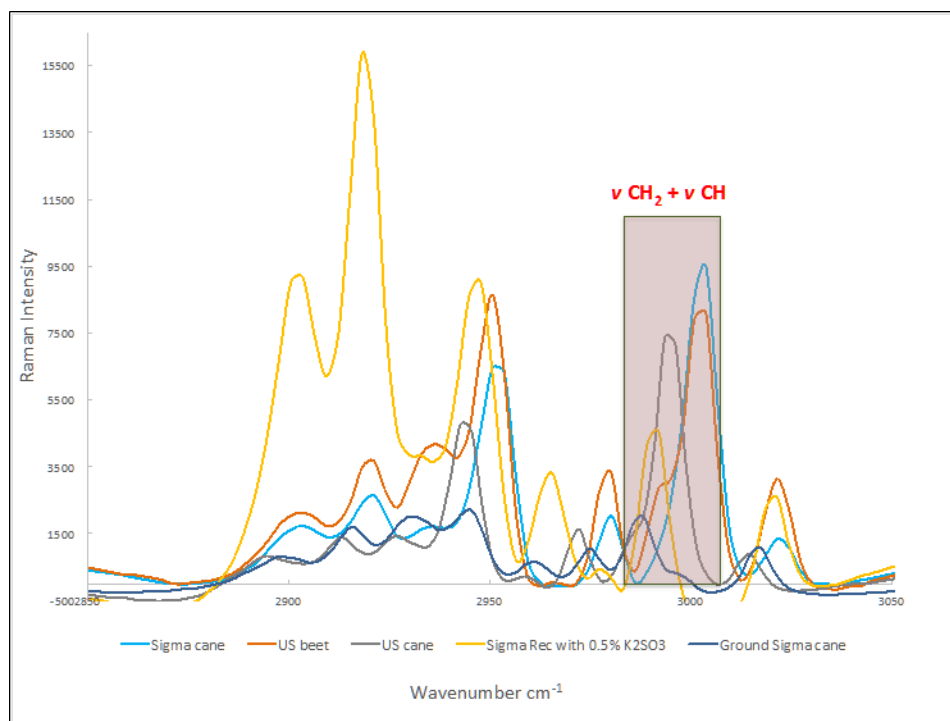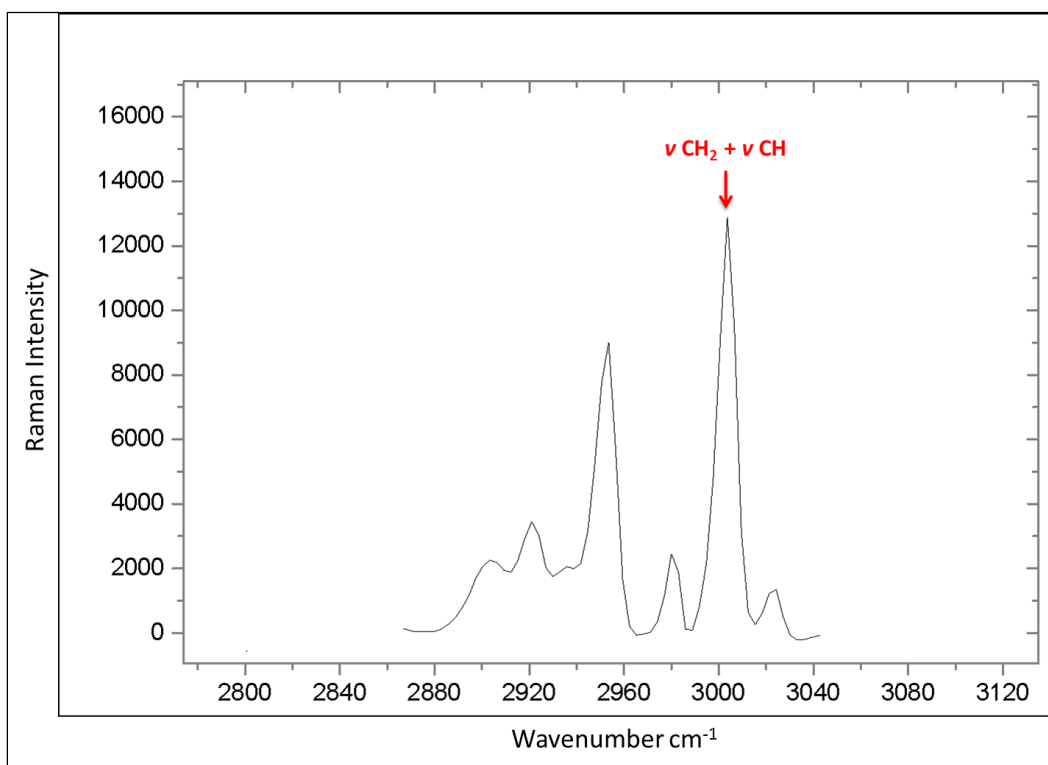
Figure 7.8 Example Raman spectrum of –CH_2 and –CH stretching vibration assigned for analytical grade Sigma cane sucrose at 25°C (~3000 cm^{-1}) using OriginPro 9.0 (top) and Raman spectra of all five sucrose samples plotted together at 25°C using Excel (bottom).
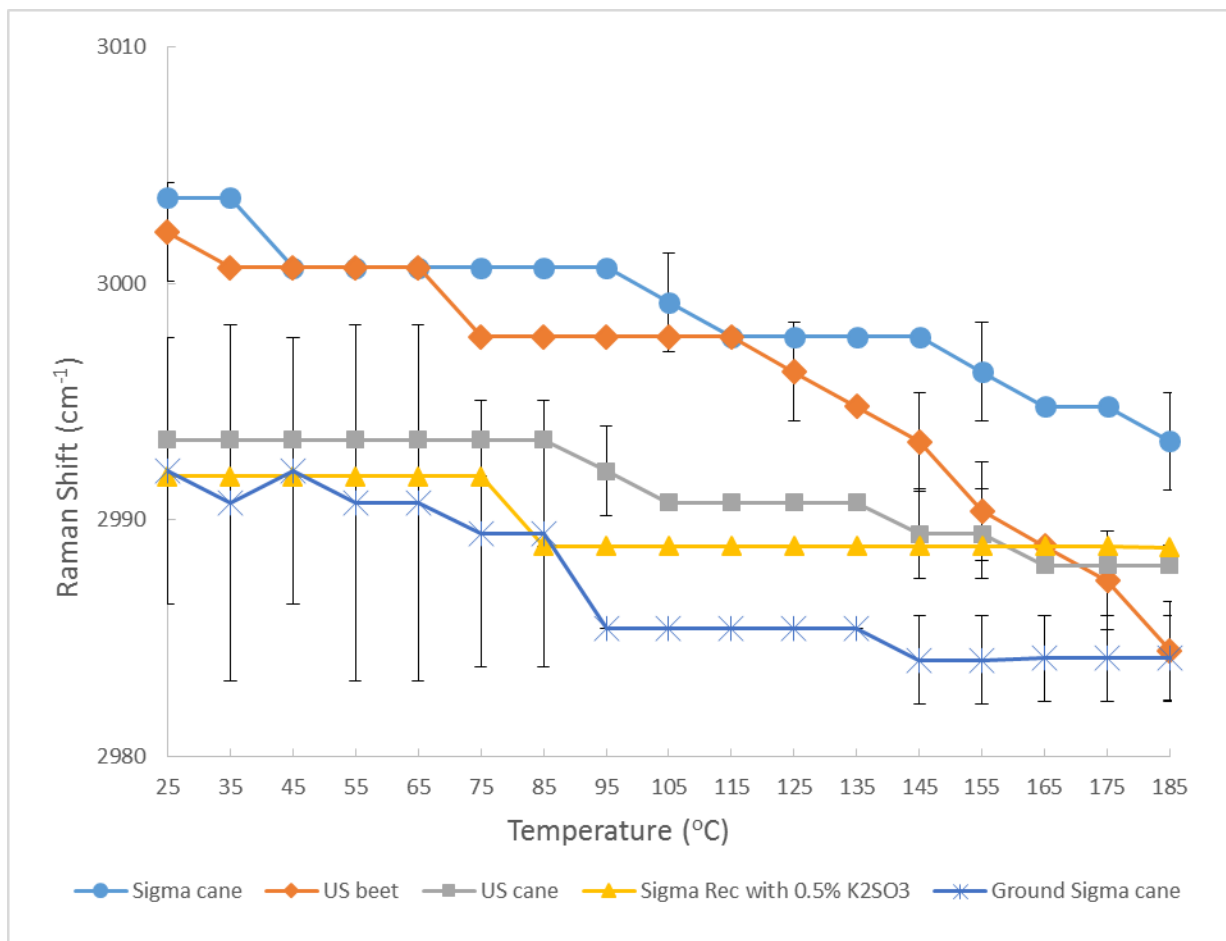
Figure 7.9 The Raman shift of –CH$_2$ and –CH stretching vibration (vCH$_2$ + vCH) mode as a function of temperature in analytical grade Sigma cane, US beet, US cane, Sigma cane recrystallized with 0.5% K$_2$SO$_3$, and ground Sigma cane sucrose samples.
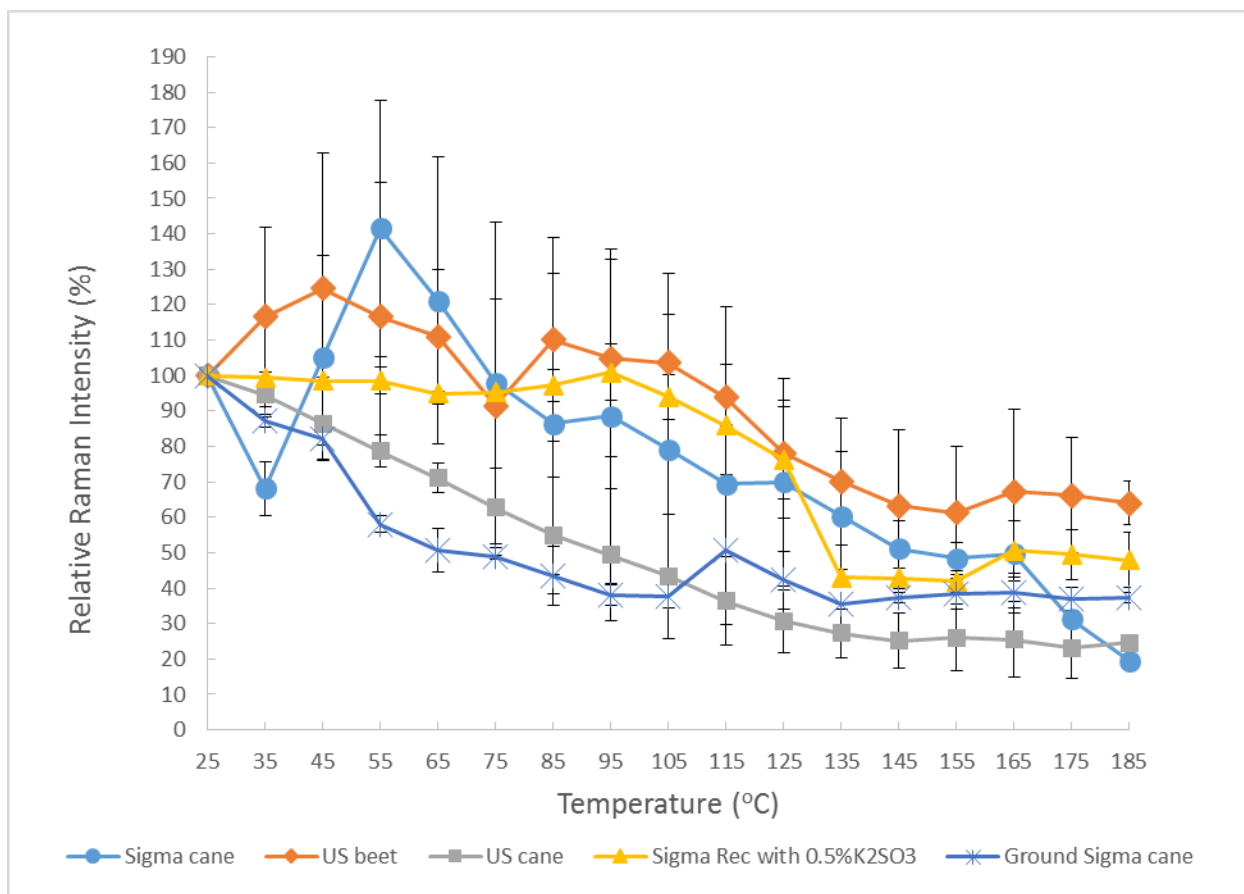
Figure 7.10 The relative Raman intensity of –CH$_2$ and –CH stretching vibration (vCH$_2$ + vCH) mode as a function of temperature in analytical grade Sigma cane, US beet, US cane, Sigma cane recrystallized with 0.5% K$_2$SO$_3$, and ground Sigma cane sucrose samples.
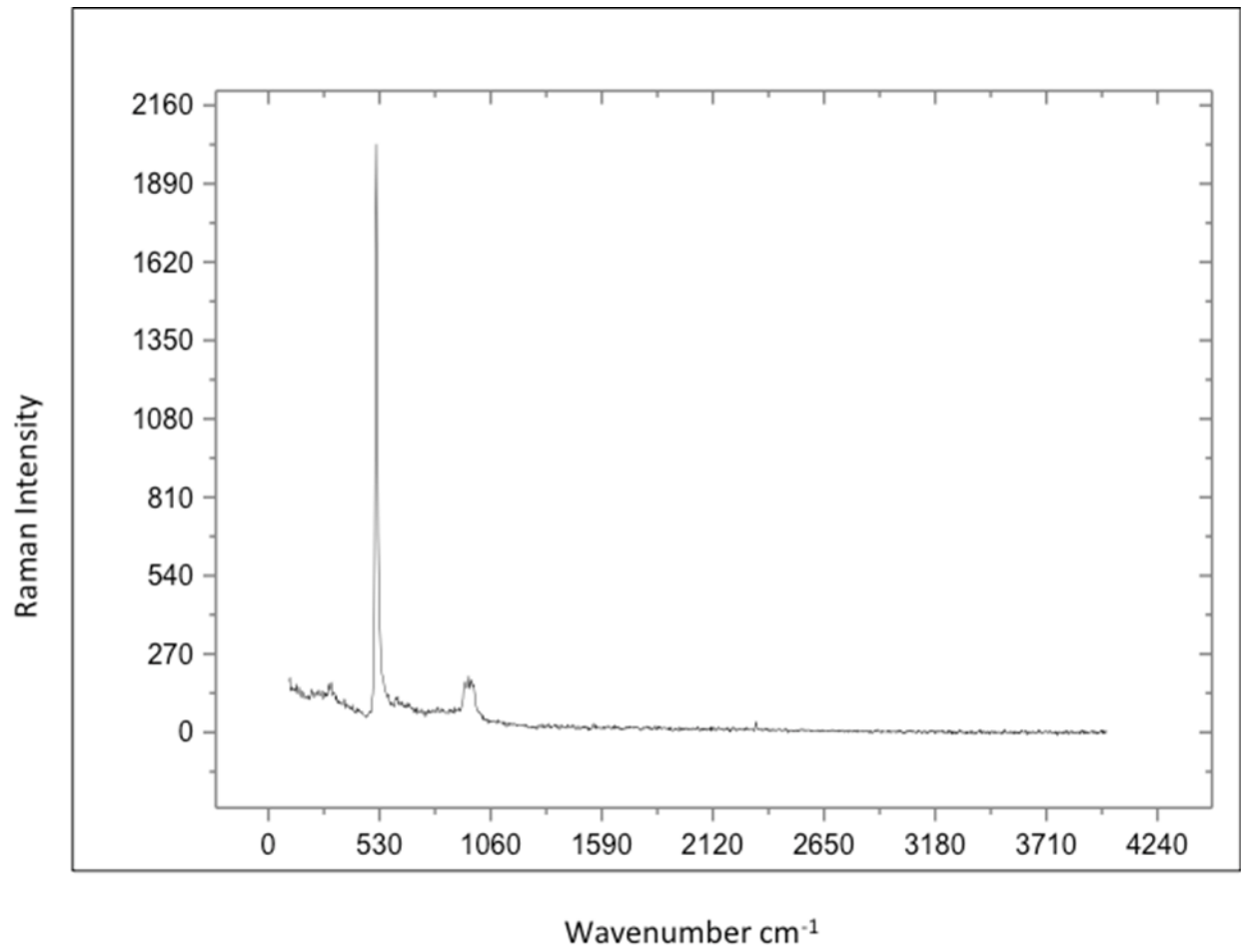
Figure 7.11 Raman Spectrum of Silicon wafer in the 100 – 4000 cm^{-1} range at 25°C.
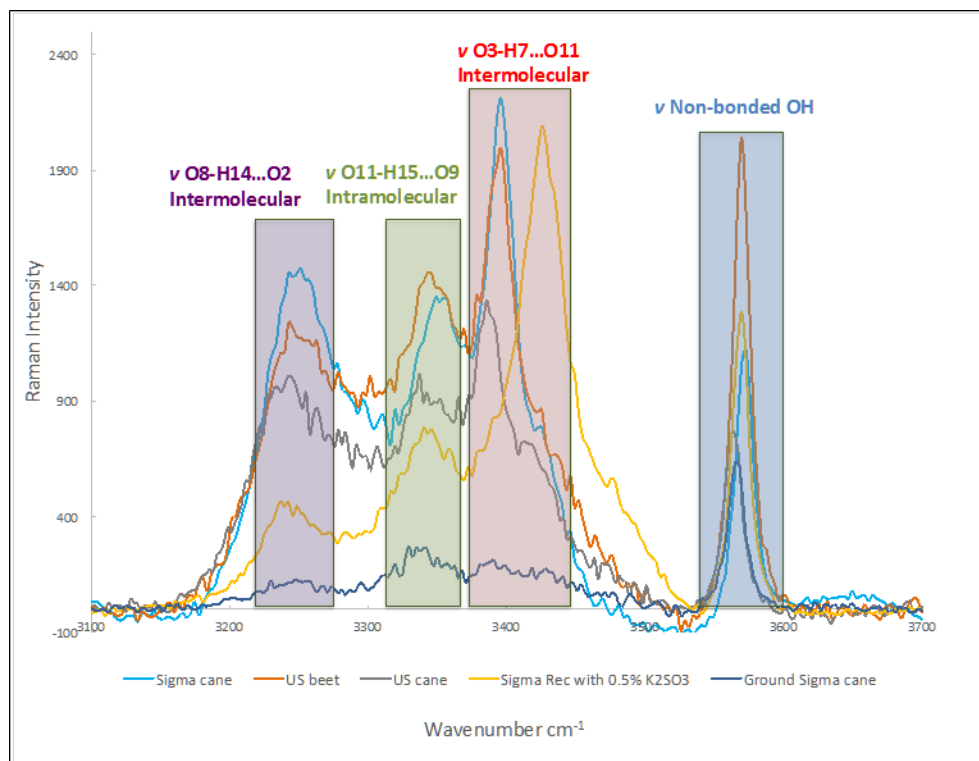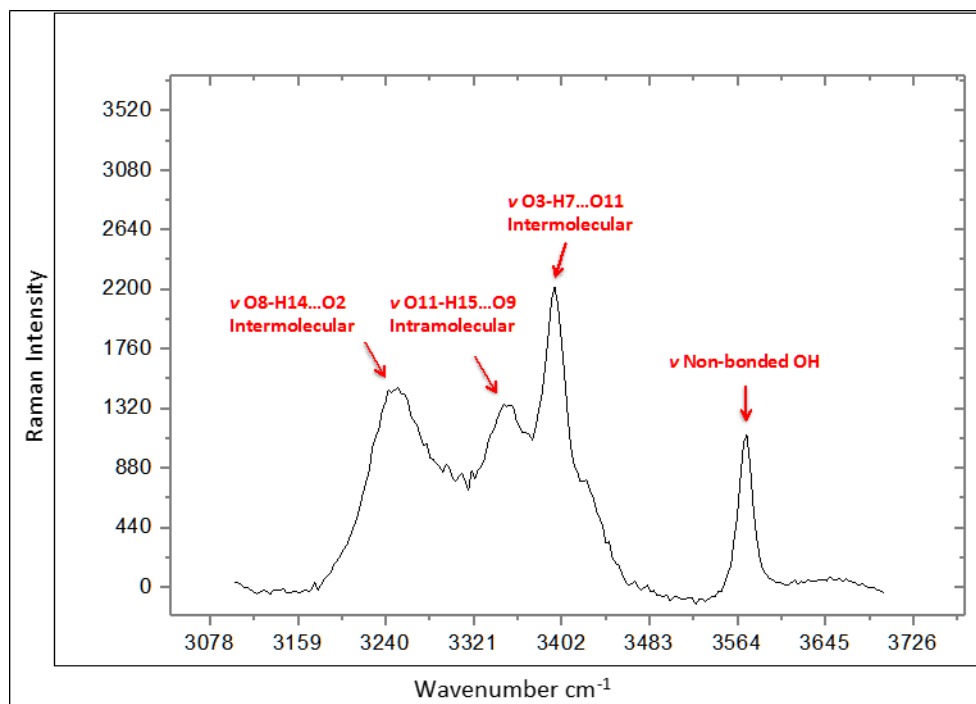
Figure 7.12 Example Raman spectrum of OH groups stretching modes assigned for analytical grade Sigma cane sucrose at 25°C (3100-3500 cm^{-1}) using OriginPro 9.0 (top) and Raman spectra of all five sucrose samples plotted together at 25°C in Excel (bottom).
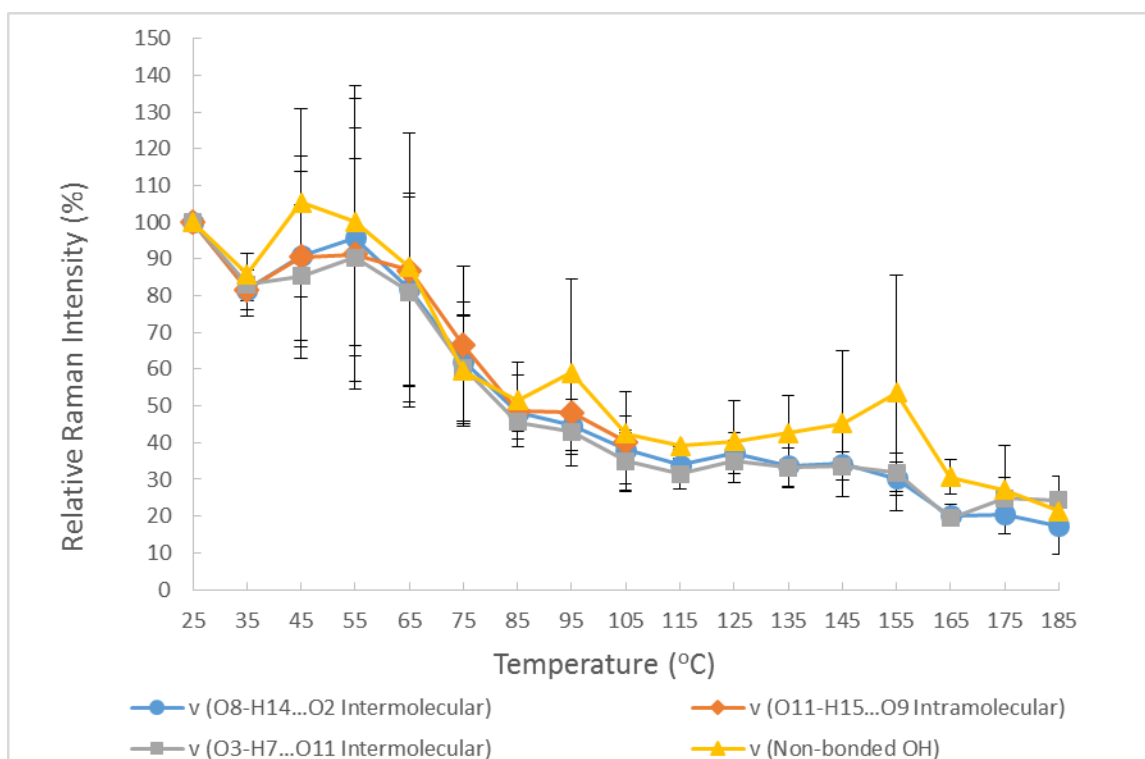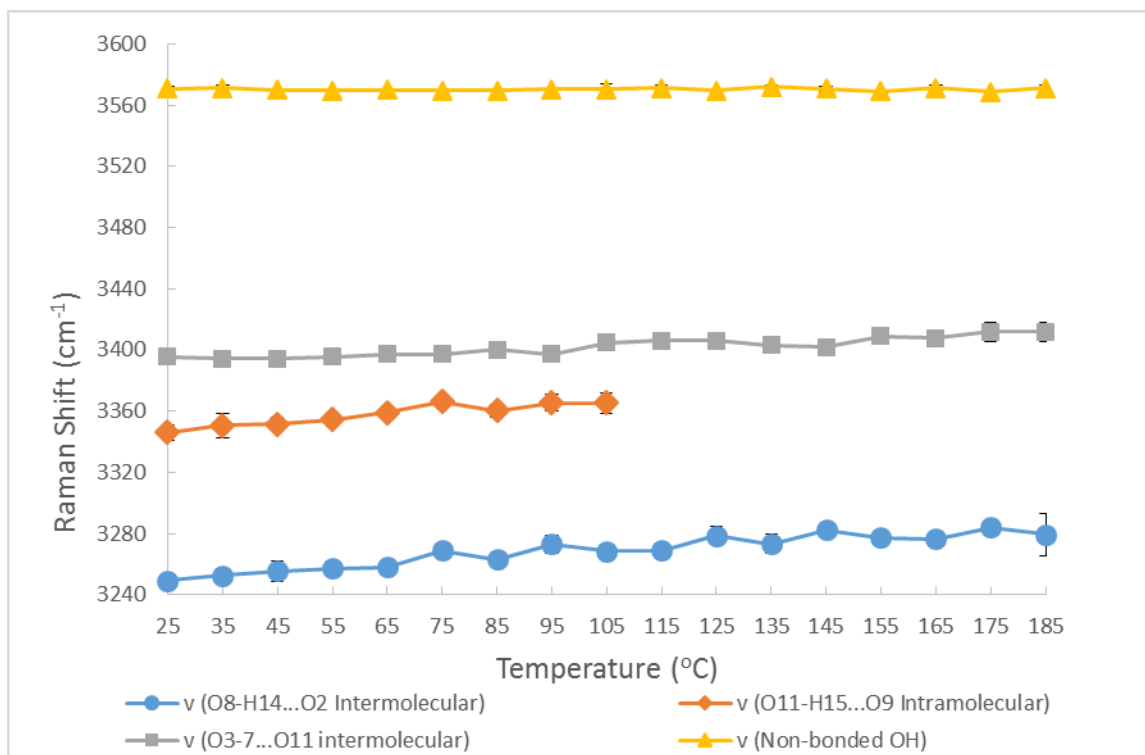
Figure 7.13 Raman shift (top) and relative Raman intensity (bottom) of OH groups stretching modes as a function of temperature in analytical grade Sigma cane sucrose.
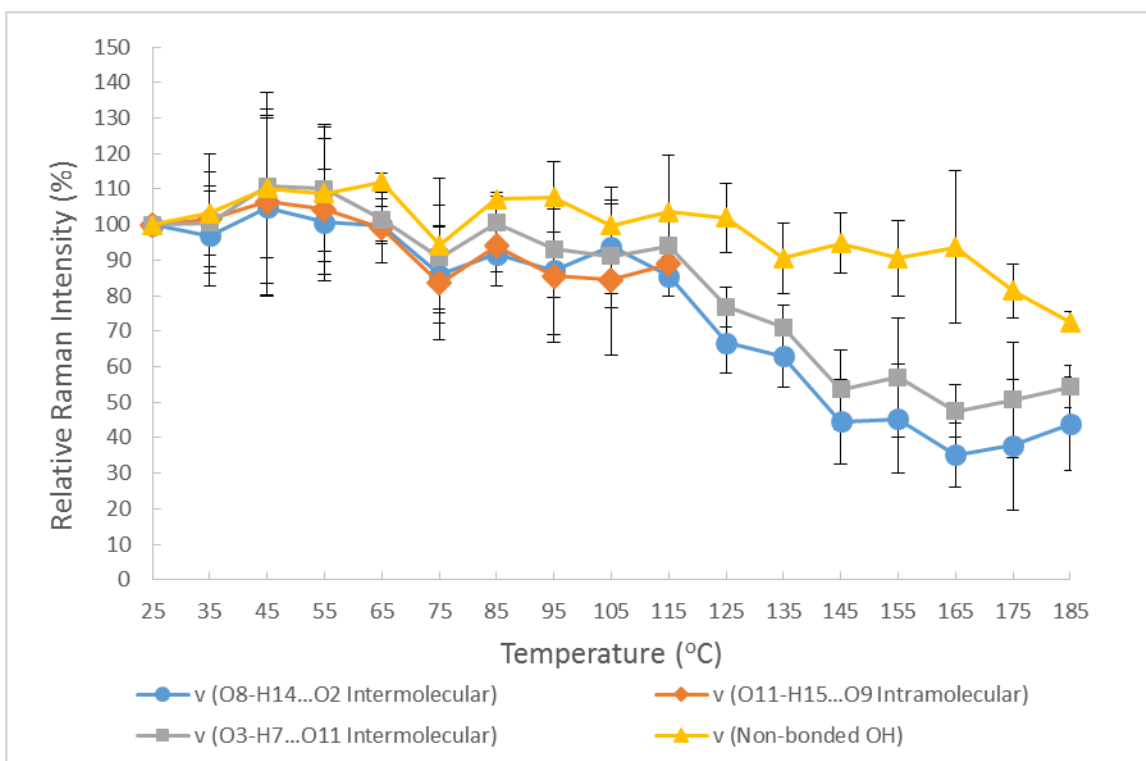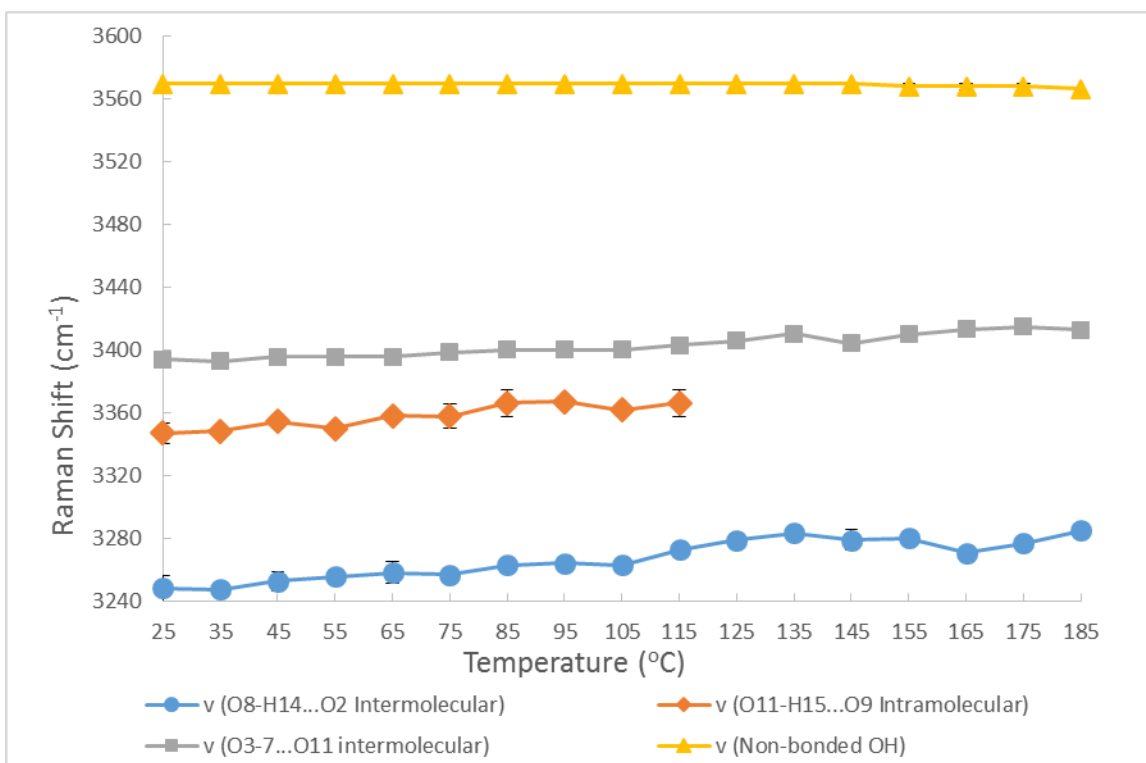
Figure 7.14 Raman shift (top) and relative Raman intensity (bottom) of OH groups stretching modes as a function of temperature in US beet sucrose.
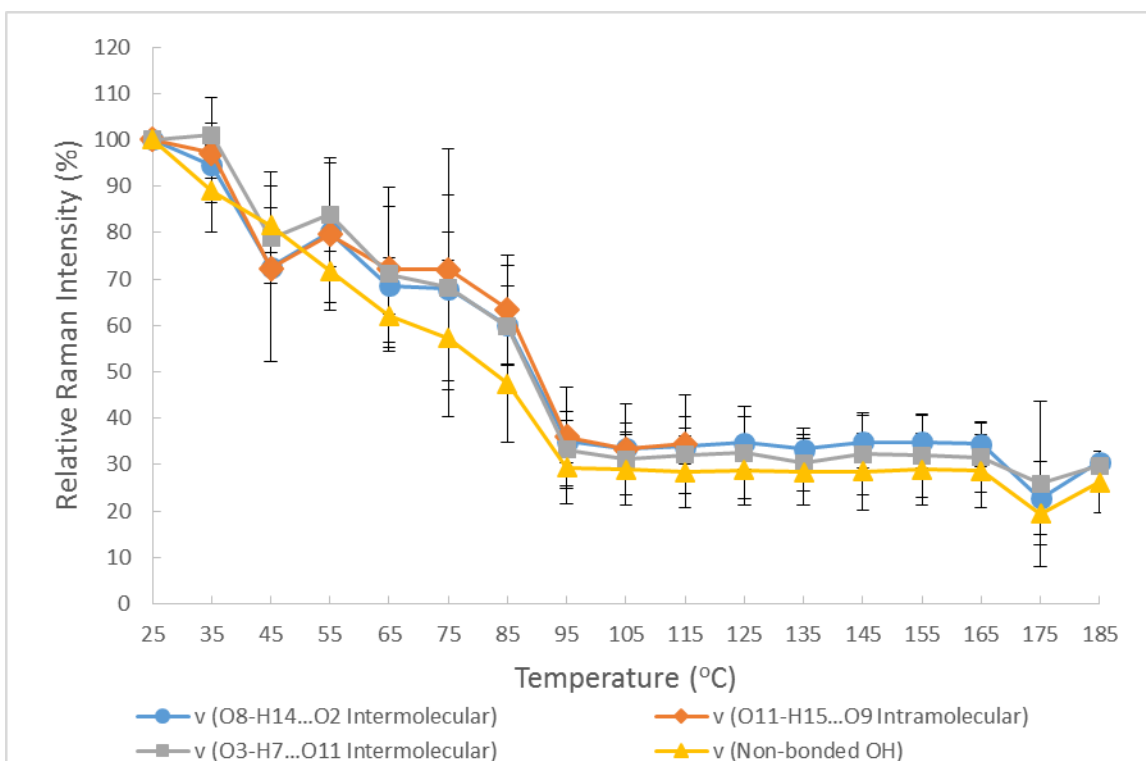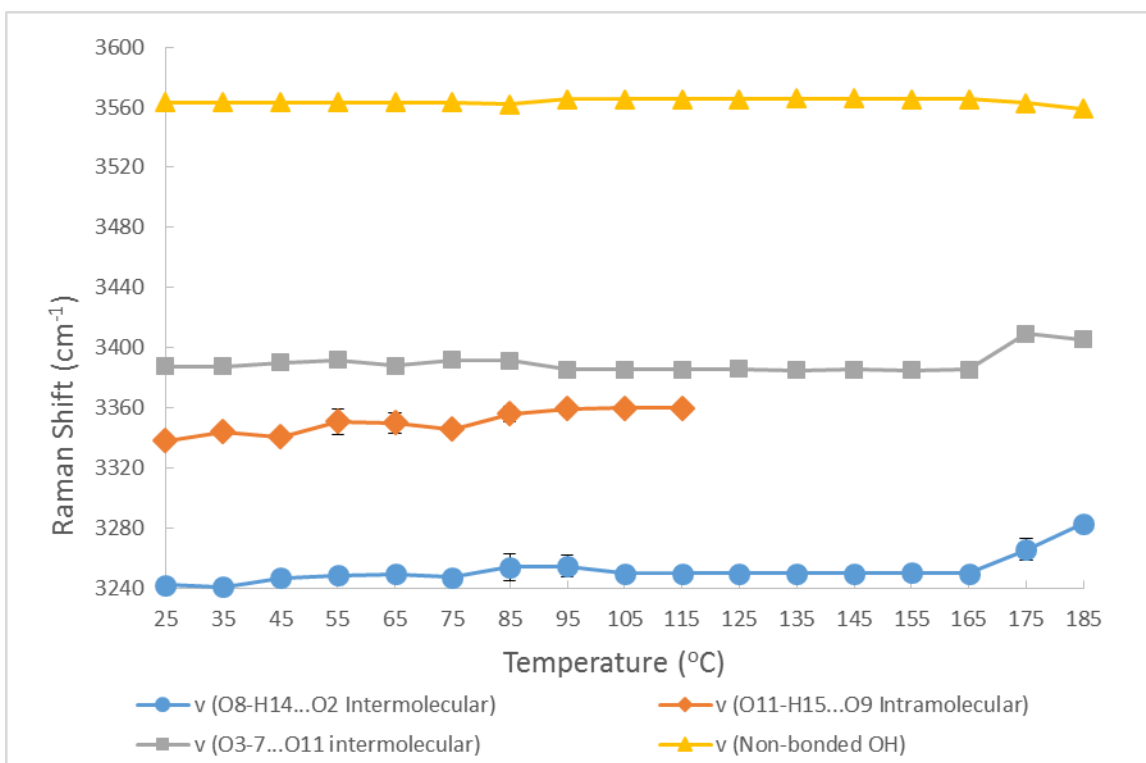
Figure 7.15 Raman shift (top) and relative Raman intensity (bottom) of OH groups stretching modes as a function of temperature in US cane sucrose.
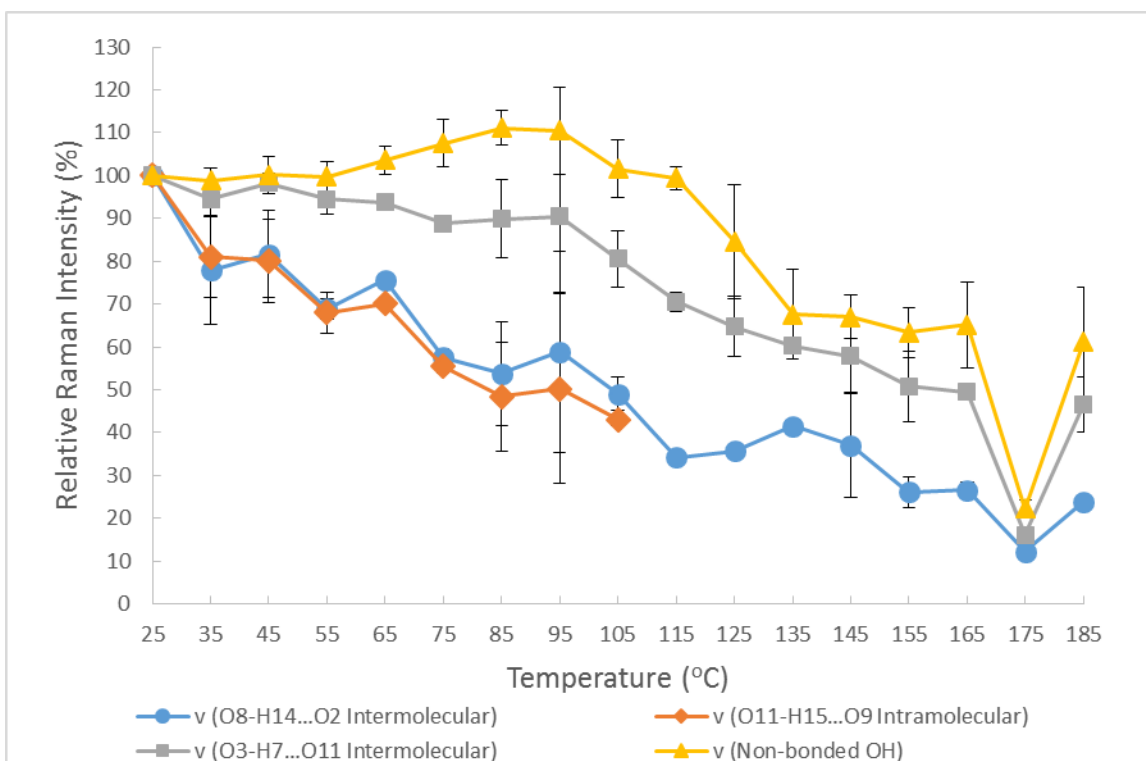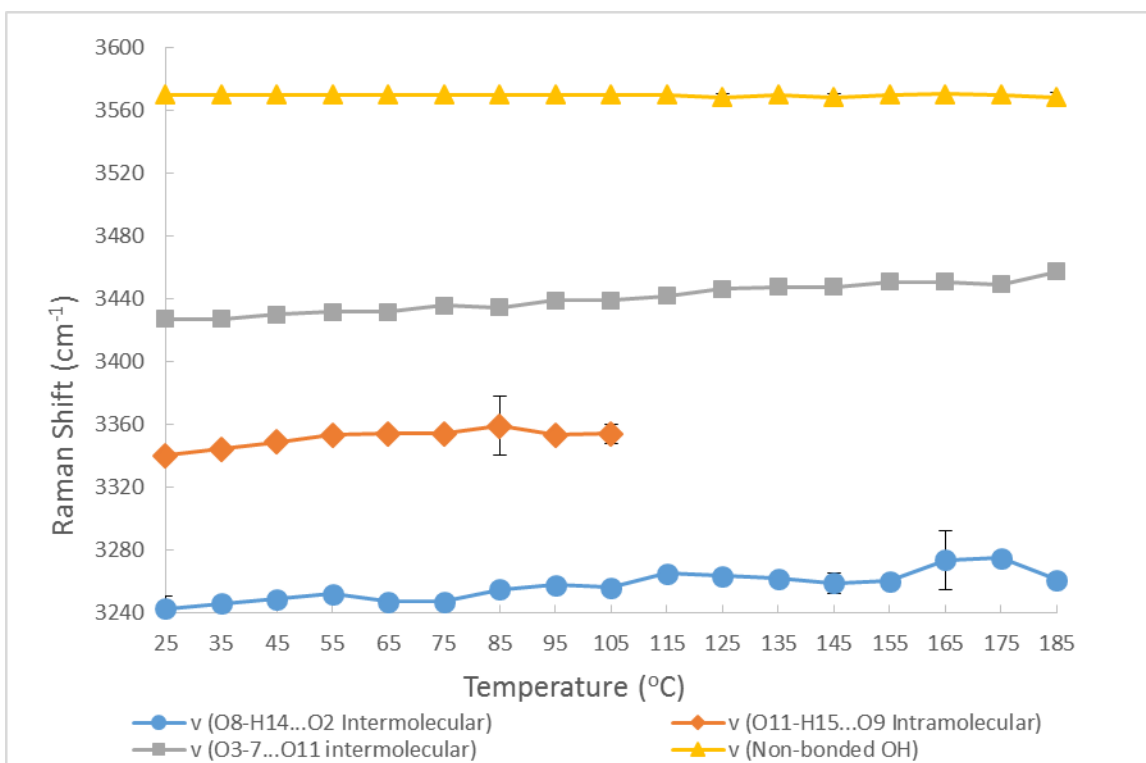
Figure 7.16 Raman shift (top) and relative Raman intensity (bottom) of OH groups stretching modes as a function of temperature in recrystallized Sigma cane sucrose with 0.5% K$_2$SO$_3$.
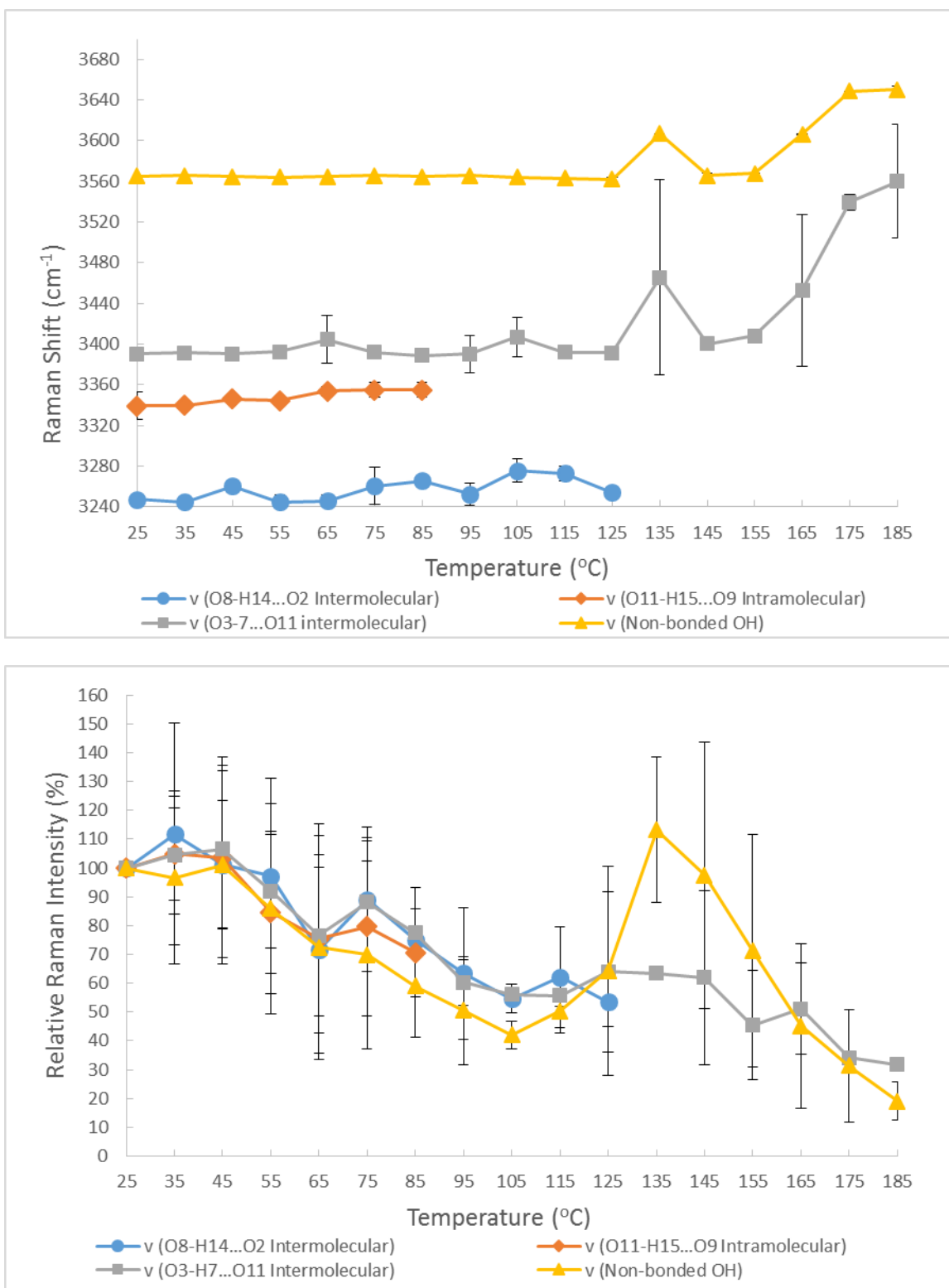
Figure 7.17 Raman shift (top) and relative Raman intensity (bottom) of OH groups stretching modes as a function of temperature in ground Sigma cane sucrose.

Chapter 8: Conclusions and future research recommendations

8.1 Conclusions

Based on the comparison of DSC and HPLC measurements for the sucrose samples studied herein, a wide variation in thermal stability behavior between and within sucrose sources was observed (Chapters 2 and 3). In general, beet and cane sucrose sources exhibit substantially different thermal behaviors, in terms of the number of endothermic DSC peaks (in general, one peak for beet samples and two peaks for cane samples), the extent of heating rate dependency (in general, cane > beet), and the degree of thermal stability (beet > cane).

The underlying cause(s) of these thermal behavior differences required further investigation, leading to the specific objective of investigating the influence of the composition and chemistry of the sucrose crystal on its thermal behavior using a variety of beet and cane sucrose sources (Chapters 5 and 6). Several analytical methods and techniques were applied to approach this research objective, including moisture content analysis, pH, conductivity ash content, total sulfite content, powder X-ray diffraction (PXRD), single crystal X-ray diffraction (SXRD), X-ray Micro-Computed Tomography (Micro-CT), Differential Scanning Calorimetry (DSC), High Performance Liquid Chromatography (HPLC), and Confocal Raman imaging and spectroscopy.

Our results suggest that the composition and chemistry of the mother liquor occlusions, formed within the sucrose crystal during the crystallization process, are responsible for the thermal behavior of the various sucrose sources studied herein. Based on these findings, by manipulating the composition and chemistry of the mother liquor occlusions, using our enhanced laboratory-recystallization method, we can manipulate the thermal behavior of the

sucrose, so that the crystalline sucrose exhibits only the small endothermic DSC peak

(laboratory-recrystallized Sigma cane in HPLC water) or only the large endothermic DSC peak

(laboratory-recrystallized Sigma cane in HPLC water plus 0.5% K_2SO_3).

Regarding the specific sucrose sources studied herein we observed the following thermal

behavior. In the case of analytical grade and white refined cane sucrose sources, the presence

of the small endothermic peak in the DSC thermogram is associated with the onset of thermal

decomposition of sucrose within mother liquor occlusions, initiated by hydrolysis and mediated

by the composition and chemistry of the sucrose crystal. These sucrose sources have low

conductivity ash values and their sulfite content was below the detection limit. In the case of

beet and Chinese cane sucrose sources, the sulfite contained in the mother liquor occlusions,

which was added during the sulfitization processing step, is responsible for the absence of the

small endothermic DSC peak. The inhibitory effect of the sulfite against thermal decomposition

in these sugar sources results in greater thermal stability compared to the analytical and white

refined cane sucrose sources. In the case of Sugar in the Raw, the high conductively ash, as well

as high pH value, are thought to be responsible for the absence of the small endothermic DSC

peak, again inhibiting the onset of thermal decomposition. The laboratory-recrystallized

analytical grade cane Sigma sucrose investigation further proved that the appearance of the

small endothermic DSC peak in Sigma cane sample was inhibited by sulfite contained in the

mother liquor occlusions.

Last but not least, this research has made a substantial impact on the thermal behavior

investigation of crystalline sucrose at the molecular level, since we successfully explored three

vibrational modes within and between each crystalline sucrose sources as a function of temperature using confocal Raman imaging and spectroscopy (Chapter 7).

Overall, this research revealed that the sucrose crystal composition and chemistry directly influence sucrose thermal behavior, which in turn, is critical to the thermal processing and reactions of sucrose in sucrose containing foods, such as baking and caramelization.

8.2 Future research recommendations

Sucrose is produced worldwide and is one of the most important carbohydrates used in food (Clemens and others 2016). Though the research herein has significantly contributed to solving many of the thermal behavior issue associated with sucrose (Chapter 4, Table 4.1), more areas of research remain. Our recommendations for future research include, but are not limited to: 1) investigate the differences in hydrolysis between beet and cane sugars in solutions, 2) determine the detailed thermal stability mechanism of action of sulfite, as well as high mineral content and pH, 3) measure the specific mineral profile of the sucrose sources studied herein uisng inductively coupled plasma (ICP) analysis, 4) manipulate the recrystallization conditions by altering the pH and impuritiy type in order to futher control and study the thermal behavior of sucrose, 5) investigate the caramelization kinetics and associated potent odorants of crystalline beet and cane sucrose sources, 6) develop alternative time-temperature caramelization processing conditions in order to optimize caramel color and flavor development for use in the food industry, as well as the field of molecular gastronomy (Lee and others 2011a and b and McGee 2012); 7) probe the effects of beet and cane sucrose on starch gelatinization and retragradtion processes, 8) continue to explore the chemical basis of

functionality differences between beet and cane sugar sources in a real food systems (Urbanus

2014).

8.3 References

Clemens RA, Jones JM, Kern M, Lee SY, Mayhew EJ, Slavin JL, and Zivanovic S. 2016. Functionality of sugars in foods and health. Comprehensive Reviews in Food Science and Food Safety, 15:433-470.

Lee JW, Thomas LC, Schmidt SJ. 2011a. Investigation of the heating rate dependency associated with the loss of crystalline structure in sucrose, glucose, and fructose using a thermal analysis approach (Part I). Journal of Agricultural and Food Chemistry, (59):684-701.

Lee JW, Thomas LC, Jerrell   J, Feng H, Cadwallader KR, Schmidt SJ. 2011b. Investigation of thermal decomposition as the kinetic process that causes the loss of crystalline structure in sucrose using a chemical analysis approach (Part II). Journal of Agricultural and Food Chemistry, (59):702-712.

McGee H. 2012. Caramelization: new science, new possibilities. Curious Cook Blog <http://www.curiouscook.com/site/2012/09/caramelization-new-science-new-possibilities.html> Last accessed March 19, 2016.

Urbanus, B.L, Schmidt, S.J. and Lee, S.Y. 2014. Sensory differences between product matrices made with beet and cane sugar sources.   Journal of Food Science, 79(11): S2354-2361.

Appendix A Composition of cane and beet refined white sugar (Godshall 2013)

Constituent	Cane	Beet
Pol	99.95	99.95
Color, pH 7	15-35	20-45
Absorbance ratio pH9/pH4	1.5-4.0	1.3
pH	6.2-6.7	6.5-8.0
Conductivity Ash %	0.01-0.03	0.01-0.03
Moisture %	0.01-0.02	0.01-0.02
Polysaccharides, ppm	70-200	20-50
Dextran, ppm	20-60	rarely present
Starch, ppm	30-50	0
Raffinose	0	30-50 ppm
Kestoses	30-50 ppm	0 to trace
Floccing potential	Low to none	Low to none
Causes of floc	Protein & ISP*	Saponins
SO_2, ppm	Not detected	ND in USA, low in Europe
Sediment, ppm	10-20	15-20
Turbidity, IU	2-25	1-5 (Higher outside US)
Turbidity, NTU	0-1.5	0-1.0
Glucose, %	0.005	0.001-0.003
Fructose, %	0.005	0.001-0.003
Volatile compounds odor**	Caramel, molasses	Earthy, VFA
Total plate count, CFU/10 g	<10	<10
Yeast & mold, CFU/10 g	<10	<10

Notes: * ISP is indigenous sugarcane polysaccharide, an arabinogalactan polymer, found in cane cell walls; ** Odors are rarely noted in either cane or beet white sugar;

Source: Sugar Processing Research Institute, Inc., New Orleans, Louisiana, USA

Appendix B Melting temperatures of sucrose found in the literature

Sugar type	Heating rate (°C/min)	Melting temp. (°C)		Enthalpy (J/g)	Analysis technique	References (most of samples source has not been specified)
		Tmonset	Tmpeak			
Sucrose (in old literature)			160-186			Shah and Chakradeo, 1936; Powers 1958; Shallenberger and Birch, 1975
Recrystallized sucrose in alcohol			188			Shah and Chakradeo, 1936
Sucrose [B/C/R]			184-188.4/172-190.6 /173.4-174.8			Kamoda, 1960
Sucrose	5		186		DSC	Weitz and Wunderlich, 1974
Sucrose	1	160	185	120	HP-DTA	Raemy, 1983
Sucrose (fine crystals)			186-190		DTA	Mathlouthi, 1986
Sucrose	10	192			DSC	Levine and Slade, 1988, 1989, 1991
Sucrose[1/2]	5		149.85/186.85			Reynhardt, 1990
Sucrose	5		183.5		DSC	Roos and Karel, 1990, 1991
Sucrose	5	173	190	118	DSC	Roos, 1995; Bonelli and others, 1997
Sucrose	10		188		DSC	Saleki-Gerhardt and Zografi, 1994
Sucrose[P/C]			186/175-190			Schiweck and Clark, 1994
Sucrose	15		188		DSC	Eggleston et al, 1996
Sucrose	10		190		DSC	Vanhal and Blond, 1999

Sucrose	10	176	183	135	DSC	Gloria and Sievert, 2001
Recrystallized sucrose (magnetic treated)[1/2]	5		152/175-190		DSC	Miller, 2001
Sucrose	10	185	189		DSC	Bhandari and Hartel, 2002
Sucrose	10	165	188.7	135.7	DSC	Smidova and others, 2003
Sucrose[A/B]	0.5	167.9/181.4	169.9/182.7	54.8/119.8	DSC	Hurtta and others, 2004
Sucrose[A/B]	1	173.7/184.5	176.6/186.6	72.1/126.6	DSC	Hurtta and others, 2004
Sucrose[A/B]	2	178.2/187.1	181.4/189.3	111.4/128	DSC	Hurtta and others, 2004
Commercial sucrose	10		170-192		DSC	Okuno and others, 2003
Reagent sucrose	10		182		DSC	Okuno and others, 2003
Recrystallized reagent Sucrose	10		166		DSC	Okuno and others, 2003
Recrystallized reagent sucrose with 0.01% KCl	10		174		DSC	Okuno and others, 2003
Recrystallized reagent sucrose with 0.05% KCl	10		174		DSC	Okuno and others, 2003
Recrystallized reagent sucrose with 0.1% KCl	10		175		DSC	Okuno and others, 2003
Recrystallized reagent sucrose with	10		176		DSC	Okuno and others, 2003

0.5% KCl					
Recrystallized reagent sucrose with 1% KCl	10		178		DSC	Okuno and others, 2003
Low ash sucrose[1/2]	10		154.3/190.5	1.1/116.0	DSC	Maulny, 2003
Low ash sucrose recrystallized with no salts[1/2]	10		154.8/180.8	33.3/85.4	DSC	Maulny, 2003
Low ash sucrose recrystallized with 0.1% of KCl	10		188.4	119.8	DSC	Maulny, 2003
Low ash sucrose recrystallized with 0.5% of KCl	10		186.1	110.0	DSC	Maulny, 2003
Low ash sucrose recrystallized with 1% of KCl	10		184.1	112.6	DSC	Maulny, 2003
Low ash sucrose recrystallized with 0.1% of NaCl	10		189.1	122.7	DSC	Maulny, 2003
Low ash sucrose recrystallized with 0.5% of NaCl	10		183.8	111.0	DSC	Maulny, 2003
Low ash sucrose recrystallized with 1% of NaCl	10		184.3	112.5	DSC	Maulny, 2003
Low ash sucrose recrystallized with 0.1% of K_2SO_4	10		189.0	117.7	DSC	Maulny, 2003
Low ash sucrose recrystallized with	10		190.1	125.2	DSC	Maulny, 2003

0.5% of K$_2$SO$_4$						
Low ash sucrose recrystallized with 1% of K2SO4	10		190.8	124.5	DSC	Maulny, 2003
Sucrose[A/B]	10	185.9/188.9	190.5/191.5	126.4/134.4	DSC	Hurtta and others, 2004
Sucrose[A/B]	20	187.5/189.6	191.9/192.9	130.8/135.4	DSC	Hurtta and others, 2004
Sucrose[A/B]	50	188.3/191.1	193.7/196.1	136.9/138.8	DSC	Hurtta and others, 2004
Sucrose[A/B]	100	189.0/190.8	196.1/196.5	143.2/145.4	DSC	Hurtta and others, 2004
Sucrose			168-183		DSC	Kishihara and others, 2004
Sucrose[1/2]			150/(170-180)		DSC	Kishihara and others, 2004
Crystalline sucrose	10		187.4		DSC	Kawakami and others, 2005
Sucrose[C/R(1,2)]	10		191.7/(154.3, 186.8)	132.8/(3.9, 108.5)	DSC	Beckett and others, 2006
Sucrose[1/2]	2	138.01/173.24	146.00/179.84	9.77/115.07	DSC	Lee and others, 2011a
Sucrose[1/2]	5	145.15/179.64	154.48/188.28	6.59/117.80	DSC	Lee and others, 2011a
Sucrose[1/2]	10	150.97/186.19	156.64/190.55	10.03/127.10	DSC	Lee and others, 2011a
Sucrose	20	177.13	193.88	203.54	SDT	Saavedra-Leos and others, 2012
Beet Sucrose (18 samples)	10	188.41	190.33	132.53	DSC	Lu and others, 2013
Cane (26 samples)	10	153.80/187.39	168.99/190.07	4.79/132.40	DSC	Lu and others, 2013
Sugar in the Raw cane	10	188.34	191.67	129.80	DSC	Lu and others, 2013
Sucrose[1/2]	0.5	130.55/157.65	134.75/168.45	116.86	DSC	Magoń and others,

						2014
Sucrose[1/2]	1	136.25/161.95	138.35/174.05	125.62	DSC	Magoń and others, 2014
Sucrose[1/2]	2	141.65/169.55	143.55/181.15	128.54	DSC	Magoń and others, 2014
Sucrose[1/2]	5	148.15/178.65	150.95/189.15	131.46	DSC	Magoń and others, 2014
Sucrose[1/2]	10	153.55/184.05	156.75/191.25	131.46	DSC	Magoń and others, 2014
Sucrose[1/2]	20	158.85/185.45	162.95/191.35	134.39	DSC	Magoń and others, 2014
Sucrose	20	184.85			FSC	Magoń and others, 2014
Sucrose	60	189.85			FSC	Magoń and others, 2014
Sucrose	600	182.85			FSC	Magoń and others, 2014
Sucrose	6000	192.85			FSC	Magoń and others, 2014
Sucrose	60000	196.85	209.85		FSC	Magoń and others, 2014

Sucrose [B/C/R] indicates three different sugars categories, B was 7 beet sugar samples, C was 11 cane sugars samples, R was 4 recrystallized sucrose samples.

**Sucrose[C/P] indicates two different sugar categories, P was pure sucrose, C was commercial sucrose samples.

***Sucrose[A/B] indicates two different sugar samples. Sucrose A was bulk materials, the others were fine chemicals made for laboratory use.

****Sucrose[C/R(1,2)] indicates two different sugar categories (C was commercial sucrose and R was C Recrystallized in purified water) and two endothermic peaks were found in R, 1 was the first small endothermic peak, 2 was the main endothermic peak.

*****Sucrose[1/2] indicates two endothermic peaks were found in the same scanning run, 1 was the first small endothermic peak, 2 was the main endothermic peak.

Appendix C Product information for analytical grade cane sucrose

![SIGMA]

ProductInformation

Sucrose

Product Number **S 0389**
Store at Room Temperature

Product Description
Molecular Formula: $C_{12}H_{22}O_{11}$
Molecular Weight: 342.3
CAS Number: 57-50-1
Melting point: >160 C
Rotation: +66.5 (2.6 %, water, 25 °C)

This product is a disaccharide composed of glucose and fructose, which is used for a variety of applications. It is isolated from cane sugar; it is not synthetic. This product is suitable for molecular biology applications. It is free of DNase, RNase, and protease impurities.

This product can be used to prepare density gradients for cell/organelle separation.[1,2] The refractive index of the solution will be directly related to the density.[2] In addition, sucrose can be used as a supplement in plant, insect, and bacterial culture media. It can also be used in various enzymatic assays.

Precautions and Disclaimer
For Laboratory Use Only. Not for drug, household or other uses.

Preparation Instructions
This product is soluble in water (500 mg/ml).

Storage/Stability
Solutions can be autoclaved for 15-20 minutes at a maximum of 121 °C. There will be some hydrolysis to glucose and fructose, depending in part on how rapidly the autoclave comes to the required temperature and pressure. Care must be taken to prevent solutions from caramelizing.

References
1. Data for Biochemical Research, 3rd ed., Dawson, R. M. C., et al., Oxford University Press (New York, NY: 1986), pp. 545-546.
2. Centrifugation, a Practical Approach, 2nd ed., Rickwood, D., ed., IRL Press (Oxford, UK: 1984) Appendix IV.

CMH/ 12/02

Figure C.1 Product information for Sigma-Aldrich sucrose S0389

Figure C.1 Continued

SIGMA-ALDRICH®

Product Specification

Product Name:
Sucrose – for molecular biology, ≥99.5% (GC)

Product Number:	**S0389**
CAS Number:	57-50-1
MDL:	MFCD00006626
Formula:	C12H22O11
Formula Weight:	342.30 g/mol
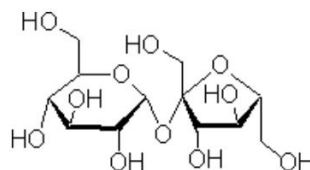
TEST	Specification
Appearance (Color)	White
Appearance (Form)	Crystals
Solubility (Color)	Colorless
Solubility (Turbidity)	Clear
5 g plus 10 mL H2O	
Infrared spectrum	Conforms to Structure
Heavy Metals (as Lead)	$\leq$ 5 ppm
Purity (GC)	$\geq$ 99.5 %
A260 UV Absorption	$\leq$ 0.15
50% w/v in H2O	
A280 UV Absorption	$\leq$ 0.15
50% w/v in H2O	
DNAse, Exonuclease Detection	None Detected
RNAse Detection	None Detected
Protease Impurity	None Detected
Free Glucose	$\leq$ 0.1 %
Recommended Retest Period	------------------------
5 Years	

1 of 1

Fisher Scientific

1 Reagent Lane
Fairlawn, NJ 07410
201.796.7100 tel
201.796.1329 fax

Certificate of Analysis

Fisher Scientific's Quality System has been found to conform to Quality Management System
Standard ISO9001:2000 standard by DNV Certificate number CERT-08052-2006-AQ-HOU-ANAB

This is to certify that units of the above mentioned lot number were tested and found to comply with the specifications of the grade listed. Certain data have been supplied by third parties. Fisher Scientific expressly disclaims all warranties, expressed or implied, including the implied warranties of merchantability and fitness for a particular purpose. Certain products (USP/FCC/NF/EP/BP/JP grades) are sold for use in food, drug, or medical device manufacturing. Fisher does not claim regulatory coverage under 21 CFR nor maintain DMF's with the FDA. The following are the actual analytical results obtained:

Catalog Number	S5	Mfg. Date	11/7/2008
Lot Number	085691		
Description	SUCROSE, A.C.S.		
Country of Origin	United States		

Result name	Units	Specifications	Test Value
APPEARANCE		REPORT	White crystals
CHLORIDE	%	<= 0.005	<0.005
HEAVY METALS (as Pb)	ppm	<= 5	<5.0
IDENTIFICATION	PASS/FAIL	= PASS TEST	PASS TEST
IGNITION RESIDUE	%	<= 0.01	0.0090
INSOLUBLE MATTER	%	<= 0.005	<0.0050
INVERT SUGAR	%	<= 0.05	<0.01
IRON (Fe)	ppm	<= 5	<5.0
LOSS ON DRYING @ 105 C	%	<= 0.03	0.030
SPECIFIC ROTATION @ 25 C	DEGREES (+ OR -)	Inclusive Between +66.3 +66.8	66.3
SULFATE & SULFITE	%	<= 0.005	<0.005
TITRATABLE ACID	mEq/g	<= 0.0008	0.0008

CERTIFIED BY   *Edgar E. Hans*

Lab Manager Fairlawn

Note: The data listed is valid for all package sizes of this lot of this product, expressed as a extension of this catalog number listed above. If there are any questions with this certificate, please call Chemical Services at (800) 227-6701.

Figure C.2 Product information for Fisher sucrose S5-500

Figure C.2 Continued

Description & Specifications

Chemical Identifiers

CASRegistryNumber1	57-50-1
Molecular Formula	$C_{12}H_{22}O_{11}$
Formula Weight	342.3
MFCD Number	MFCD00006626
Synonym	Cane Sugar
Chemical Name or Material	Sucrose
Grade	Certified ACS

Specifications

Chloride	0.005% max.
Identification	Pass Test
Heavy Metals (as Pb)	5ppm max.
Ignition Residue	0.01% max.
Insoluble Matter	0.005% max.
Iron (Fe)	5ppm max.
Invert Sugars	0.05% max.
Loss on Drying	0.03% max.
Packaging	Poly Bottle
Quantity	500g
Specific Rotation	+66.3 to +66.8° (+ or −)
Sulfate and Sulfite	0.005% max.
Titratable Acid	0.0008mEq/g max.
CASRegistryNumber1	57-50-1
Molecular Formula	$C_{12}H_{22}O_{11}$
Formula Weight	342.3
MFCD Number	MFCD00006626
Synonym	Cane Sugar
ChemAlert Storage Symbol	Gray

Appendix D Available origin information for the 10 beet and 10 cane sucrose samples

obtained from the Sugar Processing Research Institute, Inc. (New Orleans, LA)

# Number	Beet or cane source	Available origin information
1	Beet sugar	Hungary
2	Beet sugar	Canada
3	Beet sugar	Unknown
4	Beet sugar	United States
5	Beet sugar	United States
6	Beet sugar	Canada
7	Beet sugar	Canada
8	Beet sugar	Canada
9	Beet sugar	Canada
10	Beet sugar	Canada
11	Cane sugar	Refined in Brazil (High ash)
12	Cane sugar	Refined in Canada, raw sugar from Brazil
13	Cane sugar	Refined in United States
14	Cane sugar	Refined in United States
15	Cane sugar	Refined in United States, raw sugar from Brazil
16	Cane sugar	Refined in United States
17	Cane sugar	Refined in Saudi Arabia
18	Cane sugar	Refined in Vietnam
19	Cane sugar	Refined in United States
20	Cane sugar	Refined in United States

Appendix E Sample information for commercially obtained sugar samples

Label Name	Source	Product #, Lot # or Batch #
Sigma-Aldrich sucrose	Cane	S0389 Lot#s 128K00852/SLBF6473/SLBK4686V
Fisher sucrose	Cane	S5-500 Lot 085691
C&H pure cane sugar (4 lb)	Cane	70375C206/72162A315/52426A2/72144A210
C&H granulated white (1 lb)	Cane	79272A15
C&H sugar cubes	Cane	72135CD3
C&H Baker's sugar	Cane	2322
Meijer pure granulated	Cane	C166C313
Domino granulated	Cane	50012B1/61375B2
Domino polished white	Cane	Not provided
Domino low color, metal, turbidity sucrose (LCMT) Special ingredient	Cane	Not provided
Safeway granulated (United Sugar)	Cane	F0358DS2571
United Sugar (50 lb)	Cane	F12323
Turbinado raw cane sugar	Cane	Sugar in the Raw Packets
Dixie Crystals Pure Cane	Cane	S162D
Chinese Lump Candy (Guangdong, China)	Cane	6940033410824
Chinese granulated (Beijing, China)	Cane	6932764300024
Chinese castor (Beijing, China)	Cane	6920010302663
Price Rite extra fine granulated	Cane	F11324D
Azúcar refinery cane (Mexico) (1 Kg)	Cane	02A2
Refinery sugar (Brazil)	Cane	Unknown
Market Pantry granulated (from Target)	Beet	MLL343
Pioneer sugar	Beet	Y082C/Y249B/Y067C/Y083C
Schnucks granulated	Beet	12287X0402
Meijer pure granulated	Beet	Y279C-2
Kroger sugar granulated (United Sugar)	Beet	M1037/E9251
United Sugar (50 lb)	Beet	K12307 and E9251
Dansukker (Sweden) (1Kg)	Beet	501026

Appendix F HPLC results for crystalline sucrose samples

Table F.1 HPLC results for crystalline analytical grade Sigma cane (Figure 4.3)

Target Temperature $^{\circ}$C	Sucrose % (avg±std)	Glucose % (avg±std)	Fructose % (avg±std)	5-HMF % (avg±std)
25 ("as is")	98.587±0.958			
140	98.178±2.352			
150	99.721±1.071			
160	98.441±0.798	0.598±0.224		
170	97.013±1.404	0.609±0.166		
180	96.892±0.329	1.158±0.110		
190	93.572±1.331	2.396±0.092		0.017±0.002
200	73.157±4.498	8.793±0.610	1.076±0.108	0.024±0.000

Table F.2 HPLC results for crystalline analytical grade Fisher cane (Figure 4.4)

Target temperature $^{\circ}$C	Sucrose % (avg±std)	Glucose % (avg±std)	Fructose % (avg±std)	5-HMF % (avg±std)
25 ("as is")	98.364±0.708			
140	96.926±2.078			
150	98.430±0.772			
160	97.815±1.621	0.393±0.499		
170	98.119±0.920	0.804±0.210		
180	97.506±1.872	1.240±0.179		
190	95.138±1.131	2.357±0.782		0.015±0.001
200	78.981±2.984	7.719±0.705	0.519±0.053	0.020±0.002

Table F.3 HPLC results for crystalline white refined US cane (Figure 4.5)

Target temperature $^{\circ}$C	Sucrose % (avg±std)	Glucose % (avg±std)	Fructose % (avg±std)	5-HMF % (avg±std)
25 ("as is")	99.301±1.559			
140	98.617±1.281			
150	98.998±2.094			
160	98.580±1.588			
170	97.751±0.476	0.687±0.124		
180	98.041±1.782	0.801±0.132		
190	96.193±1.333	1.273±0.386		0.017±0.002
200	87.510±1.613	4.284±0.441	0.473±0.037	0.017±0.002

Table F.4 HPLC results for crystalline white refined C&H cane (Figure 4.6)

Target temperature °C	Sucrose % (avg±std)	Glucose % (avg±std)	Fructose % (avg±std)	5-HMF % (avg±std)
25 ("as is")	98.631±0.323			
140	99.671±0.511			
150	99.446±0.584			
160	99.050±1.008			
170	98.595±0.496	0.375±0.033		
180	99.334±0.635	0.420±0.017		
190	98.325±0.166	0.539±0.011		0.016±0.001
200	91.035±0.956	2.759±0.254	0.691±0.084	0.019±0.001

Table F.5 HPLC results for crystalline white refined US beet (Figure 4.7)

Target temperature °C	Sucrose % (avg±std)	Glucose % (avg±std)	Fructose % (avg±std)	5-HMF % (avg±std)
25 ("as is")	98.190±3.180			
140	99.246±9.489			
150	98.831±1.811			
160	99.800±0.482			
170	99.007±0.969			
180	99.380±1.097			
190	99.158±1.134			
200	93.613±0.694	2.128±0.176	0.621±0.083	0.017±0.002

Table F.6 HPLC results for crystalline white refined Pioneer beet (Figure 4.8)

Target temperature °C	Sucrose % (avg±std)	Glucose % (avg±std)	Fructose % (avg±std)	5-HMF % (avg±std)
25 ("as is")	98.678±0.266			
140	98.808±0.423			
150	98.003±1.049			
160	98.373±1.274			
170	97.767±1.084			
180	98.694±2.460			
190	96.537±0.760			
200	92.319±2.098	3.036±0.161	0.605±0.120	0.017±0.001

Table F.7 HPLC results for crystalline white refined Meijer beet (Figure 4.9)

Target temperature °C	Sucrose % (avg±std)	Glucose % (avg±std)	Fructose % (avg±std)	5-HMF % (avg±std)
25 ("as is")	98.763±1.399			
140	97.689±0.445			
150	98.738±0.672			
160	99.608±0.387			
170	98.440±1.155			
180	98.907±0.984			
190	97.326±1.002			
200	93.184±0.461	2.766±0.158	0.726±0.115	0.019±0.004

Table F.8 HPLC results for crystalline High ash cane (Figure 4.10)

Target temperature °C	Sucrose % (avg±std)	Glucose % (avg±std)	Fructose % (avg±std)	5-HMF % (avg±std)
25 ("as is")	97.480±2.9080			
140	99.643±0.738			
150	99.668±0.545			
160	99.519±0.827			
170	98.684±0.265	0.629±0.183		
180	94.265±0.797	1.821±0.249	1.272±0.313	
190	81.840±4.545	4.647±1.166	1.393±0.110	0.023±0.003
200	39.795±0.495	19.440±0.346	3.791±0.394	0.046±0.003

Table F.9 HPLC results for crystalline Sugar in the Raw (Figure 4.11)

Target temperature °C	Sucrose % (avg±std)	Glucose % (avg±std)	Fructose % (avg±std)	5-HMF % (avg±std)
25 ("as is")	99.554±1.167			
140	98.873±1.399			
150	99.117±0.955			
160	99.150±0.146			
170	99.571±0.534			
180	100.108±0.393			
190	98.600±1.453			
200	92.140±0.445	2.735±0.197	0.706±0.038	0.016±0.002

Table F.10 HPLC results for crystalline Chinese Cane (Figure 4.12)

Target temperature °C	Sucrose % (avg±std)	Glucose % (avg±std)	Fructose % (avg±std)	5-HMF % (avg±std)
25 ("as is")	100.947±0.222			
140	100.146±0.244			
150	100.256±0.478			
160	99.989±0.072			
170	99.935±0.097			
180	99.873±0.133			
190	99.809±0.097			
200	96.907±1.474	1.499±0.139	0.362±0.052	0.014±0.000

Table F.11 HPLC results for crystalline laboratory recrystallized US beet (Figure 4.13)

Target temperature °C	Sucrose % (avg±std)	Glucose % (avg±std)	Fructose % (avg±std)	5-HMF % (avg±std)
25 ("as is")	96.195±1.386			
140	99.882±0.261			
150	96.894±0.709	1.464±0.191		0.024±0.001
160	89.247±1.194	4.439±0.538	0.949±0.087	0.048±0.004
170	84.538±0.657	6.462±0.350	1.030±0.096	0.059±0.003
180	82.451±2.015	6.920±0.867	1.324±0.126	0.059±0.004
190	62.607±2.075	14.524±1.129	1.593±0.053	0.102±0.009
200	49.214±4.072	19.761±2.124	1.944±0.341	0.211±0.017

Table F.12 HPLC results for 120 °C isothermal 480 min Sigma cane sucrose (Figure 4.14)

Target temperature °C	Sucrose % (avg±std)	Glucose % (avg±std)	Fructose % (avg±std)	5-HMF % (avg±std)
25 ("as is")	98.631±0.323			
120 (iso 480min)	97.499±1.979	1.033±0.390		0.016±0.001

Appendix G Summary for ICP analysis for "as is" and Recrystallized sucrose samples using 10%

(w/v) sucrose solution or muffle furnace ashed methods

Table G.1 ICP analysis using 10% sucrose solution

Sucrose (ppm)	Sigma cane		US beet		Domino cane	
	as-is	1st recrystallized	as-is	1st recrystallized	as-is	1st recrystallized
Ca	0.00	0.00	0.05	0.00	0.48	0.10
Fe	0.00	0.00	0.03	0.00	0.00	0.00
K	0.25	0.16	5.39	0.21	2.09	0.25
Mg	0.00	0.00	0.11	0.00	0.04	0.00
Na	0.41	0.39	3.55	0.16	0.48	0.72
P	0.12	0.14	1.44	0.12	0.12	0.54
S	4.42	4.47	125.15	4.86	4.18	13.50
Si	0.19	0.29	2.29	0.04	0.55	0.62
Zn	0.03	0.03	0.30	0.03	0.03	0.10
Tmonset (^{o}C)	149.40	146.92	188.73	155.13	188.08	150.21

Table G.2 ICP-AES analysis of muffle furnace ashed US beet and US cane sucrose

Element	US beet (ppm)	US cane (ppm)
Ca	2.2411	14.3
Fe	0.1046	0.072
K	29.8123	5.09
Mg	0.3148	0.838
Na	0.7197	3.25
P	0.5801	0.81
S	3.2021	8.74
Si	4.2833	5.97
Zn	0.2998	0.18

US beet and US cane samples were weighed (5 ± 0.1 g) into a ceramic crucible with lid and placed into the cold muffle furnace. Each sugar sample was prepared in duplicate. The muffle furnace was heated up to a temperature at 450 °C and held for 12 hours (Generally, ashing at 450 °C for 12 hours was satisfactory for the sugar sample). Contrary to expectations, beet sugar (US beet), which includes a sulfitation step during refining, has a lower elemental sulfur content compared to cane sugar (US cane). This could be related to the loss of sulfur during the ashing process. An interesting phenomenon was observed after the ashing process, the ash from US beet exhibits a dark grayish color; whereas the ash from US cane has a white color.

Appendix H Moisture content measurements of sugar samples by Donlevy Laboratories

DonLevy Laboratories
The Science of Prevention

11165 Delaware Parkway, Crown Point, IN 46307   Lab Phone: (219) 226-0001   Lab Fax: (219) 226-2050

Certificate of Analysis

Dr. Shelly Schmidt
University of Illinois
260 Bevier Hall 905 S. Goodwin Ave.
Urbana, IL 61801

	Report#:	UIL6R
	Report Date:	March 17, 2014
	Samples Received:	March 10, 2014
	P. O. #:	
	Temp.on Receipt:	Ambient
	Start Date:	March 10, 2014

Sample Description	Karl Fischer Method Moisture %	Karl Fischer Method Moisture %
Sample SGM Sigma Sucrose	0.03	0.02
Sample USB US Beet Sucrose	0.07	0.05
Sample USC US Cane Sucrose	0.03	0.03

Used 50/50 Formamide/methanol as solvent.
Relative Humidity = 21.82
Temperature = 24.51

Information contained in this report has been revised and
replaces the information contained in DonLevy
Laboratories report UIL6, report date 03/14/2014.

Page 1 of 1   NOTE: Results pertain only to the sample(s) received.

Final Review Performed By:
Andrew Miller
Chemistry Supervisor

Figure H.1 Moisture content measurments for "as is" analytical grade Sigma cane, US beet, and US cane sucrose samples using volumetric Karl Fisher titration.

DonLevy Laboratories
The Science of Prevention

Certificate of Analysis

Dr. Shelly Schmidt
University of Illinois
367 Bevier Hall 905 S. Goodwin Ave.
Urbana, IL 61801

Report#:	UIL8
Report Date:	October 31, 2014
Samples Received:	September 16, 2014
P. O. #:	
Temp.on Receipt:	Ambient
Start Date:	October 3, 2014

Sample Description	Karl Fischer Method Moisture %
Sample (1) FSR Fisher Sucrose	0.06
Sample (1) FSR Fisher Sucrose	0.08
Sample (2) C&H C&H Cane Sucrose	0.08
Sample (2) C&H C&H Cane Sucrose	0.10
Sample (3) PNR Pioneer Beet Sucrose	0.11
Sample (3) PNR Pioneer Beet Sucrose	0.12
Sample (4) MJR Meijer Beet Sucrose	0.09

Page 1 of 3

Figure H.2 Moisture content measurments for "as is" analytical grade Fisher cane, white refined commerical beet and cane, Sugar in the Raw (cane), ground analytical grade Sigma cane, ground US beet, and ground US cane sucrose samples using volumetric Karl Fisher titration.

Figure H.2 continued.

DonLevy Laboratories
The Science of Prevention

11165 Delaware Parkway, Crown Point, IN 46307   Lab Phone: (219) 226-0001   Lab Fax: (219) 226-2050

Certificate of Analysis

Dr. Shelly Schmidt
University of Illinois
367 Bevier Hall 905 S. Goodwin Ave.
Urbana, IL 61801

Report#:	UIL8
Report Date:	October 31, 2014
Samples Received:	September 16, 2014
P. O. #:	
Temp.on Receipt:	Ambient
Start Date:	October 3, 2014

Sample Description	Karl Fischer Method Moisture %
Sample (4) MJR Meijer Beet Sucrose	0.09
Sample (5) SRW Sugar in the Raw	0.15
Sample (5) SRW Sugar in the Raw	0.13
Sample (6) CCC Chinese Crystalline Cane Sucrose	0.14
Sample (6) CCC Chinese Crystalline Cane Sucrose	0.14
Sample (7) GSM Ground Sigma Sucrose Powder	0.03
Sample (7) GSM Ground Sigma Sucrose Powder	0.03

Page 2 of 3

308

Figure H.2 continued.

DonLevy Laboratories
The Science of Prevention

Certificate of Analysis

Dr. Shelly Schmidt	Report#: UIL8
University of Illinois	Report Date: October 31, 2014
367 Bevier Hall 905 S. Goodwin Ave.	Samples Received: September 16, 2014
Urbana, IL 61801	P. O. #:
	Temp.on Receipt: Ambient
	Start Date: October 3, 2014

Sample Description	Karl Fischer Method Moisture %
Sample (8) GUB Ground US Beet Sucrose Powder	0.06
Sample (8) GUB Ground US Beet Sucrose Powder	0.06
Sample (9) GUC Ground US Cane Sucrose Powder	0.04
Sample (9) GUC Ground US Cane Sucrose Powder	0.04

Used 50/50 Formamide/Methanol as Solvent
Relative Humidity 24.6%
Temperature 21.4° C

Final Review Performed By:
Andrew Miller
Chemistry Supervisor

Page 3 of 3   NOTE: Results pertain only to the sample(s) received.

11165 Delaware Parkway, Crown Point, IN 46307   Lab Phone: (219) 226-0001   Lab Fax: (219) 226-2050

Certificate of Analysis

Dr. Shelly Schmidt
University of Illinois
367 Bevier Hall 905 S. Goodwin Ave.
Urbana, IL 61801

Report#:	UIL9
Report Date:	April 29, 2015
Samples Received:	April 27, 2015
P. O. #:	
Temp.on Receipt:	Ambient
Start Date:	April 27, 2015

Sample Description	Karl Fischer Method Moisture % *
Sample (1) DXE Dixie Sucrose	0.03
Sample (1) DXE Dixie Sucrose	0.05
Sample (2) MTP Market Pantry Sucrose	0.04
Sample (2) MTP Market Pantry Sucrose	0.07
Sample (3) DMN Domino Sucrose	0.03
Sample (3) DMN Domino Sucrose	0.04

*Relative Humidity 24.5% 50:50
Formamide/Method Solvent Used

Final Review Performed By:

Andrew Miller
Chemistry Supervisor

Page 1 of 1   NOTE: Results pertain only to the sample(s) received.

Figure H.3 Moisture content measurments for white refined commerical beet and cane sucrose samples using volumetric Karl Fisher titration

Appendix I HPLC results for ground samples from beet and cane sources

Table I.1 HPLC results for ground Sigma

Target Temperature °C	Sucrose % (avg±std)	Glucose % (avg±std)	Fructose % (avg±std)	5-HMF % (avg±std)
25 ("as is")	100.742±0.702			
140	100.932±0.219			
150	99.673±0.141			
160	99.439±0.267			
170	98.827±0.440			
180	98.072±0.415	1.413±0.276		
190	87.318±2.974	4.807±0.852		
200	57.096±5.427	14.424±3.666	1.667±0.579	0.015±0.004

Table I.2 HPLC results for ground Fisher

Target Temperature °C	Sucrose % (avg±std)	Glucose % (avg±std)	Fructose % (avg±std)	5-HMF % (avg±std)
25 ("as is")	101.826±0.182			
140	100.667±0.908			
150	100.962±0.492			
160	100.175±0.783			
170	99.991±0.208			
180	99.207±0.371	0.571±0.197		
190	85.877±5.711	6.292±2.964		
200	49.517±5.618	18.785±1.833	1.353±0.162	0.055±0.020

Table I.3 HPLC results for ground US cane

Target Temperature °C	Sucrose % (avg±std)	Glucose % (avg±std)	Fructose % (avg±std)	5-HMF % (avg±std)
25 ("as is")	100.877±0.189			
140	100.833±0.164			
150	101.001±0.660			
160	100.400±0.618			
170	100.151±0.465			
180	99.951±0.138			
190	97.860±0.661	0.858±0.227		
200	88.974±4.853	4.290±0.866	0.353±0.020	0.016±0.001

Table I.4 HPLC results for ground US beet

Target Temperature °C	Sucrose % (avg±std)	Glucose % (avg±std)	Fructose % (avg±std)	5-HMF % (avg±std)
25 ("as is")	100.761±0.226			
140	100.111±0.475			
150	100.353±0.075			
160	99.764±0.579			
170	100.376±0.411			
180	99.822±0.228			
190	99.668±0.107			
200	96.065±0.660	2.088±0.291		

Table I.5 HPLC results for ground Chinese Cane

Target Temperature °C	Sucrose % (avg±std)	Glucose % (avg±std)	Fructose % (avg±std)	5-HMF % (avg±std)
25 ("as is")	101.652±0.089			
140	101.214±0.087			
150	100.991±0.160			
160	100.985±0.330			
170	100.158±0.274			
180	100.134±0.254			
190	99.862±0.388			
200	95.551±1.093	1.664±0.099	0.400±0.087	0.013±0.001

Table I.6 HPLC results for ground Recrystallized US beet

Target temperature °C	Sucrose % (avg±std)	Glucose % (avg±std)	Fructose % (avg±std)	5-HMF % (avg±std)
25 ("as is")	101.341±0.509			
140	100.663±1.514			
150	99.334±0.592			
160	95.302±2.108	3.236±0.386		0.024±0.006
170	89.610±1.950	4.868±0.838		0.022±0.007
180	67.964±4.607	11.615±1.730	0.760±0.263	0.053±0.019
190	56.226±3.988	15.368±2.789	0.608±0.173	0.077±0.020
200	32.731±6.297	26.915±4.031	2.896±0.888	0.192±0.055

Appendix J Morphology information for commercially available or laboratory-recrystallized

sucrose samples collected using a Leica M205C Microsystem
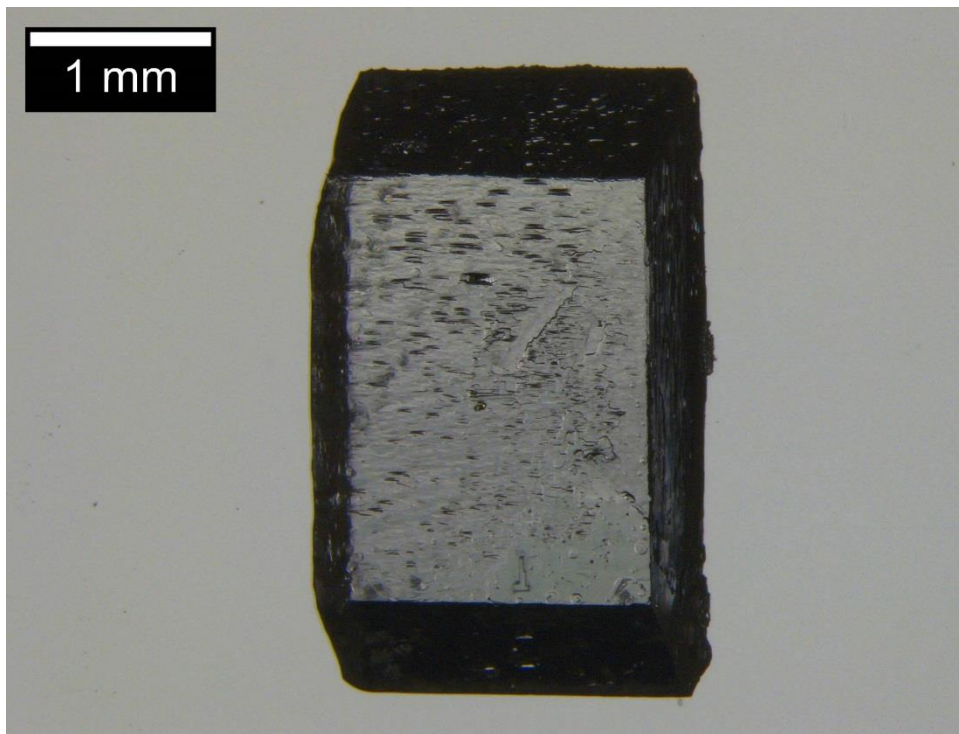
Figure J.1 Appearance of Sigma cane sucrose recrystallized with 0.1% K2SO3 in HPLC water.
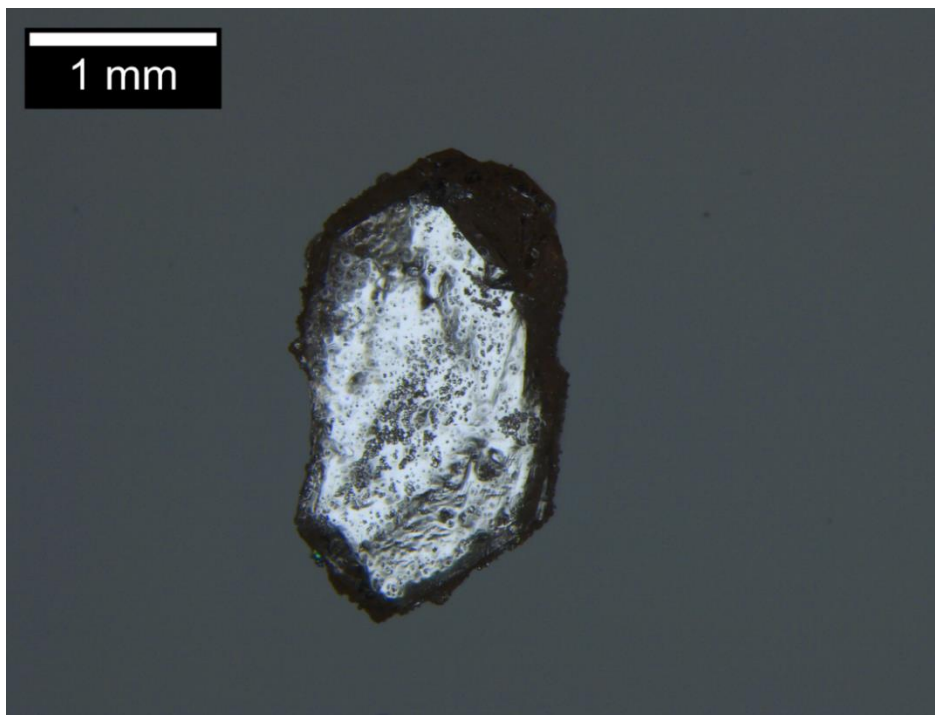
Figure J.2 Appearance of Sigma cane sucrose recrystallized with 0.2% K_2SO_3 in HPLC water.
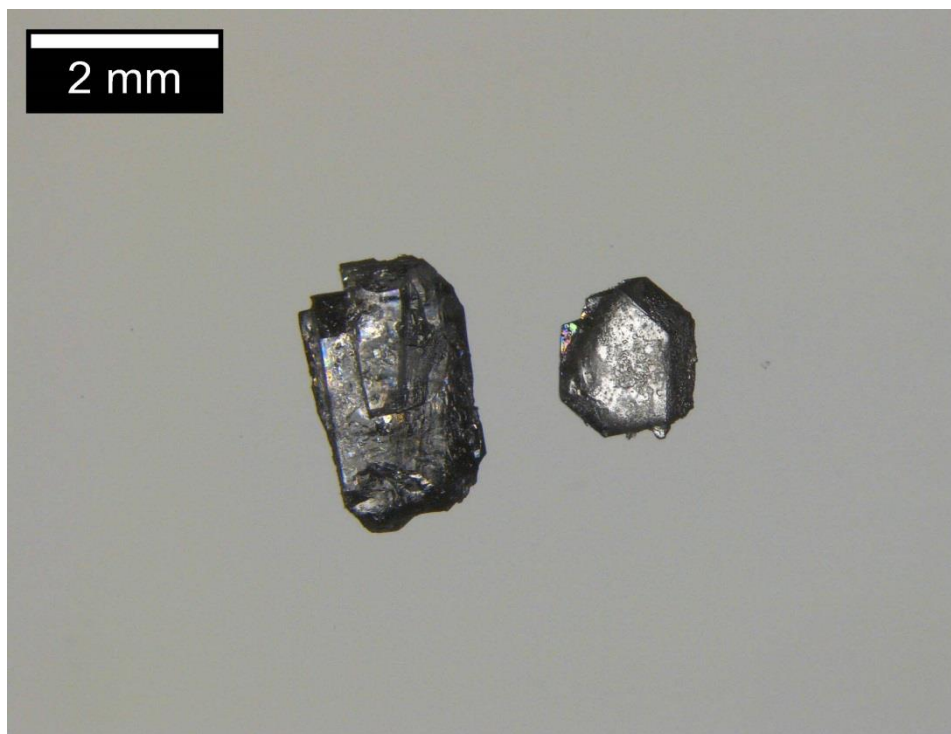
Figure J.3 Appearance of Sigma cane sucrose recrystallized with 0.8% K_2SO_3 in HPLC water.
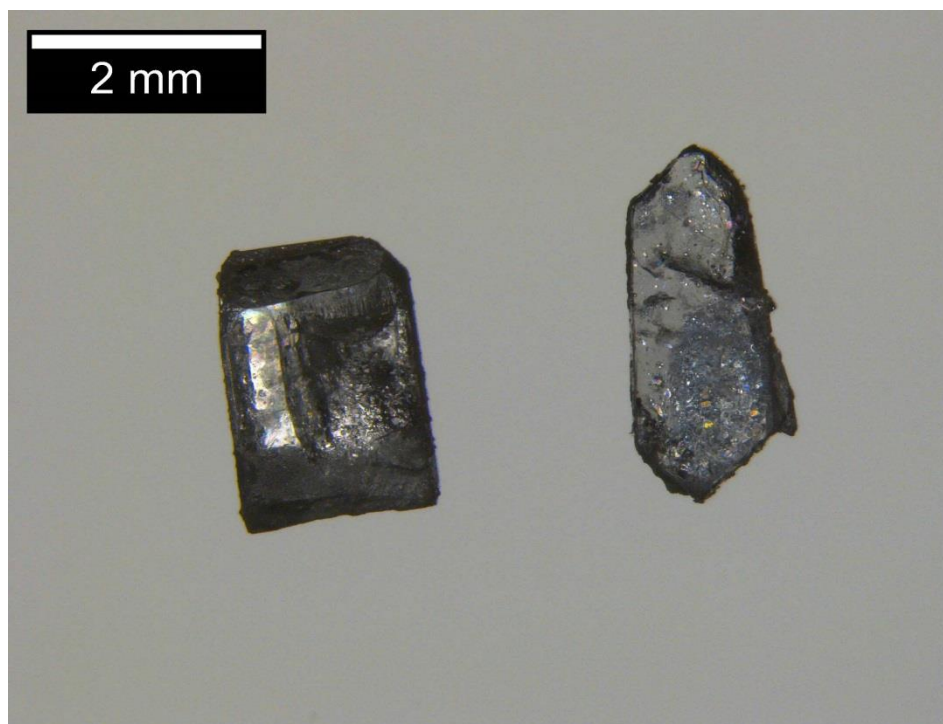
Figure J.4 Appearance of Sigma cane sucrose recrystallized with 1% K_2SO_3 in HPLC water.
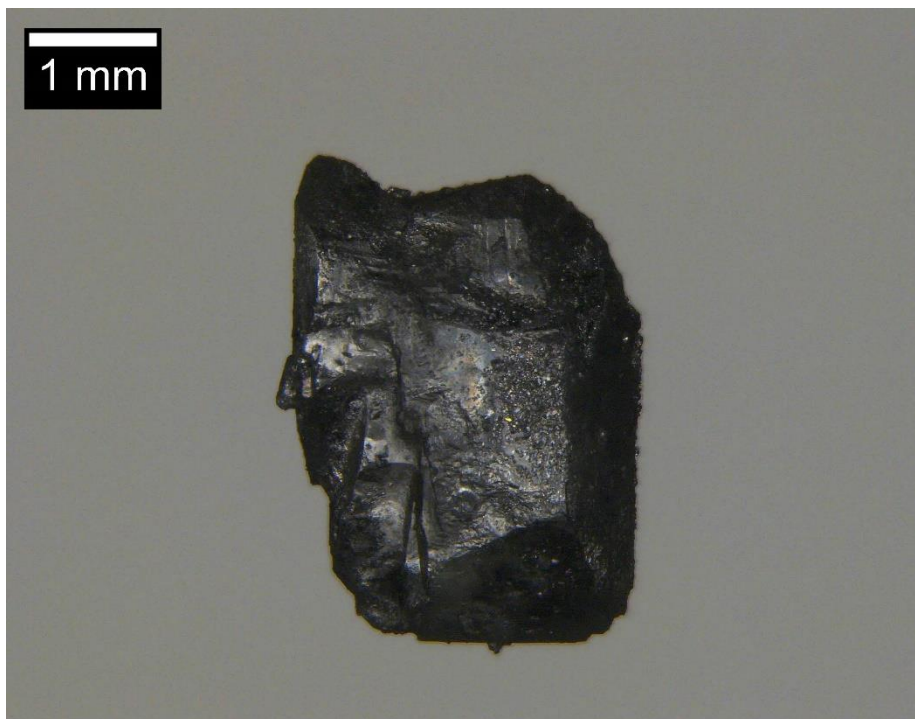
Figure J.5 Appearance of Sigma cane sucrose recrystallized with 1% K_2SO_4 in HPLC water.
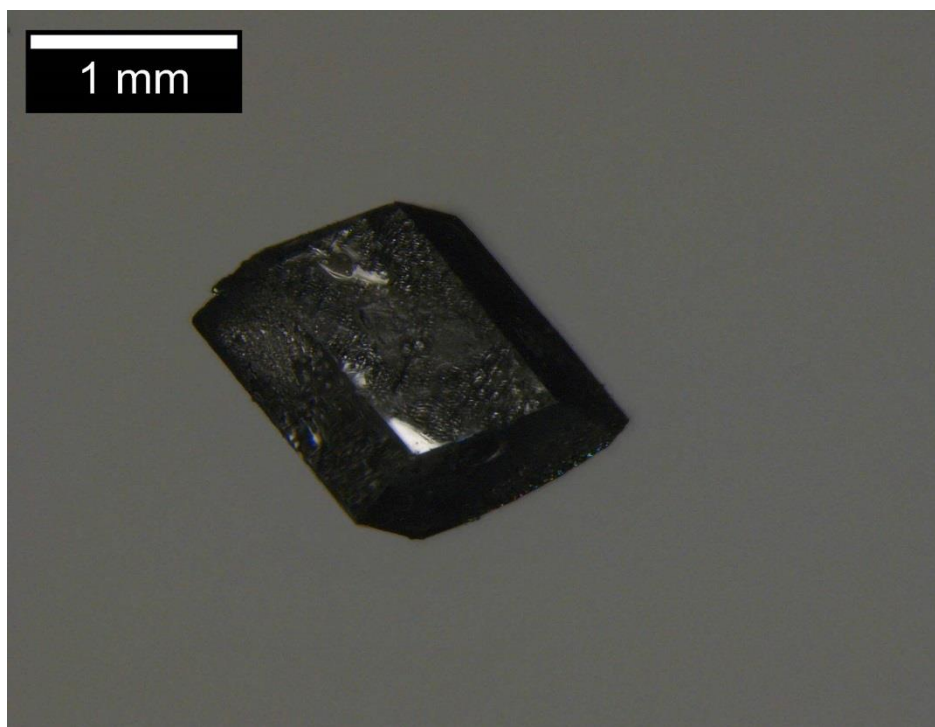
Figure J.6 Appearance of Sigma cane sucrose recrystallized with 1% CsI in HPLC water.
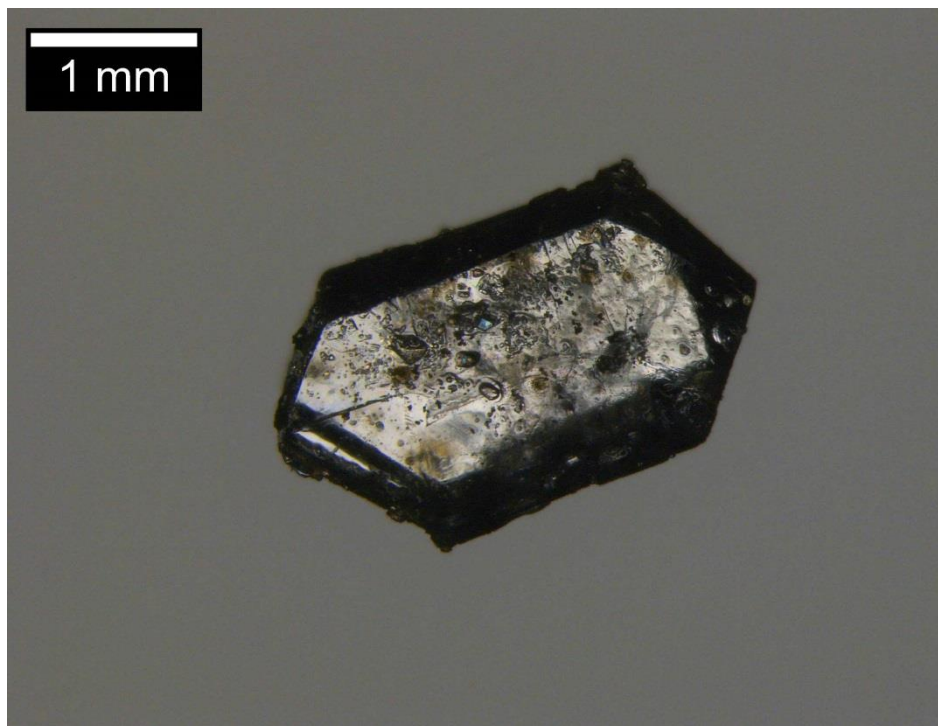
Figure J.7 Appearance of Sigma cane sucrose recrystallized with 1% CuCl in HPLC water.
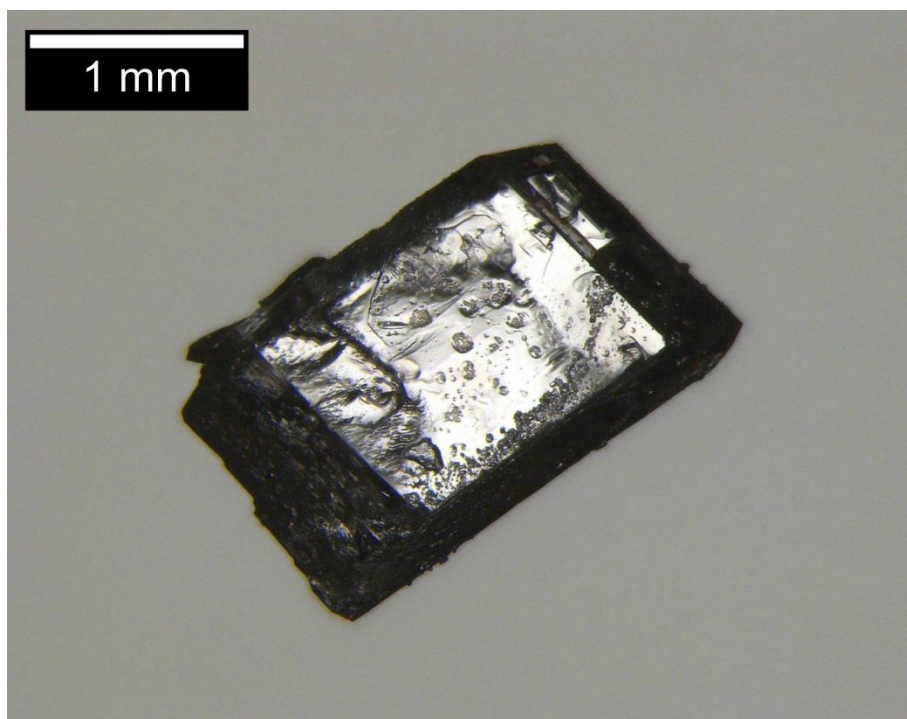
Figure J.8 Appearance of Sigma cane sucrose recrystallized with 1% Na_2SO_3 in HPLC water.
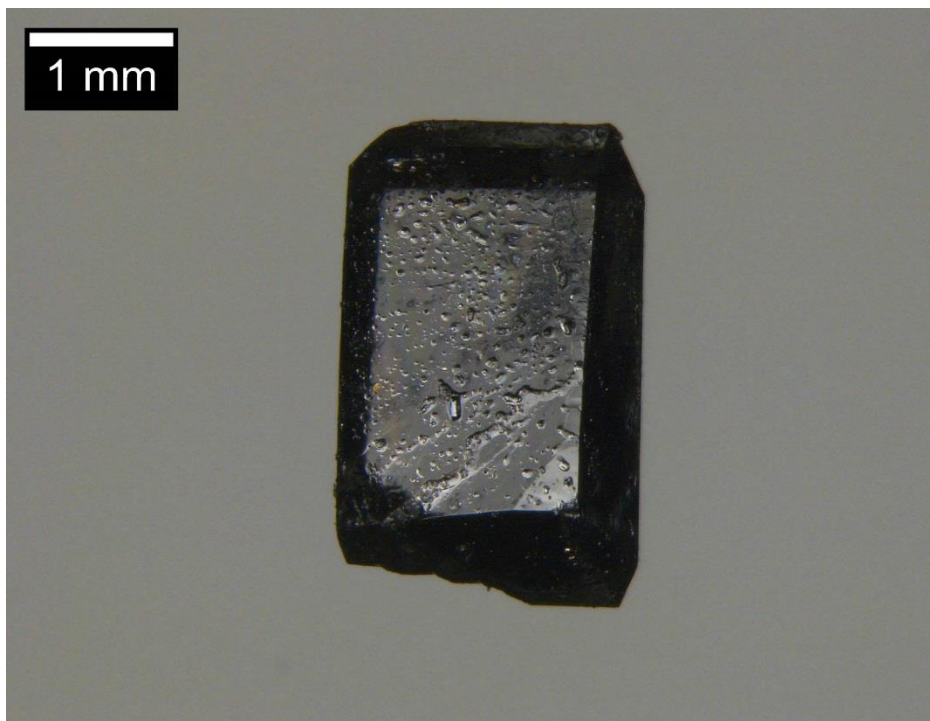
Figure J.9 Appearance of Sigma cane sucrose recrystallized with 1% NaCl in HPLC water.
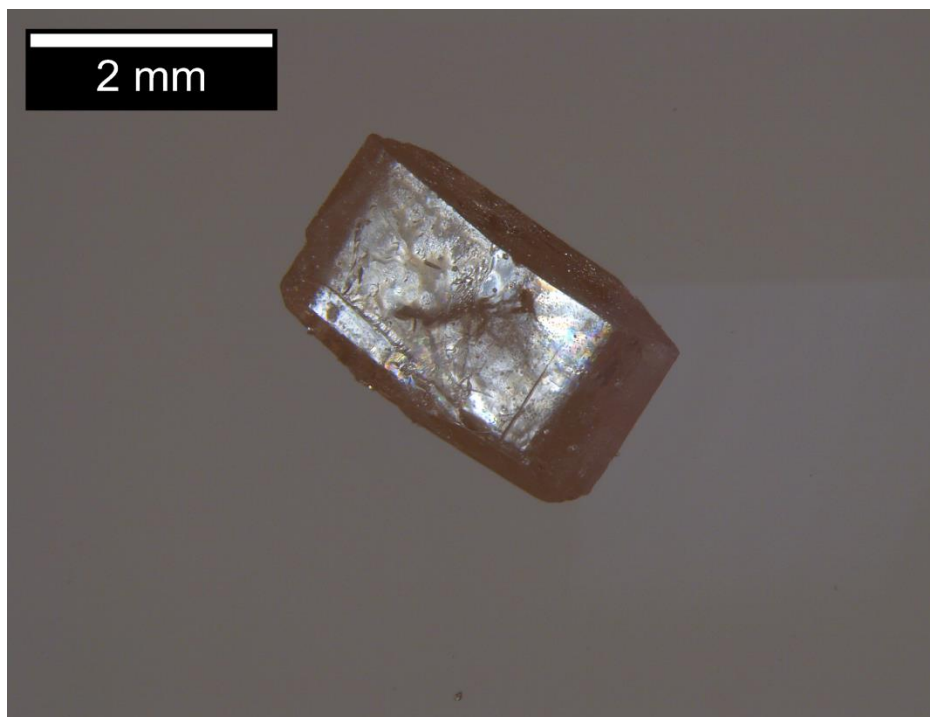
Figure J.10 Appearance of Sigma cane sucrose recrystallized with 1% NaCl in HPLC water.
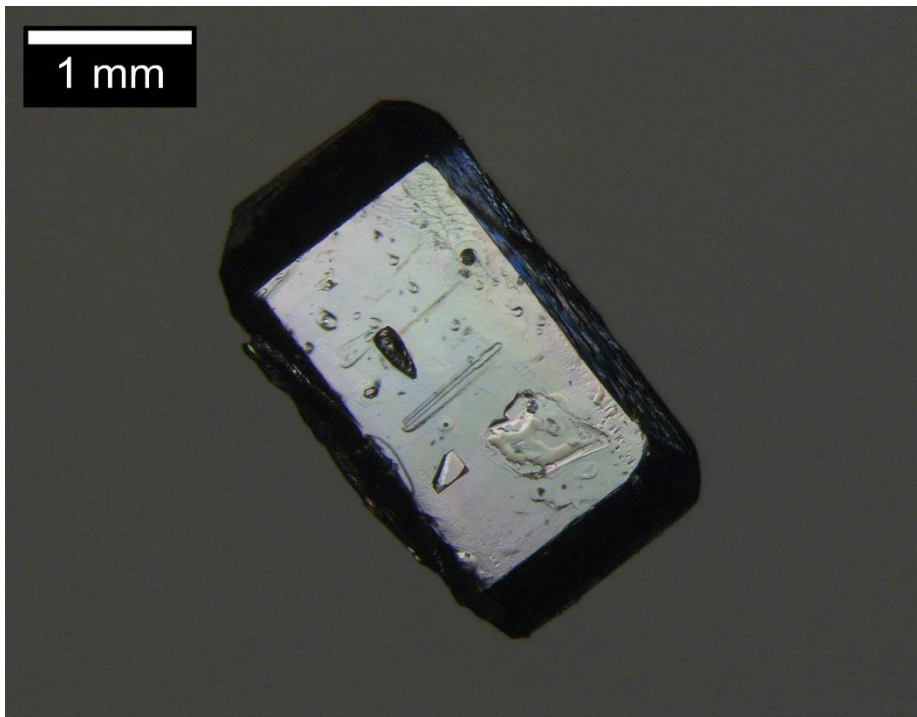
Figure J.11 Appearance of Sigma cane sucrose recrystallized in pure Ethanol.
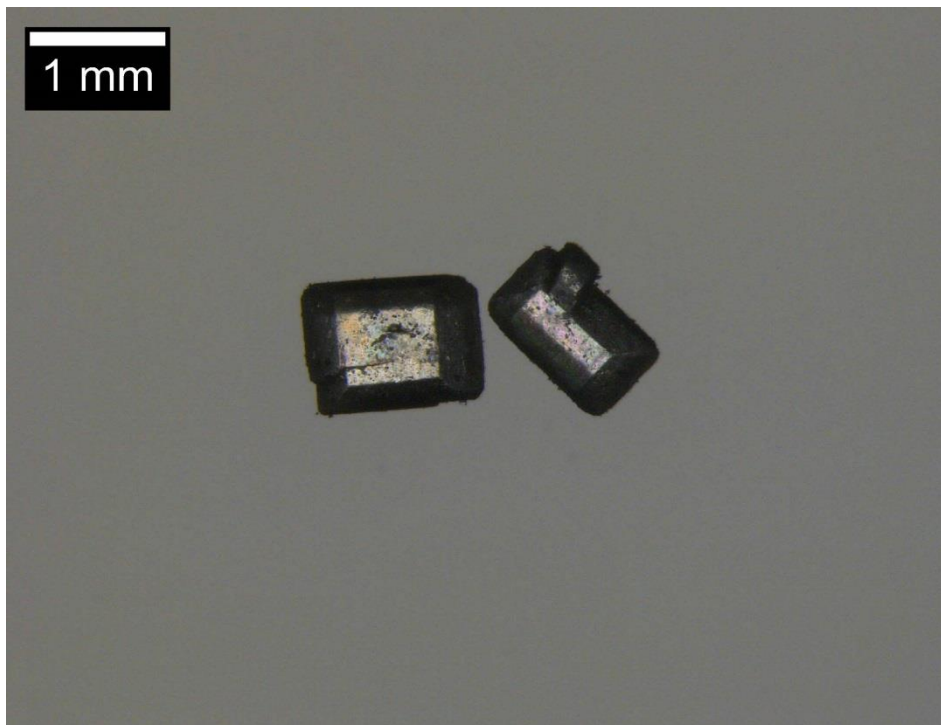
Figure J.12 Appearance of "as is" Fisher cane sucrose.
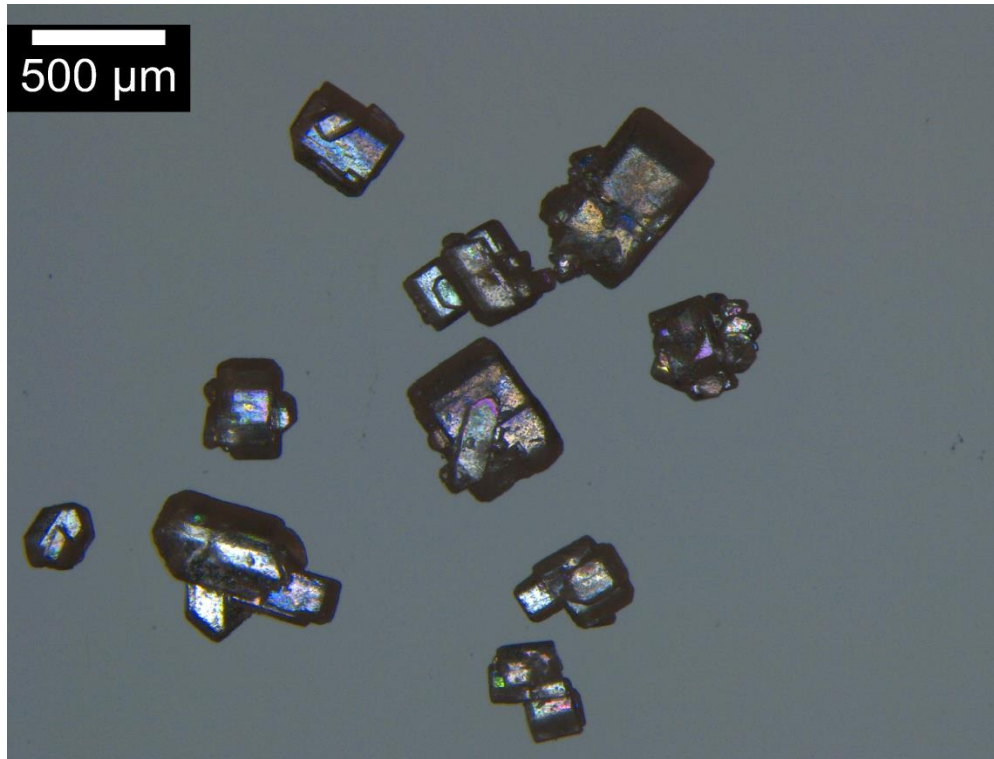
Figure J.13 Appearance of "as is" C&H cane sucrose.
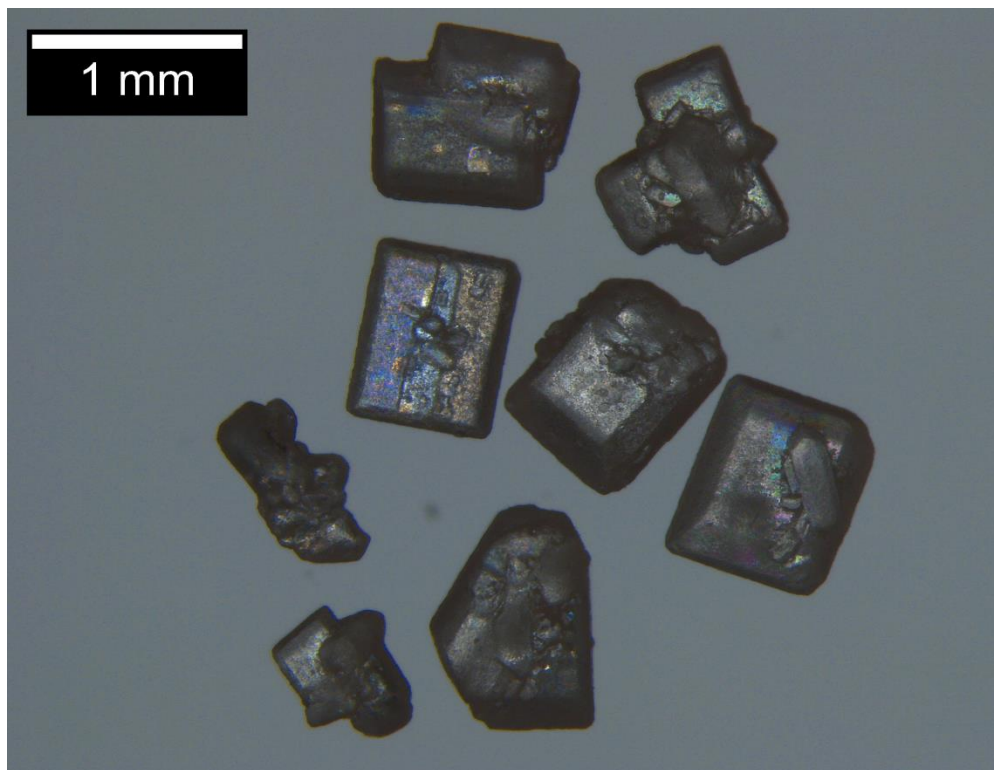
Figure J.14 Appearance of "as is" Domino cane sucrose.
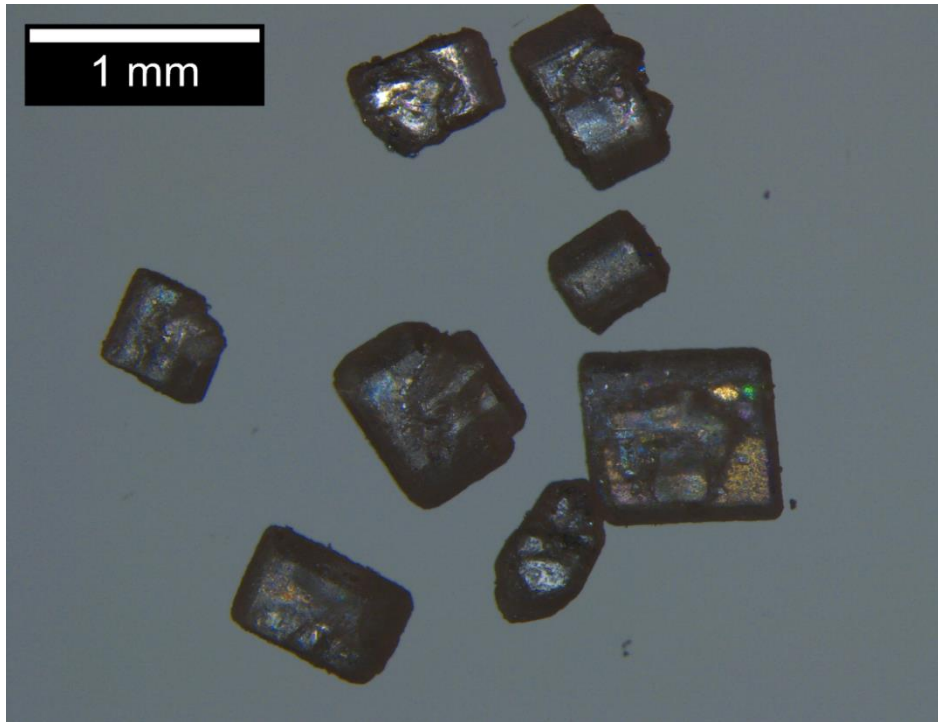
Figure J.15 Appearance of "as is" Dixie cane sucrose.
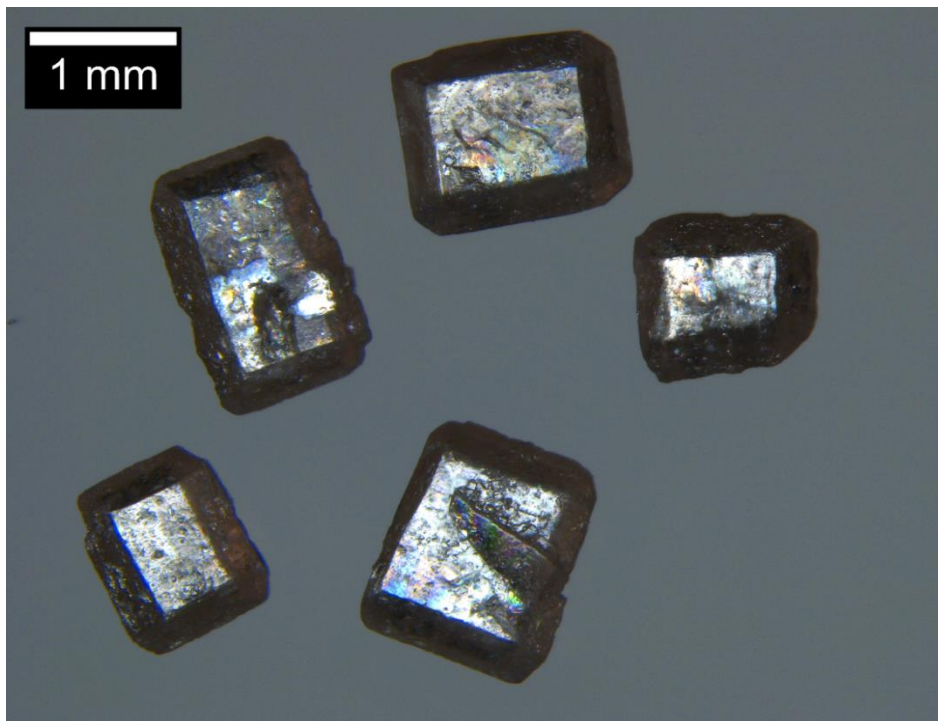
Figure J.16 Appearance of "as is" Chinese cane sucrose.
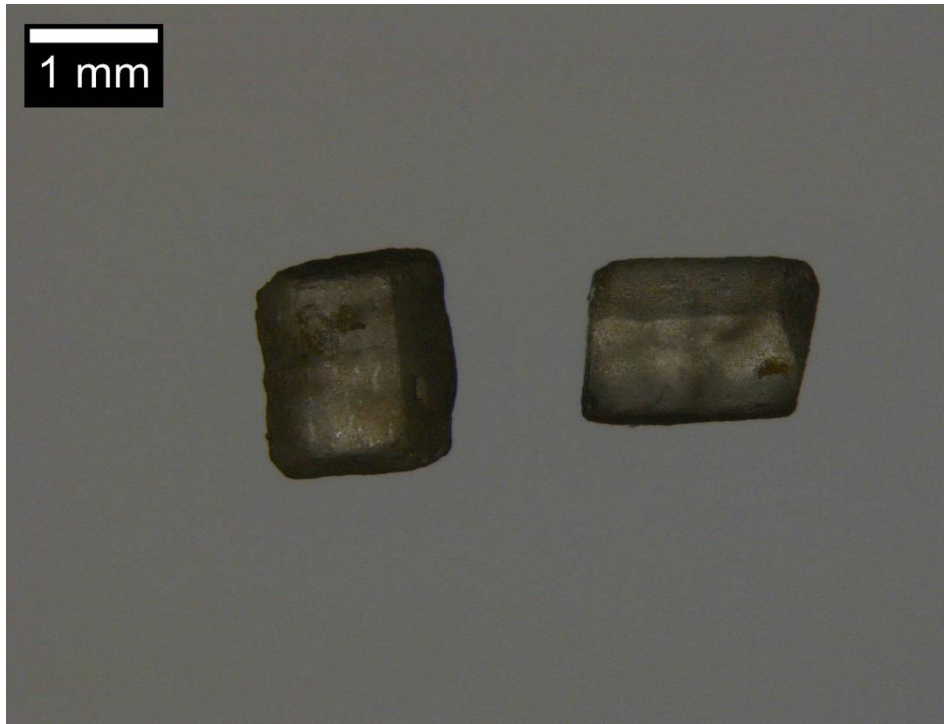
Figure J.17 Appearance of "as is" Sugar in the Raw cane sucrose.
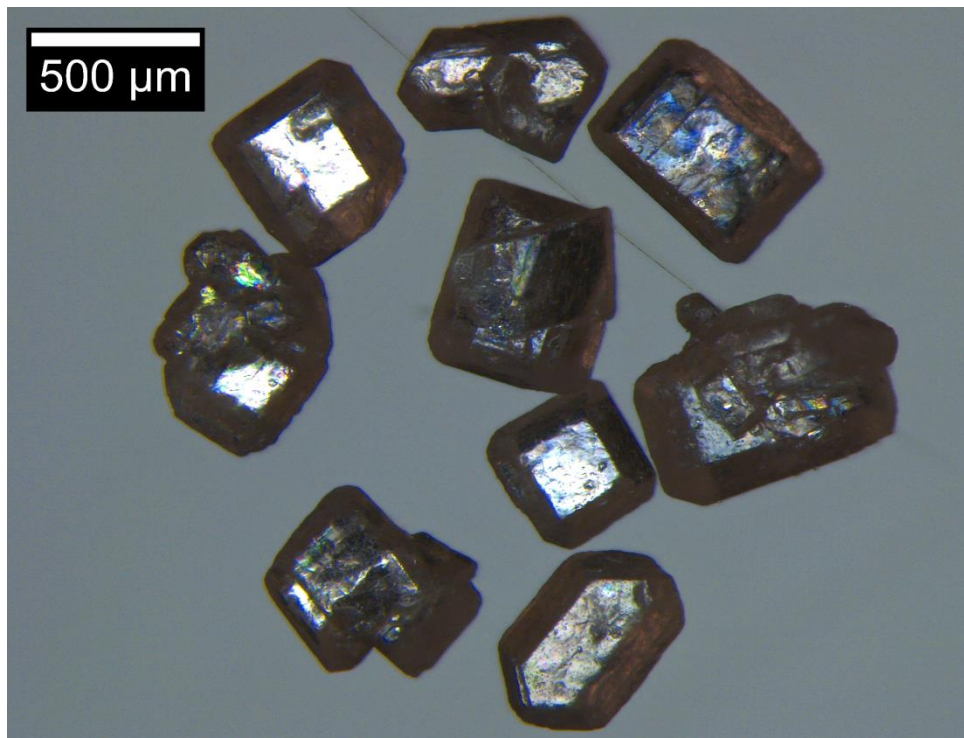
Figure J.18 Appearance of "as is" Pioneer beet sucrose.
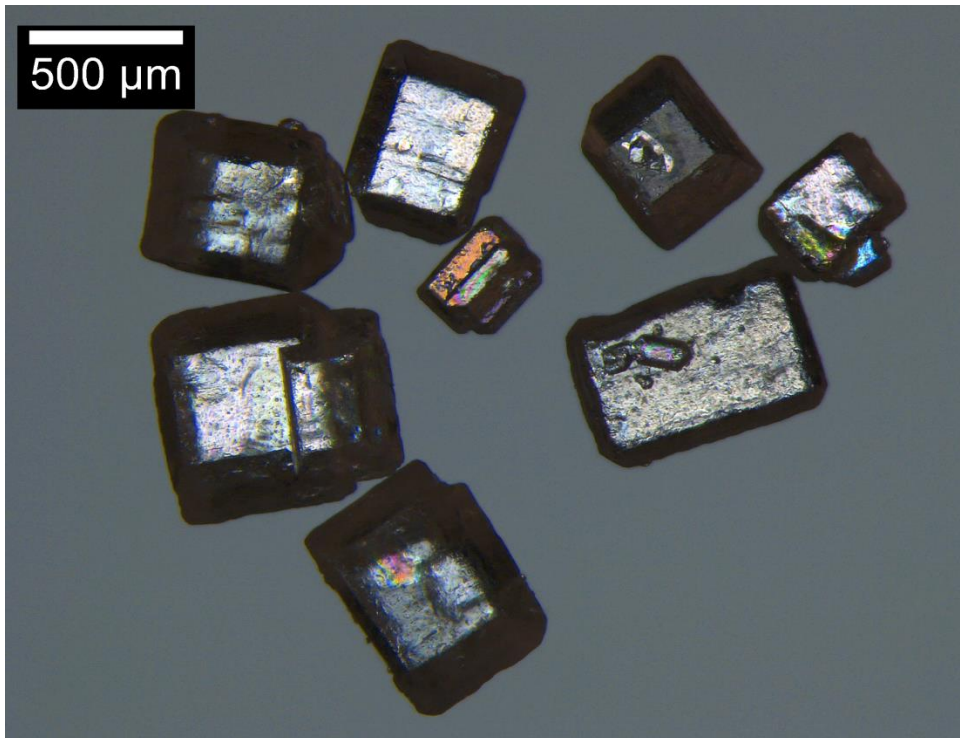
Figure J.19 Appearance of "as is" Meijer beet sucrose.
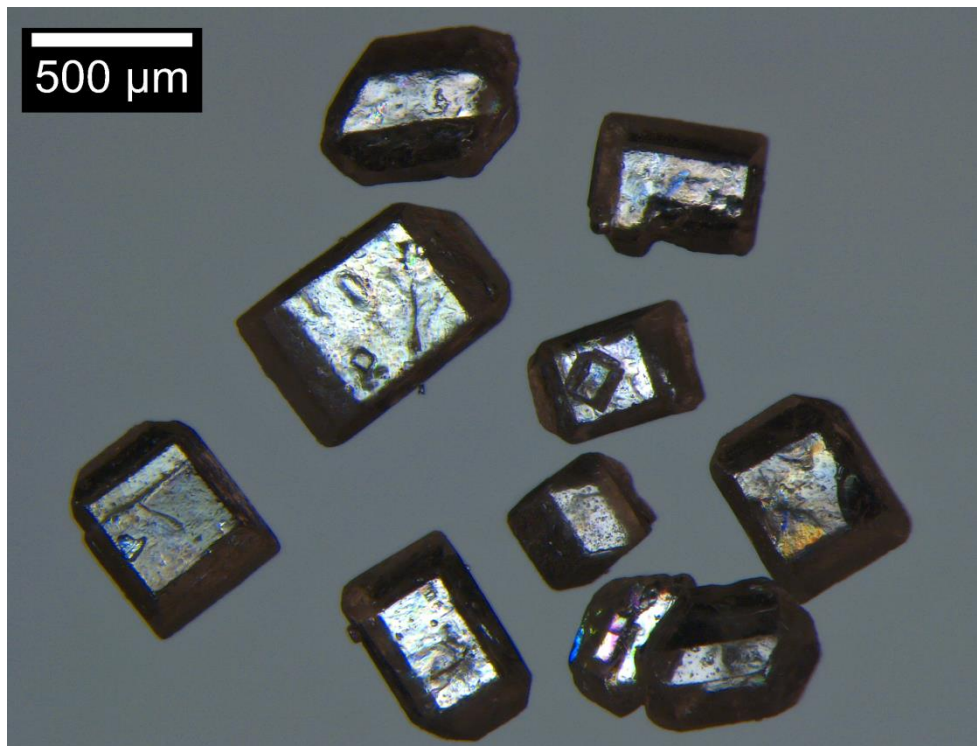
Figure J.20 Appearance of "as is" Market Pantry beet sucrose.

Appendix K HPLC analysis for selected cane, beet and laboratory-recrystallized sucrose samples

Sample Name	Target Temperature °C	Sucrose % (avg±std)	Glucose % (avg±std)	Fructose % (avg±std)
Sigma cane	"as is"	101.25±0.51		
	150	99.31±0.79		
	160	95.04±0.05	2.68±0.41	
	200	37.10±16.26	27.43±7.91	1.87±1.37
US beet	"as is"	103.21±3.46		
	190	100.11±4.03		
	200	98.54±6.99	1.90±0.29	0.35±0.03
Sigma recrystallized in HPLC water	"as is"	101.76±1.58		
	140	99.05±4.58		
	150	74.50±0.48	11.36±1.05	1.28±0.05
	160	52.12±22.84	17.61±16.10	1.54±1.43
Sigma recrystallized with 0.5% K2SO3	"as is"	101.64±2.79		
	160	101.29±1.28		
	170	101.34±0.53		
	180	101.58±2.60		
	190	103.62±0.47		
	200	97.41±2.24	2.77±0.99	

Appendix L Refined structure for analytical grade Sigma cane crystal (CCDC#1473968)

Table L.1 Crystal data and structure refinement for CCDC#1473968.

Identification code	CCDC#1473968
Empirical formula	C12 H22 O11
Formula weight	342.30
Temperature	182(2) K
Wavelength	0.71073 Å
Crystal system	Monoclinic
Space group	P2(1)
Unit cell dimensions	a = 7.7277(10) Å $\quad$ a= 90°
	b = 8.6776(11) Å $\quad$ b= 102.9640(10)°
	c = 10.8341(13) Å $\quad$ g = 90°
Volume	707.99(15) Å^3
Z	2
Density (calculated)	1.606 Mg/m^3
Absorption coefficient	0.144 mm^{-1}
F(000)	364
Crystal size	0.451 x 0.377 x 0.362 mm^3
Theta range for data collection	1.93 to 26.32°
Index ranges	-9<=h<=9, -10<=k<=10, -13<=l<=13
Reflections collected	8132
Independent reflections	2882 [R(int) = 0.0319]
Completeness to theta = 26.32°	99.9 %
Absorption correction	Integration
Max. and min. transmission	0.9985 and 0.9038
Refinement method	Full-matrix least-squares on F^2
Data / restraints / parameters	2882 / 1 / 274
Goodness-of-fit on F^2	1.039
Final R indices [I>2sigma(I)]	R1 = 0.0290, wR2 = 0.0681
R indices (all data)	R1 = 0.0306, wR2 = 0.0690
Absolute structure parameter	-0.7(7)
Largest diff. peak and hole	0.164 and -0.175 e.Å^{-3}

Table L.2 Atomic coordinates (x 10^4) and equivalent isotropic displacement parameters (Å^2x 10^3) for CCDC#1473968. U(eq) is defined as one third of the trace of the orthogonalized U^{ij} tensor.

	x	y	z	U
C(1)	5135(2)	3143(2)	6997(1)	14(1)
C(2)	3630(2)	1972(2)	6868(2)	16(1)
C(3)	4344(2)	349(2)	7142(2)	17(1)
C(4)	5565(2)	2(2)	6254(2)	18(1)
C(5)	7041(2)	1200(2)	6399(2)	16(1)
C(6)	8160(2)	1011(2)	5414(2)	20(1)
C(7)	6296(2)	4791(2)	8762(1)	14(1)
C(8)	8709(2)	6116(2)	8231(2)	16(1)
C(9)	9450(2)	5070(2)	9348(1)	14(1)
C(10)	7858(2)	4820(2)	9936(1)	15(1)
C(11)	4548(2)	5401(2)	8980(2)	16(1)
C(12)	9513(2)	5910(2)	7096(2)	20(1)
O(1)	6312(1)	2737(1)	6220(1)	16(1)
O(2)	2499(2)	2363(2)	7708(1)	19(1)
O(3)	2950(2)	-772(2)	6910(1)	24(1)
O(4)	6450(2)	-1429(2)	6510(1)	28(1)
O(5)	7128(2)	1269(2)	4166(1)	22(1)
O(6)	6087(1)	3245(1)	8292(1)	14(1)
O(7)	6818(1)	5780(1)	7878(1)	16(1)
O(8)	10904(2)	5777(2)	10216(1)	19(1)
O(9)	7970(2)	3548(2)	10755(1)	18(1)
O(10)	3781(2)	4342(2)	9718(1)	19(1)
O(11)	9593(2)	4332(2)	6728(1)	21(1)

Table L.3 Bond lengths [Å] and angles [°] for CCDC#1473968.

C(1)-O(1)	1.4154(19)
C(1)-O(6)	1.4339(18)
C(1)-C(2)	1.527(2)
C(1)-H(1A)	0.93(2)
C(2)-O(2)	1.437(2)
C(2)-C(3)	1.518(2)
C(2)-H(2A)	0.966(19)
C(3)-O(3)	1.431(2)
C(3)-C(4)	1.521(2)
C(3)-H(3A)	0.94(2)
C(4)-O(4)	1.415(2)
C(4)-C(5)	1.525(2)
C(4)-H(4A)	0.961(19)
C(5)-O(1)	1.444(2)
C(5)-C(6)	1.525(2)
C(5)-H(5A)	0.954(19)
C(6)-O(5)	1.425(2)
C(6)-H(6A)	0.98(2)
C(6)-H(6B)	1.00(2)
C(7)-O(7)	1.4101(19)
C(7)-O(6)	1.4311(19)
C(7)-C(11)	1.518(2)
C(7)-C(10)	1.545(2)
C(8)-O(7)	1.4542(19)
C(8)-C(12)	1.508(2)
C(8)-C(9)	1.519(2)
C(8)-H(8A)	0.94(2)
C(9)-O(8)	1.4306(19)
C(9)-C(10)	1.522(2)
C(9)-H(9A)	0.96(2)
C(10)-O(9)	1.4075(19)
C(10)-H(10A)	0.99(2)
C(11)-O(10)	1.431(2)
C(11)-H(11A)	0.990(18)
C(11)-H(11B)	1.01(2)
C(12)-O(11)	1.431(2)
C(12)-H(12A)	0.99(2)
C(12)-H(12B)	0.99(2)
O(2)-H(2)	0.84(2)
O(3)-H(3)	0.79(2)
O(4)-H(4)	0.74(3)
O(5)-H(5)	0.81(3)
O(8)-H(8)	0.83(2)

Table L.3 continued.

O(9)-H(9)	0.80(2)
O(10)-H(10)	0.80(2)
O(11)-H(11)	0.88(2)
O(1)-C(1)-O(6)	109.89(12)
O(1)-C(1)-C(2)	110.96(12)
O(6)-C(1)-C(2)	110.10(12)
O(1)-C(1)-H(1A)	105.1(12)
O(6)-C(1)-H(1A)	109.6(11)
C(2)-C(1)-H(1A)	111.1(12)
O(2)-C(2)-C(3)	109.97(13)
O(2)-C(2)-C(1)	110.10(13)
C(3)-C(2)-C(1)	111.32(13)
O(2)-C(2)-H(2A)	107.0(11)
C(3)-C(2)-H(2A)	109.2(12)
C(1)-C(2)-H(2A)	109.1(12)
O(3)-C(3)-C(2)	111.70(14)
O(3)-C(3)-C(4)	107.68(13)
C(2)-C(3)-C(4)	108.07(14)
O(3)-C(3)-H(3A)	110.5(12)
C(2)-C(3)-H(3A)	108.4(13)
C(4)-C(3)-H(3A)	110.5(11)
O(4)-C(4)-C(3)	113.01(14)
O(4)-C(4)-C(5)	105.11(14)
C(3)-C(4)-C(5)	110.81(14)
O(4)-C(4)-H(4A)	112.4(13)
C(3)-C(4)-H(4A)	107.2(11)
C(5)-C(4)-H(4A)	108.3(12)
O(1)-C(5)-C(4)	110.83(12)
O(1)-C(5)-C(6)	105.71(14)
C(4)-C(5)-C(6)	112.49(13)
O(1)-C(5)-H(5A)	112.2(12)
C(4)-C(5)-H(5A)	107.9(12)
C(6)-C(5)-H(5A)	107.7(11)
O(5)-C(6)-C(5)	111.25(14)
O(5)-C(6)-H(6A)	110.0(12)
C(5)-C(6)-H(6A)	111.5(12)
O(5)-C(6)-H(6B)	108.5(12)
C(5)-C(6)-H(6B)	107.6(11)
H(6A)-C(6)-H(6B)	107.9(17)
O(7)-C(7)-O(6)	110.83(12)
O(7)-C(7)-C(11)	107.10(13)
O(6)-C(7)-C(11)	110.40(13)
O(7)-C(7)-C(10)	105.02(12)

Table L.3 continued.

O(6)-C(7)-C(10)	108.24(12)
C(11)-C(7)-C(10)	115.12(13)
O(7)-C(8)-C(12)	109.61(13)
O(7)-C(8)-C(9)	105.45(12)
C(12)-C(8)-C(9)	115.35(14)
O(7)-C(8)-H(8A)	107.5(12)
C(12)-C(8)-H(8A)	108.0(12)
C(9)-C(8)-H(8A)	110.6(11)
O(8)-C(9)-C(8)	111.58(14)
O(8)-C(9)-C(10)	112.08(13)
C(8)-C(9)-C(10)	102.87(12)
O(8)-C(9)-H(9A)	111.0(11)
C(8)-C(9)-H(9A)	109.9(11)
C(10)-C(9)-H(9A)	109.1(11)
O(9)-C(10)-C(9)	115.75(13)
O(9)-C(10)-C(7)	115.63(13)
C(9)-C(10)-C(7)	102.34(12)
O(9)-C(10)-H(10A)	107.7(11)
C(9)-C(10)-H(10A)	108.3(11)
C(7)-C(10)-H(10A)	106.5(11)
O(10)-C(11)-C(7)	110.93(14)
O(10)-C(11)-H(11A)	110.1(11)
C(7)-C(11)-H(11A)	107.9(11)
O(10)-C(11)-H(11B)	109.8(11)
C(7)-C(11)-H(11B)	108.0(12)
H(11A)-C(11)-H(11B)	110.1(16)
O(11)-C(12)-C(8)	113.12(14)
O(11)-C(12)-H(12A)	101.4(12)
C(8)-C(12)-H(12A)	111.8(11)
O(11)-C(12)-H(12B)	109.8(12)
C(8)-C(12)-H(12B)	111.0(12)
H(12A)-C(12)-H(12B)	109.2(17)
C(1)-O(1)-C(5)	115.71(12)
C(2)-O(2)-H(2)	110.5(14)
C(3)-O(3)-H(3)	109.2(18)
C(4)-O(4)-H(4)	110(2)
C(6)-O(5)-H(5)	108.0(16)
C(7)-O(6)-C(1)	113.46(12)
C(7)-O(7)-C(8)	111.57(11)
C(9)-O(8)-H(8)	103.5(15)
C(10)-O(9)-H(9)	110.5(16)
C(11)-O(10)-H(10)	106.1(16)
C(12)-O(11)-H(11)	106.4(15)

Table L.4 Anisotropic displacement parameters ($Å^2 x 10^3$) for CCDC#1473968. The anisotropic displacement factor exponent takes the form: $-2p^2[h^2 a^{*2}U^{11} + ... + 2 h k a^* b^* U^{12}]$

	U^{11}	U^{22}	U^{33}	U^{23}	U^{13}	U^{12}
C(1)	16(1)	14(1)	12(1)	0(1)	5(1)	1(1)
C(2)	16(1)	19(1)	13(1)	-2(1)	4(1)	0(1)
C(3)	20(1)	16(1)	15(1)	-1(1)	5(1)	-3(1)
C(4)	23(1)	15(1)	18(1)	1(1)	7(1)	3(1)
C(5)	17(1)	16(1)	16(1)	-1(1)	5(1)	5(1)
C(6)	18(1)	21(1)	23(1)	-4(1)	8(1)	0(1)
C(7)	15(1)	10(1)	17(1)	0(1)	5(1)	-1(1)
C(8)	12(1)	14(1)	21(1)	0(1)	4(1)	-1(1)
C(9)	13(1)	13(1)	16(1)	-3(1)	3(1)	-1(1)
C(10)	15(1)	14(1)	16(1)	-1(1)	5(1)	0(1)
C(11)	13(1)	16(1)	20(1)	-1(1)	5(1)	0(1)
C(12)	18(1)	20(1)	21(1)	3(1)	7(1)	-2(1)
O(1)	18(1)	14(1)	16(1)	0(1)	8(1)	1(1)
O(2)	15(1)	22(1)	22(1)	-1(1)	7(1)	1(1)
O(3)	33(1)	20(1)	24(1)	-5(1)	16(1)	-11(1)
O(4)	31(1)	14(1)	44(1)	3(1)	17(1)	4(1)
O(5)	30(1)	21(1)	18(1)	-2(1)	11(1)	-5(1)
O(6)	16(1)	11(1)	14(1)	-1(1)	3(1)	1(1)
O(7)	13(1)	17(1)	18(1)	4(1)	3(1)	-2(1)
O(8)	12(1)	23(1)	22(1)	-4(1)	2(1)	-1(1)
O(9)	21(1)	17(1)	16(1)	2(1)	6(1)	2(1)
O(10)	18(1)	22(1)	20(1)	-3(1)	10(1)	-2(1)
O(11)	17(1)	23(1)	25(1)	-4(1)	9(1)	-1(1)

Table L.5 Hydrogen coordinates (x 10^4) and isotropic displacement parameters (Å^2x 10 ^{3}) for CCDC#1473968.

	x	y	z	U(eq)
H(1A)	4700(20)	4110(30)	6712(17)	17
H(2A)	2910(20)	2010(20)	6017(18)	19
H(3A)	4980(20)	300(20)	7992(19)	20
H(4A)	4860(20)	60(20)	5404(18)	22
H(5A)	7810(20)	1070(20)	7215(18)	19
H(6A)	9190(30)	1700(30)	5586(19)	24
H(6B)	8610(30)	-70(30)	5470(19)	24
H(8A)	8830(20)	7160(30)	8476(17)	19
H(9A)	9800(20)	4100(20)	9052(17)	17
H(10A)	7700(20)	5760(30)	10424(16)	18
H(11A)	3740(20)	5560(20)	8142(17)	19
H(11B)	4790(30)	6420(30)	9440(17)	19
H(12A)	10780(30)	6200(30)	7285(17)	23
H(12B)	8860(30)	6530(30)	6366(19)	23
H(2)	1630(30)	2890(30)	7327(19)	29
H(3)	2660(30)	-950(30)	7550(20)	36
H(4)	5790(30)	-2050(30)	6520(20)	42
H(5)	7180(30)	2180(30)	4010(20)	33
H(8)	11780(30)	5270(30)	10122(19)	29
H(9)	8220(30)	2780(30)	10420(19)	27
H(10)	3440(30)	3620(30)	9260(20)	29
H(11)	8500(30)	3980(30)	6570(20)	31

Table L.6 Torsion angles [°] for CCDC#1473968.

O(1)-C(1)-C(2)-O(2)	177.21(12)
O(6)-C(1)-C(2)-O(2)	55.35(17)
O(1)-C(1)-C(2)-C(3)	54.99(17)
O(6)-C(1)-C(2)-C(3)	-66.88(16)
O(2)-C(2)-C(3)-O(3)	63.09(16)
C(1)-C(2)-C(3)-O(3)	-174.61(12)
O(2)-C(2)-C(3)-C(4)	-178.65(13)
C(1)-C(2)-C(3)-C(4)	-56.34(16)
O(3)-C(3)-C(4)-O(4)	-65.13(18)
C(2)-C(3)-C(4)-O(4)	174.07(14)
O(3)-C(3)-C(4)-C(5)	177.19(13)
C(2)-C(3)-C(4)-C(5)	56.39(16)
O(4)-C(4)-C(5)-O(1)	-177.25(13)
C(3)-C(4)-C(5)-O(1)	-54.84(17)
O(4)-C(4)-C(5)-C(6)	64.65(17)
C(3)-C(4)-C(5)-C(6)	-172.95(14)
O(1)-C(5)-C(6)-O(5)	-56.97(17)
C(4)-C(5)-C(6)-O(5)	64.11(19)
O(7)-C(8)-C(9)-O(8)	-147.40(13)
C(12)-C(8)-C(9)-O(8)	91.52(17)
O(7)-C(8)-C(9)-C(10)	-27.07(16)
C(12)-C(8)-C(9)-C(10)	-148.15(14)
O(8)-C(9)-C(10)-O(9)	-78.29(18)
C(8)-C(9)-C(10)-O(9)	161.72(13)
O(8)-C(9)-C(10)-C(7)	155.04(13)
C(8)-C(9)-C(10)-C(7)	35.06(16)
O(7)-C(7)-C(10)-O(9)	-157.91(13)
O(6)-C(7)-C(10)-O(9)	-39.48(18)
C(11)-C(7)-C(10)-O(9)	84.57(17)
O(7)-C(7)-C(10)-C(9)	-31.17(16)
O(6)-C(7)-C(10)-C(9)	87.26(15)
C(11)-C(7)-C(10)-C(9)	-148.69(14)
O(7)-C(7)-C(11)-O(10)	171.32(12)
O(6)-C(7)-C(11)-O(10)	50.56(17)
C(10)-C(7)-C(11)-O(10)	-72.34(17)
O(7)-C(8)-C(12)-O(11)	-70.19(17)
C(9)-C(8)-C(12)-O(11)	48.6(2)
O(6)-C(1)-O(1)-C(5)	67.72(16)
C(2)-C(1)-O(1)-C(5)	-54.27(17)
C(4)-C(5)-O(1)-C(1)	54.54(16)
C(6)-C(5)-O(1)-C(1)	176.69(12)
O(7)-C(7)-O(6)-C(1)	-45.00(16)
C(11)-C(7)-O(6)-C(1)	73.50(15)

Table L.6 continued

C(10)-C(7)-O(6)-C(1)	-159.66(12)
O(1)-C(1)-O(6)-C(7)	108.46(14)
C(2)-C(1)-O(6)-C(7)	-129.04(14)
O(6)-C(7)-O(7)-C(8)	-101.79(14)
C(11)-C(7)-O(7)-C(8)	137.72(13)
C(10)-C(7)-O(7)-C(8)	14.87(16)
C(12)-C(8)-O(7)-C(7)	132.43(14)
C(9)-C(8)-O(7)-C(7)	7.68(17)

Table L.7 Hydrogen bonds for CCDC#1473968 [Å and °].

D-H...A	d(D-H)	d(H...A)	d(D...A)	<(DHA)
O(2)-H(2)...O(11)#1	0.84(2)	2.00(2)	2.8319(19)	170(2)
O(3)-H(3)...O(9)#2	0.79(2)	2.05(2)	2.8392(18)	177(2)
O(4)-H(4)...O(7)#3	0.74(3)	2.41(3)	2.8203(18)	116(2)
O(4)-H(4)...O(5)#4	0.74(3)	2.65(3)	3.356(2)	160(3)
O(5)-H(5)...O(3)#5	0.81(3)	2.03(3)	2.816(2)	163(2)
O(8)-H(8)...O(10)#6	0.83(2)	1.88(2)	2.7063(17)	171(2)
O(9)-H(9)...O(8)#7	0.80(2)	2.04(2)	2.8382(19)	172(2)
O(10)-H(10)...O(2)	0.80(2)	2.00(2)	2.7752(18)	161(2)
O(11)-H(11)...O(1)	0.88(2)	1.97(2)	2.8325(17)	167(2)

Symmetry transformations used to generate equivalent atoms:

#1 x-1,y,z   #2 -x+1,y-1/2,-z+2   #3 x,y-1,z

#4 -x+1,y-1/2,-z+1   #5 -x+1,y+1/2,-z+1   #6 x+1,y,z

#7 -x+2,y-1/2,-z+2

Appendix M Refined structure for US beet crystal (CCDC#1473969)

Table M.1 Crystal data and structure refinement for CCDC#1473969.

Identification code	CCDC#1473969
Empirical formula	C12 H22 O11
Formula weight	342.30
Temperature	182(2) K
Wavelength	0.71073 Å
Crystal system	Monoclinic
Space group	P2(1)
Unit cell dimensions	a = 7.741(2) Å a= 90°
	b = 8.691(2) Å b= 102.981(3)°
	c = 10.853(3) Å g = 90°
Volume	711.5(3) Å^3
Z	2
Density (calculated)	1.598 Mg/m^3
Absorption coefficient	0.143 mm^{-1}
F(000)	364
Crystal size	0.402 x 0.275 x 0.198 mm^3
Theta range for data collection	1.93 to 26.52°
Index ranges	-9<=h<=9, -10<=k<=10, -13<=l<=13
Reflections collected	2964
Independent reflections	2954 [R(int) = 0.0000]
Completeness to theta = 26.52°	99.6 %
Absorption correction	Semi-empirical from equivalents
Max. and min. transmission	0.745374 and 0.358843
Refinement method	Full-matrix least-squares on F^2
Data / restraints / parameters	2954 / 1 / 274
Goodness-of-fit on F^2	0.918
Final R indices [I>2sigma(I)]	R1 = 0.0343, wR2 = 0.0603
R indices (all data)	R1 = 0.0435, wR2 = 0.0631
Absolute structure parameter	-0.6(9)
Largest diff. peak and hole	0.174 and -0.196 e.Å^{-3}

Table M.2 Atomic coordinates (x 10^4) and equivalent isotropic displacement parameters (Å^2x 10^3) for CCDC#1473969. U(eq) is defined as one third of the trace of the orthogonalized U^{ij} tensor.

	x	y	z	U(eq)
C(1)	5135(3)	3147(3)	6997(2)	15(1)
C(2)	3629(3)	1968(3)	6865(2)	17(1)
C(3)	4347(3)	348(3)	7144(2)	17(1)
C(4)	5565(3)	9(3)	6254(2)	18(1)
C(5)	7046(3)	1191(3)	6399(2)	18(1)
C(6)	8156(3)	1002(3)	5417(2)	21(1)
C(7)	6299(3)	4796(2)	8762(2)	15(1)
C(8)	8708(3)	6120(3)	8233(2)	18(1)
C(9)	9454(3)	5071(3)	9345(2)	16(1)
C(10)	7853(3)	4821(3)	9930(2)	15(1)
C(11)	4551(3)	5403(3)	8980(2)	18(1)
C(12)	9512(3)	5914(3)	7094(2)	21(1)
O(1)	6316(2)	2738(2)	6218(1)	17(1)
O(2)	2501(2)	2365(2)	7709(2)	21(1)
O(3)	2958(2)	-777(2)	6910(2)	25(1)
O(4)	6450(2)	-1427(2)	6512(2)	29(1)
O(5)	7128(2)	1266(2)	4169(1)	24(1)
O(6)	6084(2)	3244(2)	8292(1)	14(1)
O(7)	6816(2)	5783(2)	7874(1)	17(1)
O(8)	10901(2)	5776(2)	10215(1)	21(1)
O(9)	7970(2)	3546(2)	10754(1)	19(1)
O(10)	3776(2)	4340(2)	9718(1)	21(1)
O(11)	9598(2)	4332(2)	6728(1)	23(1)

Table M.3 Bond lengths [Å] and angles [°] for CCDC#1473969.

C(1)-O(1)	1.422(2)
C(1)-O(6)	1.434(2)
C(1)-C(2)	1.535(3)
C(1)-H(1A)	0.97(2)
C(2)-O(2)	1.442(3)
C(2)-C(3)	1.519(3)
C(2)-H(2A)	1.01(2)
C(3)-O(3)	1.433(3)
C(3)-C(4)	1.523(3)
C(3)-H(3A)	1.00(2)
C(4)-O(4)	1.421(3)
C(4)-C(5)	1.521(3)
C(4)-H(4A)	0.970(19)
C(5)-O(1)	1.455(3)
C(5)-C(6)	1.521(3)
C(5)-H(5A)	0.958(19)
C(6)-O(5)	1.427(3)
C(6)-H(6A)	1.02(2)
C(6)-H(6B)	1.00(2)
C(7)-O(7)	1.412(2)
C(7)-O(6)	1.439(3)
C(7)-C(11)	1.520(3)
C(7)-C(10)	1.539(3)
C(8)-O(7)	1.458(2)
C(8)-C(12)	1.514(3)
C(8)-C(9)	1.519(3)
C(8)-H(8A)	0.94(2)
C(9)-O(8)	1.431(2)
C(9)-C(10)	1.530(3)
C(9)-H(9A)	1.00(2)
C(10)-O(9)	1.414(2)
C(10)-H(10A)	1.05(2)
C(11)-O(10)	1.439(3)
C(11)-H(11A)	0.988(19)
C(11)-H(11B)	1.05(2)
C(12)-O(11)	1.437(3)
C(12)-H(12A)	0.98(2)
C(12)-H(12B)	1.02(2)
O(2)-H(2)	0.87(2)
O(3)-H(3)	0.83(2)
O(4)-H(4)	0.78(3)
O(5)-H(5)	0.86(3)
O(8)-H(8)	0.78(2)

O(9)-H(9)	0.84(3)
O(10)-H(10)	0.82(2)
O(11)-H(11)	0.85(2)
O(1)-C(1)-O(6)	109.92(16)
O(1)-C(1)-C(2)	110.73(16)
O(6)-C(1)-C(2)	109.98(17)
O(1)-C(1)-H(1A)	104.6(12)
O(6)-C(1)-H(1A)	111.6(12)
C(2)-C(1)-H(1A)	109.9(13)
O(2)-C(2)-C(3)	110.03(17)
O(2)-C(2)-C(1)	109.66(17)
C(3)-C(2)-C(1)	111.35(17)
O(2)-C(2)-H(2A)	107.6(12)
C(3)-C(2)-H(2A)	108.7(12)
C(1)-C(2)-H(2A)	109.4(12)
O(3)-C(3)-C(2)	111.75(17)
O(3)-C(3)-C(4)	107.63(17)
C(2)-C(3)-C(4)	107.72(17)
O(3)-C(3)-H(3A)	110.0(13)
C(2)-C(3)-H(3A)	110.7(13)
C(4)-C(3)-H(3A)	108.8(11)
O(4)-C(4)-C(5)	104.73(17)
O(4)-C(4)-C(3)	112.63(18)
C(5)-C(4)-C(3)	111.28(18)
O(4)-C(4)-H(4A)	109.7(14)
C(5)-C(4)-H(4A)	110.2(12)
C(3)-C(4)-H(4A)	108.3(12)
O(1)-C(5)-C(6)	105.62(18)
O(1)-C(5)-C(4)	110.46(16)
C(6)-C(5)-C(4)	112.68(18)
O(1)-C(5)-H(5A)	108.7(14)
C(6)-C(5)-H(5A)	108.8(12)
C(4)-C(5)-H(5A)	110.4(13)
O(5)-C(6)-C(5)	111.42(17)
O(5)-C(6)-H(6A)	110.6(12)
C(5)-C(6)-H(6A)	110.7(13)
O(5)-C(6)-H(6B)	107.9(13)
C(5)-C(6)-H(6B)	109.9(13)
H(6A)-C(6)-H(6B)	106.2(17)
O(7)-C(7)-O(6)	110.83(15)
O(7)-C(7)-C(11)	107.12(16)
O(6)-C(7)-C(11)	110.14(17)
O(7)-C(7)-C(10)	105.34(16)

O(6)-C(7)-C(10)	108.16(16)
C(11)-C(7)-C(10)	115.15(17)
O(7)-C(8)-C(12)	109.33(17)
O(7)-C(8)-C(9)	105.71(16)
C(12)-C(8)-C(9)	115.13(18)
O(7)-C(8)-H(8A)	110.3(13)
C(12)-C(8)-H(8A)	106.7(13)
C(9)-C(8)-H(8A)	109.7(13)
O(8)-C(9)-C(8)	111.62(19)
O(8)-C(9)-C(10)	111.98(17)
C(8)-C(9)-C(10)	102.49(16)
O(8)-C(9)-H(9A)	111.4(12)
C(8)-C(9)-H(9A)	109.7(12)
C(10)-C(9)-H(9A)	109.2(12)
O(9)-C(10)-C(9)	115.52(18)
O(9)-C(10)-C(7)	115.98(17)
C(9)-C(10)-C(7)	102.49(16)
O(9)-C(10)-H(10A)	106.7(11)
C(9)-C(10)-H(10A)	107.0(11)
C(7)-C(10)-H(10A)	108.7(11)
O(10)-C(11)-C(7)	111.18(18)
O(10)-C(11)-H(11A)	110.7(12)
C(7)-C(11)-H(11A)	108.4(12)
O(10)-C(11)-H(11B)	107.8(12)
C(7)-C(11)-H(11B)	110.0(13)
H(11A)-C(11)-H(11B)	108.8(18)
O(11)-C(12)-C(8)	113.11(18)
O(11)-C(12)-H(12A)	103.4(14)
C(8)-C(12)-H(12A)	111.8(12)
O(11)-C(12)-H(12B)	110.9(13)
C(8)-C(12)-H(12B)	111.3(13)
H(12A)-C(12)-H(12B)	105.9(18)
C(1)-O(1)-C(5)	115.66(16)
C(2)-O(2)-H(2)	111.6(15)
C(3)-O(3)-H(3)	109.7(18)
C(4)-O(4)-H(4)	111(2)
C(6)-O(5)-H(5)	111.0(17)
C(1)-O(6)-C(7)	113.30(15)
C(7)-O(7)-C(8)	111.18(15)
C(9)-O(8)-H(8)	108.4(19)
C(10)-O(9)-H(9)	107.4(17)
C(11)-O(10)-H(10)	103.4(18)
C(12)-O(11)-H(11)	106.7(17)

Table M.4 Anisotropic displacement parameters ($Å^2$ x 10^3) for CCDC#1473969. The anisotropic displacement factor exponent takes the form: $-2p^2[h^2 a^{*2}U^{11} + ... + 2hk a^* b^* U^{12}]$

	U^{11}	U^{22}	U^{33}	U^{23}	U^{13}	U^{12}
C(1)	15(1)	16(1)	13(1)	-1(1)	3(1)	1(1)
C(2)	17(1)	19(1)	14(1)	-2(1)	3(1)	1(1)
C(3)	20(1)	15(1)	16(1)	-1(1)	4(1)	-4(1)
C(4)	23(1)	11(1)	20(1)	3(1)	5(1)	3(1)
C(5)	19(1)	16(1)	17(1)	0(1)	2(1)	4(1)
C(6)	20(1)	22(2)	22(1)	-4(1)	5(1)	-1(1)
C(7)	15(1)	13(1)	18(1)	0(1)	4(1)	-1(1)
C(8)	13(1)	15(1)	24(1)	-2(1)	3(1)	-4(1)
C(9)	13(1)	18(1)	17(1)	-5(1)	4(1)	-1(1)
C(10)	18(1)	14(1)	15(1)	1(1)	4(1)	0(1)
C(11)	14(1)	19(1)	20(1)	0(1)	5(1)	2(1)
C(12)	20(1)	22(2)	21(1)	2(1)	6(1)	-1(1)
O(1)	19(1)	16(1)	18(1)	0(1)	7(1)	1(1)
O(2)	17(1)	22(1)	24(1)	-1(1)	7(1)	1(1)
O(3)	34(1)	22(1)	25(1)	-6(1)	16(1)	-12(1)
O(4)	30(1)	15(1)	46(1)	4(1)	16(1)	3(1)
O(5)	31(1)	25(1)	19(1)	-2(1)	10(1)	-6(1)
O(6)	17(1)	11(1)	14(1)	-1(1)	1(1)	0(1)
O(7)	13(1)	18(1)	19(1)	6(1)	3(1)	-1(1)
O(8)	12(1)	26(1)	24(1)	-4(1)	2(1)	0(1)
O(9)	22(1)	18(1)	18(1)	2(1)	5(1)	2(1)
O(10)	20(1)	24(1)	22(1)	-3(1)	10(1)	-2(1)
O(11)	18(1)	26(1)	26(1)	-6(1)	8(1)	-2(1)

Table M.5 Hydrogen coordinates (x 10^4) and isotropic displacement parameters (Å^2x 10^3) for CCDC#1473969.

	x	y	z	U(eq)
H(1A)	4660(30)	4140(30)	6676(19)	18
H(2A)	2880(30)	2000(20)	5980(20)	20
H(3A)	5050(20)	260(30)	8039(19)	21
H(4A)	4860(30)	10(30)	5394(18)	21
H(5A)	7810(30)	1130(30)	7225(19)	21
H(6A)	9230(30)	1710(30)	5610(20)	25
H(6B)	8640(30)	-70(30)	5450(20)	25
H(8A)	8890(30)	7150(30)	8484(19)	21
H(9A)	9810(30)	4060(30)	9029(18)	19
H(10A)	7740(20)	5800(30)	10468(17)	19
H(11A)	3740(30)	5580(30)	8149(18)	21
H(11B)	4760(30)	6450(30)	9478(18)	21
H(12A)	10760(30)	6250(30)	7270(18)	25
H(12B)	8870(30)	6570(30)	6350(20)	25
H(2)	1640(30)	2970(30)	7340(20)	31
H(3)	2600(30)	-920(30)	7570(20)	38
H(4)	5780(40)	-2100(30)	6480(20)	44
H(5)	7220(30)	2210(30)	3940(20)	37
H(8)	11780(30)	5390(30)	10140(20)	32
H(9)	8180(30)	2770(30)	10360(20)	29
H(10)	3440(30)	3630(30)	9230(20)	31
H(11)	8540(30)	3990(30)	6560(20)	34

Table M.6 Torsion angles [°] for CCDC#1473969.

O(1)-C(1)-C(2)-O(2)	177.19(16)
O(6)-C(1)-C(2)-O(2)	55.5(2)
O(1)-C(1)-C(2)-C(3)	55.2(2)
O(6)-C(1)-C(2)-C(3)	-66.5(2)
O(2)-C(2)-C(3)-O(3)	63.6(2)
C(1)-C(2)-C(3)-O(3)	-174.64(17)
O(2)-C(2)-C(3)-C(4)	-178.42(17)
C(1)-C(2)-C(3)-C(4)	-56.6(2)
O(3)-C(3)-C(4)-O(4)	-65.0(2)
C(2)-C(3)-C(4)-O(4)	174.32(17)
O(3)-C(3)-C(4)-C(5)	177.72(17)
C(2)-C(3)-C(4)-C(5)	57.1(2)
O(4)-C(4)-C(5)-O(1)	-177.20(16)
C(3)-C(4)-C(5)-O(1)	-55.2(2)
O(4)-C(4)-C(5)-C(6)	64.9(2)
C(3)-C(4)-C(5)-C(6)	-173.11(18)
O(1)-C(5)-C(6)-O(5)	-56.7(2)
C(4)-C(5)-C(6)-O(5)	64.0(3)
O(7)-C(8)-C(9)-O(8)	-147.26(16)
C(12)-C(8)-C(9)-O(8)	91.9(2)
O(7)-C(8)-C(9)-C(10)	-27.3(2)
C(12)-C(8)-C(9)-C(10)	-148.05(19)
O(8)-C(9)-C(10)-O(9)	-78.1(2)
C(8)-C(9)-C(10)-O(9)	162.18(17)
O(8)-C(9)-C(10)-C(7)	154.85(17)
C(8)-C(9)-C(10)-C(7)	35.1(2)
O(7)-C(7)-C(10)-O(9)	-157.89(16)
O(6)-C(7)-C(10)-O(9)	-39.3(2)
C(11)-C(7)-C(10)-O(9)	84.3(2)
O(7)-C(7)-C(10)-C(9)	-31.1(2)
O(6)-C(7)-C(10)-C(9)	87.46(19)
C(11)-C(7)-C(10)-C(9)	-148.88(19)
O(7)-C(7)-C(11)-O(10)	170.93(16)
O(6)-C(7)-C(11)-O(10)	50.3(2)
C(10)-C(7)-C(11)-O(10)	-72.3(2)
O(7)-C(8)-C(12)-O(11)	-70.5(2)
C(9)-C(8)-C(12)-O(11)	48.3(3)
O(6)-C(1)-O(1)-C(5)	67.6(2)
C(2)-C(1)-O(1)-C(5)	-54.1(2)
C(6)-C(5)-O(1)-C(1)	176.58(15)
C(4)-C(5)-O(1)-C(1)	54.5(2)
O(1)-C(1)-O(6)-C(7)	108.32(18)
C(2)-C(1)-O(6)-C(7)	-129.51(17)

Table M.6 continued

O(7)-C(7)-O(6)-C(1)	-44.6(2)
C(11)-C(7)-O(6)-C(1)	73.79(19)
C(10)-C(7)-O(6)-C(1)	-159.58(16)
O(6)-C(7)-O(7)-C(8)	-102.17(18)
C(11)-C(7)-O(7)-C(8)	137.65(17)
C(10)-C(7)-O(7)-C(8)	14.6(2)
C(12)-C(8)-O(7)-C(7)	132.64(18)
C(9)-C(8)-O(7)-C(7)	8.1(2)

Table M.7 Hydrogen bonds for CCDC#1473969 [Å and °].

D-H...A	d(D-H)	d(H...A)	d(D...A)	<(DHA)
O(2)-H(2)...O(11)#1	0.87(2)	1.97(3)	2.833(2)	173(2)
O(3)-H(3)...O(9)#2	0.83(2)	2.02(2)	2.846(2)	172(3)
O(4)-H(4)...O(7)#3	0.78(3)	2.41(3)	2.821(2)	115(2)
O(4)-H(4)...O(5)#4	0.78(3)	2.62(3)	3.364(2)	161(3)
O(5)-H(5)...O(3)#5	0.86(3)	1.97(3)	2.820(3)	167(2)
O(8)-H(8)...O(10)#6	0.78(2)	1.93(2)	2.710(2)	172(2)
O(9)-H(9)...O(8)#7	0.84(3)	2.02(3)	2.842(2)	166(2)
O(10)-H(10)...O(2)	0.82(2)	1.98(2)	2.776(2)	165(3)
O(11)-H(11)...O(1)	0.85(2)	2.00(2)	2.837(2)	167(2)

Symmetry transformations used to generate equivalent atoms:

#1 x-1,y,z   #2 -x+1,y-1/2,-z+2   #3 x,y-1,z

#4 -x+1,y-1/2,-z+1   #5 -x+1,y+1/2,-z+1   #6 x+1,y,z

#7 -x+2,y-1/2,-z+2

Appendix N Refined structure for US cane crystal (CCDC#1473970)

Table N.1 Crystal data and structure refinement for CCDC#1473970.

Identification code	CCDC#1473970	
Empirical formula	C12 H22 O11	
Formula weight	342.30	
Temperature	173(2) K	
Wavelength	0.71073 Å	
Crystal system	Monoclinic	
Space group	P2(1)	
Unit cell dimensions	a = 7.7376(15) Å	a= 90°
	b = 8.6930(16) Å	b= 102.991(2)°
	c = 10.833(2) Å	g = 90°
Volume	710.0(2) Å^3	
Z	2	
Density (calculated)	1.601 Mg/m^3	
Absorption coefficient	0.143 mm^{-1}	
F(000)	364	
Crystal size	0.294 x 0.281 x 0.164 mm^3	
Theta range for data collection	2.70 to 30.52°.	
Index ranges	-11<=h<=11, -12<=k<=12, -15<=l<=15	
Reflections collected	19351	
Independent reflections	4314 [R(int) = 0.0330]	
Completeness to theta = 30.52°	99.7 %	
Absorption correction	Integration	
Max. and min. transmission	0.9796 and 0.9647	
Refinement method	Full-matrix least-squares on F^2	
Data / restraints / parameters	4314 / 1 / 233	
Goodness-of-fit on F^2	1.029	
Final R indices [I>2sigma(I)]	R1 = 0.0292, wR2 = 0.0758	
R indices (all data)	R1 = 0.0313, wR2 = 0.0771	
Absolute structure parameter	-0.3(5)	
Largest diff. peak and hole	0.342 and -0.199 e.Å^{-3}	

Table N.2 Atomic coordinates (x 10^4) and equivalent isotropic displacement parameters ($Å^2$x 10^3) for CCDC#1473970. U(eq) is defined as one third of the trace of the orthogonalized U^{ij} tensor.

	x	y	z	U(eq)
C(1)	5138(1)	3142(1)	7001(1)	12(1)
C(2)	3626(1)	1971(1)	6868(1)	13(1)
C(3)	4345(2)	343(1)	7147(1)	14(1)
C(4)	5564(2)	3(1)	6250(1)	15(1)
C(5)	7047(1)	1200(1)	6404(1)	14(1)
C(6)	8157(2)	1008(1)	5414(1)	18(1)
C(7)	6296(1)	4796(1)	8764(1)	11(1)
C(8)	8706(1)	6120(1)	8231(1)	13(1)
C(9)	9452(1)	5068(1)	9350(1)	12(1)
C(10)	7855(1)	4824(1)	9935(1)	11(1)
C(11)	4544(1)	5403(1)	8980(1)	14(1)
C(12)	9515(1)	5911(1)	7094(1)	17(1)
O(1)	6312(1)	2738(1)	6220(1)	13(1)
O(2)	2501(1)	2365(1)	7709(1)	16(1)
O(3)	2947(1)	-773(1)	6912(1)	21(1)
O(4)	6448(1)	-1432(1)	6508(1)	24(1)
O(5)	7128(1)	1270(1)	4167(1)	20(1)
O(6)	6084(1)	3245(1)	8292(1)	11(1)
O(7)	6816(1)	5783(1)	7875(1)	13(1)
O(8)	10904(1)	5776(1)	10215(1)	17(1)
O(9)	7972(1)	3544(1)	10754(1)	15(1)
O(10)	3778(1)	4340(1)	9717(1)	17(1)
O(11)	9591(1)	4332(1)	6726(1)	19(1)

Table N.3 Bond lengths [Å] and angles [°] for CCDC#1473970.

C(1)-O(1)	1.4176(13)
C(1)-O(6)	1.4278(13)
C(1)-C(2)	1.5339(15)
C(1)-H(1A)	1.0000
C(2)-O(2)	1.4353(13)
C(2)-C(3)	1.5256(15)
C(2)-H(2A)	1.0000
C(3)-O(3)	1.4330(14)
C(3)-C(4)	1.5272(15)
C(3)-H(3A)	1.0000
C(4)-O(4)	1.4195(14)
C(4)-C(5)	1.5303(16)
C(4)-H(4A)	1.0000
C(5)-O(1)	1.4484(13)
C(5)-C(6)	1.5271(15)
C(5)-H(5A)	1.0000
C(6)-O(5)	1.4239(15)
C(6)-H(6A)	0.9900
C(6)-H(6B)	0.9900
C(7)-O(7)	1.4140(12)
C(7)-O(6)	1.4386(13)
C(7)-C(11)	1.5213(14)
C(7)-C(10)	1.5415(15)
C(8)-O(7)	1.4553(12)
C(8)-C(12)	1.5132(15)
C(8)-C(9)	1.5241(15)
C(8)-H(8A)	1.0000
C(9)-O(8)	1.4301(13)
C(9)-C(10)	1.5250(15)
C(9)-H(9A)	1.0000
C(10)-O(9)	1.4135(13)
C(10)-H(10A)	1.0000
C(11)-O(10)	1.4331(14)
C(11)-H(11A)	0.9900
C(11)-H(11B)	0.9900
C(12)-O(11)	1.4340(15)
C(12)-H(12A)	0.9900
C(12)-H(12B)	0.9900
O(2)-H(2)	0.860(19)
O(3)-H(3)	0.81(2)
O(4)-H(4)	0.75(2)
O(5)-H(5)	0.78(2)
O(8)-H(8)	0.871(18)

O(9)-H(9)	0.83(2)
O(10)-H(10)	0.81(2)
O(11)-H(11)	0.873(19)
O(1)-C(1)-O(6)	110.15(8)
O(1)-C(1)-C(2)	110.92(8)
O(6)-C(1)-C(2)	110.20(8)
O(1)-C(1)-H(1A)	108.5
O(6)-C(1)-H(1A)	108.5
C(2)-C(1)-H(1A)	108.5
O(2)-C(2)-C(3)	110.02(9)
O(2)-C(2)-C(1)	109.91(9)
C(3)-C(2)-C(1)	111.12(9)
O(2)-C(2)-H(2A)	108.6
C(3)-C(2)-H(2A)	108.6
C(1)-C(2)-H(2A)	108.6
O(3)-C(3)-C(2)	111.43(9)
O(3)-C(3)-C(4)	107.77(9)
C(2)-C(3)-C(4)	107.71(9)
O(3)-C(3)-H(3A)	110.0
C(2)-C(3)-H(3A)	110.0
C(4)-C(3)-H(3A)	110.0
O(4)-C(4)-C(3)	112.62(9)
O(4)-C(4)-C(5)	105.08(9)
C(3)-C(4)-C(5)	110.72(9)
O(4)-C(4)-H(4A)	109.4
C(3)-C(4)-H(4A)	109.4
C(5)-C(4)-H(4A)	109.4
O(1)-C(5)-C(6)	105.66(9)
O(1)-C(5)-C(4)	110.57(8)
C(6)-C(5)-C(4)	112.04(9)
O(1)-C(5)-H(5A)	109.5
C(6)-C(5)-H(5A)	109.5
C(4)-C(5)-H(5A)	109.5
O(5)-C(6)-C(5)	111.44(9)
O(5)-C(6)-H(6A)	109.3
C(5)-C(6)-H(6A)	109.3
O(5)-C(6)-H(6B)	109.3
C(5)-C(6)-H(6B)	109.3
H(6A)-C(6)-H(6B)	108.0
O(7)-C(7)-O(6)	110.69(8)
O(7)-C(7)-C(11)	107.12(8)
O(6)-C(7)-C(11)	110.18(8)
O(7)-C(7)-C(10)	105.11(8)

347

O(6)-C(7)-C(10)	108.28(8)
C(11)-C(7)-C(10)	115.34(9)
O(7)-C(8)-C(12)	109.59(9)
O(7)-C(8)-C(9)	105.57(8)
C(12)-C(8)-C(9)	115.05(9)
O(7)-C(8)-H(8A)	108.8
C(12)-C(8)-H(8A)	108.8
C(9)-C(8)-H(8A)	108.8
O(8)-C(9)-C(8)	111.37(9)
O(8)-C(9)-C(10)	112.21(9)
C(8)-C(9)-C(10)	102.49(8)
O(8)-C(9)-H(9A)	110.2
C(8)-C(9)-H(9A)	110.2
C(10)-C(9)-H(9A)	110.2
O(9)-C(10)-C(9)	115.26(8)
O(9)-C(10)-C(7)	115.56(9)
C(9)-C(10)-C(7)	102.57(8)
O(9)-C(10)-H(10A)	107.7
C(9)-C(10)-H(10A)	107.7
C(7)-C(10)-H(10A)	107.7
O(10)-C(11)-C(7)	110.88(9)
O(10)-C(11)-H(11A)	109.5
C(7)-C(11)-H(11A)	109.5
O(10)-C(11)-H(11B)	109.5
C(7)-C(11)-H(11B)	109.5
H(11A)-C(11)-H(11B)	108.1
O(11)-C(12)-C(8)	113.02(9)
O(11)-C(12)-H(12A)	109.0
C(8)-C(12)-H(12A)	109.0
O(11)-C(12)-H(12B)	109.0
C(8)-C(12)-H(12B)	109.0
H(12A)-C(12)-H(12B)	107.8
C(1)-O(1)-C(5)	115.52(8)
C(2)-O(2)-H(2)	108.6(12)
C(3)-O(3)-H(3)	109.7(14)
C(4)-O(4)-H(4)	112.6(17)
C(6)-O(5)-H(5)	109.2(14)
C(1)-O(6)-C(7)	113.56(8)
C(7)-O(7)-C(8)	111.38(8)
C(9)-O(8)-H(8)	104.6(12)
C(10)-O(9)-H(9)	109.0(15)
C(11)-O(10)-H(10)	106.3(13)
C(12)-O(11)-H(11)	105.7(13)

Table N.4 Anisotropic displacement parameters Å^{2}x 10^3) for CCDC#1473970. The anisotropic displacement factor exponent takes the form: -2p^2[h^2 a*^{2}U^{11} + ... + 2 h k a* b* U^{12}]

	U^{11}	U^{22}	U^{33}	U^{23}	U^{13}	U^{12}
C(1)	12(1)	12(1)	12(1)	0(1)	4(1)	0(1)
C(2)	13(1)	13(1)	12(1)	-1(1)	3(1)	0(1)
C(3)	17(1)	11(1)	14(1)	-1(1)	5(1)	-2(1)
C(4)	19(1)	11(1)	16(1)	0(1)	6(1)	1(1)
C(5)	15(1)	13(1)	14(1)	0(1)	4(1)	3(1)
C(6)	17(1)	19(1)	19(1)	-3(1)	8(1)	0(1)
C(7)	10(1)	10(1)	13(1)	0(1)	3(1)	0(1)
C(8)	11(1)	12(1)	16(1)	1(1)	4(1)	-1(1)
C(9)	10(1)	13(1)	14(1)	-2(1)	3(1)	-1(1)
C(10)	11(1)	11(1)	12(1)	0(1)	3(1)	0(1)
C(11)	11(1)	14(1)	17(1)	-1(1)	5(1)	2(1)
C(12)	16(1)	18(1)	18(1)	1(1)	7(1)	-2(1)
O(1)	16(1)	12(1)	14(1)	0(1)	6(1)	1(1)
O(2)	12(1)	18(1)	18(1)	-1(1)	6(1)	1(1)
O(3)	29(1)	17(1)	21(1)	-6(1)	13(1)	-11(1)
O(4)	27(1)	12(1)	37(1)	3(1)	14(1)	4(1)
O(5)	26(1)	19(1)	15(1)	-2(1)	8(1)	-4(1)
O(6)	14(1)	9(1)	11(1)	0(1)	2(1)	0(1)
O(7)	10(1)	14(1)	15(1)	4(1)	2(1)	-2(1)
O(8)	10(1)	20(1)	19(1)	-4(1)	1(1)	-2(1)
O(9)	18(1)	15(1)	14(1)	2(1)	4(1)	1(1)
O(10)	15(1)	20(1)	18(1)	-2(1)	8(1)	-2(1)
O(11)	16(1)	20(1)	21(1)	-4(1)	7(1)	0(1)

Table N.5 Hydrogen coordinates (x 10^4) and isotropic displacement parameters (Å^2x 10^3) for CCDC#1473970.

	x	y	z	U(eq)
H(1A)	4615	4173	6728	14
H(2A)	2905	2006	5978	15
H(3A)	5026	269	8046	16
H(4A)	4857	13	5356	18
H(5A)	7831	1116	7271	17
H(6A)	9162	1741	5594	21
H(6B)	8652	-47	5468	21
H(8A)	8869	7213	8520	15
H(9A)	9834	4067	9043	15
H(10A)	7723	5766	10436	14
H(11A)	4742	6404	9425	17
H(11B)	3711	5571	8153	17
H(12A)	8809	6500	6372	20
H(12B)	10731	6341	7292	20
H(2)	1640(20)	2920(20)	7304(17)	24
H(3)	2670(20)	-990(20)	7570(20)	32
H(4)	5830(30)	-2070(30)	6570(20)	36
H(5)	7160(20)	2140(30)	4007(18)	30
H(8)	11840(20)	5270(20)	10112(17)	25
H(9)	8160(30)	2760(30)	10370(20)	39(5)
H(10)	3460(20)	3610(20)	9267(18)	25
H(11)	8490(20)	4020(20)	6519(18)	28

Table N.6 Torsion angles [°] for CCDC#1473970.

O(1)-C(1)-C(2)-O(2)	177.41(8)
O(6)-C(1)-C(2)-O(2)	55.17(11)
O(1)-C(1)-C(2)-C(3)	55.38(12)
O(6)-C(1)-C(2)-C(3)	-66.86(11)
O(2)-C(2)-C(3)-O(3)	63.41(11)
C(1)-C(2)-C(3)-O(3)	-174.63(9)
O(2)-C(2)-C(3)-C(4)	-178.59(9)
C(1)-C(2)-C(3)-C(4)	-56.63(11)
O(3)-C(3)-C(4)-O(4)	-65.38(12)
C(2)-C(3)-C(4)-O(4)	174.28(9)
O(3)-C(3)-C(4)-C(5)	177.29(9)
C(2)-C(3)-C(4)-C(5)	56.95(11)
O(4)-C(4)-C(5)-O(1)	-177.44(9)
C(3)-C(4)-C(5)-O(1)	-55.58(12)
O(4)-C(4)-C(5)-C(6)	64.98(12)
C(3)-C(4)-C(5)-C(6)	-173.16(9)
O(1)-C(5)-C(6)-O(5)	-56.39(11)
C(4)-C(5)-C(6)-O(5)	64.09(12)
O(7)-C(8)-C(9)-O(8)	-147.50(8)
C(12)-C(8)-C(9)-O(8)	91.55(11)
O(7)-C(8)-C(9)-C(10)	-27.34(10)
C(12)-C(8)-C(9)-C(10)	-148.29(9)
O(8)-C(9)-C(10)-O(9)	-78.73(11)
C(8)-C(9)-C(10)-O(9)	161.70(9)
O(8)-C(9)-C(10)-C(7)	154.82(9)
C(8)-C(9)-C(10)-C(7)	35.25(10)
O(7)-C(7)-C(10)-O(9)	-157.53(8)
O(6)-C(7)-C(10)-O(9)	-39.19(12)
C(11)-C(7)-C(10)-O(9)	84.76(11)
O(7)-C(7)-C(10)-C(9)	-31.27(10)
O(6)-C(7)-C(10)-C(9)	87.06(9)
C(11)-C(7)-C(10)-C(9)	-148.99(9)
O(7)-C(7)-C(11)-O(10)	171.02(8)
O(6)-C(7)-C(11)-O(10)	50.55(12)
C(10)-C(7)-C(11)-O(10)	-72.39(11)
O(7)-C(8)-C(12)-O(11)	-70.05(11)
C(9)-C(8)-C(12)-O(11)	48.68(13)
O(6)-C(1)-O(1)-C(5)	67.47(11)
C(2)-C(1)-O(1)-C(5)	-54.80(11)
C(6)-C(5)-O(1)-C(1)	176.60(8)
C(4)-C(5)-O(1)-C(1)	55.17(11)
O(1)-C(1)-O(6)-C(7)	108.29(9)
C(2)-C(1)-O(6)-C(7)	-129.01(9)

Table N.6 continued

O(7)-C(7)-O(6)-C(1)	-44.76(10)
C(11)-C(7)-O(6)-C(1)	73.53(10)
C(10)-C(7)-O(6)-C(1)	-159.48(8)
O(6)-C(7)-O(7)-C(8)	-102.04(9)
C(11)-C(7)-O(7)-C(8)	137.81(9)
C(10)-C(7)-O(7)-C(8)	14.66(11)
C(12)-C(8)-O(7)-C(7)	132.51(9)
C(9)-C(8)-O(7)-C(7)	8.07(11)
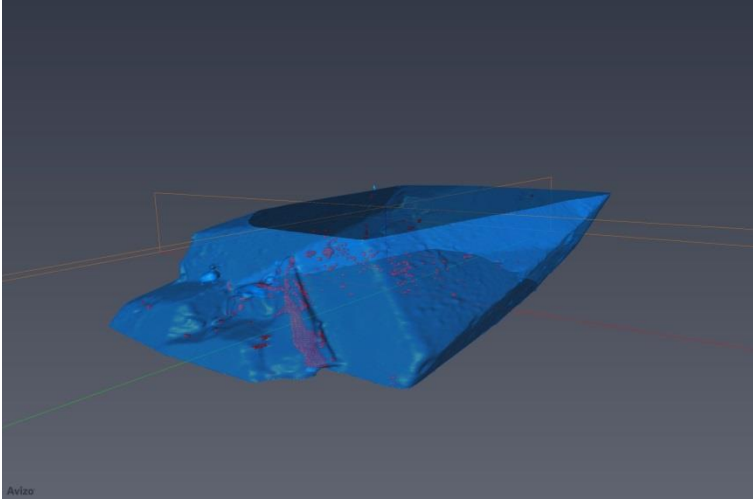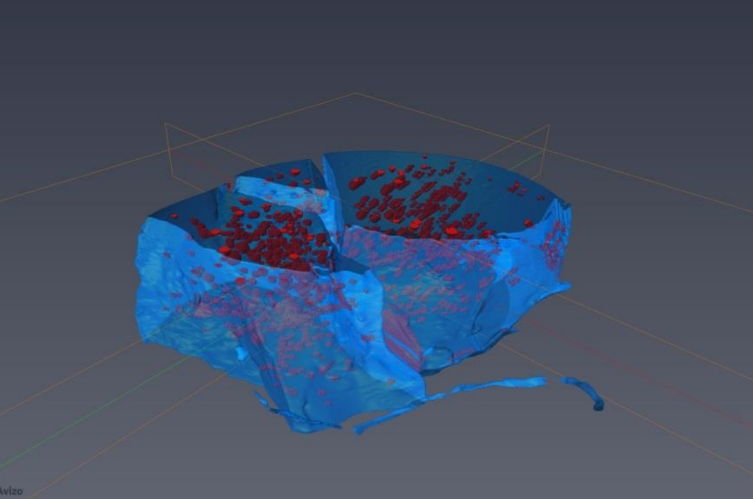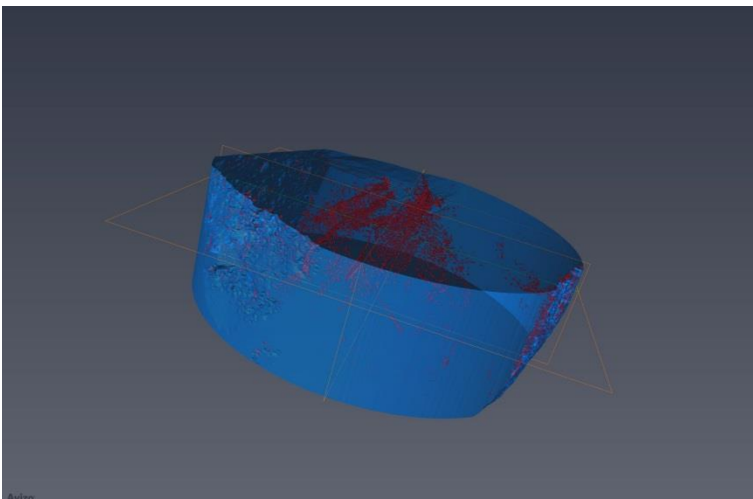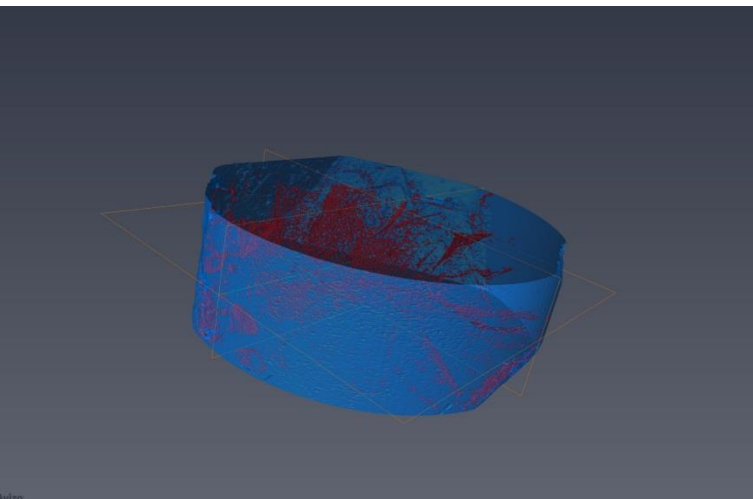
Table N.7 Hydrogen bonds for CCDC#1473970 [Å and °].

D-H...A	d(D-H)	d(H...A)	d(D...A)	<(DHA)
O(2)-H(2)...O(11)#1	0.860(19)	1.991(19)	2.8372(13)	168.0(17)
O(3)-H(3)...O(9)#2	0.81(2)	2.03(2)	2.8396(14)	178(2)
O(4)-H(4)...O(7)#3	0.75(2)	2.36(2)	2.8194(13)	121(2)
O(4)-H(4)...O(5)#4	0.75(2)	2.67(2)	3.3570(15)	154(2)
O(5)-H(5)...O(3)#5	0.78(2)	2.06(2)	2.8185(14)	165(2)
O(8)-H(8)...O(10)#6	0.871(18)	1.841(18)	2.7081(12)	173.2(17)
O(9)-H(9)...O(8)#7	0.83(2)	2.03(2)	2.8384(13)	167(2)
O(10)-H(10)...O(2)	0.81(2)	2.00(2)	2.7728(13)	160.3(19)
O(11)-H(11)...O(1)	0.873(19)	1.987(19)	2.8343(12)	163.5(18)
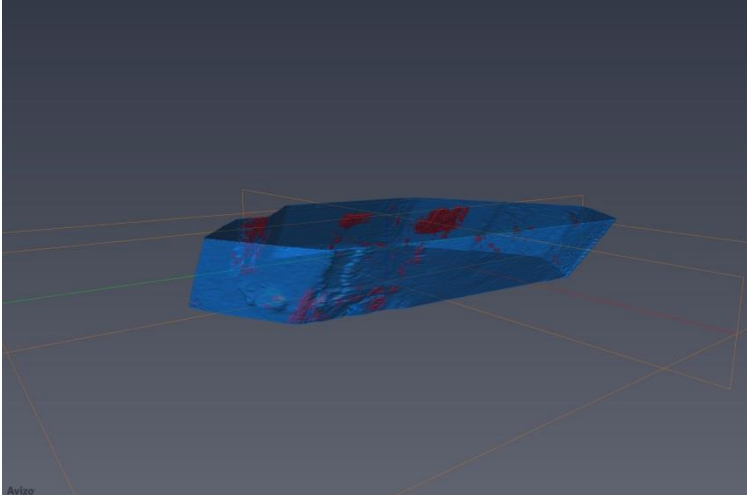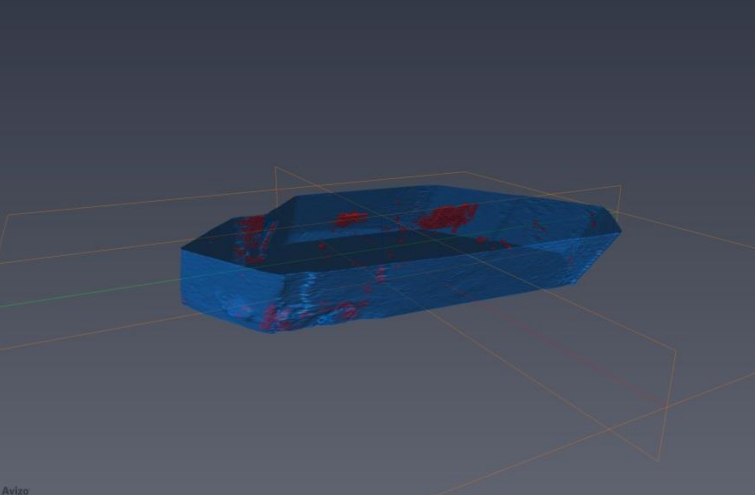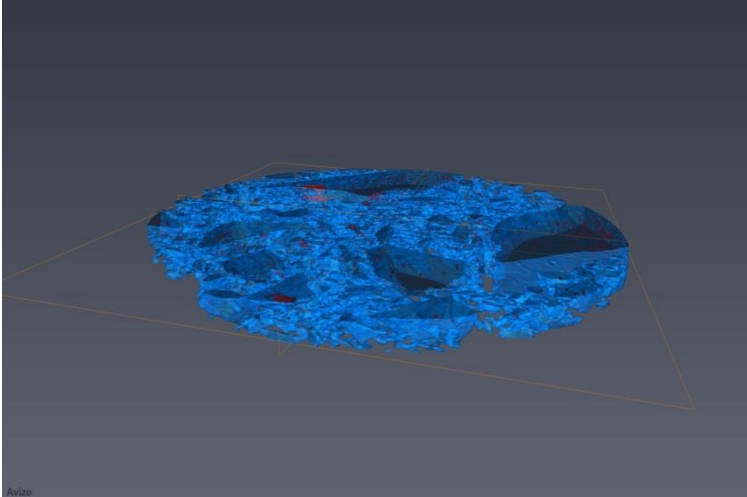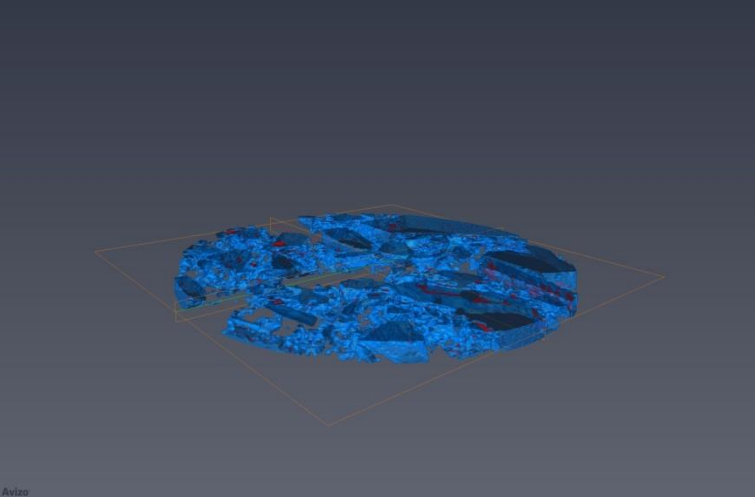
Symmetry transformations used to generate equivalent atoms:

#1 x-1,y,z #2 -x+1,y-1/2,-z+2 #3 x,y-1,z
#4 -x+1,y-1/2,-z+1 #5 -x+1,y+1/2,-z+1 #6 x+1,y,z
#7 -x+2,y-1/2,-z+2

Appendix O 3D Micro-CT images for selected sucrose samples at different temperatures

US beet	"as is"	195ºC
	Porosity%: 0.05280 ± 0.03486	Porosity%: 1.60460 ± 0.24619
Sigma cane recrystallized in HPLC water	"as is"	140ºC
	Porosity%: 0.10621 ± 0.05152	Porosity%: 0.13250 ± 0.01972

Appendix O continued.		
Sigma cane	"as is"	145°C
	Porosity%: 0.00742 ± 0.00830	Porosity%: 0.11873 ± 0.10334
Ground Sigma cane	"as is"	165°C
	Porosity%: 0.21917 ± 0.01068	Porosity%: 0.24927 ± 0.06025

Appendix P Observed and calculated wavenumbers (cm^{-1}) and assignment for sucrose

(Brizuela and others 2012)

Modes	IR[a] solid	Raman[a] solid	SQM[b]	IR int.[c]	Raman act.[d]	Assignment[a]
1	3566 s		3619	35.5	69.1	ν (O14–H15)
2			3609	19.8	60.5	ν (O21–H22)
3			3604	20.4	144.9	ν (O43–H45)
4	3414 sh	3338 w, br	3593	29.1	139.2	ν (O34–H40)
4	3391 vs	3296 w	3579	10.4	87.8	ν (O12–H13)
6	3339 vs	3272	3576	28.8	98.3	ν (O30–H35)
7	3263 sh		3568	25.2	78.0	ν (O16–H17)
8		3244 w	3528	50.2	70.5	ν (O39–H44)
9	3014 vw	3014 w	3021	11.4	63.4	ν (C24–H26)
10			3013	1.7	67.0	ν (C4–H7)
11	2995 w	2994 w	3001	13.9	55.8	ν$_a$ CH$_2$
12			2994	18.5	30.8	ν$_a$ CH$_2$
13	2983 vw	2985 w	2966	29.4	28.5	ν$_a$ CH$_2$
14	2972 w	2972 w	2958	18.9	44.1	ν (C28–H33)
15	2958 w	2959 w	2933	6.6	66.7	ν (C31–H36)
16	2942 m	2943 s	2932	30.0	70.3	ν$_s$ CH$_2$
17	2933 sh	2929 sh	2904	23.9	75.2	ν$_s$ CH$_2$
18	2914 w	2913 vs	2895	58.9	108.7	ν$_s$ CH$_2$
19	2896 vw	2913 vs	2881	96.9	196.6	ν$_s$ C–H
20	2880 sh		2874	9.9	19.8	ν$_a$ C–H
21	2847 sh	2841 vw	2850	59.7	83.9	ν$_a$ C–H
22		2822 vw	2825	67.9	85.9	ν (C32–H38)
23	1477 m	1474 sh	1469	4.4	12.8	δCH$_2$
24	1460 m	1462 m	1465	2.9	4.2	δCH$_2$
25	1440 m, br		1448	3.4	8.6	wag CH$_2$
26			1442	3.3	0.8	δCH$_2$
27	1431 m	1432 w, br	1437	8.4	5.9	ρ C4–H7
28	1426 sh	1428 w	1426	6.8	2.7	wag CH$_2$
29			1420	4.6	4.9	ρ C28–H33, ρ′ C25–H29
30	1409 w	1411 w, br	1413	2.4	3.6	ρ C5–H8
31			1409	26.3	7.9	ρ C25–H29, ν (C24–C25)
32	1391 sh		1398	39.1	1.4	wag CH$_2$
33			1396	38.0	1.9	ρ′ C 31–H36
34	1386 w		1385	14.8	1.2	δ (O39–H44)
35			1380	11.3	2.1	ρ C3–H6
36	1375 w	1378 w	1375	6.7	1.8	ρ C 5–H8
37	1366 w	1367 w	1364	26.2	6.4	ρ C31–H36
38	1348 m	1349 w	1352	11.4	5.5	ρ C H$_2$
39			1351	17.2	4.0	ρ′ C 5–H8
40			1348	5.8	2.9	ρ C H$_2$
41	1343 sh		1339	11.9	9.2	ρ C H$_2$
42	1327 sh	1327 w	1337	13.8	8.3	ρ′ C 5–H8
43	1323 m		1314	21.7	5.7	ρ′ C 4–H7
44	1304 w	1305 vw	1303	76.2	6.9	ρ′ C 4–H7
45	1280 m	1293 vvw	1298	12.4	5.1	ρ C32–H38
46	1274 sh	1278 w	1261	2.2	2.3	ρ C H$_2$
47		1262 w	1258	55.2	9.2	ρ′ C 3–H6
48	1238 m, br	1239 m	1249	13.5	4.7	δ (O14–H15)
49			1227	14.7	6.8	δ (O30–H35)
50			1222	47.8	1.3	δ (O21–H22)
51	1209 w	1209 w	1217	17.0	4.6	δ (O43–H45)
52			1210	26.5	10.1	δ (O16–H17)
53			1208	75.8	3.8	ρ′ C 32–H38
54		1189 vvw	1197	11.9	3.1	δ (O34–H40)
55	1171 m	1171 sh	1181	58.3	4.7	ν (C1–C18)
56	1161 m	1162 w	1171	44.3	3.6	δ (O12–H13)
57	1138 sh		1133	115.8	1.9	ν (C25–O30)
58	1129 m	1126 m	1125	38.9	1.6	ν (C5–O16)
59	1116 m		1115	48.2	1.5	ν (C4–O14)
60	1104 m	1105 w	1107	16.3	5.8	ν (C32–O39)
61	1087 sh	1089 w	1097	100.6	2.9	ν (C24–O23)
62	1073 sh		1078	23.2	3.9	ν (C3–C9), ν (C1–C5)
63	1069 vs	1071 sh	1070	7.6	4.4	ν (C31–C37)
64			1067	62.9	4.2	ν (C9–O12)
65			1060	78.7	3.1	ν (C18–O21)
66	1053 vs	1052 sh	1058	147.7	4.3	ν (C9–O12)

67			1055	45.7	2.9	ν (C18–O21)
68	1038 s	1039 m	1043	7.5	4.9	ν (C4–C3)
69			1036	204.8	3.9	ν (C3–O2)
70			1025	89.8	5.1	ν (C37–O43)
71	1014 s	1014 w	1011	53.7	2.9	ν (C3–O2)
72	1004 s	993 vw	995	58.2	1.5	ν (C24–O27)
73	991 vs, br		981	156.9	1.0	ν (C28–O34)
74			970	241.3	2.4	ν (C1–O23)
75		967 vvw	967	82.2	0.3	ν (C4–C5)
76	943 m	946 w	947	22.9	7.5	ν (C28–C32)
77	921 w	922 w	900	33.4	0.6	ν (C32–C31)
78	914 sh	913 sh	880	55.2	0.9	ν (C1–O2)
79	909 s		865	14.1	4.3	τw CH₂
80	868 m	871 w	832	31.1	3.5	δ (O23–C24–C25)
81	850 m	850 vs	801	52.0	3.2	τw CH₂
82		780 vw	796	28.0	8.1	τw CH₂
83	734 m	738 w	758	20.1	11.0	ν (C31–O27), βR₁ (A6)
84	695 sh	701 vw	712	14.8	2.6	ν (C25–C28)
85	682 w	680 vw	688	50.7	2.3	δ (O34–C28–C32)
86			675	2.3	1.4	δ (O23–C24–O27)
87	642 w	641 w	629	8.2	4.7	βR₁ (A5)
88	595 sh		602	18.8	2.5	δ (C5–C1–O23)
89	583 w	585 w	587	16.1	0.8	δ (O16–C5–C4)
90	552 m	552 m	561	15.7	0.6	δ (O2–C1–O23)
91	537 m	526 w	539	123.1	2.9	βR₂ (A5)
92	523 w	497 w	496	33.6	3.6	τO39–H44
93	499 sh		495	10.6	1.8	τO39–H44
94	472 m	475 w	460	1.3	0.9	δ (O14–C4–C5)
95	440 w	443 m	451	24.5	1.8	δ (C31–C37–O43)
96	417 sh		435	32.8	1.9	δ (O30–C25–C28), ν (C24–C25)
97	405 w	403 vs	393	8.6	1.7	δ (C9–C3–O2), δ (O14–C4–C3)
98			377	80.6	4.2	βR₂ (A6), δ (O30–C25–C28)
99		365 w	360	84.5	1.9	τO16–H17
100			356	17.5	0.5	τO30–H35
101		347 vw	349	7.7	2.4	τO16–H17
102		336 vvw	334	0.8	2.5	δ (C3–C9–O12)
103		315 w	331	2.7	3.3	δ (C31–C37–O43)
104		297 w	298	36.9	2.9	δ (O39–C32–C31), δ (C37–C31–O27)
105			296	32.9	2.3	δ (O39–C32–C28)
106		284 w	286	130.0	2.5	τO34–H40
107			273	114.7	1.4	δ (O34–C28–C25)
108			268	66.4	3.1	τO21–H22
109		257 w	263	21.1	1.2	δ (O16–C5–C1)
110			253	43.9	2.2	δ (O34–C28–C32)
111		231 s	243	1.8	1.2	τO12–H13
112		219 sh	223	10.7	0.6	δ (O2–C1–C18)
113			208	89.1	2.5	δ (C5–C1–C18)
114			204	9.8	0.1	τO43–H45, δ (C1–O23–C24)
115			190	9.0	0.6	δ (C1–C18–O21)
116		183 vvw	184	2.9	0.5	δ (C37–C31–C32), βR₃ (A6)
117		174 vvw	167	27.6	0.9	δ (C9–C3–C4)
118		159 vvw	161	3.9	0.2	τO14–H15
119		148 vvw	144	2.4	0.2	τR₁ (A6)
120		125 vvw	127	3.4	0.5	τR₂ (A6)
121		115 vvw	113	4.6	0.1	τwO21–C18
122		105 vvw	110	1.1	0.1	τwO21–C18
123			89	2.9	0.3	τwO42–C37
124			76	2.3	0.3	τwO12–C9
125			65	1.5	0.0	τw(A6)
126			60	0.7	0.2	τR₃ (A6)
127			49	5.2	0.0	τR₂ (A5)
128			32	3.2	0.3	τR₁ (A5)
129			19	0.7	0.4	τw(A5)

Abbreviations: ν, stretching; β, deformation in the plane; γ, deformation out of plane; wag, wagging; τ, torsion; β_R, deformation ring τ_R, torsion ring; ρ, rocking; τw, twisting δ, deformation; a, antisymmetric; s, symmetric; A5, Ring glucofuran; A6, Ring glucopyran.

[a] This work.
[b] From scaled quantum mechanics force field.
[c] Units are km mol⁻¹.
[d] Raman activities in Å⁴ (amu)⁻¹.

Appendix Q Assignments of –OH, CH₂ and CH vibrational modes of sucrose crystal (Szostak and others 2014)

Tentative assignments of sucrose IR and Raman bands in the –CH₂ and –CH stretching vibration region (3100–2800 cm⁻¹)

	ν_{IR} (cm⁻¹)		ν_R (cm⁻¹); crystal polarization				Calcd[1] (cm⁻¹)	Assignment
	In KBr	ATR	X(YY)X	X(YZ)X	X(ZY)X	X(ZZ)X		
1	3013w	3014vw	3013w	3013m	3013m	3013m	3021	$\nu^{as}_{CH2} + \nu_{CH}$
2	2993w	2994vw	2994s	2994s	2994s	2994w	3013	$\nu^{as}_{C2H2} + \nu_{CH}$
3	2984w	2983vw		2984m	2984m	2984s	3001	$\nu^{as}_{CH2} + \nu_{CH}$
4	2972m	2971w	2972w	2972s	2972s	2972s	2994	ν^{as}_{CH2}
5	2958w			2960w	2961w	2960sh	2966	ν_{CH}
6					2956vw	2957w	2958	ν_{CH}
7			2944m		2944s		2933	$\nu^{s}_{CH2} + \nu_{CH}$
8	2941s	2941w		2943s		2943m	2932	ν^{s}_{CH2}
9	2934	2933sh			2931m		2904	$\nu^{s}_{CH2} + \nu_{CH}$
10				2929m		2929m	2895	ν_{CH}
11			2926w		2925w		2881	ν^{s}_{CH2}
12	2912m	2913w	2913m	2913m	2913m	2915m	2874	ν_{CH}
13			2899vw				2850	ν^{s}_{CH2}
14	2895m	2895w			2895w		2825	ν_{CH}

Assignments of OH group stretching (ν), bending in plane (δ), and out of plane (γ) vibrations participating in hydrogen bonds (or not) to the bands observed in IR, Raman, and INS spectra of crystalline sucrose

No.	Description[44]/(Scheme 1)	l^a_{OH} (Å)	$R^a_{O\cdots O}$ (Å)	Angle[a] (°)	ν^b (cm⁻¹)	δ (cm⁻¹) assign.[c]	γ (cm⁻¹) assign.[c]
1	Non-bonded O4–H/O7–H9	0.913			3560	942 ν(CC)	472 δ(O–C–O)
2	Intermolecular O6–H⋯O3/O10–H10⋯O5	0.955	2.848	162.9	3475	1004 ν(CO)	522 τ(OH)
3	Intermolecular O3–H⋯O′3/O5–H8⋯O6	0.960	2.862	178.8	3452	1039 ν(CO)	552 δ(O–C–O)
4	Intermolecular O′3–H⋯O′4/O6–H13⋯O8	0.969	2.864	168.5	3430	1053 ν(CO)	583 δ(O–C–C)
5	Intermolecular O2–H⋯O′6/O3–H7⋯O11	0.973	2.855	170.2	3392	1117 ν(CO)	619 INS*
6	Intramolecular O′6–H⋯O5/O11–H15⋯O9	0.973	2.850	167.1	3342	1209 δ(OH)	642 βR fruct
7	Intramolecular O′1–H⋯O2/O2–H11⋯O3	0.974	2.781	158.6	3290	1239 δ(OH)	683 δ(O–C–C)
8	Intermolecular O′4–H⋯O′1/O8–H14⋯O2	0.977	2.716	165.4	3245	1280 ρ(CH)	733 ν(CO)